

***Laboratory Testing of Railroad Flatcars  
for use as Highway Bridges on Low-Volume Roads  
to Determine Ultimate Strength and Redundancy***

December 2013  
TR-2-2013

**Indiana LTAP Center  
Purdue University School of Civil Engineering  
Indiana LTAP Center  
3000 Kent Avenue  
West Lafayette, Indiana 47906**

**Telephone: 765.494.2164  
Toll Free in Indiana: 1.800.428.7639  
Facsimile: 765.496.1176**

This document is disseminated under the sponsorship of the Indiana LTAP Center at Purdue University in the interest of information exchange. Purdue University and the Indiana LTAP Center assume no liability for its contents or use thereof. Purdue University and the Indiana LTAP Center do not endorse products or manufacturers. Trademarks or manufacturers names may appear herein only because they are considered essential to the objective of this document. The contents of this report reflect the views of the authors, who are responsible for the facts and accuracy of the data presented herein. The contents do not necessarily reflect the official policy of Purdue University or the Indiana LTAP Center. This report does not constitute a standard, specification, or regulation.

**Form DOT F 1700.7 (8-72)**

1. Report No. TR-2-2013		2. Government Accession No.		3. Recipient's Catalog No.	
4. Title and Subtitle: Laboratory Testing of Railroad Flatcars for use as Highway Bridges on Low-Volume Roads to Determine Ultimate Strength and Redundancy				5. Report Date: December 2013	
				6. Performing Organization Code:	
7. Author(s): Teresa L. Washeleski, Robert J. Connor, Jason B. Lloyd				8. Performing Organization Report No.	
9. Performing Organization Name and Address: Purdue University School of Civil Engineering, 550 Stadium Mall Drive, West Lafayette, Indiana 47907-2051				10. Work Unit No.	
				11. Contract or Grant No.	
12. Sponsoring Agency Name and Address: Purdue University School of Civil Engineering, Indiana Local Technical Assistance Program, 3000 Kent Avenue, Suite C2-118, West Lafayette, Indiana 47906				13. Type of Report and Period Covered: Manual	
				14. Sponsoring Agency Code	
15. Supplementary Notes					
<p>16. Abstract: Railroad flatcars (RRFCs) are a convenient option to replace existing deteriorating bridge structures on low-volume roads. They are typically used as the bridge superstructure by placing two or more flatcars side-by-side to achieve the desired bridge width. Utilizing RRFCs as a bridge allows for rapid construction and greater cost savings compared to traditional practices. These benefits make them an attractive solution for rural communities in Indiana, as well as other states.</p> <p>Uncertainty remains about the response under higher loads than could be easily achieved in the field and the level of redundancy of railroad flatcar bridges. Using RRFCs as bridges becomes less economical for counties if they do not display adequate load-path redundancy and are labeled "fracture critical." If labeled as such, life-cycle costs would rise due to the requirement of an arms-length inspection for each 24 month inspection period. Laboratory testing of a RRFC bridge with two flatcars placed side-by-side allowed for experimental testing under higher loads, as well as increased amounts of instrumentation to better understand the behavior of the RRFCs.</p> <p>As a result of the experimental data, load rating guidelines were developed for RRFC bridges constructed with a fully composite concrete deck. The research also focused on the level of system redundancy in a RRFC bridge after failure of one of the two main box girders. Procedures were developed to estimate whether the remaining longitudinal members provide sufficient available capacity to carry traffic loads.</p>					
17. Key Words: Bridge Rehabilitation, Retired Railroad Flatcar, Bridge Superstructure, Load Rating Guidelines, Railroad Flatcar Bridge, RRFC, Level of System Redundancy			18. Distribution Statement: No Restrictions		
19. Security Classif. (of this report): Unclassified		20. Security Classif. (of this page): Unclassified		21. No. of Pages: 271	22. Price: N/A



**LABORATORY TESTING OF RAILROAD FLATCARS  
FOR USE AS HIGHWAY BRIDGES ON LOW-VOLUME  
ROADS TO DETERMINE ULTIMATE STRENGTH AND  
REDUNDANCY**

**-FINAL REPORT-**

Prepared for

The Indiana Local Technical Assistance Program (LTAP)

Prepared by

Teresa L. Washeleski

Robert J. Connor

Jason B. Lloyd

December 2013

Purdue University

School of Civil Engineering

West Lafayette, Indiana



## ACKNOWLEDGEMENTS

The authors would like to thank the Indiana Local Technical Assistance Program (LTAP) for funding this laboratory study on the use of railroad flatcars as bridges on low volume roads.

Additionally, the authors would like to recognize Rick Franklin Corporation (RFC) in Lebanon, Oregon, for providing the purchase of the two railroad flatcars used for this research project. Specifically, the authors would like to thank John Stolsig from RFC for his assistance, knowledge, and corporation throughout the purchasing process.

The authors would like to thank Dr. Christopher Higgins from Oregon State University for aiding in the inspection process before purchasing the railroad flatcars.

Lastly, the authors appreciate the assistance of staff and students of Bowen Laboratory at Purdue University. Specifically, Mr. Luke Snyder, Mr. Matt Hebdon, Mr. Ryan Sherman, Mrs. Lindsey Lyrenmann, Mr. Tom Spragg, Mr. Tom Bradt, Mr. Tom Garyson, Mr. David Koppes, Ms. Becky Reising, and Ms. Grace Kenney.

## TABLE OF CONTENTS

Page	
	iii
LIST OF TABLES .....	viii
LIST OF FIGURES .....	x
LIST OF EQUATIONS .....	xiv
ABSTRACT .....	xv
CHAPTER 1. INTRODUCTION .....	1
1.1. Background.....	1
1.2. Research Objectives .....	2
1.3. Organization .....	2
CHAPTER 2. CRITICAL REVIEW OF LITERATURE.....	4
2.1. Using Railroad Flatcars as Bridges .....	4
2.1.1. Montana State University.....	5
2.1.2. Arkansas State University .....	5
2.1.3. California Emergency Bridge System.....	6
2.1.4. Bridge Diagnostics Inc. Load Rating .....	6
2.1.5. Iowa State University .....	7
2.2. Purdue University Railroad Flatcar Bridge Research (Phase I) .....	8
2.2.1. Indiana Inventory .....	9
2.2.2. Field Instrumentation & Testing .....	10
2.2.3. Load Rating Guidelines.....	11
2.2.3.1. Main Girders .....	12
2.2.3.2. Exterior Girders & Stringers .....	12
2.2.4. Selecting a RRFC .....	13
2.2.4.1. Geometry.....	13
2.2.4.2. Condition.....	14
2.3. Queensland University of Technology Railroad Flatcar Bridge Research.....	14
2.3.1. Laboratory Testing .....	15
2.3.1.1. Finite Element Analysis .....	16

2.3.1.2. Experimental Set-up.....	16
2.3.1.3. Laboratory Load Tests .....	17
2.3.2. Field Testing.....	19
2.3.3. Research Conclusions.....	20
2.3.3.1. Laboratory Test Conclusions .....	20
2.3.3.2. Field Test Conclusions .....	20
2.4. Exploring Load-Path Redundancy in Bridges .....	21
2.4.1. University of Texas .....	21
2.4.2. New Mexico State University .....	22
2.4.3. Purdue University.....	22
2.5. Spring Analogy to Predict Live Load Response of Girders .....	23
2.5.1. Spring Analogy Method .....	24
2.5.2. Model Comparison.....	25
2.6. Summary.....	26
CHAPTER 3. SELECTION OF RAILROAD FLATCARS .....	27
3.1. Selection Criteria .....	27
3.1.1. Geometry .....	27
3.1.1.1. “Car Haulers” vs. Traditional RRFCs .....	27
3.1.1.2. Length .....	28
3.1.1.3. Width.....	28
3.1.1.4. Cross Section.....	28
3.1.1.5. Connections.....	28
3.1.1.6. Number of RRFCs.....	29
3.1.2. Condition .....	29
3.2. Final Selection .....	29
3.2.1. Specimen Acquisition.....	29
3.2.2. Geometry .....	30
3.2.3. Condition.....	31
3.2.4. History of RRFCs Selected for Research .....	32
CHAPTER 4. INSTRUMENTATION & EQUIPMENT .....	34
4.1. Uniaxial Strain Gages.....	34
4.1.1. Location of Uniaxial Strain Gages .....	35
4.2. Rectangular Rosette Strain Gages .....	37
4.2.1. Location of Rectangular Rosette Strain Gages.....	37
4.3. Displacement Sensors.....	38
4.3.1. Location of Displacement Sensors .....	38
4.4. Load Cell .....	39
4.5. Hydraulic Cylinder .....	39

4.6. Data Acquisition .....	40
4.7. Thermocouples .....	40
CHAPTER 5. EXPERIMENTAL CONFIGURATIONS AND PROCEDURES .....	42
5.1. Railroad Flatcar Bridge Overview .....	42
5.2. Load Tests .....	43
5.3. No Bridge Deck .....	44
5.4. Timber Deck Patch .....	45
5.4.1. Timber Deck Design .....	46
5.4.2. Timber Deck Cost Estimate .....	47
5.4.3. Load Tests with Timber Deck .....	47
5.5. Concrete Bridge Deck .....	48
5.5.1. Concrete Deck Design .....	49
5.5.1.1. Formwork .....	49
5.5.1.2. Shear Connectors .....	50
5.5.1.3. Steel Reinforcement .....	50
5.5.1.4. Concrete Type .....	51
5.5.2. Concrete Deck Cost Estimate .....	52
5.5.3. Load Tests with Composite Concrete Deck .....	53
5.5.3.1. Single Patch Load Tests .....	53
5.5.3.2. Axle Load Tests .....	54
5.5.3.3. Load Centered Between Railroad Flatcars .....	55
5.5.3.4. Load at Quarter Points .....	57
5.6. Fracture Tests .....	58
5.6.1. Fracture Test 1 Overview .....	58
5.6.2. Fracture Test 2 Overview .....	60
CHAPTER 6. RESULTS OF LABORATORY LOAD TESTING .....	62
6.1. No Bridge Deck .....	63
6.1.1. Test 1 & Test 2: Single Patch Load .....	63
6.2. Timber Deck Patch .....	70
6.2.1. Test 3: Single Patch Load .....	70
6.2.2. Test 4: Axle Load .....	72
6.3. Concrete Bridge Deck .....	73
6.3.1. Concrete Pour .....	73
6.3.2. Test 5 & Test 7: Single Patch Load .....	74
6.3.3. Test 6 & Test 8: Axle Load .....	80
6.3.4. Test 9 & Test 10: Load Centered Between Railroad Flatcars .....	81
6.3.5. Test 11 & Test 12: Load at Quarter Point .....	84
6.4. Fracture Test Results .....	86

6.4.1. Fracture Test 1 Results .....	86
6.4.1.1. Fracture Test 1 Load Redistribution .....	87
6.4.1.2. Fracture Test 1 Concrete Deck Response .....	92
6.4.2. Fracture Test 2 Results .....	94
6.4.2.1. Fracture Test 2 Load Redistribution .....	96
6.4.2.2. Fracture Test 2 Concrete Deck Response .....	100
CHAPTER 7. REVISIONS AND PROPOSED ADDITIONS TO LOAD RATING GUIDELINES.....	101
7.1. Revisions to Phase I Load Rating Guidelines .....	101
7.2. Railroad Flatcar Bridges Constructed with a Composite Concrete Deck .....	102
7.2.1. Effective Section .....	104
7.2.2. Girder Distribution Factors Using Spring Analogy .....	107
7.2.2.1. Model Calibration .....	108
7.2.2.2. Parametric Study .....	110
7.2.2.3. Distribution Factor Results .....	113
7.2.2.4. Car Distribution Factor Results.....	118
7.2.3. Stress Modification Factor .....	121
7.3. Capacity After Fracture .....	122
7.3.1. Capacity Limit.....	123
7.3.2. Redistribution of Locked-in Loads.....	124
7.3.2.1. Distribution Factor for Redistribution of Locked-in Loads .....	126
7.3.2.2. Car Distribution Factor for Redistribution of Locked-in Loads ...	126
7.3.3. Redistribution of Live Load .....	126
7.3.3.1. Distribution Factor for Redistribution of Live Load.....	128
7.3.3.2. Car Distribution Factor for Redistribution of Live Load.....	129
7.4. Shear .....	129
CHAPTER 8. RESULTS, CONCLUSIONS, & RECOMMENDATIONS .....	132
8.1. Results .....	132
8.2. Conclusions .....	133
8.3. Future Research Recommendations .....	134
LIST OF REFERENCES.....	135
APPENDIX A. RAILROAD FLATCAR DIMENSIONS .....	138
APPENDIX B. INSTRUMENTATION PLANS .....	142
APPENDIX C. RAILROAD FLATCAR BRIDGE DECK DESIGNS.....	152



APPENDIX D. LABORATORY TEST RESULTS.....	163
APPENDIX E. DEVELOPMENT OF PROPOSED GUIDELINES .....	181
APPENDIX F. PROPOSED GUIDELINES FOR LOAD RATING BRIDGES CONSTRUCTED FROM RAILROAD FLATCARS .....	196
APPENDIX G. LOAD RATING AND FRACTURE CAPACITY EXAMPLE .....	227
APPENDIX H. GUIDANCE FOR ESTABLISHING RELIABILITY-BASED INSPECTION INTERVAL FOR RRFC BRIDGES WITH FULLY COMPOSITE CONCRETE DECKS .....	242

## LIST OF TABLES

Table	Page
Table 2.1: Deck types from Indiana RRFC bridge inventory (Provines et al., 2011) .....	9
Table 2.2: RRFC bridge selection for field testing (Provines et al., 2011).....	11
Table 2.3: Interior girder GDFs for bridges in study (Akinici et al., 2013).....	25
Table 5.1: RRFC bridge load tests .....	44
Table 5.2: Cost estimate for timber deck patch .....	47
Table 5.3: Concrete compressive strength for RRFC bridge deck .....	52
Table 5.4: Cost estimate for concrete deck.....	53
Table 6.1: RRFC bridge load tests.....	63
Table 6.2: Concrete dead load stress.....	74
Table 6.3: Concrete dead load displacement .....	74
Table 6.4: Displacement results for Test 9 & Test 10 .....	84
Table 6.5: Displacement results for Test 11 .....	86
Table 7.1: Composite section properties.....	105
Table 7.2: Total bridge moment near midspan .....	106
Table 7.3: Total bridge moment near quarter point .....	107
Table 7.4: Stiffness values used for spring analogy calibration .....	108
Table 7.5: Comparison of actual versus model girder distribution factors (GDF) .....	109
Table 7.6: Test 5 Distribution factors (DF) and car distribution factors (CDF).....	110
Table 7.7: Relative flexural stiffness values for parametric study.....	111
Table 7.8: Distance between flatcars for parametric study.....	111
Table 7.9: Truck wheel locations for parametric study .....	111
Table 7.10: Parametric Study 1 combinations .....	112

Table 7.11: Parametric Study 2 combinations .....	112
Table 7.12: Maximum distribution factors for LOC5-LOC6 .....	115
Table 7.13: Distribution factor for calculating live load stress for single lane loaded ...	118
Table 7.14: Distribution factor for calculating live load stress for two lanes loaded .....	118
Table 7.15: Maximum car distribution factors for LOC1-LOC6 .....	121
Table 7.16: Maximum car distribution factors for DIST1-DIST7.....	121
Table 7.17: Car distribution factor results for calculating live load stress .....	121
Table 7.18: Maximum total stress in outer exterior girder of fractured flatcar .....	124
Table 7.19: Fracture 1 redistribution of locked-in loads.....	125
Table 7.20: Fracture 1 redistribution of live load .....	128
Table 7.21: Section J-J maximum shear values with no deck .....	131
Table 7.22: Section J-J maximum shear values with composite concrete deck .....	131

## LIST OF FIGURES

Figure	Page
Figure 2.1: Elevation view (A), longitudinal members (B), & transverse members (C) of a typical RRFC (Provines et al., 2011) .....	10
Figure 2.2: Flat bottom rail wagon tested at QUT (McDonald, 2011) .....	15
Figure 2.3: FBW boundary constraints (McDonald, 2011) .....	17
Figure 2.4: M1600 load case (McDonald, 2011) .....	18
Figure 2.5: FBW field bridge cross section at midspan, units in mm (Jamtsho & Dhanasekar, 2013) .....	19
Figure 2.6: Idealized model using the spring analogy method (Akinci et al, 2013).....	24
Figure 3.1: RRFC delivery to Bowen Laboratory .....	30
Figure 3.2: RRFC members from underneath (A) & members from top (B) as erected in the laboratory .....	31
Figure 3.3: Local burn-through on bottom flange of a transverse member .....	32
Figure 3.4: Visible stenciled markings, load limit and light weight (A) & type of flatcar and date built (B) .....	33
Figure 4.1: Example of a uniaxial strain gage after installation .....	35
Figure 4.2: Placement of RRFCs in laboratory.....	36
Figure 4.3: Example of installed rectangular rosette strain gage.....	37
Figure 4.4: Linear motion position sensor near support (A) & position transducer attached to a main girder (B).....	38
Figure 4.5: Test set-up containing the load cell and hydraulic cylinder .....	40
Figure 4.6: Thermocouples installed on the outside of the main girder (A) & on the inside of the main girder (B) .....	41

Figure 5.1: Roller support (A) & pin support (B) at wheel truck locations.....	43
Figure 5.2: Test 1 & Test 2 load set-up .....	45
Figure 5.3: Test 1 on East RRFC (A) & Test 2 on West RRFC (B).....	45
Figure 5.4: Completed timber deck patch.....	47
Figure 5.5: Test 3 (A) & Test 4 (B) load set-up.....	48
Figure 5.6: Test 3 (A) & Test 4 (B) with timber deck patch .....	48
Figure 5.7: Completed formwork construction & shear stud installation.....	50
Figure 5.8: RRFC bridge after installing steel reinforcement.....	51
Figure 5.9: RRFC bridge concrete deck pour .....	52
Figure 5.10: Test 5 (A) & Test 7 (B) load set-up at midspan (looking south).....	54
Figure 5.11: Test 5 (A) on East RRFC (A) & Test 7 on West RRFC (B) (looking south).....	54
Figure 5.12: Test 6 (A) & Test 8 (B) load set-up at midspan (looking south).....	55
Figure 5.13: Test 6 on East RRFC (A) & Test 8 on West RRFC (B) (looking south) .....	55
Figure 5.14: Test 9 (A) & Test 10 (B) load set-up at Section E (looking south).....	56
Figure 5.15: Test 9 (A) & Test 10 (B) (looking south).....	56
Figure 5.16: Test 11 (A) & Test 12 (B) load set-up at Section E (looking south).....	57
Figure 5.17: Test 11 (A) on East RRFC & Test 12 (B) on West RRFC (looking south) .	58
Figure 5.18: Cooling chamber .....	59
Figure 5.19: Bottom flange cut (A), side flange cuts (B), & web cuts (C).....	60
Figure 5.20: Initial cut in West RRFC main girder before fracture (looking up at bottom flange) .....	61
Figure 6.1: Test 1 versus Test 2 main girder response at Sections C & I.....	64
Figure 6.2: Test 1 response at Section C for an applied load of 150 kips .....	65
Figure 6.3: Test 1 neutral axis location for Section C .....	66
Figure 6.4: Test 1 response at Section B for an applied load of 150 kips .....	67
Figure 6.5: Test 1 response at Section A for an applied load of 150 kips .....	67
Figure 6.6: Test 1 main girder stress results for Sections B & E.....	68
Figure 6.7: Test 1 versus Test 2 main girder displacement response .....	69
Figure 6.8: Test 3 response for Section C at an applied load of 150 kips .....	71
Figure 6.9: Test 3 neutral axis location for Section C .....	71

Figure 6.10: Test 3 versus Test 4 exterior girder response for Section C.....	73
Figure 6.11: Test 1 versus Test 5 main girder stress results for Section C.....	75
Figure 6.12: Test 5 response for Section C at an applied load of 150 kips .....	76
Figure 6.13: Test 5 neutral axis location for Section C .....	77
Figure 6.14: Test 5 main girder stress results for Sections C & I.....	78
Figure 6.15: Test 5 exterior girder stress results for Section C & I.....	79
Figure 6.16: Test 5 main girder displacement results .....	80
Figure 6.17: Test 6 response for Section C at an applied load of 150 kips .....	81
Figure 6.18: Test 9 response for Section C at an applied load of 150 kips .....	82
Figure 6.19: Test 10 response for Section C at an applied load of 150 kips .....	83
Figure 6.20: Location of displacement sensors during Test 9 & Test 10 .....	83
Figure 6.21: Test 11 response for Section E at an applied load of 150 kips.....	85
Figure 6.22: Test 11 & Test 12 main girder stress results for Section E .....	85
Figure 6.23: Fracture Test 1 fractured main girder bottom flange (A) & web (B).....	87
Figure 6.24: Fracture Test 1 stress results at Sections C & I.....	89
Figure 6.25: Fracture Test 1 stress results at Section B.....	90
Figure 6.26: Fracture Test 1 stress results at Section B (exterior girders).....	91
Figure 6.27: Fracture Test 1 stress results at Section C (stringers) .....	92
Figure 6.28: Separation of shear stud in concrete deck after Fracture Test 1 .....	93
Figure 6.29: Separation of concrete deck on West RRFC .....	93
Figure 6.30: Concrete deck delamination on East RRFC after Fracture Test 1 .....	94
Figure 6.31: Fracture Test 2 load sequence .....	95
Figure 6.32: Fracture Test 2 fractured main girder web (A) & bottom flange (B).....	95
Figure 6.33: West RRFC displacement results for Fracture Test 2 .....	97
Figure 6.34: East RRFC displacement results for Fracture Test 2 .....	98
Figure 6.35: After-fracture loading of RRFC bridge .....	99
Figure 6.36: After-fracture loading of RRFC bridge (deck view) .....	99
Figure 6.37: Concrete deck delamination on West RRFC after Fracture Test 2 .....	100
Figure 7.1: Assumed effective sections for each primary member near midspan .....	105
Figure 7.2: Assumed effective sections for each primary member near quarter point ...	106

Figure 7.3: RRFC bridge modeled using the spring analogy.....	108
Figure 7.4: Schematic for “DIST” and “LOC” .....	110
Figure 7.5: Parametric Study 1 results varying relative stiffness .....	114
Figure 7.6: Parametric Study 1 results varying truck location.....	115
Figure 7.7: Parametric Study 2 when varying distance between flatcars .....	116
Figure 7.8: Distribution factors for Case 1 .....	117
Figure 7.9: Schematic for determining the distribution factor for one lane loaded .....	118
Figure 7.10: Car distribution factor when varying truck location .....	119
Figure 7.11: Car distribution factor when varying distance between flatcars .....	120
Figure 7.12: Percent of total moment carried by primary members before and after fracture .....	127
Figure 7.13: Location of rectangular rosette strain gages on East RRFC.....	130

**LIST OF EQUATIONS**

Equation	Page
Equation 1: Live load bending stress equation (Provines et al., 2011).....	11
Equation 2: Live load bending stress equation developed in Phase I (Provines et al., 2011). .....	103



## ABSTRACT

Washeski, Teresa Lynn. M.S.C.E., Purdue University, December 2013. Laboratory Testing of Railroad Flatcars for Use as Highway Bridges on Low-Volume Roads to Determine Ultimate Strength and Redundancy Major Professor: Robert J. Connor.

Railroad flatcars (RRFCs) are a convenient option to replace existing deteriorating bridge structures on low-volume roads. They are typically used as the bridge superstructure by placing two or more flatcars side-by-side to achieve the desired bridge width. Utilizing RRFCs as a bridge allows for rapid construction and greater cost savings compared to traditional practices. These benefits make them an attractive solution for rural communities in Indiana, as well as other states.

Uncertainty remains about the response under higher loads than could be easily achieved in the field and the level of redundancy of railroad flatcar bridges. Using RRFCs as bridges becomes less economical for counties if they do not display adequate load-path redundancy and are labeled “fracture critical.” If labeled as such, life-cycle costs would rise due to the requirement of an arms-length inspection for each 24 month inspection period. Laboratory testing of a RRFC bridge with two flatcars placed side-by-side allowed for experimental testing under higher loads, as well as increased amounts of instrumentation to better understand the behavior of the RRFCs.

As a result of the experimental data, load rating guidelines were developed for RRFC bridges constructed with a fully composite concrete deck. The research also focused on the level of system redundancy in a RRFC bridge after failure of one of the two main box girders. Procedures were developed to estimate whether the remaining longitudinal members provide sufficient available capacity to carry traffic loads.

## CHAPTER 1. INTRODUCTION

### 1.1. Background

Railroad flatcars (RRFCs) are a convenient option to replace existing deteriorating bridge structures on low-volume roads. They are typically used as the bridge superstructure by placing two or more flatcars side-by-side to achieve the desired bridge width. Utilizing RRFCs as a bridge allows for rapid construction and greater cost savings compared to traditional practices. These benefits make them an attractive solution for rural communities in Indiana, as well as other states.

The unique superstructure of RRFCs could create a challenge when attempting to load rate these types of bridges. There is limited guidance in existing AASHTO Specifications on load rating RRFC bridges, often resulting in overly conservative load postings. Previous research conducted by researchers from Purdue University addressed this issue by load testing seven existing RRFC bridges in Indiana (Provines, Connor, & Sherman, 2011). Proposed load rating guidelines were developed as a result of this research. The objective was to develop guidelines that were simple, yet more accurately predicted the actual capacity of the flatcars. This phase was labeled Phase I of a two part research study.

However, uncertainty remained about the response under higher loads than could be easily achieved in the field, shear behavior, response with a composite concrete deck, and the level of redundancy of railroad flatcar bridges with two flatcars placed side-by-side. Using RRFCs as bridges becomes less economical if they do not display adequate load-path redundancy and are labeled “fracture critical.” If labeled as such, life-cycle costs would rise due to the requirement of an arms-length inspection for each 24 month

inspection period. Laboratory testing of a RRFC bridge with two flatcars placed side-by-side allowed for experimental testing under higher loads, as well as increased amounts of instrumentation to better understand the behavior of the RRFCs.

## **1.2. Research Objectives**

To provide more data regarding these uncertainties, a second phase of research was proposed. The research objectives of Phase II are as follows:

- Evaluate the behavior of railroad flatcar bridges subjected to higher loads (over 175 kips) through controlled laboratory load testing.
- Investigate the following: load distribution within a single flatcar; load distribution between two flatcars placed side-by-side; shear live load response; bending live load response; behavior effects of a timber deck; behavior effects of a composite concrete deck.
- Demonstrate load-path redundancy in railroad flatcar bridges by simulating a fracture in a primary load carrying member.
- Calibrate and revise the proposed load rating guidelines developed in Phase I.

## **1.3. Organization**

This document is organized into eight chapters plus appendices. Chapter 2 provides a literature review of previous research on railroad flatcar bridges, as well as other relative industry research. Chapter 3 presents the criteria and final selection of the two railroad flatcars used for testing in the laboratory. Chapter 4 describes the instrumentation and equipment used during laboratory testing. The different experimental load tests and procedures are discussed in Chapter 5. Chapter 6 contains the results of the laboratory load tests. The application of the experimental results to refine the proposed guidelines is described in Chapter 7. Chapter 8 provides the research project conclusions and recommendations for future work.

Instrumentation plans, bridge deck designs, laboratory tests results, and development of the additional load rating guidelines are provided in Appendix A-E. The proposed load rating guidelines are provided in Appendix F. These proposed guidelines include that of Phase I, as well as revisions and additions as a result of the findings from Phase II. Appendix G provides a load rating and a redundancy evaluation example using the proposed guidelines.

## CHAPTER 2. CRITICAL REVIEW OF LITERATURE

A comprehensive literature review related to the use of railroad flatcars (RRFCs) as low-volume road bridges was performed in Phase I. The review included information from informal surveys conducted by telephone and email to railroad companies and railroad car manufacturers. The review began with a background of RRFCs before being implemented as low-volume road bridges. The background included the following: geometry and structural features, design specifications according to the Association of American Railroads (AAR), in-service use, and reasons for retirement. Also, the review focused on previous research performed by other universities and agencies regarding load rating, inspection, and acquisition of RRFC bridges (Provines et al., 2011).

The focus of this literature review was to collect research pertaining to the current study. This includes previous RRFC bridge research, after-fracture studies performed on traditional bridges, and an alternate approach to determine the distribution of live load moment in a slab-on-girder bridge. The review of these topics was essential to successfully complete the current study.

The section begins with a brief background of RRFC bridge research performed prior to, during, and following the completion of Phase I. The section continues with a discussion of past research on the redundancy of bridges. Lastly, the spring analogy to predict the live load response of girders is presented.

### **2.1. Using Railroad Flatcars as Bridges**

Past research focused on the benefits of using RRFCs as bridges on low-volume roads, criteria on selecting flatcars to use, and suggestions for load rating procedures. The

following lists the research reviewed and a brief description of the project objectives and results.

### **2.1.1. Montana State University**

- The main objective of this study was to determine which RRFCs should be used to replace existing aging low-volume road bridges.
- The research indicated that RRFCs should be selected based on evaluation of the following: (1) condition survey, (2) strength, (3) fatigue (remaining life), (4) simple testing methods to estimate the performance of RRFCs as bridges (Suprenant, 1987a; Suprenant, 1987b).

### **2.1.2. Arkansas State University**

- The main objectives of this study were to compile a RRFC bridge database for the state of Arkansas, perform field testing of four existing railcar bridges, construct and test a one-third scale model of a RRFC bridge, and develop load rating software for future use (Parsons, 1991).
- Destructive tests were performed on a scaled model of a single boxcar to simulate corrosion and cracking in a longitudinal member. The finite element model created could adequately predict the strains when only the bottom flange of the side sill was cut or removed. The model did not reasonably predict the behavior when a large portion of the web was cut (Parsons, 1991).
- Load rating software was created in the study to load rate flatcars and boxcars. The software was calibrated using the scaled model. The software had good agreement with the flatcar bridges, but not with the boxcar bridges load tested. The software was unable to adequately load rate a RRFC bridge with large damage (Parsons, 1991). During a conversation

with Arkansas DOT representatives, it was stated that the program is no longer being used due to time inefficiency and the need for finite element modeling background (Provines et al., 2011).

### **2.1.3. California Emergency Bridge System**

- The California Department of Transportation (Caltrans) was in need of economical and reliable bridge replacement solutions following the 1994 Northridge earthquake. RRFCs were used as the bridge superstructure for this temporary solution. Before implementing this system, a finite element model was analyzed for earthquake loading and a prototype built and loaded (Roberts, 1995a; Roberts, 1995b; Wattenburg, 1995).
- The finite element model concluded that the main structural members had enough strength to withstand any earthquake aftershock (Wattenburg, 1995). Also, the tested prototype displayed enough strength to support AASHTO live loads (Robert, 1995a). The field application of these temporary structures resulted in quicker assembly and greater cost savings for Caltrans, compared to other solutions (Robert, 1995b).

### **2.1.4. Bridge Diagnostics Inc. Load Rating**

- The objectives of this research were to perform field testing of two existing RRFC bridges and conduct finite element modeling to determine load ratings (Bridge Diagnostics Inc., 1995; Bridge Diagnostics Inc. 2002).
- It was concluded from the field instrumentation and testing that the main girders carried the majority of the load. The exterior girders displayed local behavior and also carried global load (Bridge Diagnostics Inc., 1995). The finite element modeling showed that the structural members were adequate for carrying traffic loads (Bridge Diagnostics Inc., 2002).

### 2.1.5. Iowa State University

- Numerous studies were performed on the use of RRFCs as low-volume road bridges and were sponsored by Iowa Department of Transportation. These studies on the use of RRFCs as bridges on low-volume roads focused on: guidelines for selecting RRFCs, field testing, laboratory testing of longitudinal connections, and developing load rating procedures.
- According to the research, the following items should be considered when selecting a RRFC for use as a low-volume bridge: (1) structural element sizes, load distributing capabilities, and support locations, (2) member straightness/damage, (3) structural element configuration, (4) uniform, matching cambers, (5) RRFC availability. Fatigue considerations when using a RRFC as a bridge were also addressed. Through contacted agencies who implement RRFC bridges, it was concluded that fatigue is not a concern (Wipf, Klaiber, & Doornink, 2003).
- Several field tests were conducted on existing RRFC bridges and RRFC bridges built purposefully for ISU testing. The tested bridges varied in length and number of RRFCs side-by-side. All of the RRFC bridges tested provided adequate strength to carry Iowa legal loads, as well as remain within the AASHTO live load deflection limit. Different longitudinal connections between adjacent RRFCs were considered throughout field testing including angles, concrete beams with longitudinal reinforcement and threaded rods, welded steel plates, and bolting the exterior girders together. All connections, with the exception of the angles, were deemed adequate to transfer load between adjacent RRFCs. It was also concluded that the interior girders within the RRFC bridge system carry the majority of the dead load and live load. Finally, with regards to the multi-span RRFC bridges tested, the shallow end of the tapered section was concluded to be the critical section to analyze for flexure (Wipf et al.,



1999; Wipf et al., 2003; Doornink, Wipf, & Klaiber, 2003a; Wipf et al., 2007a; Wipf et al., 2007b).

- A grillage model was constructed to analyze the RRFC bridges that were load tested. It was determined to conduct a grillage model instead of a finite element model due to the ease and fast results of the grillage model. The model showed good agreement with data from field testing. Therefore, it was deemed acceptable to analyze the behavior of RRFC bridges using this type of model (Wipf et al., 2003).
- ISU conducted laboratory testing on a specific longitudinal connection. A reinforced concrete beam with longitudinal reinforcement transverse threaded rods was constructed between two W-shapes to simulate the connection between adjacent RRFC exterior girders. The connection was tested in torsion and flexure under service loads and failed in torsion. As a result of the testing, ISU concluded that this type of connection is adequate to use for 56 feet long RRFCs, compared to 89 feet long RRFCs (Wipf et al., 2003; Doornink, Wipf, & Klaiber, 2003b).
- ISU created two load rating methods; the first using load and resistance factor rating (LRFR), and the second using allowable stress rating (ASR). The first method requires field testing data to complete the load rating process. The second method requires the unknown of the live load effect. ISU developed a series of equations to assist in estimating the live load effect in order to adequately load rate the bridge (Wipf et al., 1999; Wipf et al., 2007b).

## **2.2. Purdue University Railroad Flatcar Bridge Research (Phase I)**

Researchers at Purdue University conducted field studies on the use of RRFCs as low-volume road bridges in 2011. The research was sponsored by the Indiana Local Technical Assistance Program (LTAP). The objectives of this study were to develop

guidelines in acquiring, inspecting, and load rating RRFCs to be used as low-volume road bridges. The acquisition and inspection guidelines were based on the inventory and site visits of RRFC bridges in Indiana. The guidelines for load rating focused on live load bending stress and were developed based on field data from seven instrumented RRFC bridges in Indiana (Provines et al., 2011).

### 2.2.1. Indiana Inventory

An inventory was provided of over 120 bridges constructed from RRFCs in Indiana. This inventory allowed the researchers to become familiar with common construction practices of RRFC bridges in the state. RRFCs typically come in lengths of 56 or 89 feet; it was determined that the majority of the RRFC bridges in Indiana are constructed from RRFCs with a length of 89 feet. Two or three RRFCs are typically used to achieve the desired bridge width. The majority of RRFC bridges in the inventory are constructed with two flatcars side-by-side. As shown in Table 2.1, common RRFC bridge deck types range from steel plate, concrete cast-in-place, timber, corrugated steel, and open grating (Provines et al., 2011).

**Table 2.1: Deck types from Indiana RRFC bridge inventory (Provines et al., 2011)**

Deck Type	# of Bridges	Percentage
Steel Plate	77	62%
Concrete Cast-in-Place	34	27%
Timber	8	7%
Corrugated Steel	4	3%
Open Grating	1	1%
<b>Total</b>	<b>124</b>	<b>100%</b>

A representative sample of 25 RRFC bridges in Indiana was chosen to perform field visits and further investigate the geometry and common construction of RRFC bridges. It was observed that most RRFCs used for bridges in the sample had one main girder and two exterior girders, along with a system of stringers between the main girder and each exterior girder. Figure 2.1 shows an example of a bridge constructed with “typical” RRFCs (Provines et al., 2011).



**Figure 2.1: Elevation view (A), longitudinal members (B), & transverse members (C) of a typical RRFC (Provines et al., 2011)**

### 2.2.2. Field Instrumentation & Testing

The research team selected seven existing RRFC bridges in Indiana to instrument and load test. The selection is provided in Table 2.2 with details including span length, deck type, exterior girder size, type of longitudinal connection, and load posting (if any). Uniaxial strain gages were installed near midspan for each bridge, typically on the top and bottom flanges of the main girders and exterior girders, as well as on one or two stringers. The strain gages allowed for stress data to be collected during load testing. An empty and a loaded tandem axle dump truck were used for load testing the seven bridges. The tests were performed on three lanes: upstream, downstream, and on the centerline. Two tests were performed in each lane: static park test and crawl test. The data collected aided in the development of the proposed load rating guidelines (Provines et al., 2011).

**Table 2.2: RRFC bridge selection for field testing (Provines et al., 2011).**

Bridge	Span Length	Deck Type	Exterior Girder Size	Longitudinal Connection	Load Posting (tons)
CL-53	34'-0"	Asphalt	Small	Welded steel plate	None
CL-179	31'-6"	Asphalt	Small	Welded steel plate	None
CL-406	42'-0"	Asphalt	Car hauler	Large steel beam & plate	4
FO-25	70'-0"	Timber	Small	Steel beams	None
FO-54	81'-0"	Steel	Small	Steel beams & plate	None
FO-256	82'-0"	Steel	Small	Steel beams & plate	4
VE-24	50'-0"	Concrete	Large	One steel beam at midspan	None

### 2.2.3. Load Rating Guidelines

The goal of the proposed load rating guidelines was to develop procedures that were simple, yet accurately predicted the live load bending response of RRFC bridges. The procedures focus on load rating for a single lane loaded. These procedures were developed based on field test results of the seven RRFC bridges. This research aided in the development of Equation 1 to determine the live load bending stress of a longitudinal member (Provines et al., 2011). A brief overview of the different equation variables for typical RRFCs is described in the following sections.

$$\sigma_{LL} = (\alpha) (CDF) \frac{(DF) M_{LL}}{S_{eff}}$$

**Equation 1: Live load bending stress equation (Provines et al., 2011)**

where:

$\sigma_{LL}$  = Maximum positive live load bending stress

$\alpha$  = Stress modification factor

$CDF$  = Car distribution factor

$DF$  = Distribution factor

$M_{LL}$  = Maximum positive live load moment

$S_{eff}$  = Effective section modulus

#### 2.2.3.1. *Main Girders*

The maximum positive live load moment is determined using traditional methods as described in The *AASHTO Manual for Bridge Evaluation* (2011). This bridge moment is then distributed between RRFCs using the distribution factor. The research concluded that implementing the lever rule was sufficient in determining the distribution factor. According to the research, the main girders are load rated based on global bending effects. It was established that the effective section used for the main girders is the main girder plus two stringers on each side of the main girder. This effective section, the section participating in global bending of the main girder, is recommended to be used when the exterior girders are considered “small” (i.e., the moment of inertia of the exterior girder is not greater than 15% of the moment of inertia of the main girder). If the RRFC has “large” exterior girders, than the recommended effective section is the entire flatcar. A stress modification factor of 0.75 was determined sufficient to more accurately predict the bridge moment compared to actual field results (Provines et al., 2011).

#### 2.2.3.2. *Exterior Girders & Stringers*

Calculating the live load stress of the exterior girders and stringers is based on local bending effects. The research showed that the live load moment can be calculated using the moment equation for a simply-supported beam that is point loaded at midspan, with the span length taken as the center to center distance between transverse floorbeams. The distribution factor is determined based on the relative stiffness of the secondary members. It was recommended that the local bending effects for bridges with a composite concrete deck do not need to be evaluated, due to the additional stiffness of the concrete deck (Provines et al., 2011).

#### 2.2.4. Selecting a RRFC

Guidelines to acquire RRFCs to be used as low-volume road bridges were developed based on the Indiana inventory, discussions with county officials, and field test results. Considerations include the site requirements, the desired geometry of the flatcars, and the condition of the flatcars (Provines et al., 2011). The following briefly explains these considerations.

##### 2.2.4.1. Geometry

- **Span Length:** The span length of the desired bridge should be equal to or shorter than the distance between the centerlines of the wheel truck supports. The flatcars were designed to be supported at the wheel trucks; therefore, it is recommended to support them at these locations when utilizing as a bridge.
- **Main Girder:** The main girders of the RRFC bridge carry the majority of the traffic load; therefore, they should be large enough and have adequate stiffness.
- **Exterior Girders:** Typically, longitudinal connections are formed between adjacent RRFCs. The exterior girders should be sufficient to construct the desired longitudinal connection (e.g., size and any additional attachments).
- **Width:** The flatcars and longitudinal connection utilized should create the desired driving width of the bridge. Using narrower RRFCs may lead to using wider longitudinal connections, which can create unwanted problems.
- **Similar RRFCs:** Using flatcars with similar cross section and longitudinal profiles will ease in the construction of the RRFC bridge. It will also provide symmetric behavior within the bridge system.
- **Boxcars & Car Haulers:** Boxcars and car haulers are not recommended to be used as highway bridges. The research showed that these types of cars did not perform as well as typical RRFCs under live load (Provines et al., 2011).

#### 2.2.4.2. Condition

- **Main Girder:** The main girder carries the majority of the traffic load; therefore, it is recommended to thoroughly inspect these members for corrosion and cracking, specifically in the welds of the cover plates.
- **Overall RRFC:** The entire RRFC should be inspected for any bent members, cracks, corrosion, or missing members. If RRFCs have significant amounts of damage, they should not be used as bridges.
- **Deck:** The original RRFC deck should be inspected to determine if it is suitable to utilize as a driving surface, or if an additional deck system needs to be constructed.
- **Paint/Coating:** The paint or coating of the RRFCs should be inspected to determine if a new coat of paint is needed to prevent corrosion damage in the future life of the bridge (Provines et al., 2011).

### 2.3. Queensland University of Technology Railroad Flatcar Bridge Research

There exists a need in Australia for an economical replacement solution for aging bridges on low-volume roads that can safely resist heavy axle loads. Researchers at Queensland University of Technology (QUT) in Brisbane, Australia conducted laboratory and field testing of disused flat bottom rail wagons (FBW) to determine if they are structurally adequate to carry traffic loads. If FBWs are determined structurally sufficient, utilizing them as a bridge allows for shorter construction times and lower initial costs compared to using new material. These studies were funded by the Department of Infrastructure, Commonwealth of Australia through the AusLink initiative (McDonald, 2011; Dhanasekar & Bayissa, 2011; Jamtsho & Dhanasekar, 2013). The following sections briefly discuss the experimental testing performed, along with the research results.

### 2.3.1. Laboratory Testing

The flat bottom rail wagon (FBW) system in the Australian rail industry differs from railroad flatcars (RRFC) in the United States. Such differences include fewer primary members and smaller sized members. The FBW used for laboratory research was a PHO class FBW, which is an Open Goods Wagon manufactured and designed by Queensland Railways Authority (McDonald, 2011).

The FBW consisted of a center girder (main box girder) with a depth of 26 inches and a width of 16 inches. The edge beams (exterior girders) were Z-sections that were about 8 inches deep. Folded plate beams welded to the center girder and the edge beams created the FBW deck (Dhanasekar & Bayissa, 2011). Figure 2.2 shows the inverted FBW used for laboratory testing.

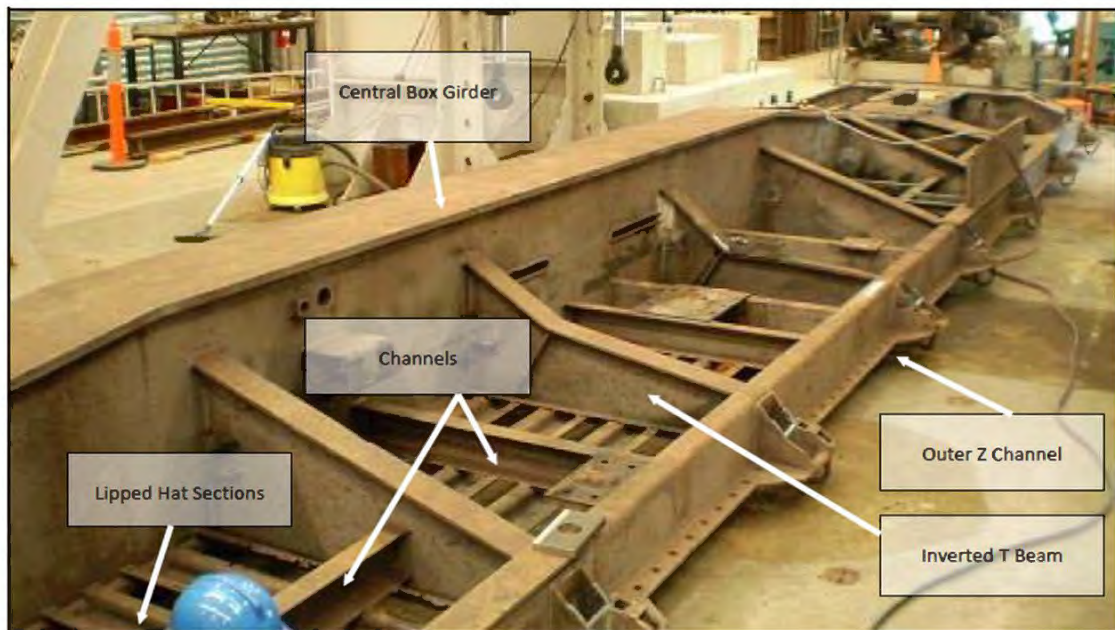


**Figure 2.2: Flat bottom rail wagon tested at QUT (McDonald, 2011)**

Two FBWs placed side-by-side was required to achieve the required driving width of the single lane, single span, low-volume road bridge. However, due to laboratory space and equipment limitations, only a single FBW (i.e., half of a FBW bridge) was able to be experimentally tested in the laboratory. The attachment of a



second FBW was simulated using constructed boundary constraints, as discussed in a later section (McDonald, 2013).

#### *2.3.1.1. Finite Element Analysis*

A three-dimensional finite element model in ABAQUS was developed for the laboratory FBW. The model was calibrated using experimental stress and deflection data from laboratory testing of the single FBW (without boundary constraints). The FE model was used to understand the behavior of a full FBW bridge, with two FBWs side-by-side (Dhanasekar & Bayissa, 2011).

#### *2.3.1.2. Experimental Set-up*

The single FBW was supported on reinforced concrete blocks at the wheel truck locations. The center girder and edge beams were all supported at this cross section. A simply supported condition was developed using elastomeric bearing pads at the supports. The total length of the FBW was about 46 feet with a span length of 33 feet and a width of 8.5 feet (McDonald, 2011).

Boundary constraints were used to simulate double FBWs to create an entire bridge. Six adjustable boundary constraints were located along the longitudinal edge of one of the edge beams. They were located where the transverse members cross the edge beams. The FE model previously mentioned was used to determine the required boundary condition adjustments, based on deflections, to adjust the constraints in the laboratory set-up (Dhanasekar & Bayissa, 2011).

Figure 2.3 shows the boundary constraints utilized in the laboratory. The assumption of similar flexural stiffness of the two FBW was made when determining the appropriate boundary adjustments. The mechanism shown consisted of individual screw jack pedestal stands connected by a bolt assembly to the edge beams. The mechanism only allowed vertical translation and no longitudinal edge beam rotations (McDonald, 2011).



**Figure 2.3: FBW boundary constraints (McDonald, 2011)**

#### *2.3.1.3. Laboratory Load Tests*

Laboratory testing was performed to investigate serviceability and ultimate limit state requirements by using two load cases. These load cases were based from the Australian bridge design standards (AS 1500, 2004). The W80 wheel load was the first load case and consisted of a 15.8 inch by 9.8 inch patch load of 18 kips. The second load case was the M1600 moving traffic load. This loading consisted of tri-axle groups that represent several trucks passing over the bridge. Each axle load group is about 81 kips (13.5 kips per wheel load) and a uniformly distributed load of about 0.4 kips/foot across the width of the traffic lane. For the serviceability tests performed, the wheel loads were increased to 14.6 kips to take into account the uniformly distributed load. The target wheel load for the ultimate load test was 34.8 kips per wheel load. These loads were positioned to create the most critical shear and bending effects in the center girder. Testing to failure was not in the scope of the research and was deemed an unnecessary risk in order to achieve the goals of the research study. Five loading configurations were tested based on the two load cases. These configurations were as follows:

- W80 load case located at the centerline of the RRFC, 1.75 feet north of midspan;

- W80 load case offset 15.75 inches from the centerline of the RRFC, 1.75 feet north of midspan;
- W80 load case offset 33 inches from the centerline of the RRFC, 1.75 feet north of midspan (no boundary constraints were used for this configuration);
- M1600 service load case, with and without boundary conditions;
- M1600 ultimate load case, with and without boundary conditions (McDonald, 2011).

A schematic of the M1600 load case is shown in Figure 2.4. A loading tree concept was used in order to create three points of contact for each simulated truck. It was assumed that the single FBW carries half of the applied load; therefore, the other wheels to create the wheel axle would theoretically be applied to the second FBW (McDonald, 2011).

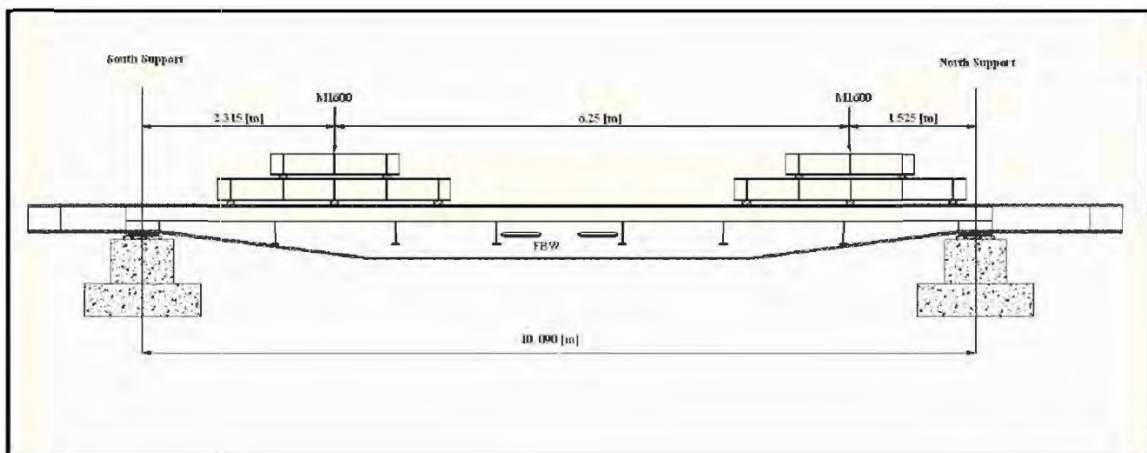


**Figure 2.4: M1600 load case (McDonald, 2011)**

Uniaxial strain gages and displacement transducers were installed at critical locations, such as locations with maximum bending. Strain gage rosettes were installed at locations of maximum shear. The goal was to understand the behavior of the center girder and edge beams before and after applying boundary constraints. The data acquisition

system only allowed 31 channels at a time; therefore, the experimental load tests were repeated to acquire the desired amount of data (McDonald, 2011).

### 2.3.2. Field Testing

As a part of the research study, a bridge was constructed from disused FBWs on a low-volume road in Queensland, Australia and performance field tested. The bridge consisted of two FBWs placed side-by-side and a reinforced concrete deck. The deck was made composite with the use of shear studs. Pairs of shear studs were placed longitudinally about every 6 inches. The midspan cross section of the bridge is shown in Figure 2.5. As shown, curbs were also utilized in this bridge system (Jamtsho & Dhanasekar, 2013).

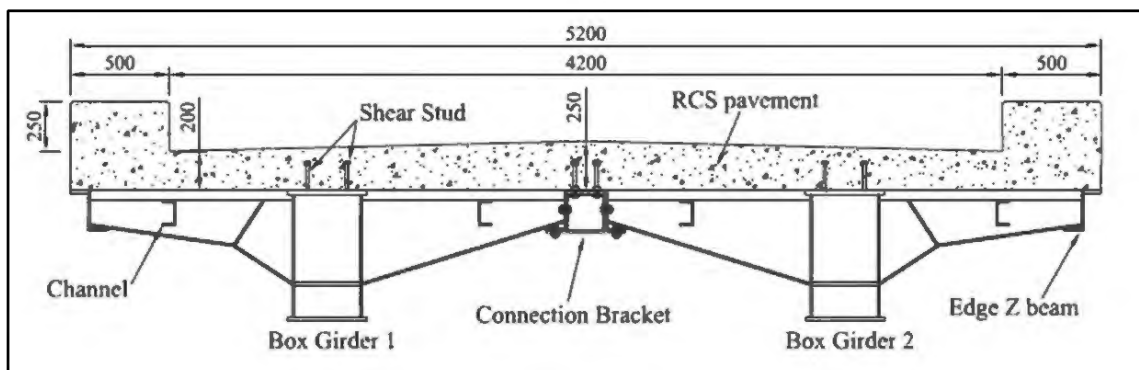


**Figure 2.5: FBW field bridge cross section at midspan, units in mm (Jamtsho & Dhanasekar, 2013)**

Load tests were performed using tandem trucks loaded with crushed rocks. The gross weight of the truck was about 51 kips. Two load positions were implemented: down the centerline of the bridge and offset about 2.5 feet from the centerline. The tests consisted of four different speeds: static, crawl, and two moving load tests. Strain gages and displacement transducers were used to measure the bridge behavior when loaded (Jamtsho & Dhanasekar, 2013).

### 2.3.3. Research Conclusions

Laboratory and field research was performed to assess the structural adequacy of flat bottom rail wagons used as low-volume road bridges. Both studies concluded that the FBW bridges tested were sufficient in resisting the Australian bridge design traffic loads (McDonald, 2011; Dhanasekar & Bayissa, 2011; Jamtsho & Dhanasekar, 2013). The following sections review the laboratory and field research conclusions.

#### 2.3.3.1. Laboratory Test Conclusions

The following were key conclusions made from the experimental testing and finite element analysis of the FBW laboratory bridge.

- Deflections caused by the M1600 serviceability loading were within specified standard limits. The bending and shear strains were below yield for this loading.
- Bending moments and shear forces in the FBW girders remained below capacity limits.
- The FBW sufficiently carried the applied loads without the need for additional structural members (Dhanasekar & Bayissa, 2011).

#### 2.3.3.2. Field Test Conclusions

The following were relevant conclusions made from field testing of a FBW bridge.

- The critical location of the M1600 load was offset from centerline, creating an eccentric load condition.
- Linear strain and deflection responses were observed and increased as the truck speed increased.
- Maximum deflections remained below the serviceability deflection limit.

- The maximum moment at midspan and the shear force near the supports with the ultimate load applied remained under the member capacities.
- The composite concrete deck increased the strength of the bridge and reduced the moment measured in the center girder (Jamtsho & Dhanasekar, 2013).

#### **2.4. Exploring Load-Path Redundancy in Bridges**

According to the *National Bridge Inspection Standards*, the definition of a fracture critical member is “a steel member in tension, or with a tension element, whose failure would probably cause a portion of or the entire bridge to collapse” (NBIS, 2012). The *AASHTO Manual for Bridge Evaluation* (2011) presents a similar definition. The definition of a fracture critical member in the *AASHTO LRFD Bridge Design Specifications* is a “component in tension whose failure is expected to result in the collapse of the bridge or the inability of the bridge to perform its function” (AASHTO, 2012). Previous research exploring after-fracture redundancy of a bridge system has shown that failure of a fracture critical member has not always lead to collapse. The bridges studied possessed adequate load-path redundancy that is not accounted for during evaluation. This section will introduce these research studies and their outcomes. It is noted that these studies also performed finite element analysis of the bridge systems; however, only experimental test results will be discussed due to the scope of this report.

##### **2.4.1. University of Texas**

Researchers at the University of Texas, in conjunction with the Texas Department of Transportation and the Federal Highway Administration, studied the redundancy of a full-scale steel twin box-girder bridge. This bridge type is considered a fracture critical bridge and is commonly seen throughout Texas. The bridge was decommissioned and rebuilt at the Ferguson Structural Engineering Laboratory for testing (Neuman, 2009).

A final fracture through the bottom flange that extended the full depth of the webs was induced in one of the girders at midspan. A truck load of 76 kips was applied to the

bridge at midspan where the fracture occurred. Although significant deflections and damage were observed, the bridge did not collapse. The bridge was then over-loaded to collapse in order to determine its ultimate load. The two girder bridge was able to resist a load four times its design load (Neuman, 2009).

#### **2.4.2. New Mexico State University**

Destructive field testing was performed on the I-40 bridges over the Rio Grande in Albuquerque, New Mexico in 1993, before being demolished by the state. The bridges were two girder steel bridges that were non-composite with the concrete deck. This bridge type is considered fracture critical. The study focused on three of the spans totaling 425 feet (Idriss et al., 1995).

A fracture was induced in the middle span of the three spans considered. The final damage was a 6 foot deep crack in one of the two 10 foot deep plate girders. The bridge was loaded to a truck static load of 82 kips. The strain gage results from the applied load, along with redistribution of dead load, indicated that the load was longitudinally redistributed through cantilever action to the supports. Elements such as the floor beams, lateral bracing system, and deck transferred the load to the non-fractured girder. No yielding was detected in the remaining elements and collapse of the fracture critical labeled bridge did not occur (Idriss et al., 1995).

#### **2.4.3. Purdue University**

Researchers at Purdue University were presented with an opportunity to perform destructive testing on April 25, 2012 on the northernmost approach span of the US-421 Bridge carrying traffic between Madison, IN and Milton, KY over the Ohio River. The approach span is considered a Pratt truss that was 149 feet long (Diggelmann, Connor, & Sherman, 2012).

The middle lower cord on the upstream side was chosen to fracture using controlled demolition. This member was a main chord and was classified as a fracture

critical member. A distributed live load totaling 145 kips was simulated using sand across the bridge. Strain gages were placed at critical locations to determine the behavior before and after fracture occurred. After fracture occurred, the bridge did not collapse and displayed system redundancy to adequately carry the redistributed dead load and applied live load (Diggelmann et al., 2012).

### **2.5. Spring Analogy to Predict Live Load Response of Girders**

Traditional methods of determining the live load response of girders are often conservative compared to detailed finite element analysis (FEA). The spring analogy was developed to more accurately predict the live load response of girders from the FEA using a simplified method. Traditionally, a bridge is analyzed as a beam line to determine maximum bending moment and shear values as a result of traffic design loads. The maximum values are multiplied by girder distribution factors (GDF) to distribute the load to individual girders in that cross section. The *AASHTO LRFD Bridge Design Specifications* (2012) provides equations and procedures for calculating the GDFs. This method was found to be conservative for several bridges studied (Akinci, Liu, & Bowman, 2013).

The spring analogy provides an alternative approach to determine the girder distribution factors used to calculate the member bending moments and transverse deflected shape, at a specific cross section. It is not intended to replace the GDF procedures currently in AASHTO; although results indicate a more accurate prediction of the live load distribution compared to those in AASHTO. This method can easily account for different size girders, different girder spacing, and even the effects of a standard Jersey type parapet (Akinci et al., 2013).

Researchers at Purdue University used four existing highway structures to aid in development of the spring analogy. Three of the four bridges were instrumented to collect live load response data. This data was used to calibrate three-dimensional finite element models of the specific bridges. The results of the spring analogy were then compared against those of the finite element modeling. A reasonable correlation between the field



instrumentation, finite element models, and spring analogy existed for the bridges studied (Akinci et al., 2013).

### 2.5.1. Spring Analogy Method

The bridge system in the spring analogy is idealized as a series of rotational springs connected by torsion bars for a specific bridge cross section. The rotational springs represent the bridge girders and the torsion bars represent the bridge deck. The truck load is divided into two applied moments located at the center of the truck wheels at a desired transverse location. The system is then analyzed (typically using structural analysis software) to determine the rotational reactions of the springs. These reactions are the girder distribution factors for the specific case. Figure 2.6 shows an example of the model set-up for an eight girder bridge (Akinci et al., 2013).

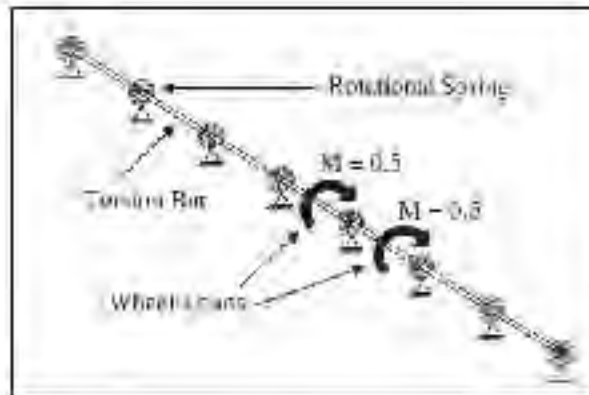


**Figure 2.6: Idealized model using the spring analogy method (Akinci et al, 2013)**

#### *Rotational springs*

The rotational springs are spaced equal to that of the bridge girders. Rotational stiffness values are assigned to each spring based on their relative flexural stiffness. For example, the interior girders may be assigned a rotational stiffness of unity. The rotational stiffness of the exterior girders is then set equal to the ratio of the moment of inertia of the exterior girder to the moment of inertia of the interior girder. This procedure can be easily adjusted to accommodate for composite sections and irregular shaped girders (Akinci et al., 2013).

### *Torsion bars*

The torsion bars represent the elements that assist in longitudinal distribution of the live load between girders (e.g., the bridge deck). It is important to adequately model the load distribution of the deck by assigning appropriate stiffness values to the torsion bars. Research found that the stiffness of a torsion bar depends on the girder spacing and span length. The stiffness of a torsion bar is made relative to the interior girder stiffness (Akinci et al., 2013).

### **2.5.2. Model Comparison**

The finite element models were calibrated using field instrumentation data from three of the four bridges studied in Indiana. Girder distribution factors were determined using the spring analogy for each bridge and compared to the results of the finite element analysis. The results of the spring analogy matched well with the FEA for the selection, as shown in Table 2.3 for the interior girders in the investigation. The results from the spring analogy were also compared to the equations provided in AASHTO to calculate girder distribution factors. As shown in the table, the AASHTO equations were conservative when compared to the FEA (Akinci et al., 2013).

**Table 2.3: Interior girder GDFs for bridges in study (Akinci et al., 2013)**

Bridge	GDF			GDF ratio	
	AASHTO Eqn.	FEA	Spring Analogy (SA)	$\frac{GDF_{AASHTO}}{GDF_{FEA}}$	$\frac{GDF_{SA}}{GDF_{FEA}}$
US-52	0.29	0.23	0.25	1.27	1.09
I-65 over Ridge Road	0.44	0.29	0.28	1.52	0.97
I-164	0.38	0.34	0.32	1.13	0.94
I-65 over US-30	0.41	0.3	0.31	1.36	1.03

Several other bridges analyzed by previous researchers were used to compare the spring analogy to the results of their finite element analysis. It was concluded that the spring analogy provided satisfactory results for steel and prestressed girder bridges when compared to FEA results (Akinci et al., 2013).

## 2.6. Summary

This literature review was intended to provide background on previous railroad flatcar bridge research, load redundancy studies performed, and an alternative approach in determining the distribution of live load in a slab-on-girder bridge system. The discussion on previous RRFC bridge research focused on a review of Phase I, and information pertaining to research conducted following the completion of Phase I.

After reviewing the literature on RRFCs being used as low-volume road solutions to replace deteriorating bridges, it was concluded that further studies were necessary to address existing concerns. The first concern relates to the ultimate strength of RRFCs being used as bridges. Through this research, laboratory testing of a RRFC bridge would allow larger loads to be applied and a greater number of instrumentation to be installed to determine the behavior of the RRFC bridge under these loads.

The second concern that remains is related to load-path redundancy of RRFC bridge systems. Due to the structural geometry of RRFCs, questions are raised as to whether or not these bridges should be labeled fracture critical. A controlled fracture of a full-scale RRFC bridge, including after-fracture load testing, has not been performed in the laboratory. This research would address this issue and provide guidance to assess the load-path redundancy in a RRFC bridge system.

## CHAPTER 3. SELECTION OF RAILROAD FLATCARS

In order to complete the laboratory study, two identical railroad flatcars were needed to construct a full-scale bridge. The purpose of this chapter is to describe the steps of the selection process. First, selection criteria were developed based on previous research. The criteria are briefly explained, along with the desired RRFC configuration for this research. Next, an extensive search for the desired type and length of flatcar was conducted. Finally, RRFCs were purchased and delivered to the laboratory. A description of the geometry and condition of the RRFCs selected is provided.

### 3.1. Selection Criteria

The following sections describe the criteria considered when selecting the flatcars used for laboratory testing. Several parameters were based on the information presented in the *Proposed Guidelines for Acquiring Railroad Flatcars to be Used as Low-Volume Road Bridges* from Phase I (Provines et al., 2011).

#### 3.1.1. Geometry

RRFCs come in a variety of lengths, widths, and cross sections. During the purchasing process, it was important to understand these differences and create a set of geometric selection criteria to pursue. The following sections briefly describe the different geometries of flatcars and the desired configuration for this research.

##### 3.1.1.1. “Car Haulers” vs. Traditional RRFCs

Traditional flatcars are railcars with an open deck, compared to “car haulers” and boxcars that are enclosed with sides and a roof. “Car haulers” and boxcars are not recommended to be used as low-volume road bridges. Field testing conducted in Phase I demonstrated that these types of railcars did not perform as well as traditional RRFCs.

The boxcar bridge previously field tested had larger deflections under controlled loading compared to the traditional RRFC bridges. One reason for this behavior was that the main girders on the boxcars were smaller and less stiff (Provines et al., 2011). As a result of these findings, traditional RRFCs were desirable for this research.

#### *3.1.1.2. Length*

RRFCs are constructed in out-to-out lengths of approximately 56 or 89 feet (span lengths are recommended to be wheel truck to wheel truck). According to the results of the Indiana inventory of RRFC bridges conducted in Phase I, the majority of bridges were constructed with 89 feet long flatcars (Provines et al., 2011). A flatcar length of 89 feet was desired for this research in order to correspond with the lengths found in the field.

#### *3.1.1.3. Width*

RRFCs range in widths between 8 to 10 feet. For field application, the appropriate flatcar width should be chosen based on the desired driving width of the bridge. Using narrower RRFCs may require a greater number of flatcars or a wider longitudinal connection (Provines et al., 2011).

#### *3.1.1.4. Cross Section*

The flatcar cross section that performed well during Phase I field testing contained one large main girder and two shallower exterior girders on each side of the main girder. This system also includes smaller stringers in the longitudinal direction and transverse floor beams. For bridge application, the exterior girders should be able to create a proper longitudinal connection between the adjacent flatcars (Provines et al., 2011). This configuration was pursued for laboratory testing.

#### *3.1.1.5. Connections*

The member elements of RRFCs are connected by rivets or welds. Studies at Iowa State University advised that RRFCs with welds, rather than rivets, be used for low-volume road bridges. Repeated loading or corrosion can cause strength loss in rivets

(Wipf et. al. 2003). Therefore, RRFCs with welded connections were desired for laboratory testing.

#### *3.1.1.6. Number of RRFCs*

RRFCs bridges typically have two or three flatcars placed side-by-side in order to achieve an adequate driving width. A greater number of RRFC bridges in Indiana were constructed with two RRFCs placed in the transverse direction; therefore, the purchase of two RRFCs was desired for this research. It was also recommended that the flatcars used in a bridge system have similar vertical cambers or longitudinal profiles for ease in construction and to provide a smoother driving surface (Provines et al., 2011).

#### **3.1.2. Condition**

A thorough inspection of the condition of the RRFCs was conducted prior to purchasing. First, the main girder was visually inspected for damage, such as corrosion and cracking. Second, the RRFC was inspected for any overall damage, including member straightness, cracks, corrosion, and any missing members. Third, it was important to note if the RRFC deck was a suitable surface for loading during research (Provines et al., 2011). The results of the condition inspection are described in Section 3.2.3.

### **3.2. Final Selection**

After discussion with several railcar vendors, two RRFCs were selected for laboratory testing. Specifics about the selection are described in the following sections.

#### **3.2.1. Specimen Acquisition**

Two identical RRFCs were purchased from Rick Franklin Corporation (RFC) in Lebanon, Oregon. Considering the selection criteria, availability, and research budget, the RRFCs provided by Rick Franklin Corporation were deemed the best option. Figure 3.1 shows the delivery of one of the two RRFCs to the laboratory. The flatcars were purchased for \$12,000 each plus a shipping cost of \$6,150 each.



**Figure 3.1: RRFC delivery to Bowen Laboratory**

### **3.2.2. Geometry**

The geometry of the flatcars was an important aspect in selecting adequate RRFCs for this research. Due to laboratory space restrictions and budget limitations, it was not feasible to purchase RRFCs that were 89 feet long. Therefore, shorter flatcars measuring approximately 56 feet in length were obtained. Each flatcar was 9 feet – 4 ¼ inches wide.

The cross section resembled a traditional RRFC; each flatcar consisted of one deep main box girder and two shallower exterior girders made from channel sections. The deep main box girder tapers near the quarter points of the flatcar into a shallower section near the supports. The other longitudinal components in this system were the small stringers. Four I-beam stringers were located on either side of the main girder. These stringers rested on the transverse members, which varied in shape and size throughout the car. Photographs of the RRFCs are shown in Figure 3.2. All connections in the RRFCs were welded and contained no rivets. Detailed dimensions of the RRFCs can be found in Appendix A.

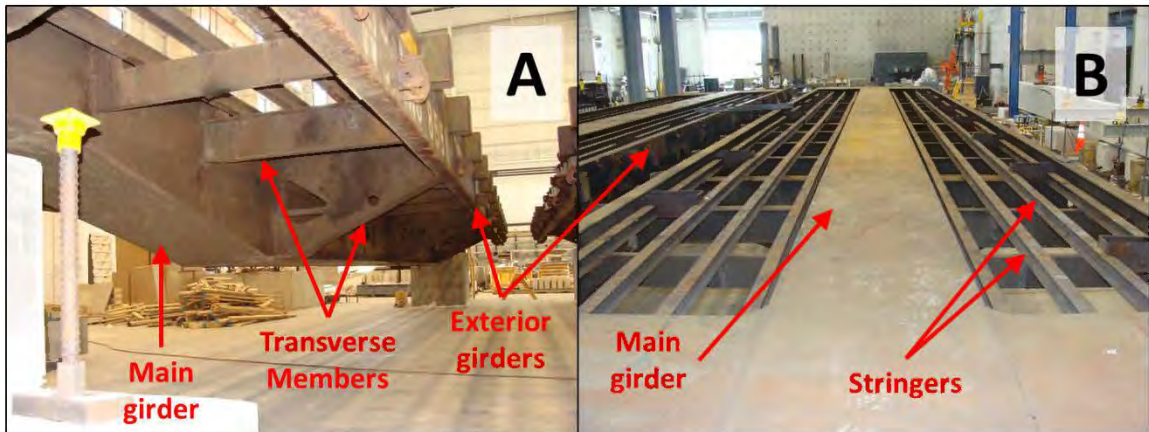


**Figure 3.2: RRFC members from underneath (A) & members from top (B) as erected in the laboratory**

### **3.2.3. Condition**

Due to the location of Rick Franklin Corporation with respect to Purdue University, Dr. Christopher Higgins from Oregon State University aided in the inspection process. Dr. Higgins was provided with the *Proposed Guidelines for Acquiring Railroad Flatcars to be Used as Low-Volume Road Bridges* from Phase I to adequately inspect the RRFCs. Since the geometry was determined acceptable before the visit, Dr. Higgins focused his inspection on the condition of the flatcars.

The condition of the RRFCs was overall satisfactory, with only minor damage found. There were a few areas on the transverse members with local burn-through from removal of the auxiliary equipment during its decommissioning (Figure 3.3). The RRFC members were straight, and there was no significant corrosion.





**Figure 3.3: Local burn-through on bottom flange of a transverse member**

Additionally, it was noted that the original wood plank decking was removed from the flatcars. Therefore, a sufficient deck needed to be constructed atop the steel members. This was not a significant disadvantage to the research due to the planned construction of a timber deck, followed by a concrete deck.

#### **3.2.4. History of RRFCs Selected for Research**

Stenciled markings on the exterior girders provided information about the design loading and history of the RRFCs. As shown in Figure 3.4, the visible stencils were the load limit, light weight, type of flatcar, and date built. The load limit of 162,300 pounds (LD LMT 162300) is the maximum weight of the cargo. The light weight of 57,700 pounds (LT WT 57700) is the total weight of the unloaded flatcar, including trucks and all accessories (e.g., brake lines, etc). As shown in Figure 3.4A, the markings were difficult to read due to the modification on the exterior girder. These were bulkhead type flatcar and were built in October 1978 (FB BLT 10-78) (AAR 2007). Bulkhead flatcars contain ends that prevent cargo from sliding out. These ends were removed prior to shipping to Purdue University.

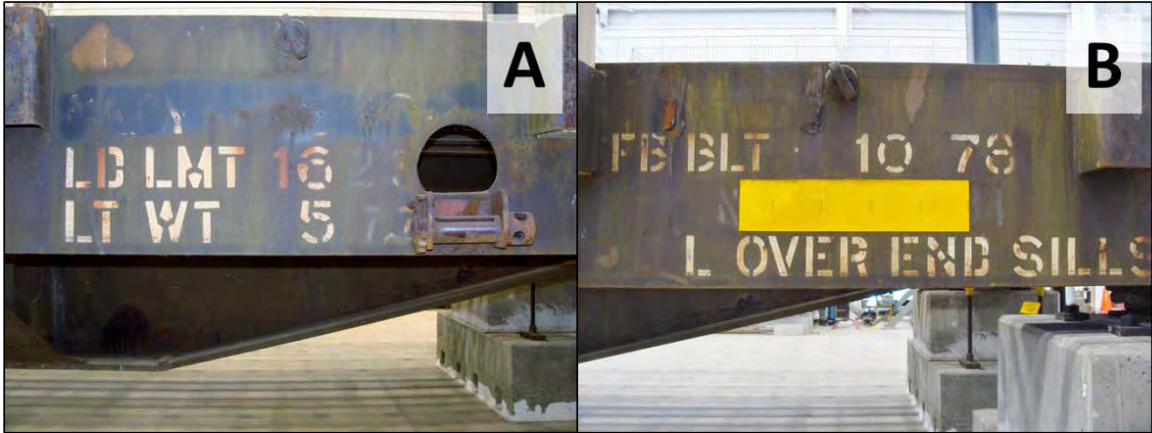


**Figure 3.4: Visible stenciled markings, load limit and light weight (A) & type of flatcar and date built (B)**

## CHAPTER 4. INSTRUMENTATION & EQUIPMENT

Instrumentation included uniaxial and rectangular rosette strain gages, displacement sensors, load cells, and thermocouples. Additional equipment to aid in load testing and data collection included a hydraulic cylinder and a data acquisition system. The following sections further explain the instrumentation and equipment.

### 4.1. Uniaxial Strain Gages

The uniaxial strain gages installed were Vishay Micro-Measurements model CEA-06-250UN-350/P2, with an active grid length of 0.25 inches and a resistance of 350 ohms. Lead wires were attached to the strain gages by the manufacturer.

A series of steps were followed to properly install the strain gages. First, the desired location of installation on the member was ground to the base metal and sanded using a variety of grit sand paper. Then, the location was cleaned using degreaser, conditioner, and neutralizer. Finally, the strain gage was attached using a bonding adhesive and covered with a general purpose coating. All products used in the installation of strain gages were produced by Vishay Micro-Measurements. Figure 4.1 shows a typical strain gage installed on the top of a longitudinal stringer.

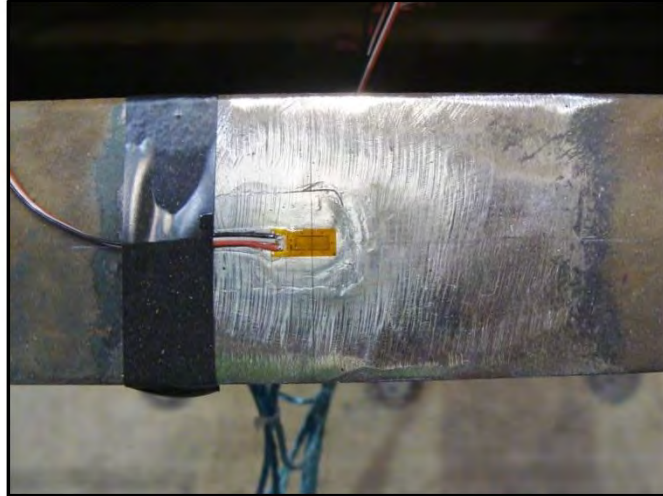


**Figure 4.1: Example of a uniaxial strain gage after installation**

#### **4.1.1. Location of Uniaxial Strain Gages**

A total of 94 uniaxial strain gages were installed on the RRFC bridge; 62 of the gages were installed on one RRFC (labeled the “East RRFC”) and 32 of the gages were installed on the second RRFC (labeled the “West RRFC”). Figure 4.2 shows the placement of the RRFCs in the laboratory with their referenced labels. The East RRFC was more heavily instrumented to determine if there was symmetrical behavior within the single RRFC and to better quantify the load distribution within a given car. All strain gage locations on the West RRFC matched with those on the East RRFC to determine if the RRFCs behaved the same when loaded individually. This allowed for direct comparison of data from different load tests of the identical RRFCs.



**Figure 4.2: Placement of RRFCs in laboratory**

The main focus during load testing was to determine the stress values within the longitudinal members. Therefore, strain gages were placed on the main girders, exterior girders, and stringers. Additionally, two strain gages were installed on the transverse floor beam at midspan. At each instrumented cross section, strain gages were installed at locations where stresses were expected to be the greatest. Thus, strain gages were located on the top and bottom flanges of the members. The strain gages on the top flanges of the main girders and exterior girders were placed on the bottom of the top flange, to accommodate the construction of the timber and concrete decks.

Five cross sections on the East RRFC and three cross sections on the West RRFC were selected for instrumentation. These cross sections were located near midspan, and on either side of the tapered sections of the main girder. It is important to mention that the location of the applied load during testing was at midspan; therefore, the midspan cross section of strain gages was offset 1 foot – 7 ½ inches from exact midspan to avoid local effects and damage from the load spreader beam. The cross sections near the tapered section of the main girder allowed for a better understanding of the load distribution within the RRFC when approaching the supports. Detailed instrumentation plans that show the exact location of all strain gages can be found in Appendix B.

## 4.2. Rectangular Rosette Strain Gages

In order to develop load rating guidelines based on shear, rectangular rosette strain gages were used to determine shear values at desired locations. The rosettes applied were Vishay Micro-Measurements model CEA-06-250UR-350 (Figure 4.3). These rectangular rosettes were single plane rosettes and contained three elements oriented at 45 degrees with respect to each other. Similar to the uniaxial strain gages, each element of a single rosette had a resistance of 350 ohms and a gage length of 0.25 inches.

The rosettes did not contain lead wires attached by the manufacturer; therefore, lead wires were soldered onto the provided solder tabs at the laboratory. The installation procedure for the rectangular rosette strain gages followed that of the uniaxial strain gages.

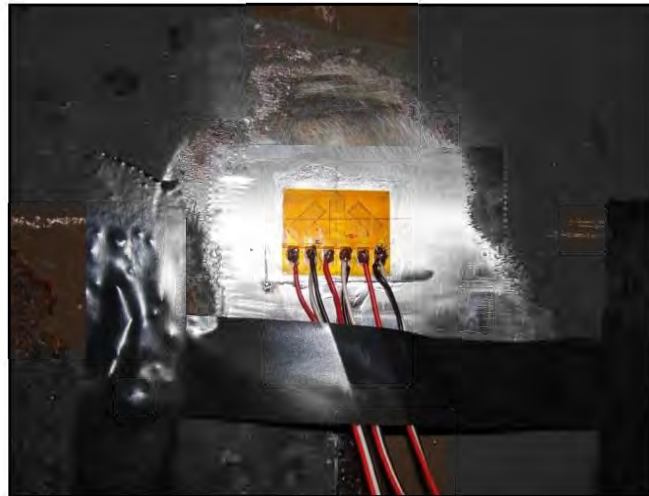


**Figure 4.3: Example of installed rectangular rosette strain gage**

### 4.2.1. Location of Rectangular Rosette Strain Gages

Rosettes were installed on the East RRFC near the bridge supports, where the shear values are the greatest. Rosettes were not installed directly at the support due to access. The two cross sections containing rosettes were located within the tapered section of the main girder, about 6 feet from the support, and at the shallow section of the main girder, about 2 feet from the support. At the two cross sections, a rosette was installed at

mid-depth on the webs of the main girder and exterior girders. There were a total of eight rosettes on the RRFC bridge. Detailed instrumentation plans that show the exact location of each rectangular rosette strain gage can be found in Appendix B.

### 4.3. Displacement Sensors

Displacement sensors were used at various locations to determine local deflections. Two different types of displacement sensors were used on the RRFC bridge. The first type were BEI Duncan Linear Motion Position Sensors (Figure 4.4A). These sensors have a 1 inch stroke and worked well within areas of limited space, such as at the supports. The second type of displacement sensors were UniMeasure PA Series position transducers (string potentiometers) with a 20 inch stroke (Figure 4.4B).

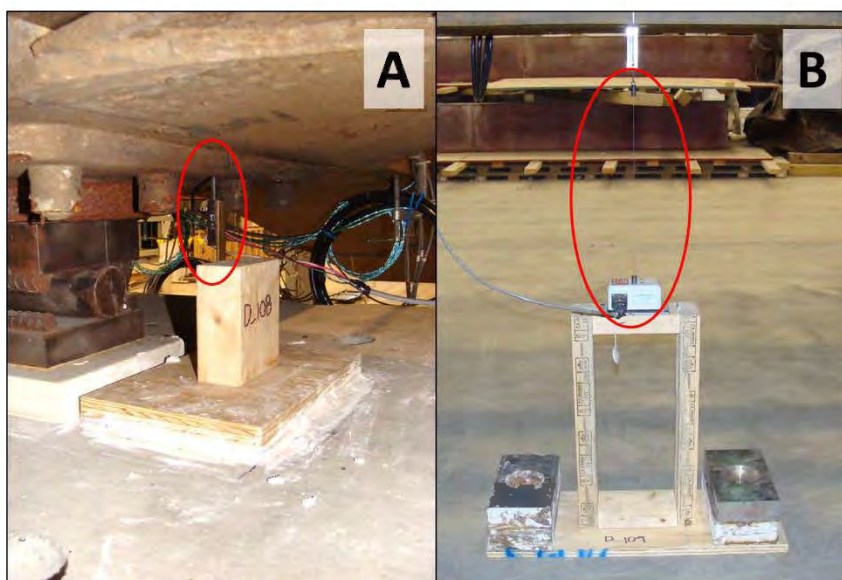


**Figure 4.4: Linear motion position sensor near support (A) & position transducer attached to a main girder (B)**

#### 4.3.1. Location of Displacement Sensors

Initially, displacement sensors were placed on the main girder at midspan, at the quarter points, and near the supports on each RRFC. A total of five displacement sensors were used on each RRFC. Recording the displacement at midspan allowed for the maximum deflections to be obtained when the load was applied at midspan. Placing

displacement sensors at the quarter points of each main girder helped to determine if there was symmetric behavior within the RRFC. Finally, displacement sensors at the supports were used to measure any settlement or uplift at this location.

The displacement sensor layout was modified throughout testing the RRFC bridge with the concrete deck. Displacement sensors at the quarter points were moved to the exterior girders at midspan and at the supports. These locations allowed comparison between the deflection of the main girder and exterior girders to better understand the behavior of the two RRFCs working as a system. The locations of the displacement sensors during each load test are provided in Appendix B.

#### **4.4. Load Cell**

Two different load cells were used throughout the laboratory testing of the RRFC bridge. The first load cell was a Honeywell Model 3156 with a capacity of 150 kips (Figure 4.5). This model was used when loading the bridge with no deck and with a timber deck. The second load cell was a Honeywell Model 3129 with a capacity of 300 kips. This model was used when loading the bridge with a concrete deck. The added capacity of the 300 kip load cell allowed for larger loads to be applied, which was necessary due to the increased stiffness of the bridge after the addition of the concrete deck.

#### **4.5. Hydraulic Cylinder**

An Enerpac RR series, double-acting hydraulic cylinder was used to apply load onto the RRFC bridge, as shown in Figure 4.5. The model used had a 6 inch stroke and 150 ton (300 kip) capacity. This specific hydraulic cylinder was chosen due to its capacity and availability in the laboratory. The location of the hydraulic cylinder varied throughout testing, depending on the desired location of the applied load.



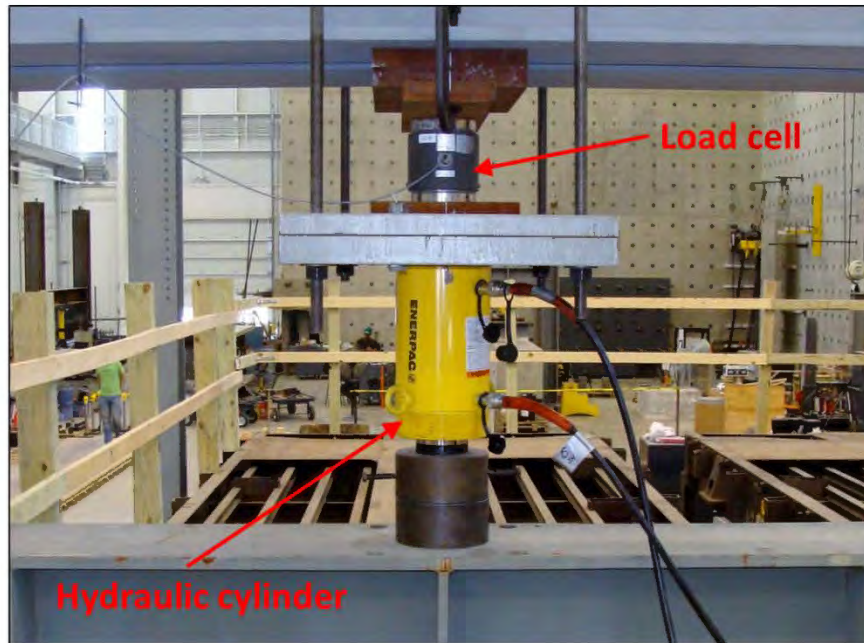


**Figure 4.5: Test set-up containing the load cell and hydraulic cylinder**

#### **4.6. Data Acquisition**

A Campbell Scientific CR9000X 16-bit data logger was used to collect the load, stress, and deflection data. This type of data logger provided the space and adequate capacity needed given the amount of instrumentation installed on the RRFC bridge. Along with the CR9000X data logger, two voltage supplies were used to excite each type of instrumentation and power the data logger. The voltage output varied depending on the type of instrumentation. All strain gages and load cells were excited with 10 volts. The displacement sensors were excited with 5 volts.

#### **4.7. Thermocouples**

Thermocouples were only used during the final fracture tests in order to monitor the temperature during the cooling process (see Section 5.6. ). Temperature data was collected using a Campbell Scientific CR5000 data logger. As shown in Figure 4.6, three thermocouples were used for the fracture tests. All thermocouples were installed on the main girder at Section C, 1 foot – 7 ½ inches north of midspan. The first thermocouple was located on the surface of the outside of one web (Figure 4.6A). The second

thermocouple was located inside a  $\frac{3}{4}$  inch deep hole drilled into the outside edge of the bottom flange (Figure 4.6A). The third thermocouple was installed on the top surface of the bottom flange inside the main box girder (Figure 4.6B).

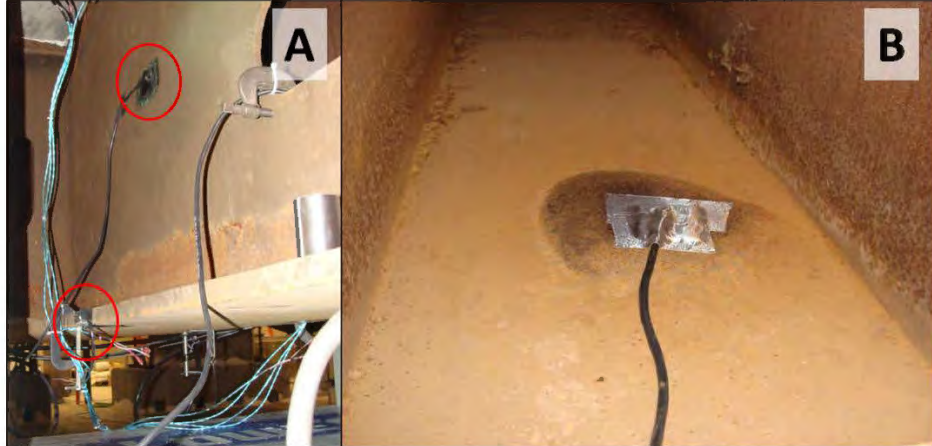


**Figure 4.6: Thermocouples installed on the outside of the main girder (A) & on the inside of the main girder (B)**

## CHAPTER 5. EXPERIMENTAL CONFIGURATIONS AND PROCEDURES

A full-scale RRFC bridge was constructed and subjected to several loading conditions in the laboratory. Testing in the laboratory created the opportunity to apply larger controlled loads and to more heavily instrument the bridge, compared to what is practical in the field. The load tests were conducted to address the research objectives mentioned in Section 1.2. This chapter describes the RRFC bridge set-up and the different experimental load tests performed in the laboratory. The results of the load tests are presented in later chapters.

### 5.1. Railroad Flatcar Bridge Overview

The RRFCs were built as a simply-supported, single-span bridge, with a span length of 47 feet – 4  $\frac{3}{4}$  inches and a total bridge width of 21 feet – 4  $\frac{3}{4}$  inches. The width included the two 9 feet – 4  $\frac{1}{4}$  inch wide RRFCs transversely spaced 12 feet on center, creating a 2 feet – 8  $\frac{1}{4}$  inch gap between the flatcars. As shown Figure 5.1, pin and roller supports placed on concrete blocks were used to simulate simply-supported conditions. Each RRFC had one pin support at the North end and one roller support at the South end. The supports were located at the RRFC wheel truck locations, as recommended in Phase I (Provines et al., 2011).



**Figure 5.1: Roller support (A) & pin support (B) at wheel truck locations**

## **5.2. Load Tests**

Several controlled load tests were performed on the RRFC bridge to aid in understanding the load distribution and the carrying capacity of the bridge system. The details about each load test are summarized in Table 5.1. The “single patch load” in the load configuration column refers to a load contact surface that was 24 inches (wide) by 16 inches (long). The dimensions of this load configuration were based on the width of the main girder flange and the width of the load spreader beam flange. The “axle load” was used to simulate a truck axle and refers to two wheel patch loads, each 20 inches (wide) by 10 inches (long), with a center-to-center spacing of 6 feet. These dimensions were based on the AASTHO tire contact area defined for the design truck (AASHTO 2012). The two patch loads used during Test 9 were each 6 inches (wide) by 14 inches (long) and placed in line with the centroids of the adjacent exterior girders on each RRFC.

The load was slowly applied in increments of 25 to 50 kips until the desired maximum load was reached. All load tests were repeated three or more times for each load configuration to ensure consistency of the data, with the exception of final load tests conducted during fracture simulation. The individual load tests and corresponding bridge decks are explained in more detail in the following sections.

**Table 5.1: RRFC bridge load tests**

Test	Load Location	Load Configuration	Maximum Load (kips)	Deck Type	Connection Between RRFCs
Test 1	Main girder of East RRFC Midspan	Single patch load	150	No deck	No connection
Test 2	Main girder of West RRFC Midspan	Single patch load	150	No deck	No connection
Test 3	Main girder of East RRFC Midspan	Single patch load	150	Timber deck	No connection
Test 4	Centered over East RRFC Midspan	Axle load	75	Timber deck	No connection
Test 5	Main girder of East RRFC Midspan	Single patch load	225	Concrete deck	Composite concrete deck
Test 6	Centered over East RRFC Midspan	Axle load	225	Concrete deck	Composite concrete deck
Test 7	Main girder of West RRFC Midspan	Single patch load	225	Concrete deck	Composite concrete deck
Test 8	Centered over West RRFC Midspan	Axle load	225	Concrete deck	Composite concrete deck
Test 9	Centered over bridge width Midspan	2 patch loads centered over exterior girders	225	Concrete deck	Composite concrete deck
Test 10	Centered over bridge width Midspan	Axle load	225	Concrete deck	Composite concrete deck
Test 11	Main girder of East RRFC 14' south of midspan	Single patch load	225	Concrete deck	Composite concrete deck
Test 12	Main girder of West RRFC 14' south of midspan	Single patch load	225	Concrete deck	Composite concrete deck
Fracture Test 1	Main girder of East RRFC Midspan	Single patch load	150 (after fracture)	Concrete deck	Composite concrete deck
Fracture Test 2	Main girder of West RRFC Midspan	Single patch load	190 (after fracture)	Concrete deck	Composite concrete deck

### 5.3. No Bridge Deck

The first two load tests were conducted with no deck and no connection between the adjacent RRFCs. This permitted each flatcar to be tested individually. Figure 5.2 offers a simplified drawing of the load set-up for these tests. Test 1 was conducted at midspan of the East RRFC with a single patch load located on the main girder (i.e., only the main girder was in contact with the spreader beam). An identical procedure was used on the West RRFC for Test 2 in order to directly compare the data and determine if the two RRFCs display the same behavior under applied load. These tests also allowed for a better understanding of the distribution of load within a single RRFC. Each test set-up is also shown in Figure 5.3.

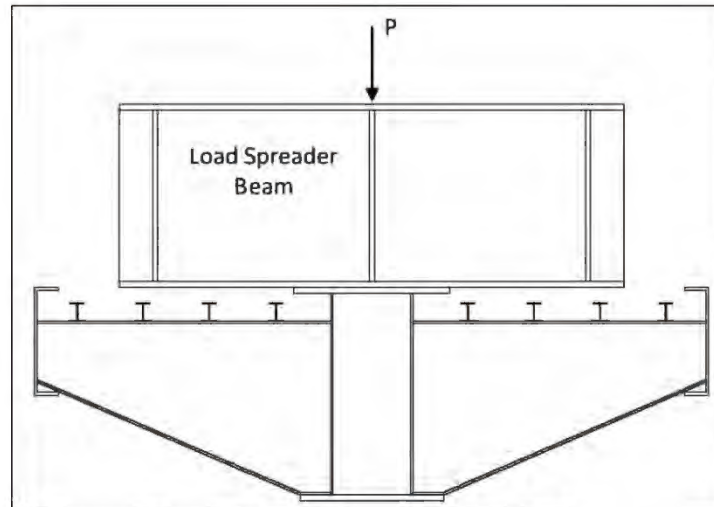


**Figure 5.2: Test 1 & Test 2 load set-up**

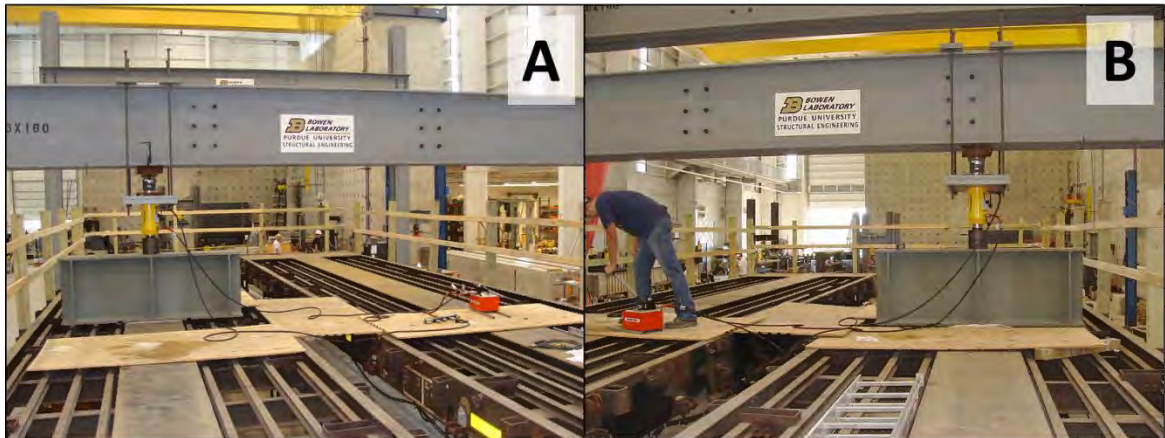


**Figure 5.3: Test 1 on East RRFC (A) & Test 2 on West RRFC (B)**

#### **5.4. Timber Deck Patch**

Timber decks are commonly used on RRFC bridges. (Provines et al., 2011). Therefore, a patch of timber decking was assembled on the East RRFC to determine the amount of load distribution it would provide. The following sections discuss the timber deck design, cost estimate, and load tests performed in the laboratory.

#### 5.4.1. Timber Deck Design

Three sizes of marine treated pine were used for the timber deck. 4x4's were cut and placed atop the stringers to support transverse 3x8's, and 2x8's were placed longitudinally on top of the 3x8's for a "driving" surface. A detailed drawing of the timber deck design can be found in Appendix C. Bridge cleats were used to secure the 3x8's to the top flanges of the main girder and exterior girders and wood screws were used to secure the individual layers of timber together. The bridge cleats can be seen in Figure 5.4. This design closely reflected the timber deck design on a RRFC bridge in Fountain County, Indiana (Peevler, 2013).

The timber deck did not extend the entire span length or width of the RRFC bridge since timber decks are known to provide only limited load distribution within a flatcar away from the applied load. Further, timber decks also provide relatively little load transfer between flatcars (Provines et al., 2011). The load distribution provided by the timber deck within the East RRFC could be determined by comparing the response with the deck to the load tests performed with no deck. The timber deck extended an arbitrary distance of 5 feet from either direction of midspan, providing a patch of timber decking that was 10 feet long and the width of one RRFC. The completed timber deck patch is shown in Figure 5.4.

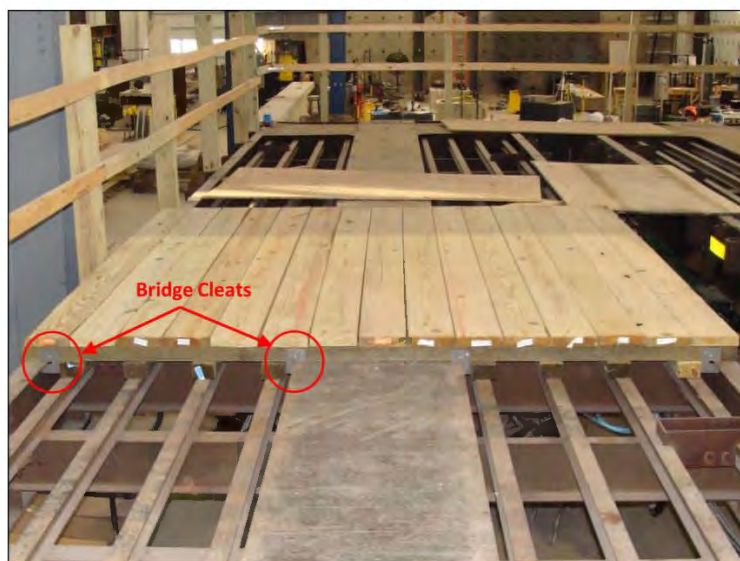


**Figure 5.4: Completed timber deck patch**

#### 5.4.2. Timber Deck Cost Estimate

Cost consideration plays a large role when counties determine what type of bridge deck to use. Table 5.2 shows the estimated costs for the timber deck constructed in the laboratory. It is important to note that these costs do not include labor, and they are estimated based on the timber deck patch constructed. An extrapolated supply cost for the entire bridge deck (both RRFCs) was calculated to be about \$12,700.

**Table 5.2: Cost estimate for timber deck patch**

COST ESTIMATE	
Supplies	Amount (\$)
Timber	790.00
Bridge Cleats	120.00
Wood Screws	50.00
<b>TOTAL</b>	<b>960.00</b>

#### 5.4.3. Load Tests with Timber Deck

As shown previously in Table 5.1, two load tests were performed with the timber deck on the East RRFC. Test 3 was conducted with a single patch load directly over the main girder, identical to Test 1 with no deck. The similar tests allowed for direct



comparison of data to determine if the timber deck played a significant load-distributing role. Test 4 was performed with an axle load to simulate a wheel truck axle. The data from this test provided information about the behavior of the RRFC when the applied load was not directed into the main girder. The load configurations for Test 3 and Test 4 are shown in Figure 5.5 and Figure 5.6.

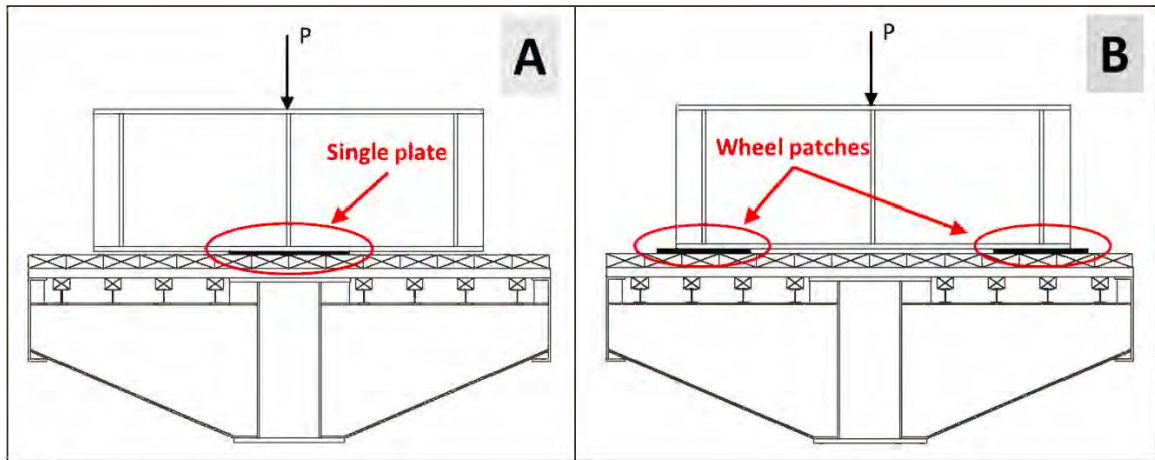


Figure 5.5: Test 3 (A) & Test 4 (B) load set-up

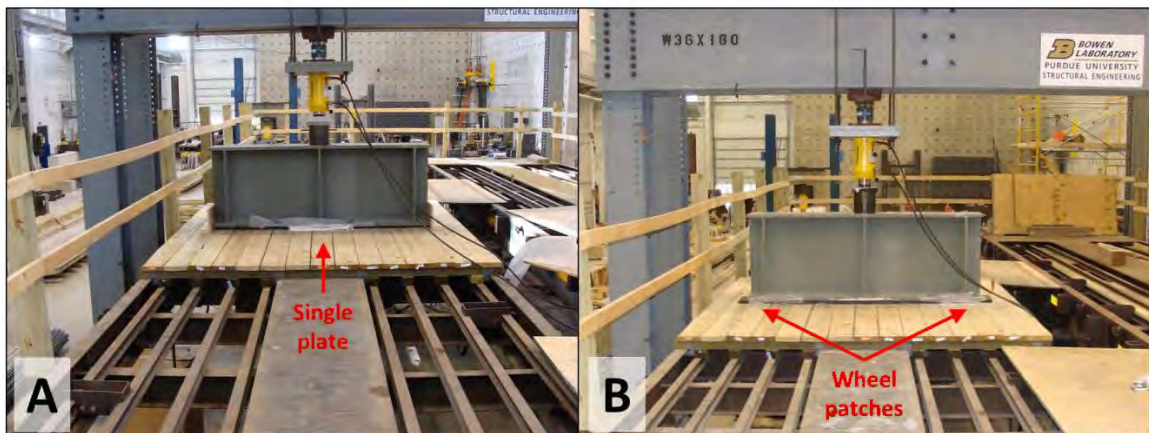


Figure 5.6: Test 3 (A) & Test 4 (B) with timber deck patch

### 5.5. Concrete Bridge Deck

Though less common, reinforced concrete decks are sometimes used as RRFC bridge decks (Provines et al., 2011). The stiffness of a concrete deck provides better load distribution than most other common alternatives. The following sections discuss the

concrete deck design, the concrete deck cost estimate, and the multiple load tests performed with the concrete bridge deck.

### **5.5.1. Concrete Deck Design**

The objective was to utilize a simple design that also provided adequate load carrying capacity and distributed load throughout and between the RRFCs. The following sections explain the components that were needed in order to sufficiently design and construct a fully composite concrete deck for the RRFC bridge.

#### *5.5.1.1. Formwork*

Removable formwork was built from plywood for the RRFC concrete bridge deck, as shown in Figure 5.7. Requiring removable formwork allowed the ability to inspect the bottom of the concrete deck during experimental load testing, in particular following the fracture simulation test when some damage was expected. The formwork was also constructed such that the top flange of the main girders, exterior girders and stringers were encased in concrete. This construction method achieved greater composite action between the RRFC steel and concrete deck. Therefore, the concrete deck thickness was 6.5 inches over the main girders, exterior girders, and between the RRFCs, and 9 inches over the stringers, as they were about 2.5 inches below the main girder. This formwork construction was time consuming and labor intensive; therefore, more simplified and typical forming techniques are recommended for actual field applications.



**Figure 5.7: Completed formwork construction & shear stud installation**

#### 5.5.1.2. Shear Connectors

Shear connectors were used to ensure composite action between the steel structure of the RRFCs and the concrete deck (i.e., to make the steel components and concrete deck act as one system). The design for the shear connectors was based on the *AASHTO LRFD Bridge Design Specifications* (2012) and installed using the procedures of the *Bridge Welding Code* (2010). Each RRFC had 296 shear connectors (Figure 5.7). All shear connectors installed were 3 inches long with a 0.75 inch diameter from Nelson Stud Welding (model S3L 3/4 x 3 3/16). A pitch of 6 inches was used for the pairs of shear connectors on the main girders. Single shear connectors were installed on all exterior girders with a pitch of 12 inches. Detailed shear connector plans can be found in Appendix C.

#### 5.5.1.3. Steel Reinforcement

Steel reinforcement for the concrete deck was designed according to the *AASHTO LRFD Bridge Design Specifications* (2012). The longitudinal reinforcement consisted of #5 bars spaced at 12 inches on the top and bottom layers. The transverse reinforcement consisted of #5 bars spaced at 10 inches on the top and bottom layers. Epoxy bars were

not used due to the controlled laboratory environment. Only 1 inch of cover was used for the top layer of rebar. This was done to simulate the potential “worst case” conditions that may occur during field construction. The bottom concrete cover in the areas with a 6.5 inch deck thickness was 1 inch, and the bottom cover was 3.5 inches where the deck was 9 inches thick. Steel reinforcement extended the entire length and width of the RRFC bridge, with a 1 inch cover at all edges. Figure 5.8 shows the RRFC bridge after installing the steel reinforcement.



**Figure 5.8: RRFC bridge after installing steel reinforcement**

#### *5.5.1.4. Concrete Type*

Indiana Department of Transportation (INDOT) Class C concrete was used for the RRFC bridge deck. This type of concrete mix is typically used for bridge decks in Indiana (Shubert 2013). A total of 34 cubic yards of concrete (four concrete trucks) was required for the bridge deck. As shown in Figure 5.9, a concrete pump truck was used to pour the concrete onto the bridge. The concrete deck was water cured for 7 days. Concrete cylinders were made and tested for each of the four concrete trucks; Table 5.3 shows the concrete compressive strengths measured during these tests.



**Figure 5.9: RRFC bridge concrete deck pour**

**Table 5.3: Concrete compressive strength for RRFC bridge deck**

Concrete Compressive Strength (psi)		
	7 Days	28 Days
Truck 1	4660	5810
Truck 2	4690	5750
Truck 3	4490	5600
Truck 4	4760	5760

### 5.5.2. Concrete Deck Cost Estimate

The estimated concrete deck costs were less expensive than the extrapolated cost estimate for the timber deck. As shown in Table 5.4, the total cost of supplies to construct the concrete deck in the laboratory was just under \$9,300. Construction time to install the shear connectors, rebar, and concrete was approximately three days. Constructing the research-necessary formwork was time consuming; however, faster and more efficient formwork construction methods are available that will not affect the behavior of the bridge system.

**Table 5.4: Cost estimate for concrete deck**

<b>COST ESTIMATE</b>	
<b>Supply</b>	<b>Amount (\$)</b>
Formwork - plywood	979.00
Shear Studs	487.50
Rebar, chairs, ties, twistors	3402.50
Concrete	4321.50
Burlap	100.00
<b>TOTAL</b>	<b>9290.50</b>

### **5.5.3. Load Tests with Composite Concrete Deck**

A total of eight load tests were conducted on the RRFC bridge with the composite concrete bridge deck, as shown previously in Table 5.1. These loads were conducted in order to determine the load distribution within and between the RRFCs. The following sections further discuss these load tests.

#### *5.5.3.1. Single Patch Load Tests*

Load tests using the same single patch load allowed for simple and direct comparison of the data without a deck and with a fully composite concrete deck. These tests differed from the tests without a deck by having the two flatcars joined creating a bridge system; however, the load distribution within a flatcar could still be evaluated. Identical tests were performed on the East RRFC and West RRFC to determine if the two RRFCs displayed similar behavior with the addition of the concrete deck. Figure 5.10 shows a simplified drawing of Test 5 and Test 7 on the East RRFC and West RRFC, respectively. Figure 5.11 shows the actual test set-ups on the RRFC bridge. Note that Figure 5.10 is oriented looking south to remain consistent with Figure 5.11 (the instrumentation plans in Appendix B are oriented looking north).

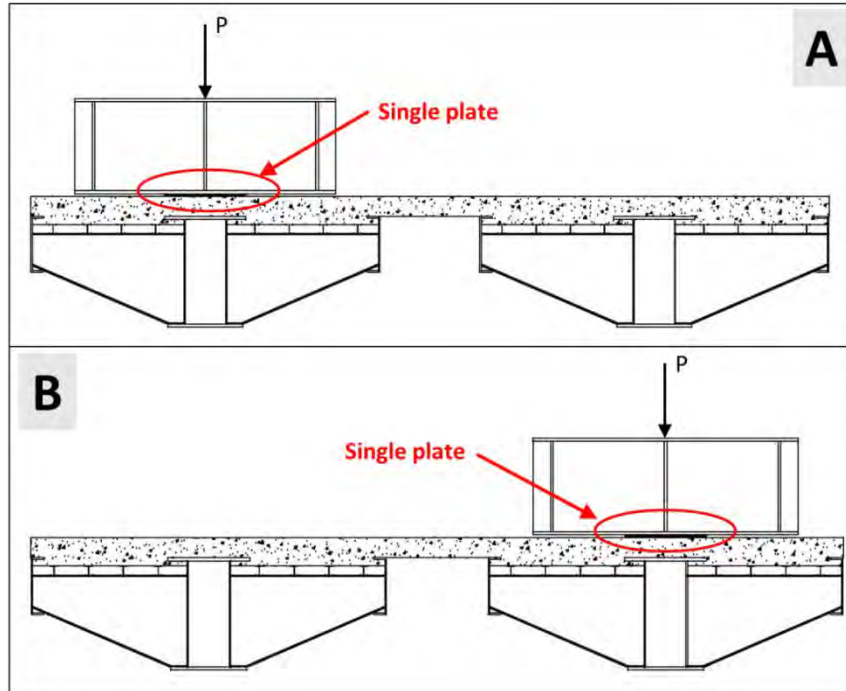


**Figure 5.10: Test 5 (A) & Test 7 (B) load set-up at midspan (looking south)**

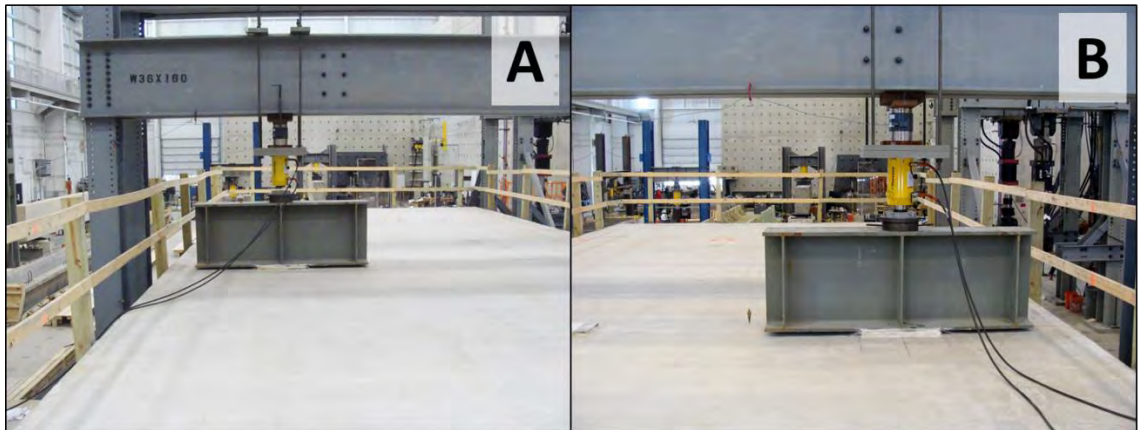


**Figure 5.11: Test 5 (A) on East RRFC (A) & Test 7 on West RRFC (B) (looking south)**

### 5.5.3.2. Axle Load Tests

Two tests were performed using an axle load to simulate a truck axle at a single location. Test 6 and Test 8 were identical tests located on the East RRFC and the West RRFC, respectively. Oriented looking South, Figure 5.12 offers a simple drawing of the two load tests. The actual test set-up is shown in Figure 5.13 for the two tests.

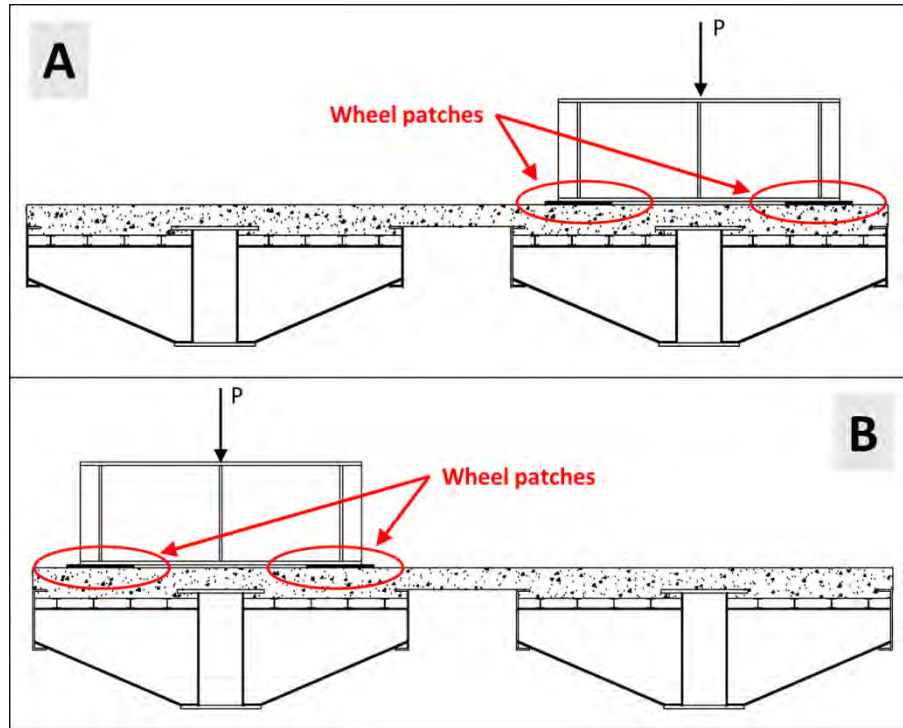


Figure 5.12: Test 6 (A) & Test 8 (B) load set-up at midspan (looking south)

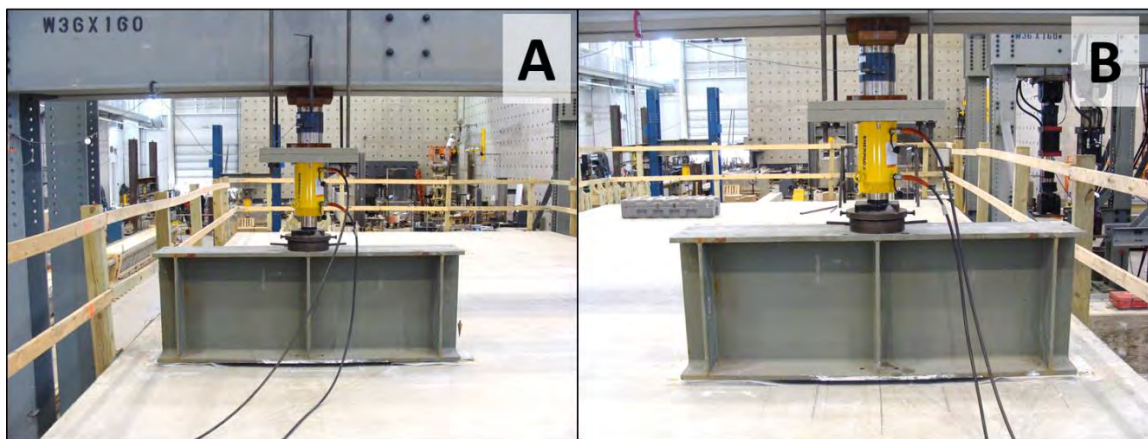


Figure 5.13: Test 6 on East RRFC (A) & Test 8 on West RRFC (B) (looking south)

### 5.5.3.3. Load Centered Between Railroad Flatcars

As shown in Figure 5.14, the load for Test 9 and Test 10 was located at the centerline of the RRFC bridge, in between the adjacent RRFCs. Test 9 consisted of two plates located in line with the centroids of the inner exterior girders, to show how the RRFC exterior girders performed with the load directly above. Test 10 consisted of axle



load to determine the behavior of the bridge when simulating a truck at this location. Figure 5.15 shows the actual load test set-ups in the laboratory.

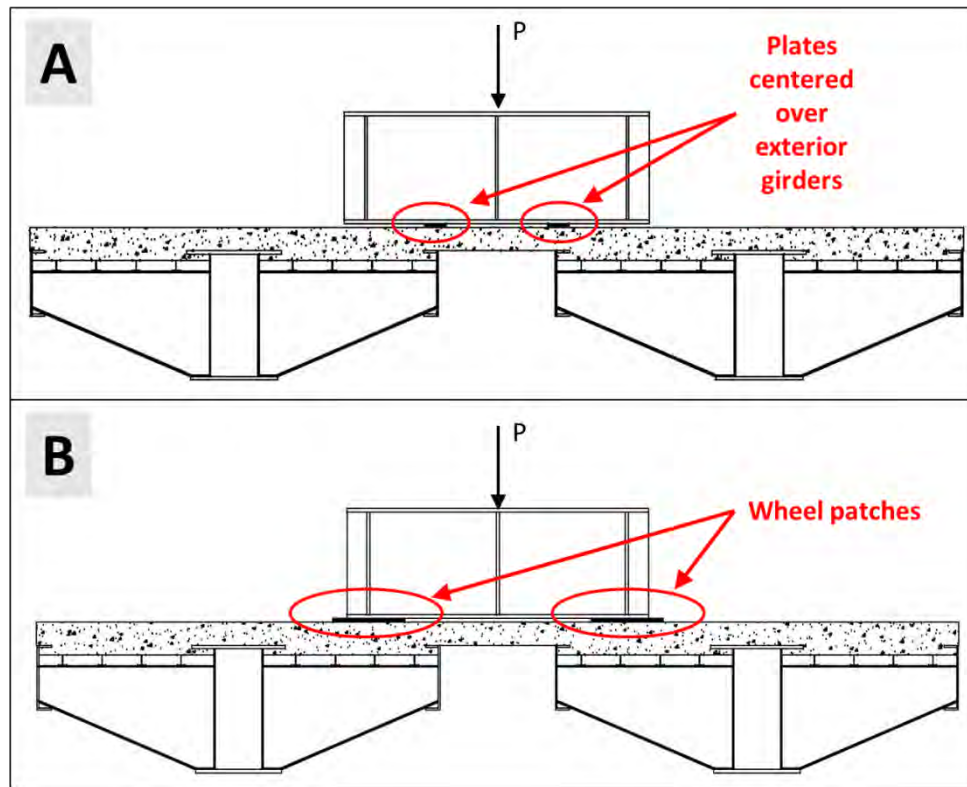


Figure 5.14: Test 9 (A) & Test 10 (B) load set-up at Section E (looking south)

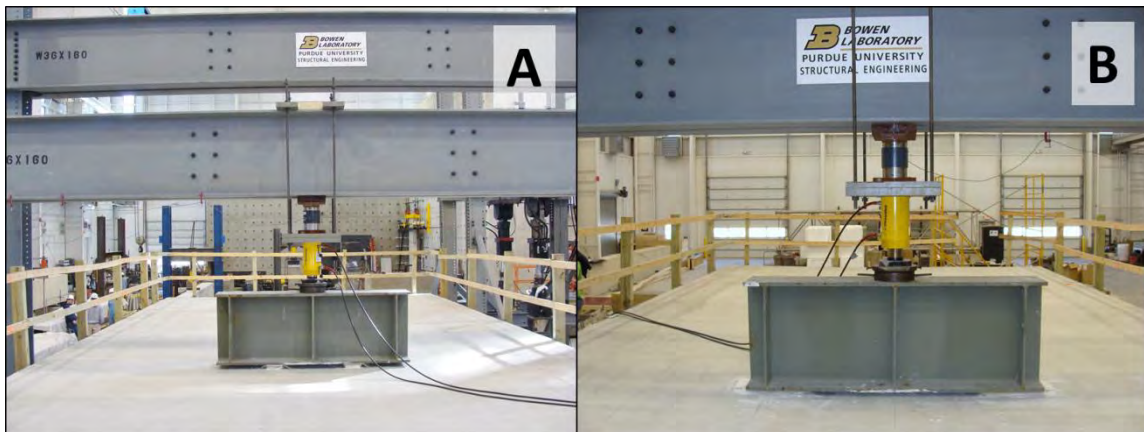


Figure 5.15: Test 9 (A) & Test 10 (B) (looking south)

#### 5.5.3.4. Load at Quarter Points

Two tests were conducted with the load applied 14 feet south of midspan. This loading condition provided a better understanding of the load distribution as the applied load moved closer to the supports. Figure 5.16 and Figure 5.17 show the load configuration for Test 11 and Test 12. Identical load tests were performed on each RRFC because the south end of the West RRFC was not instrumented and the load distribution between the RRFCs was unknown when load testing the East RRFC (Test 11). The test was repeated on the West RRFC (Test 12) to determine the load distribution between the RRFC at this location.

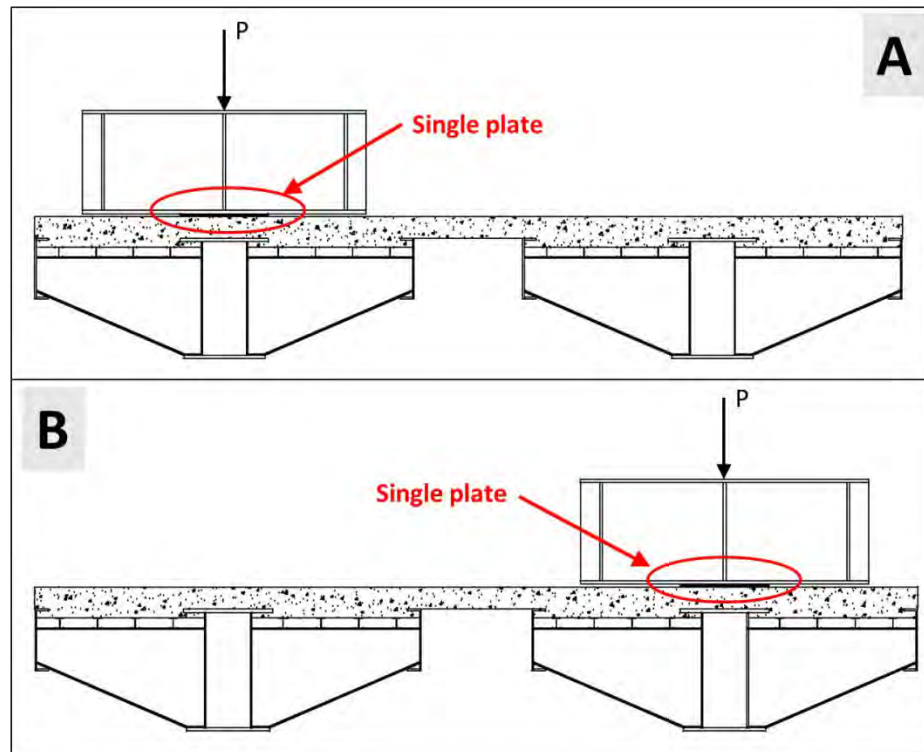
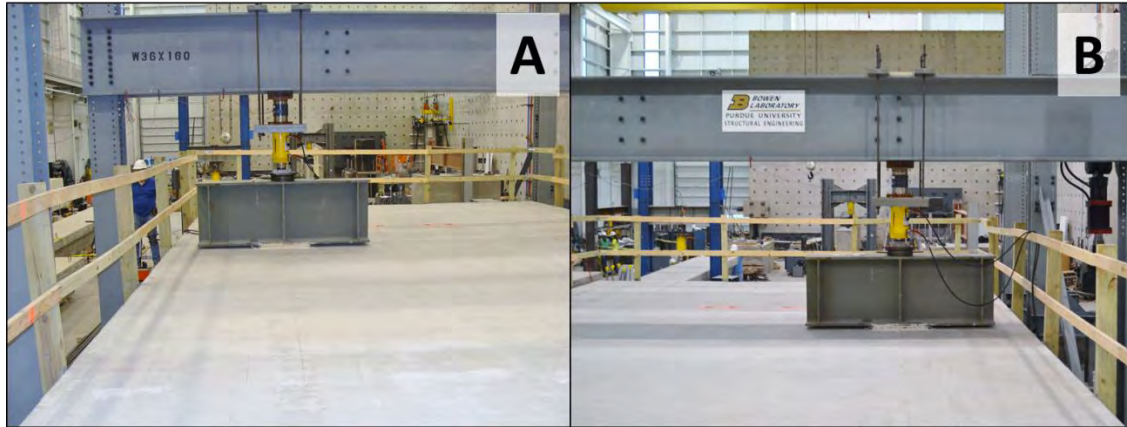


Figure 5.16: Test 11 (A) & Test 12 (B) load set-up at Section E (looking south)



**Figure 5.17: Test 11 (A) on East RRFC & Test 12 (B) on West RRFC (looking south)**

## **5.6. Fracture Tests**

Fracture tests were performed to address the issue of classifying RRFC bridges as containing fracture critical members. This issue arises due to the RRFC bridge being viewed as having only two primary load carrying members. The goal of the fracture tests was to simulate a fracture in a main girder to investigate the ability of the bridge to redistribute loads and perform as a system after fracture. The composite concrete deck previously mentioned was in place during these tests. The following sections further describe the fracture tests conducted in the laboratory.

### **5.6.1. Fracture Test 1 Overview**

The first test consisted of introducing a fracturing the East RRFC main girder, with the West RRFC main girder and all other bridge members intact. The load during this test was a single patch load centered over the East RRFC main girder. An initial center “crack” of 10.5 inches was cut into the bottom flange of the main girder, located about 2 feet north of midspan. This length cut was determined based on conservatively assumed toughness properties, known stress values at that location from previous load tests, and linear elastic fracture mechanics. As shown in Figure 5.18, a section of the main girder was cooled with liquid nitrogen in a cooling chamber to sub -100 °F in order to decrease the fracture toughness of the material. The goal was to greatly lower the

fracture toughness of the material by exposing the main girder to a large negative temperature, not to simulate a particular service temperature.



**Figure 5.18: Cooling chamber**

After multiple fracture attempts at a test load of 275 kips (approaching equipment limits), the main girder remained stable. Therefore, 3 more inches were cut on both edges of the bottom flange, leaving only about 7.5 inches of the 24 inch bottom flange still intact. Again, the main girder resisted fracture upon applying the same test load. Finally, two 15 inch cuts were created up both main girder webs (Figure 5.19). Fracture finally occurred after the main girder was cooled and loaded again.

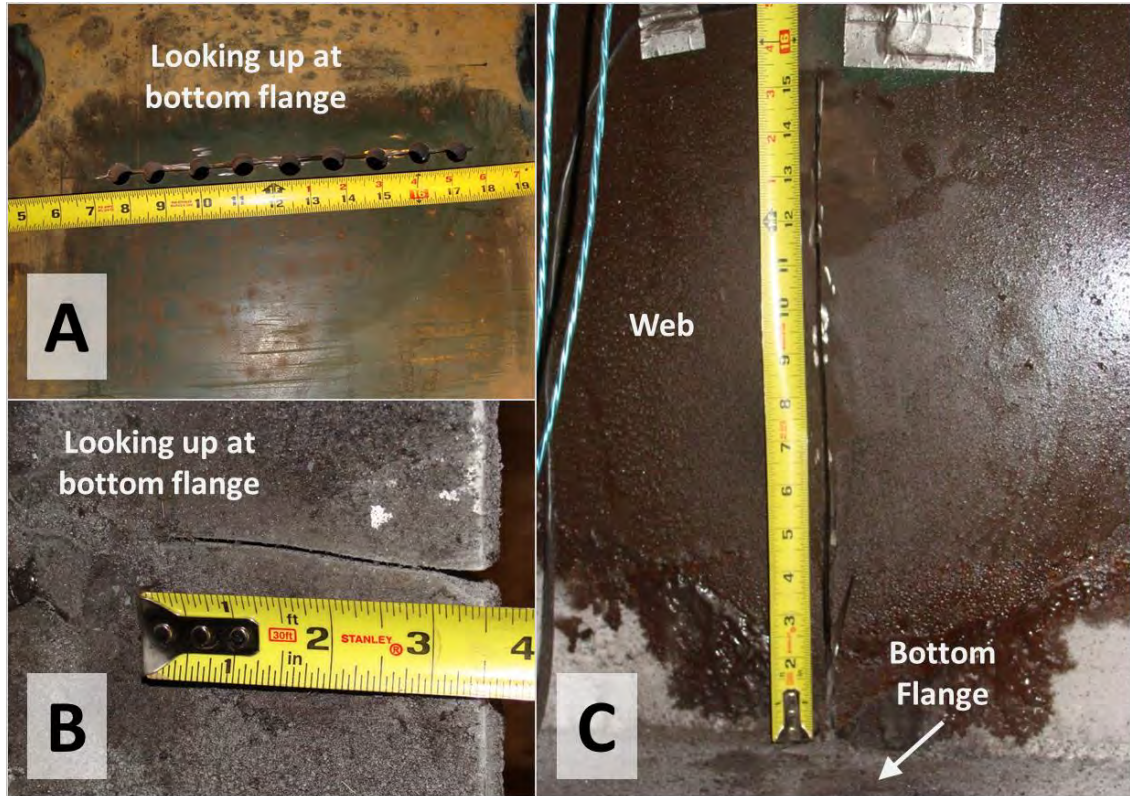


**Figure 5.19: Bottom flange cut (A), side flange cuts (B), & web cuts (C)**

### 5.6.2. Fracture Test 2 Overview

The second fracture test simulated a worst case scenario with the main girder of each RRFC fractured. This scenario, although highly unlikely, could occur if one main girder fractured, but was not detected before the other main girder fractured. Therefore, a fracture was simulated in the West RRFC main girder, with the East RRFC main girder still fractured (i.e., no repair splice). The load configuration during this test was a single patch load centered over the West RRFC main girder. An initial center “crack” of 11 inches was cut into the bottom of the main girder, located about 1.5 feet north of midspan (Figure 5.20). A section of the main girder was cooled with liquid nitrogen in a cooling chamber to sub -100 °F, as in the first fracture test. The main girder fractured under the first loading attempt; therefore, further cuts were not needed.



**Figure 5.20: Initial cut in West RRFC main girder before fracture (looking up at bottom flange)**

## CHAPTER 6. RESULTS OF LABORATORY LOAD TESTING

Several load tests were performed on the full-scale RRFC bridge in the laboratory. Each load test was repeated three or more times for each load configuration to ensure consistency of data, with the exception of the fracture tests. Excellent agreement was determined between the repeated load tests; therefore, results for one of each of the tests are presented in this chapter and the rest are presented in Appendix D.

Uniaxial strain gages were installed on the top and bottom flanges of multiple longitudinal members of the RRFC bridge. The strain measurements were converted to stress values using an elastic modulus value for steel of 29,000 ksi. Positive strain gage results indicate tension in the member and negative strain gage results indicate compression. Negative displacement readings indicate a downward displacement at that location. All instrumentation plans are located in Appendix B.

The current chapter is organized by deck type and load configuration; stress measurements are presented within particular instrumented cross sections. The different load tests are presented in Table 6.1, which is a replica of Table 5.1 and repeated for convenience. The use of this data to revise the load rating guidelines developed in Phase I are discussed in Chapter 7. Also, the rectangular rosette strain gage results are presented in Chapter 7 after converting the strain response to shear values.

**Table 6.1: RRFC bridge load tests**

Test	Load Location	Load Configuration	Maximum Load (kips)	Deck Type	Connection Between RRFCs
Test 1	Main girder of East RRFC Midspan	Single patch load	150	No deck	No connection
Test 2	Main girder of West RRFC Midspan	Single patch load	150	No deck	No connection
Test 3	Main girder of East RRFC Midspan	Single patch load	150	Timber deck	No connection
Test 4	Centered over East RRFC Midspan	Axle load	75	Timber deck	No connection
Test 5	Main girder of East RRFC Midspan	Single patch load	225	Concrete deck	Composite concrete deck
Test 6	Centered over East RRFC Midspan	Axle load	225	Concrete deck	Composite concrete deck
Test 7	Main girder of West RRFC Midspan	Single patch load	225	Concrete deck	Composite concrete deck
Test 8	Centered over West RRFC Midspan	Axle load	225	Concrete deck	Composite concrete deck
Test 9	Centered over bridge width Midspan	2 patch loads centered over exterior girders	225	Concrete deck	Composite concrete deck
Test 10	Centered over bridge width Midspan	Axle load	225	Concrete deck	Composite concrete deck
Test 11	Main girder of East RRFC 14' south of midspan	Single patch load	225	Concrete deck	Composite concrete deck
Test 12	Main girder of West RRFC 14' south of midspan	Single patch load	225	Concrete deck	Composite concrete deck
Fracture Test 1	Main girder of East RRFC Midspan	Single patch load	150 (after fracture)	Concrete deck	Composite concrete deck
Fracture Test 2	Main girder of West RRFC Midspan	Single patch load	190 (after fracture)	Concrete deck	Composite concrete deck

## 6.1. No Bridge Deck

### 6.1.1. Test 1 & Test 2: Single Patch Load

Test 1 and Test 2 were conducted with no deck and no connection between the two railroad flatcars. Detailed information about the test set-ups can be found in Section 5.3. The applied load was located at midspan of the East RRFC and the West RRFC for Test 1 and Test 2, respectively. The objectives of these tests were to understand the load distribution within one railroad flatcar and to determine if both RRFCs behaved the same under applied load. This section discusses the response of the longitudinal members for these tests. All stress values from Test 1 and Test 2 can be found in tabular form in Appendix D for an applied load of 150 kips. The structure remained linear elastic



throughout these load tests; therefore, the results provided in the appendix can be interpolated for lower loads.

Section I on the West RRFC was located at the same location as Section C on the East RRFC (1 foot – 7 ½ inches north of midspan). Test 2 performed on the West RRFC was identical to Test 1 performed on the East RRFC. The main girder response for Section C and Section I for these two tests are shown in Figure 6.1. The figure illustrates that the two RRFCs behaved the same under the applied load at midspan. For simplicity, the exterior girder and stringer stress measurements at these cross sections are not displayed on the figure. However, the two flatcars displayed similar responses for these members as well. Similar behavior was observed between Sections B and H, and between Sections A and G. Thus, it was concluded that the two RRFCs behaved the same under load and only Test 1 data will be further discussed.

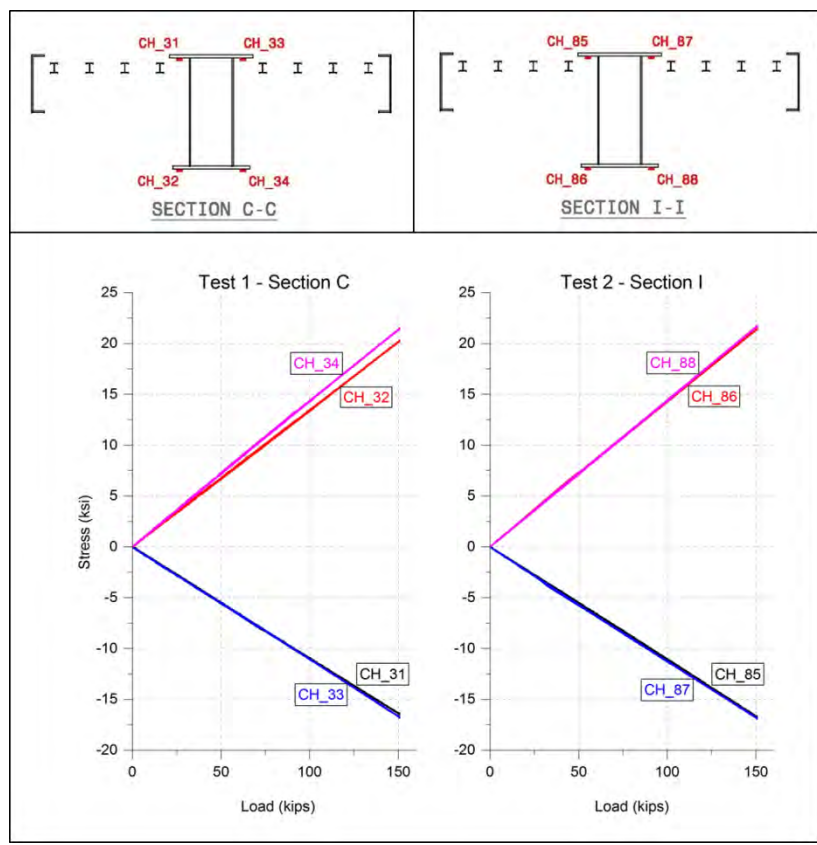
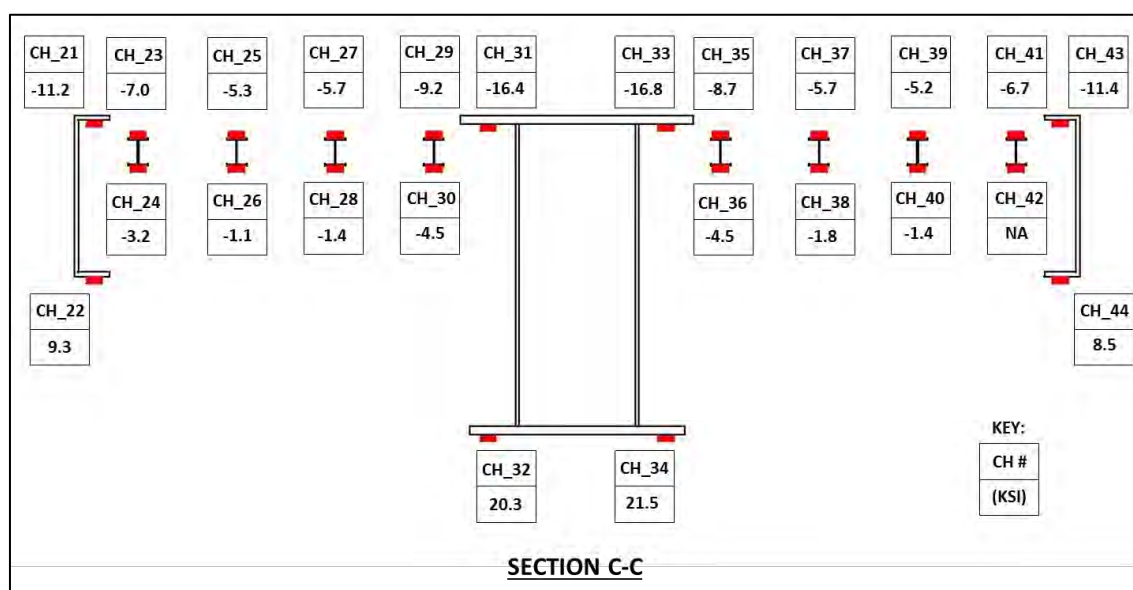


Figure 6.1: Test 1 versus Test 2 main girder response at Sections C & I

Stress measurements for Section C are displayed in Figure 6.2 at an applied load of 150 kips for all members instrumented. The stress values for the top and bottom flanges of the stringers were all in compression, indicating that these members were above the neutral axis. The exterior girder cross section is much smaller than that of the main girder; however, smaller stress values were observed in the exterior girders compared to the main girders. This indicates that less load was carried by the exterior girders than the main girder. Material tests performed on the bottom flange of the main girder indicated a yield strength of about 48 ksi; all measurements in this cross section remained below yield at the 150 kip point load.

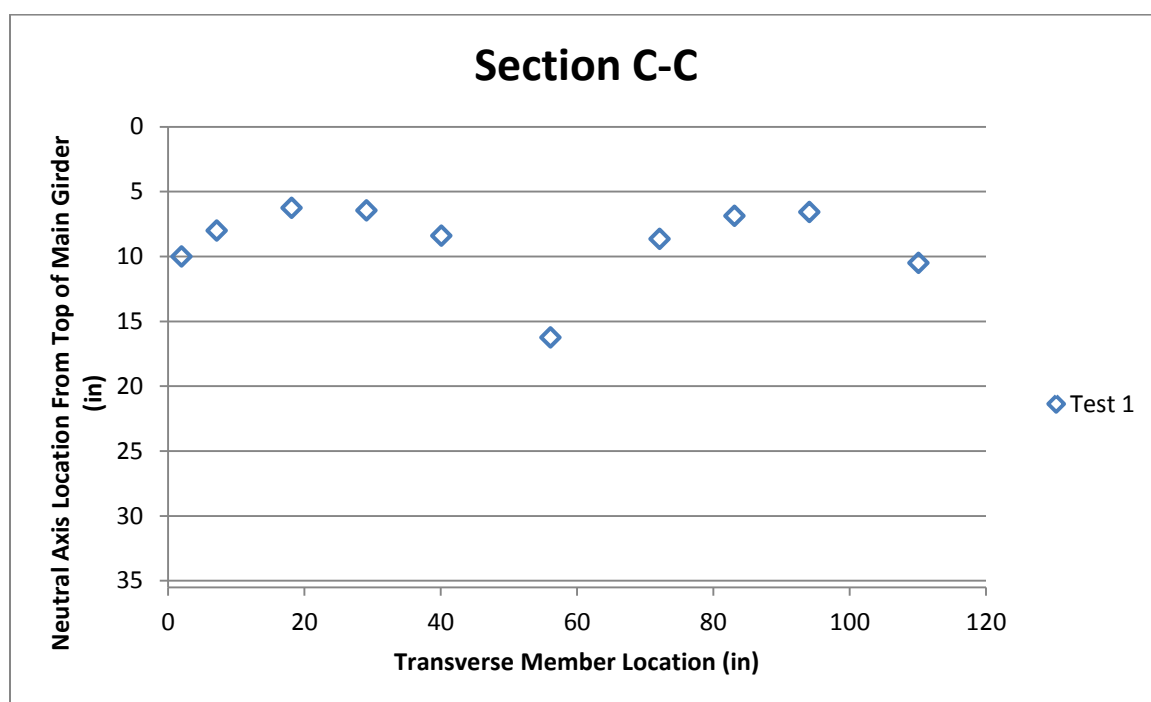


**Figure 6.2: Test 1 response at Section C for an applied load of 150 kips**

Figure 6.3 shows the neutral axis locations in each longitudinal member in Section C. The neutral axis was calculated based on top and bottom flange stress measurements for that member. The neutral axis measurement is in reference to the top of the main girder and exterior girders. For confidence, the y-axis of the plot extends to 35 inches, which is the depth of the main girder at this cross section. The members are represented by their transverse location throughout the cross section, with the outer exterior girder of the East RRFC near zero inches. The neutral axis in the main girder was calculated to be about 16.25 inches based on the stress measurements. The stringer

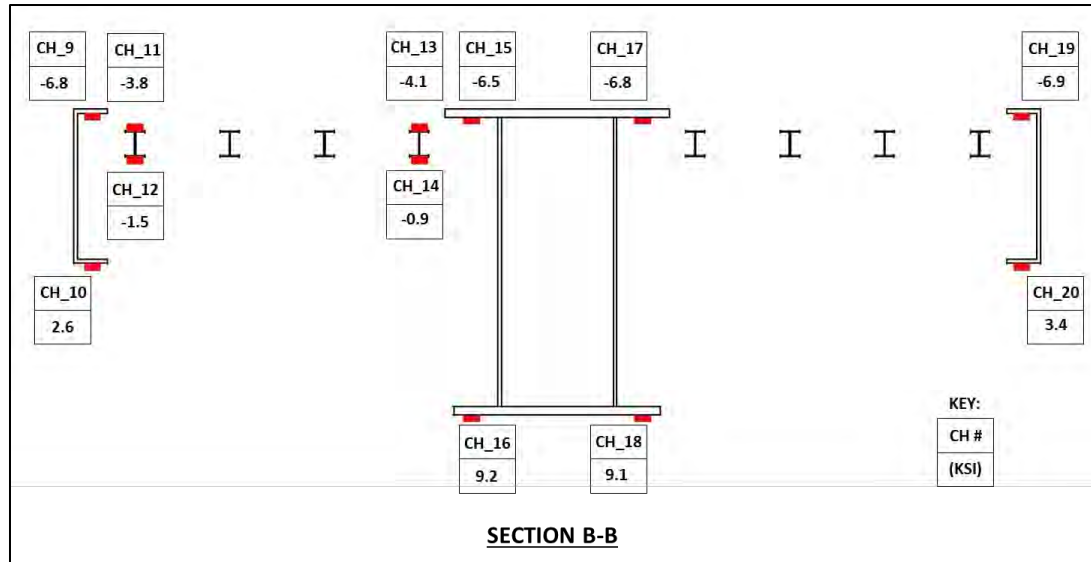
closest to the inner exterior girder (furthest point to the right) did not have a top flange stress measurement; therefore, it was not included in the plot.

If the cross section were completely rigid then the neutral axis location would be constant throughout the section. As shown in the figure, this is not the case, as the neutral axis varies throughout the cross section. One reason for this behavior is a result of shear lag. Due to the fact that the cross section was not completely rigid, there exists differential movement between the longitudinal members at this location. Although not shown, similar behavior was observed at the quarter points (Section B and Section E).



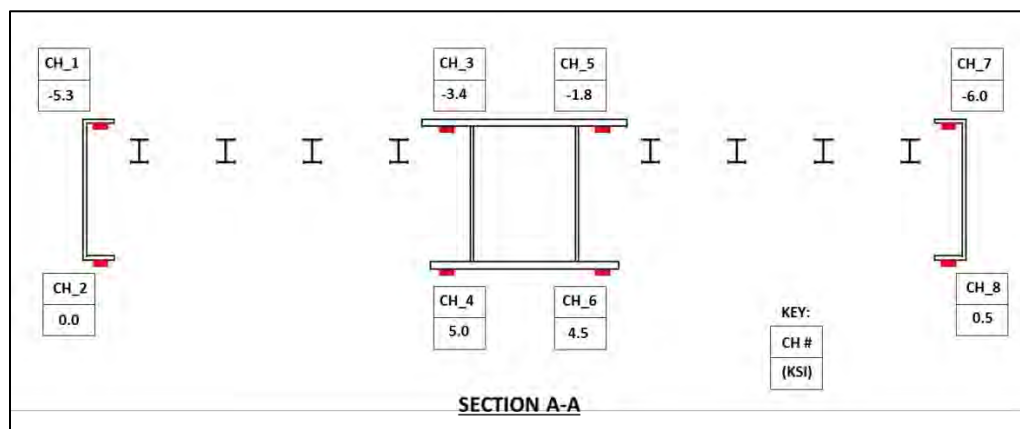
**Figure 6.3: Test 1 neutral axis location for Section C**

Figure 6.4 displays the stress measurements for the longitudinal members instrumented in Section B for an applied load of 150 kips. Section B was located near the quarter point of the span. The response for Section B was similar to that of Section C, with the exception of smaller stresses due to the location of the cross section being further away from the applied load.



**Figure 6.4: Test 1 response at Section B for an applied load of 150 kips**

Section A was located where the main girder is shallower, about 2 feet – 6 ½ inches south of the north support. The stress response for this section is shown in Figure 6.5 for an applied load of 150 kips. The small stress values observed in the bottom flange of the exterior girders show the effects of the stress distribution into the supported member (the main girder) by means of the large floorbeam located at the support. The bottom flange of the support floorbeam was welded to the webs of the exterior girders about 4 inches above the bottom flange of the exterior girders. The response shows that at this location the stress was “flowing” out of the bottom flanges of the exterior girders to get into the support floorbeam.



**Figure 6.5: Test 1 response at Section A for an applied load of 150 kips**

Sections B & E were mirrored cross sections of each other, located near the span quarter points. The main girder response for these cross sections is shown in Figure 6.6. The figure indicates that the two cross sections displayed similar behavior in the main girder due to the applied load at midspan. Not shown are the response of the exterior girders and stringers. These members also displayed similar responses between the two cross sections. Symmetric behavior was also observed between Sections A and H within the East RRFC. Thus, it was concluded that the RRFCs behave symmetrically within a single flatcar. Previous observations made for the Section A and Section B are also applicable for Section F and Section E, respectively.

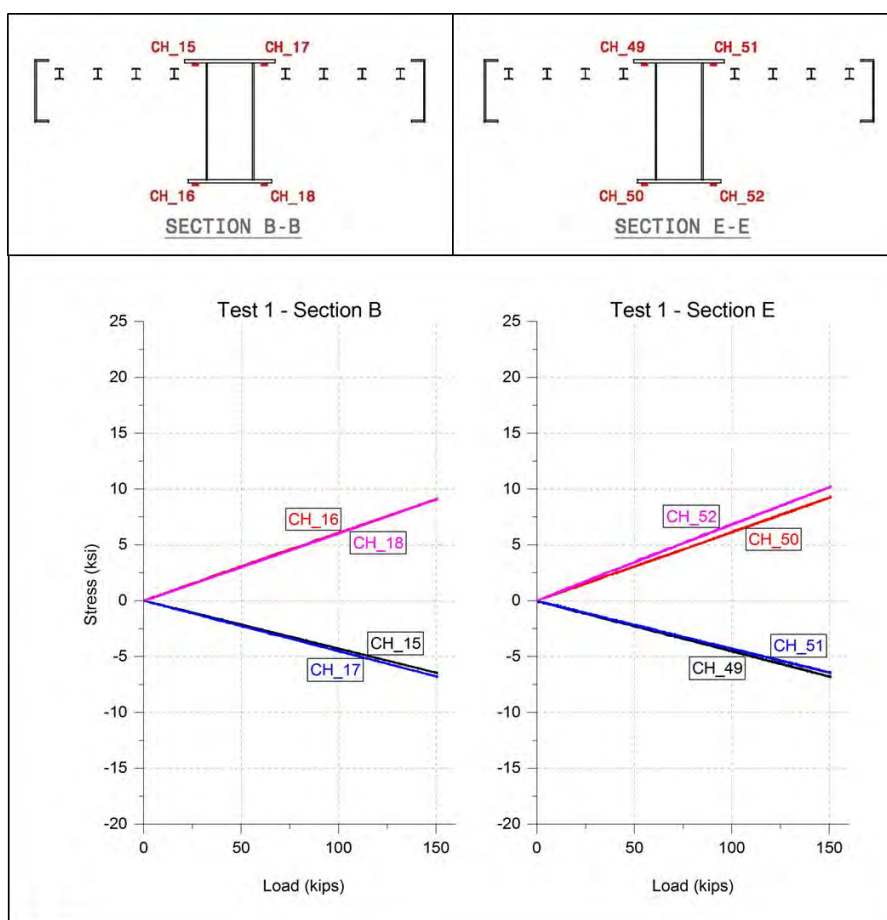


**Figure 6.6: Test 1 main girder stress results for Sections B & E**

Displacement sensors were placed at similar locations for Test 1 and Test 2. D\_110 and D\_115 (blue lines) were placed on the respective main girders at midspan,

directly under the applied load. D\_109 and D\_114 (red lines) were placed on the respective main girders at the north-end quarter points. D\_111 and D\_116 (magenta lines) were placed on the respective main girders at the south-end quarter points. D\_108 and D\_113 (black lines) were placed at the north-end supports. D\_112 and D\_117 (green lines) were placed at the south-end supports.

Figure 6.7 indicates that both RRFCs deflected the same under the applied load. The quarter point displacement sensors (red and magenta lines) show that there was symmetric behavior under the applied load in the longitudinal direction of the RRFC, as well as when comparing the two RRFCs. The midspan displacement sensors (blue lines) display maximum deflection values of 1.2 inches ( $L/475$ ) at a point load of 150 kips. Displacement sensors were installed at each support to measure any settlement or uplift at this location. Test measurements indicate small settlement at these locations (black and green lines). The support deflections were about 4% of the maximum deflection at midspan; therefore, it was determined to ignore the small deflections at the support when reporting maximum deflection values at the quarter points and at midspan.

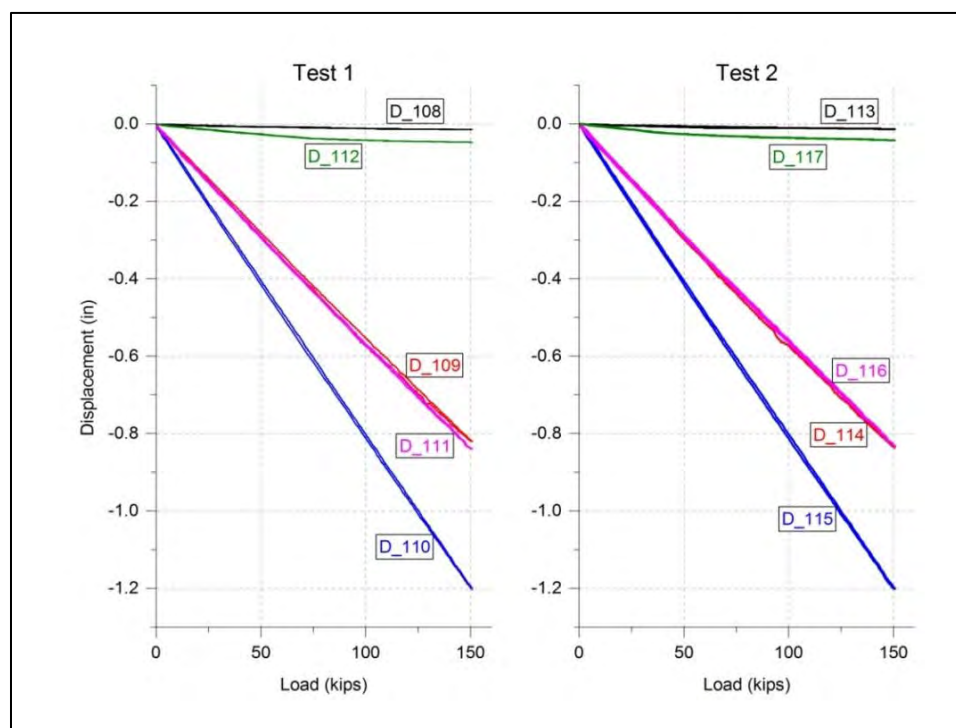


**Figure 6.7: Test 1 versus Test 2 main girder displacement response**

## 6.2. Timber Deck Patch

### 6.2.1. Test 3: Single Patch Load

Test 3 consisted of loading the East RRFC after a timber deck patch was constructed at midspan. The load configuration for Test 3 was a single patch load in order to directly compare to Test 1. Further information about the test set-up for Test 3 can be found in Section 5.4.3. The goal of this test was to determine if the timber deck provided any significant load-distribution. This section displays the response of the flatcar with the timber deck patch. Tabulated stress measurements can be found in Appendix D. The RRFC bridge was loaded to 150 kips for this test and demonstrated linear-elastic behavior up to this load.

The stress measurements at Section C are displayed in Figure 6.8. The response was similar compared to that for Section C with no timber deck (Figure 6.2). The stress measurements in the exterior girders did not change; this indicates that the stiffness of the timber deck was not adequate to distribute load out to these members. Figure 6.9 shows the neutral axis locations within each longitudinal member in the cross section for Test 3 compared to Test 1. As shown, the neutral axis locations for each member did not vary significantly. As discussed in Section 6.1.1. , the neutral axis location varied throughout the cross section due to flexibility within the section causing shear lag. Though not shown, it was also observed that there was little to no change in the response of the other four cross sections in the East RRFC when compared to Test 1 with no deck. Also, displacement measurements were similar when comparing Test 3 to Test 1 and are not discussed. These results suggest that the timber deck patch did not appreciably alter the load distribution within the flatcar.

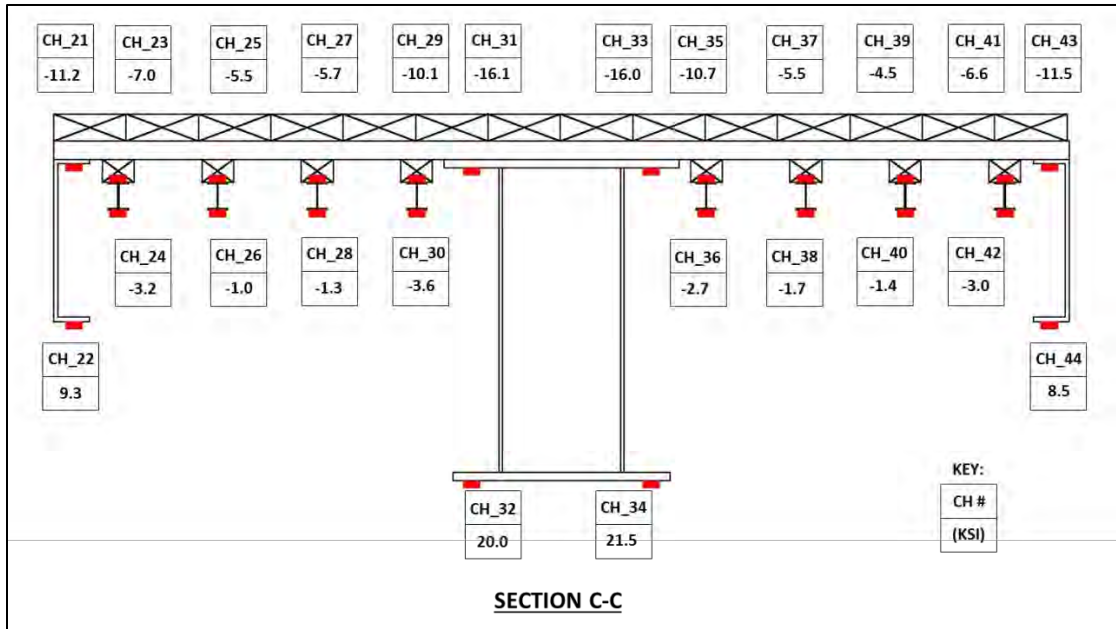


Figure 6.8: Test 3 response for Section C at an applied load of 150 kips

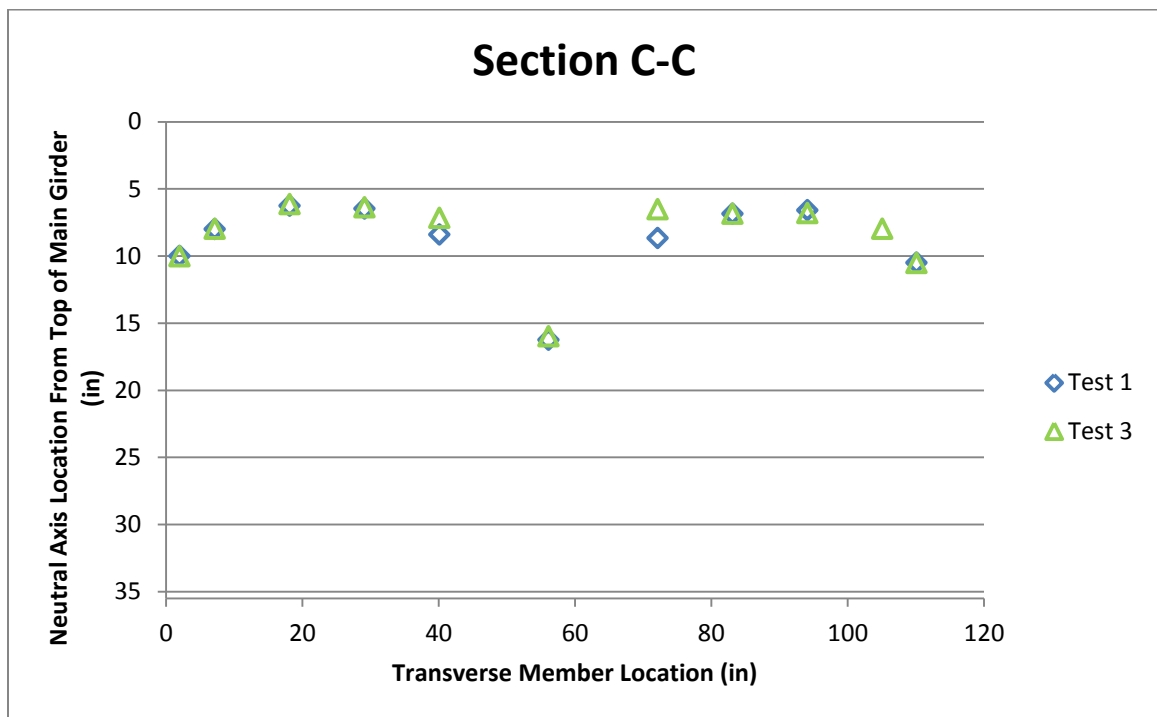


Figure 6.9: Test 3 neutral axis location for Section C



### 6.2.2. Test 4: Axle Load

Test 4 was similar to Test 3 with the exception of applying the load through two load plates instead of a single patch load. This load configuration simulates a truck axle. This section displays the flatcar response during Test 4 compared to Test 3 for Section C. Instrumentation measurements from Test 4 can be found in tabular form in Appendix D for the maximum applied load of 75 kips.

The response of the exterior girders is shown in Figure 6.10 comparing Test 3 and Test 4. A slight increase in tension and compression stresses was observed when the RRFC was loaded with an axle load (Test 4). This increase was attributed to the applied load located closer to the exterior girders, and not to the contribution of the timber deck. Displacement values did not differ from those in Test 1; therefore, they are not presented in this section. It was concluded that the timber deck patch did not provide any significant load-distribution; therefore, the results from the tests using the patch of timber decking will not be discussed further.

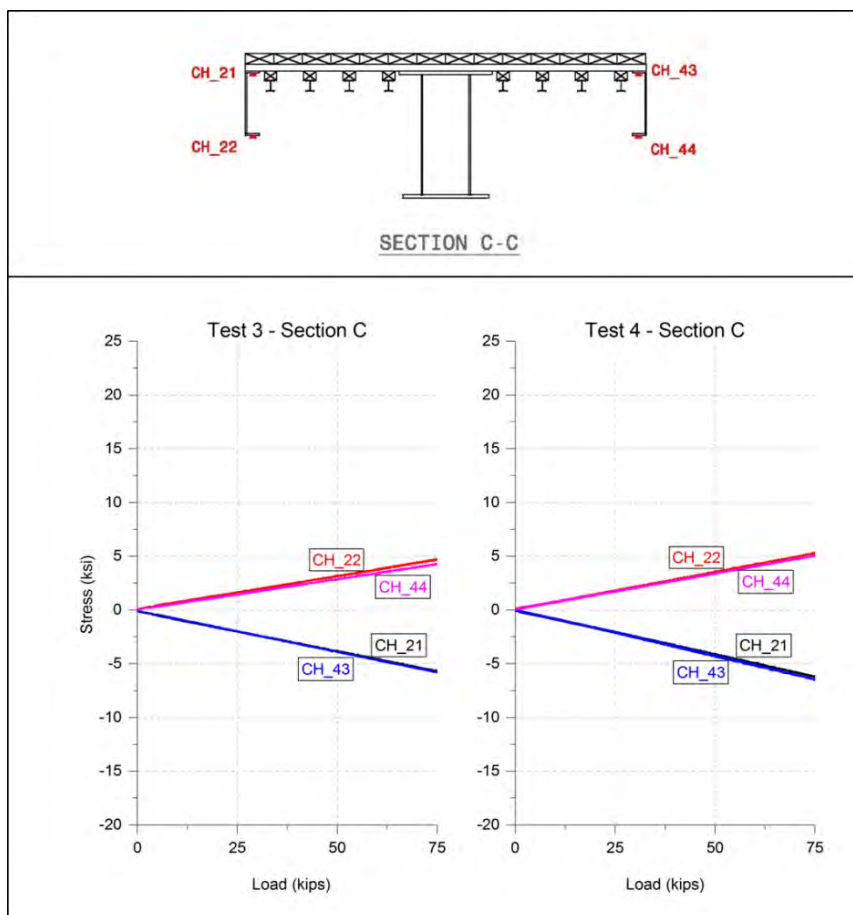


**Figure 6.10: Test 3 versus Test 4 exterior girder response for Section C**

### **6.3. Concrete Bridge Deck**

#### **6.3.1. Concrete Pour**

Instrumentation measurements were collected during placement of the concrete for the bridge deck. This data provided stress and displacement values due to the dead load of the wet concrete. Measured stresses for the gages on the bottom flange of the main girders and exterior girders at Section C and Section I (near midspan) are provided in Table 6.2 after all of the concrete was placed. Deflection values for the East RRFC are provided in Table 6.3. The locations of the displacement sensors were the same as the previous load tests. All of the instrumentation measurements from the concrete bridge deck pour can be found in Appendix D.

**Table 6.2: Concrete dead load stress**

Concrete Bridge Deck Pour	
Channel	Final Stress (ksi)
CH_22	1.9
CH_32	2.6
CH_34	3.3
CH_44	0.7
CH_80	1.4
CH_86	3.4
CH_88	3.1
CH_94	1.8

**Table 6.3: Concrete dead load displacement**

Concrete Bridge Deck Pour	
Sensor	Final Displacement (in)
D_108	-0.02
D_109	-0.11
D_110	-0.16
D_111	-0.13
D_112	-0.04

### 6.3.2. Test 5 & Test 7: Single Patch Load

Load tests 5 and 7 were performed with a single patch load located at midspan on the East RRFC and the West RRFC, respectively. Test 5 and Test 7 are described in detail in Section 5.5.3.1. The tests were used to establish if symmetric behavior would be observed with the addition of the composite concrete deck. Test results indicated that the East RRFC and the West RRFC demonstrated nearly identical response. As a result, only the results from Test 5 are provided in this section. The data from these tests was compared to Test 1 to better understand the change in behavior with the addition of the composite concrete deck. The following sections discuss the response of the main girders, exterior girders, and stringers. All measurements for Test 5 and Test 7 can be found in tabular form in Appendix D at an applied load of 150 kips. The maximum applied load for these tests was 225 kips with the RRFC bridge demonstrating linear-elastic behavior up to this load.

Figure 6.11 compares the main girder stresses from Test 1 with no deck and Test 5 with a composite concrete deck. The applied load during Test 5 was increased 75 kips in order to obtain similar maximum tension flange live load stresses (CH\_32 and CH\_34) as Test 1. This increase in load capacity was due to the addition of the composite concrete deck and the contribution from the West RRFC. The plot also shows a decrease in the compression flange stress values during Test 5 as a result of composite action between the concrete deck and RRFCs. It also illustrates that the neutral axis moved upward due to the addition of the composite concrete deck.

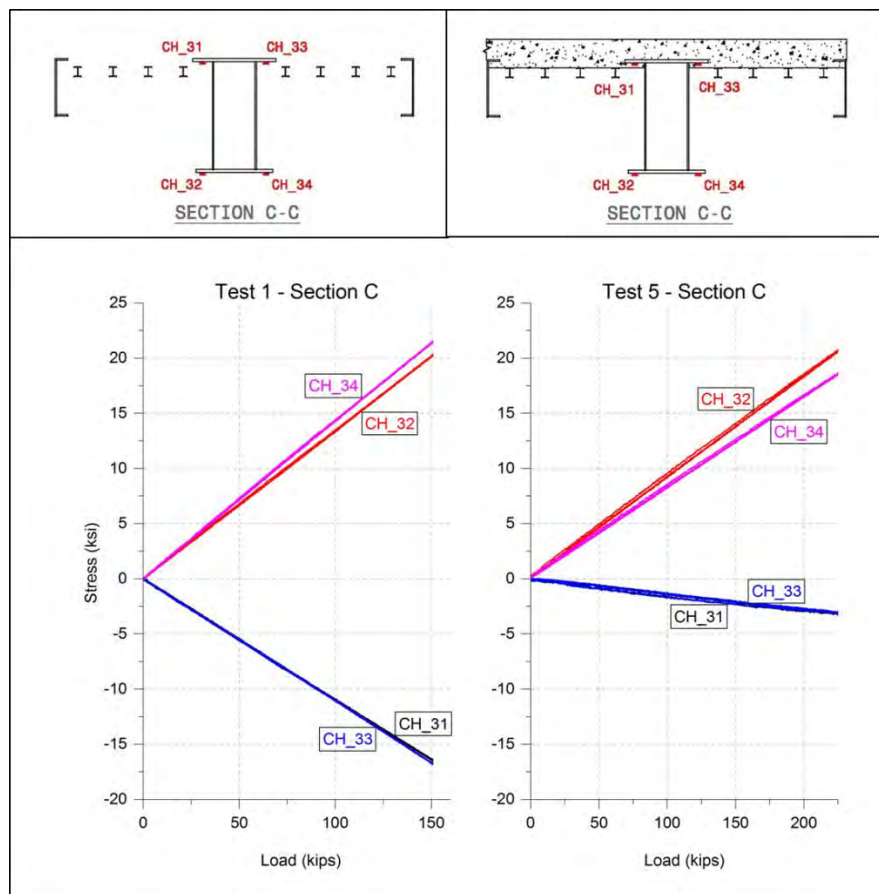


**Figure 6.11: Test 1 versus Test 5 main girder stress results for Section C**

Figure 6.12 shows the stresses in Section C during Test 5 at an applied load of 150 kips. Recall that during Test 1 (no deck) the top and bottom flanges of the stringers were both in compression. As shown in the figure, the bottom flanges of the stringers were in tension and the top flanges were close to zero. This indicates that the neutral axis moved upward as a result of composite action between the RRFC superstructure and the composite concrete deck. Figure 6.13 shows the neutral axis locations based on stress measurements for each member for Test 5 compared to Test 1. As shown, a more constant neutral axis is observed throughout the cross section compared to Test 1. This is attributed to the concrete deck adding longitudinal stiffness in the cross section. This behavior was also observed for Sections A, B, E, and F in the East RRFC.

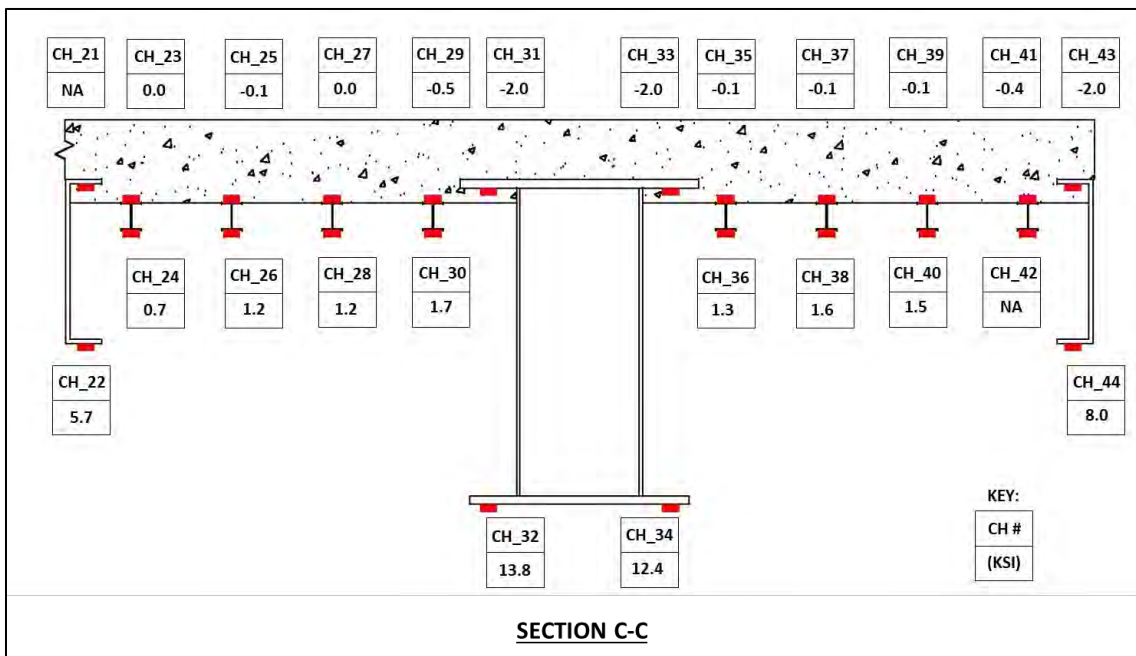
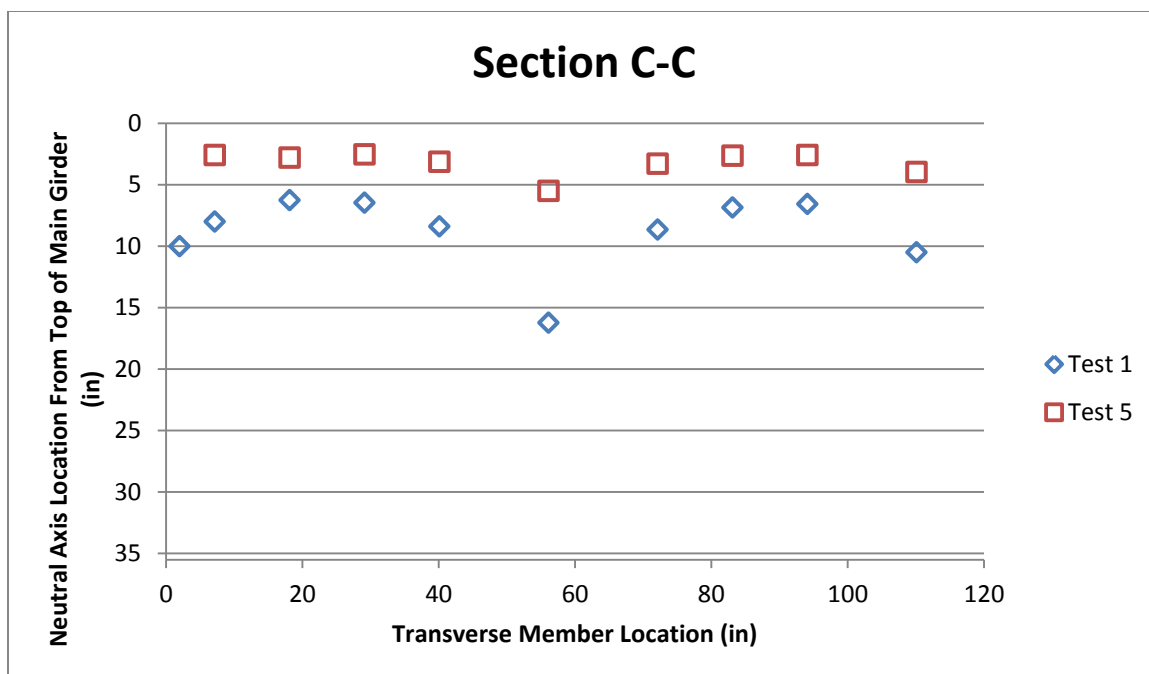
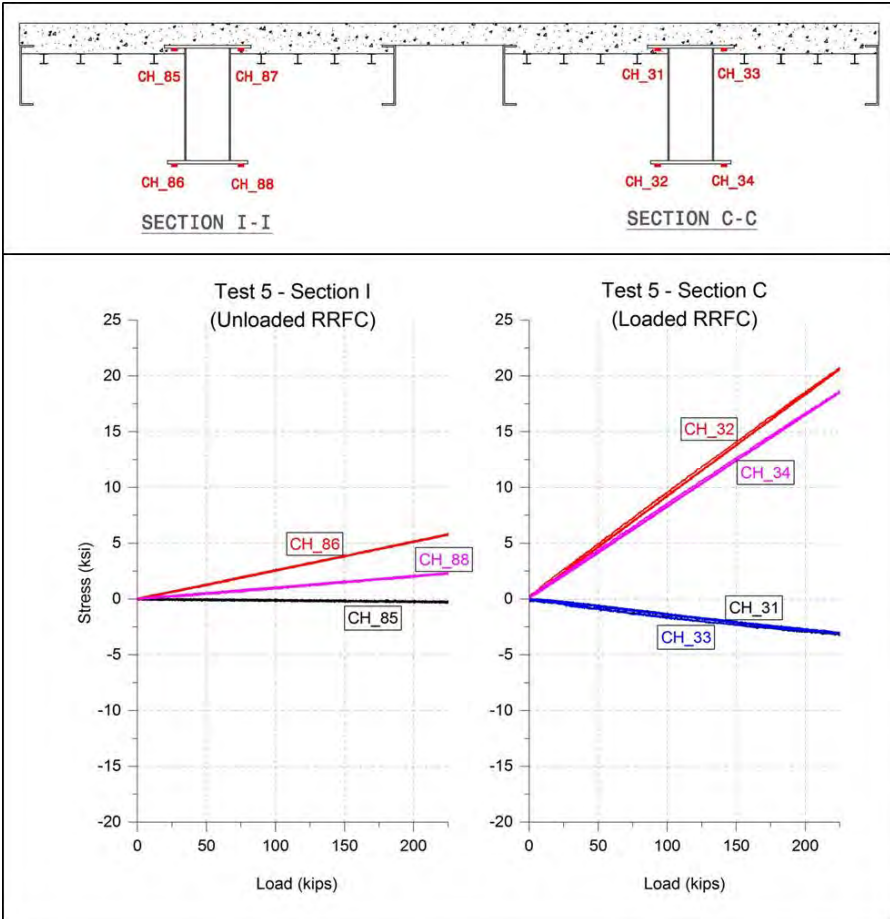


Figure 6.12: Test 5 response for Section C at an applied load of 150 kips



**Figure 6.13: Test 5 neutral axis location for Section C**

Main girder top and bottom flange stress measurements are presented in Figure 6.14. The “loaded RRFC” and “unloaded RRFC” for Test 5 are the East RRFC and West RRFC, respectively. As shown in the instrumentation plans in Appendix B, Section C and Section I were at the same locations on the East RRFC and the West RRFC, respectively. The entire bridge cross section is included in Figure 6.14; the West RRFC is on the left and the East RRFC is on the right. CH\_87 was not working properly during this test; therefore, it was not included in the figure. The plots in Figure 6.14 show the load distribution between the RRFCs by means of the concrete deck. The East RRFC displays greater stress values; in other words, more of the load was being carried by that flatcar compared to the adjacent flatcar, as expected. One reason for the stress difference in the bottom flange strain gages of the main girder could be due to slight out-of-plane bending within the member.



**Figure 6.14: Test 5 main girder stress results for Sections C & I**

Figure 6.15 shows the load distribution comparing the four exterior girders within the bridge cross section for Sections C & I. Stresses are greater in the exterior girders of the loaded RRFC, as expected. The stress values for the West RRFC outer exterior girder (CH\_79 and CH\_80) were close to zero for this load test. A simple explanation for this behavior is that the load was distributed to other longitudinal members before reaching the outer exterior girder of the West RRFC.

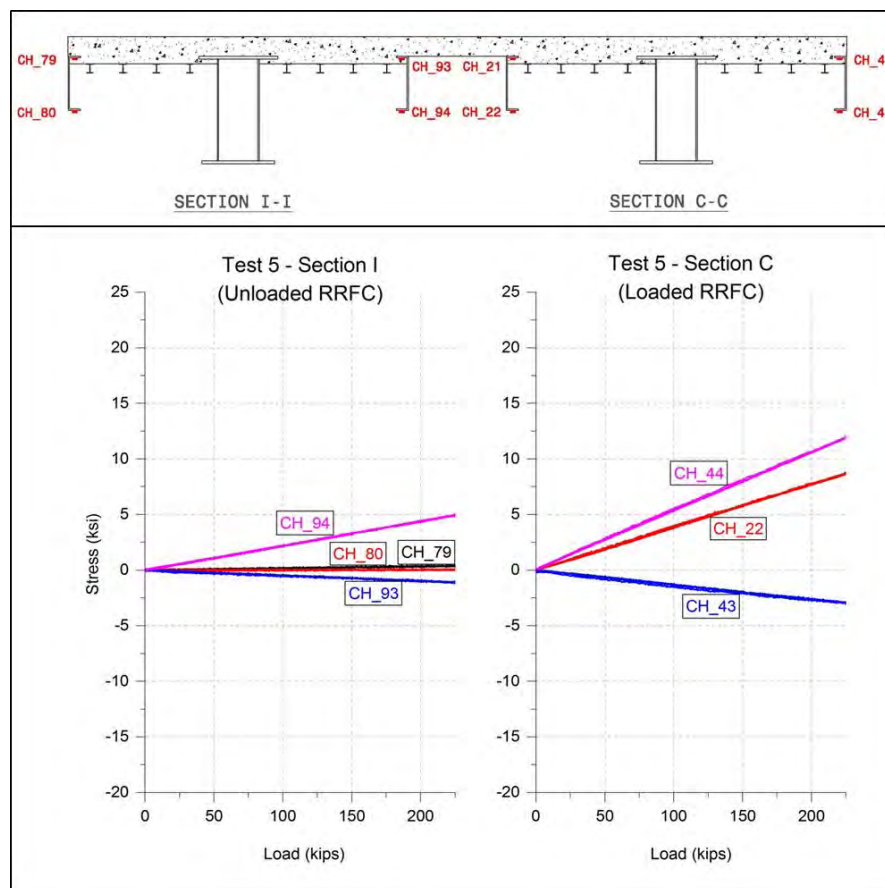


**Figure 6.15: Test 5 exterior girder stress results for Section C & I**

Displacement values were recorded for both RRFCs during Test 5. Displacement sensors were placed at similar locations as Test 1 and Test 2. D\_110 and D\_115 (blue lines) were placed on the respective main girders at midspan, directly under the applied load. D\_109 and D\_114 (red lines) were placed on the respective main girders at the north-end quarter points. D\_111 and D\_116 (magenta lines) were placed on the respective main girders at the south-end quarter points. D\_108 and D\_113 (black lines) were placed at the north-end supports. D\_112 and D\_117 (green lines) were placed at the south-end supports. The displacement sensors at the supports were installed to measure any settlement or uplift at these locations. As shown in Figure 6.16, small settlements were measured at the supports (about 0.01 inches). It was determined to ignore these displacements when reporting the maximum displacements at the quarter points and at midspan. As shown in the figure, the loaded RRFC (East RRFC) experienced larger displacements than the unloaded RRFC (West RRFC). The displacements in the West



RRFC indicate that the load was distributed to this flatcar through the composite concrete deck. The largest measured displacement due to the applied load of 225 kips was about 0.7 inches at the location of the applied load. This corresponds to a displacement of about  $L/800$ .

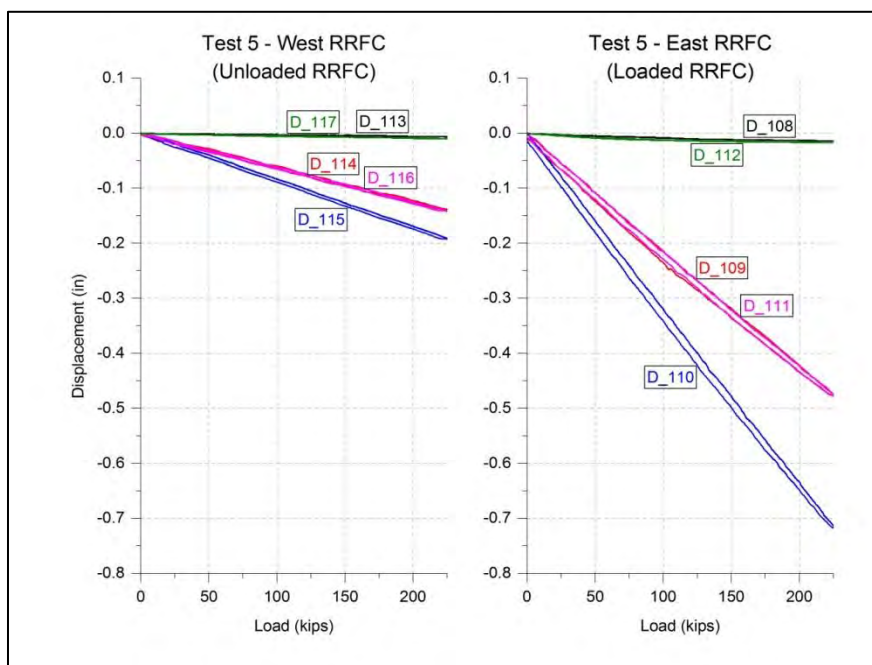


**Figure 6.16: Test 5 main girder displacement results**

### 6.3.3. Test 6 & Test 8: Axle Load

Test 6 and Test 8 were identical load tests performed on the East RRFC and West RRFC, respectively. Test 6 and Test 8 are described in detail in Section 5.5.3.2. Both RRFCs performed the same under applied load; therefore, only the results from Test 6 are presented in this section. The objective of these tests was to determine the behavior of the bridge when simulating a truck axle at a single location. All instrumentation results from Test 6 and Test 8 can be found in tabular form in Appendix D at an applied load of 150 kips. The RRFC structure displayed linear-elastic behavior throughout the load testing to 225 kips.

Test 6 stress measurements for Section C are displayed in Figure 6.17. An increase in stress was observed in the exterior girders and stringers, indicating that these

members were carrying more load, when compared to Test 5 in Figure 6.12. This is as expected due to the two patch loads located above the stringers and closer to the exterior girders.

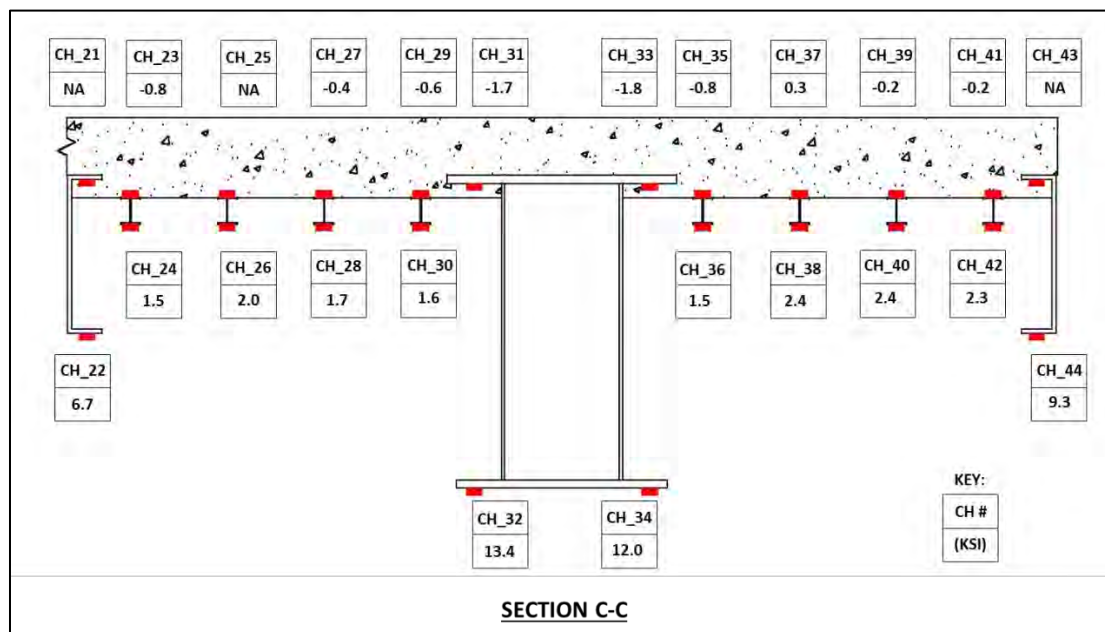
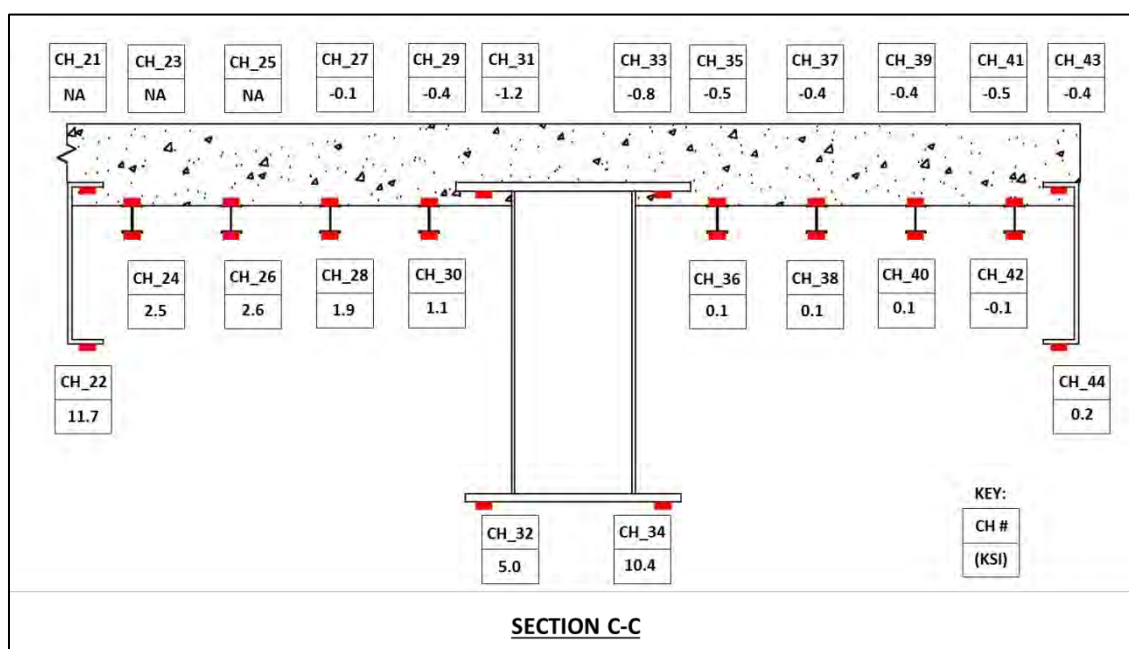


Figure 6.17: Test 6 response for Section C at an applied load of 150 kips

#### 6.3.4. Test 9 & Test 10: Load Centered Between Railroad Flatcars

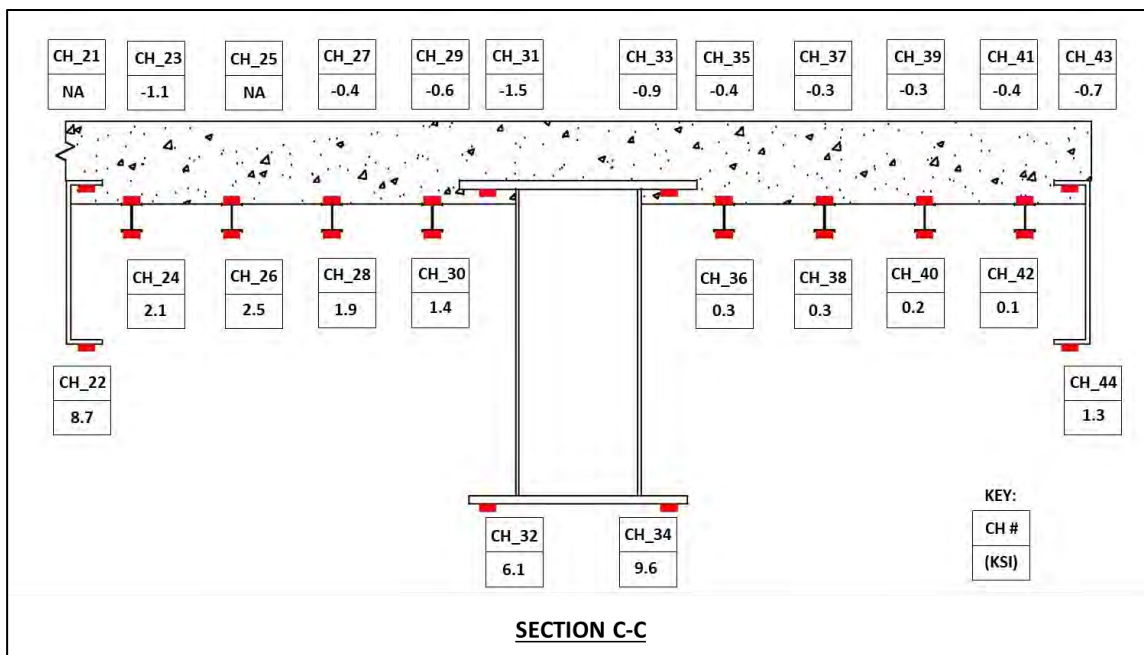
Test 9 and Test 10 were located on the centerline of the RRFC bridge. Further information about the test set-ups can be found in Section 5.5.3.3. Test 9 consisted of two plates located in line with the centroids of the inner exterior girders. Test 10 consisted of axle load plates simulating a truck axle. Section C on the East RRFC was located at the same location as Section I on the West RRFC. Due to the symmetrical load configuration, the two flatcars displayed the same behavior; therefore, only the East RRFC results are discussed in this section. All instrumentation measurements from Test 9 and Test 10 can be found in tabular form in Appendix D at an applied load of 150 kips. The RRFC Bridge was loaded to 225 kips for these load tests and displayed linear-elastic behavior up to this load.

The response for Section C on the East RRFC during Test 9 is displayed in Figure 6.18 for an applied load of 150 kips. As expected, the inner exterior girder (CH\_22) measured larger stresses compared to previous tests due to the applied load located directly above that member. Lower stresses were observed in the outer exterior girder (CH\_43 and CH\_44) compared to other load tests, and the inner exterior girder response. The stringers closest to the applied load also observed an increase in stress compared to previous tests. The difference in stress values in the bottom flange of the main girder indicates slight out-of-plane bending within that member.



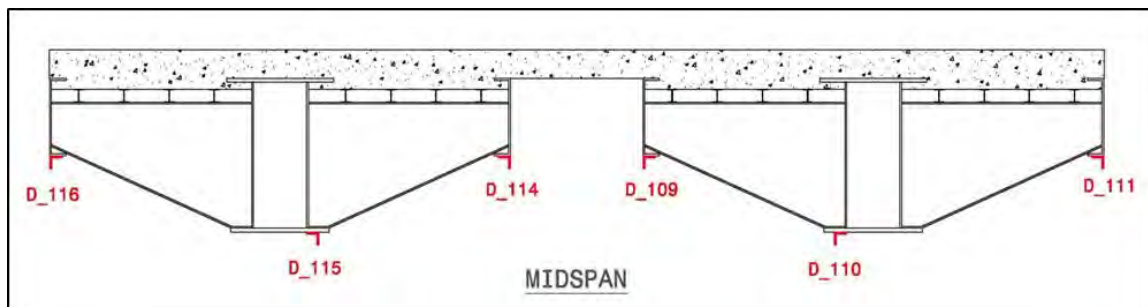
**Figure 6.18: Test 9 response for Section C at an applied load of 150 kips**

Figure 6.19 shows the response for Section C during Test 10. Similar to Test 9, larger stresses were observed in the inner exterior girder (CH\_22) and the neighboring stringers. Slight differences exist when comparing Test 10 to Test 9. The axle load configuration for Test 10 had a greater distance between the two patch loads; therefore, the load was distributed more into the other members and decreased at the location of CH\_22.



**Figure 6.19: Test 10 response for Section C at an applied load of 150 kips**

The instrumentation plans for the displacement sensors were modified for Test 9 and Test 10. Instead of placing the displacement sensors in a longitudinal orientation as in the previous tests, Test 9 and Test 10 consisted of placing the sensors in a transverse orientation at midspan. Figure 6.20 shows the location of the displacement sensors during this test. D\_108, D\_112, D\_113, and D\_117 were located at the supports as in previous tests. The displacement results are presented in Table 6.4. As shown, the displacement results of the West RRFC were similar to the East RRFC. The inner exterior girders (D\_109 and D\_114) had the largest measured displacements. This was expected because the load was located above those members.



**Figure 6.20: Location of displacement sensors during Test 9 & Test 10**

**Table 6.4: Displacement results for Test 9 & Test 10**

	<b>Test 9 at 225 kips</b>	<b>Test 10 at 225 kips</b>
<b>Sensor</b>	<b>Displacement (in)</b>	<b>Displacement (in)</b>
<b>D_108</b>	-0.04	-0.02
<b>D_109</b>	-0.91	-0.70
<b>D_110</b>	-0.50	-0.49
<b>D_111</b>	-0.05	-0.22
<b>D_112</b>	-0.02	-0.01
<b>D_113</b>	-0.02	-0.01
<b>D_114</b>	-0.90	-0.71
<b>D_115</b>	-0.49	-0.47
<b>D_116</b>	-0.05	-0.22
<b>D_117</b>	-0.03	-0.01

### 6.3.5. Test 11 & Test 12: Load at Quarter Point

Test 11 and Test 12 were located 14 feet south of midspan (at Section E from the instrumentation plans). Detailed information about the test set-ups for Test 11 and Test 12 are provided in Section 5.5.3.4. It was previously discovered that the two RRFCs behaved the same under applied load. Note that the south end of the West RRFC was not instrumented and the load distribution between the RRFCs was consequently unknown when load testing the East RRFC during Test 11. Therefore, the test was repeated on the West RRFC (Test 12) to determine the load distribution through the instrumented south end of the East RRFC. All data measurements from Test 11 and Test 12 can be found in tabular form in Appendix D for an applied load of 150 kips.

The East RRFC main girder stress results are presented in this section for Test 11 and Test 12 to show the load distribution between the loaded and unloaded RRFC main girders. Figure 6.21 shows the response of the main girder and exterior girders in Section E for Test 11. The load was located at Section E; therefore, the maximum moment in the bridge during Test 11 was at Section E. The load during Test 11 was moved closer to the support which created a smaller moment in the bridge, and resulted in lower maximum stress values for Test 11 compared to Test 5. Figure 6.22 shows the main girder stress results for Section E for Test 11 and Test 12. As expected, more load remains in the loaded RRFC than is distributed to the adjacent RRFC.

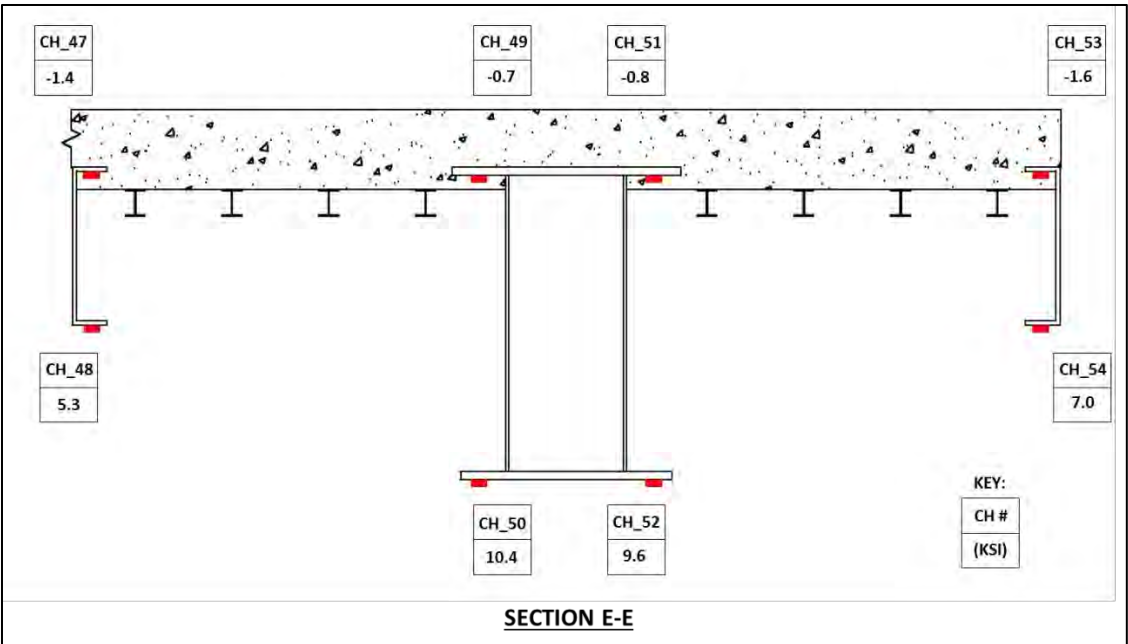


Figure 6.21: Test 11 response for Section E at an applied load of 150 kips

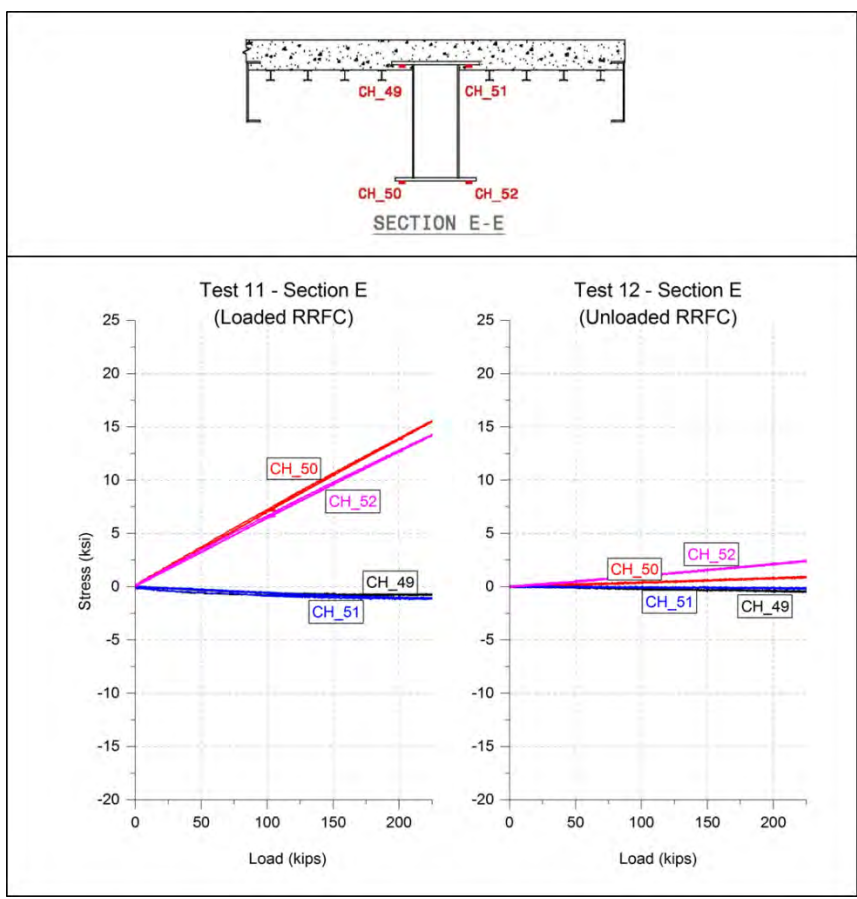


Figure 6.22: Test 11 & Test 12 main girder stress results for Section E

The main girder displacement results for Test 11 are shown in Table 6.5. The locations of the displacement sensors for Test 11 were the same as Test 5 and shown in Appendix D. The maximum displacement measurement occurred at D\_110, located at midspan, and was about 0.4 inches ( $L/1400$ ). This was a smaller maximum moment when compared to the load located at midspan (Test 5), as expected.

**Table 6.5: Displacement results for Test 11**

	<b>Test 11 at 225 kips</b>
<b>Sensor</b>	<b>Displacement (in)</b>
D_108	-0.01
D_109	-0.26
D_110	-0.42
D_111	-0.39
D_112	-0.02
D_113	0.00
D_114	-0.07
D_115	-0.10
D_116	-0.08
D_117	-0.01

#### **6.4. Fracture Test Results**

##### **6.4.1. Fracture Test 1 Results**

The first fracture test consisted of simulating a fracture in the East RRFC main girder. As mentioned in Section 5.6.1. , several loading attempts along with increasing the size of the initial flaw were needed to finally achieve sudden brittle fracture. Figure 6.23 shows the final fractured main girder. Fractures in the web propagated upward from the cuts made earlier (Figure 6.23B). These web cracks occurred during the last cooling process, before the final fracture load was applied, as a result of thermal stresses. One of these cracks bifurcated, and the other trifurcated. Also shown, the bottom flange fractured the remaining distance between initial flaws (a total of 6 inches) when subjected to an applied load of about 180 kips.

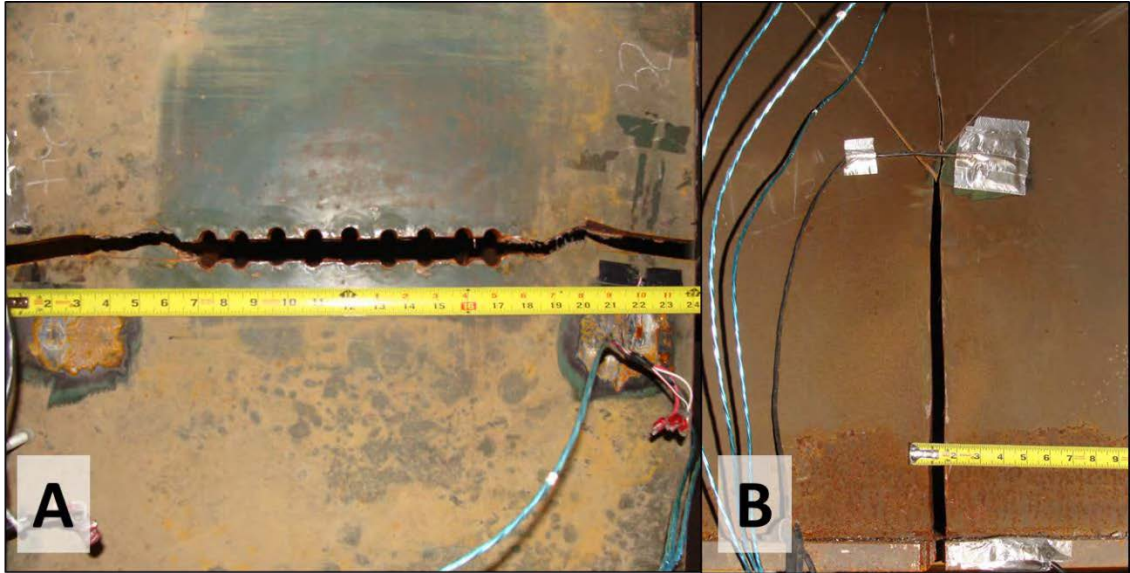


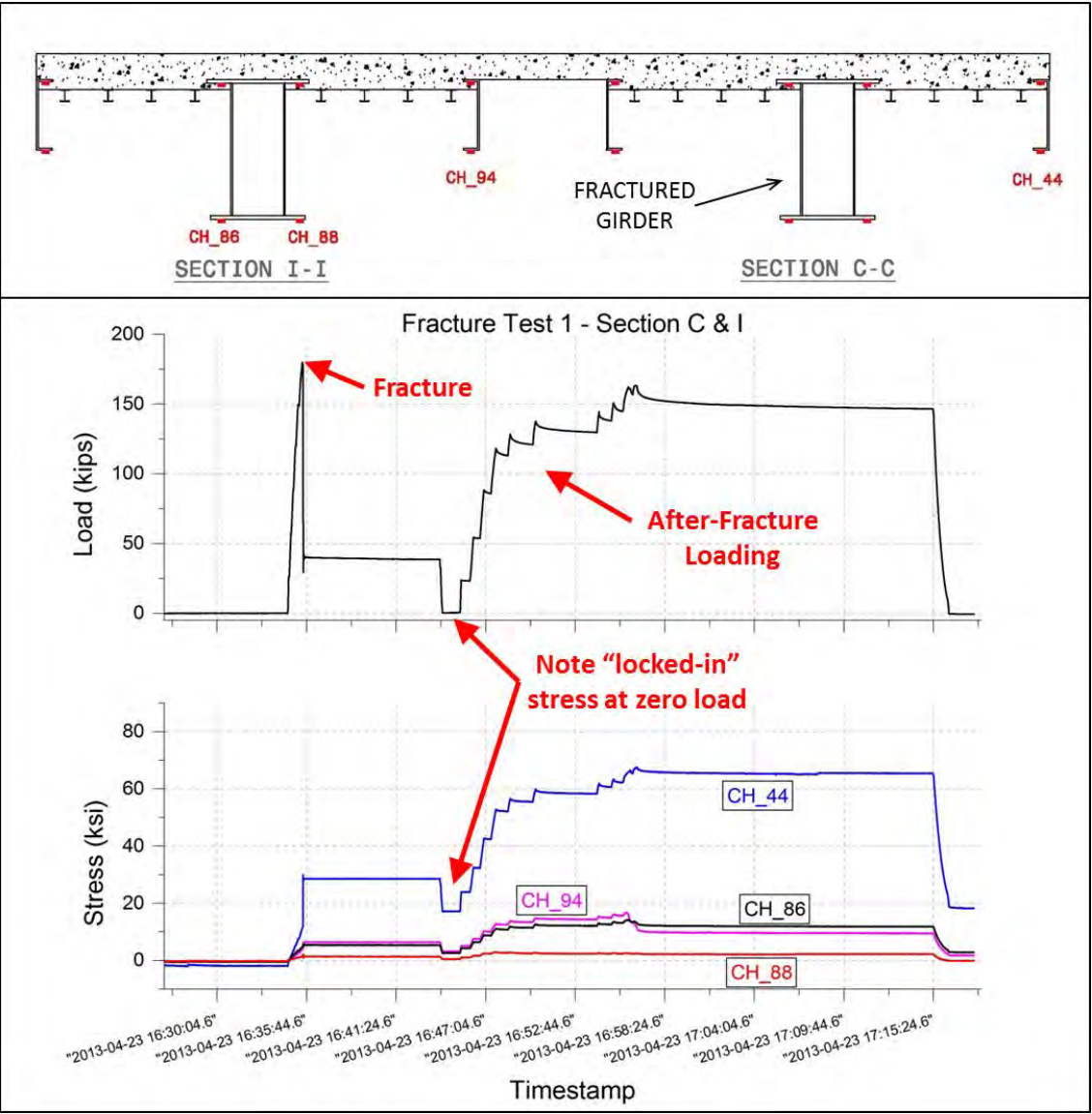
**Figure 6.23: Fracture Test 1 fractured main girder bottom flange (A) & web (B)**

#### *6.4.1.1. Fracture Test 1 Load Redistribution*

The goal of the first fracture test was to determine the load redistribution after one main girder fractured. In order to determine the new load path, the RRFC bridge was point loaded to 150 kips (about twice the weight of the AASHTO design truck) after the East RRFC main girder fractured. The following figures provide an overview of the load distribution within the RRFC bridge after fracture occurred. It is worth mentioning that several sensors and gages were damaged during the fracture test, including critical displacement sensors, rendering them unusable. Complete stress and displacement results due to the applied load for Fracture Test 1 can be found in Appendix D. The values presented in the appendix are at an after-fracture load of 0 kips (when the applied load was unloaded after fracture occurred), and at an after-fracture load of 75 kips. It is important to mention that during the higher post-fracture loads, locations of the RRFC material were likely yielding, and no longer responding with linear-elastic behavior. Thus, the stress values are presented at a sub-yield load of 75 kips. Significant yielding of the exterior girders in the fractured flatcar began at an after-fracture load of about 140 kips.

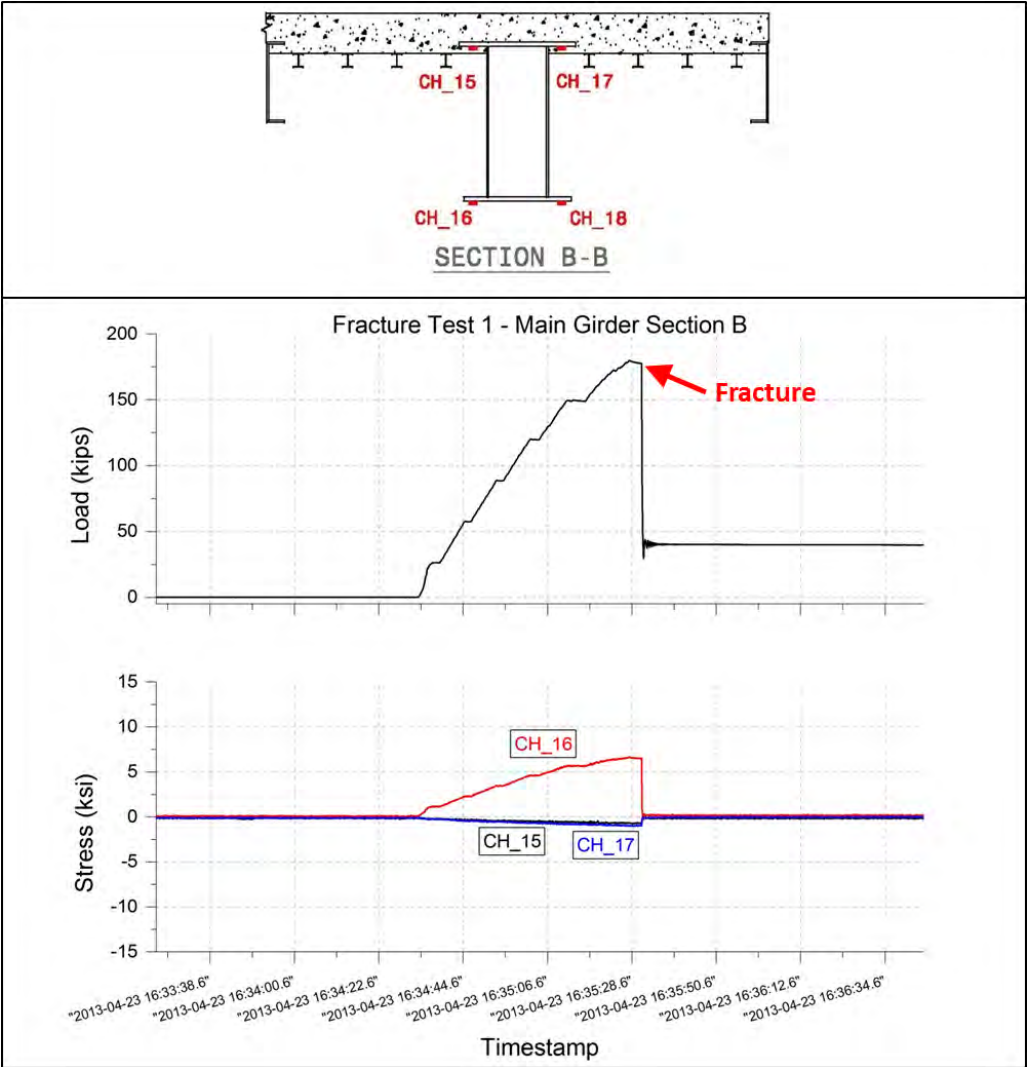


Figure 6.25 shows the stress data in Section C and Section I during the different loading stages. As shown in the load plot above, the East RRFC main girder fractured at a load of about 180 kips. After the fracture occurred, the entire load was taken off of the bridge, and then slowly reloaded to 150 kips. This was not the maximum load the bridge could sustain in a fracture state, rather a high enough load that was determined satisfactory to compare data to previous load tests. At the point of fracture, an increase in the stress in the outer exterior girder of the East RRFC (CH\_44) was observed. The plot shows that some stresses do not return to zero once the RRFC bridge was unloaded. This behavior indicates redistribution of the locked-in stresses, once carried by the East RRFC main girder, to the non-fractured members. These locked-in stresses include dead load stresses carried by the main girder and residual stresses within the main girder (it is noted that since no yielding was observed, the offsets are not attributed to nonlinear behavior). The stress measurement in the outer exterior girder of the fractured car (CH\_44) was about 8 ksi at an applied load of 75 kips before fracture (Test 5). At an applied load of 75 kips after fracture, the stress in this girder was about 21 ksi; about 2.5 times greater than the before-fracture measurement.



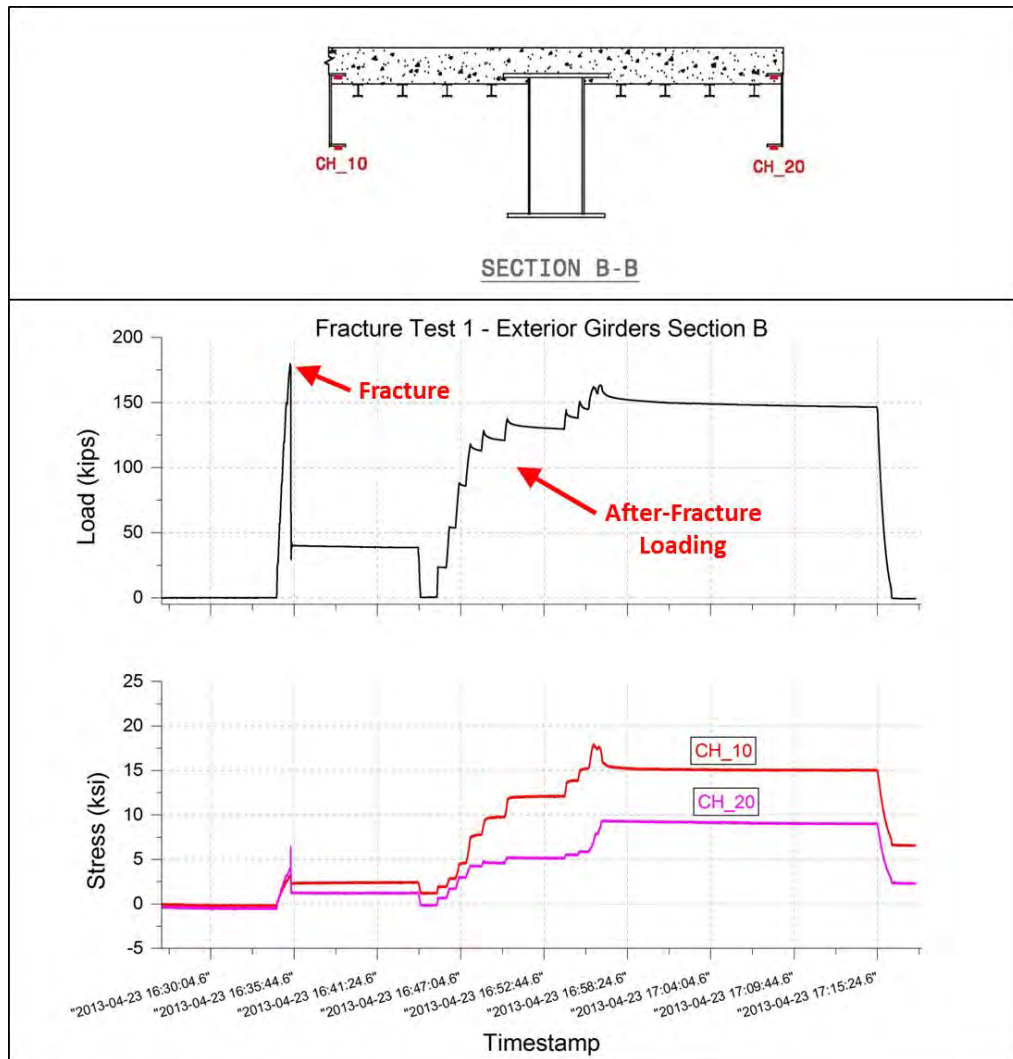
**Figure 6.24: Fracture Test 1 stress results at Sections C & I**

The strain gages on the bottom flange of the main girder at Section C (CH\_32 and CH\_34) were not working properly due to their location inside of the cooling chamber. Therefore, Figure 6.25 shows the close-up stress results at Section B for the main girder. As shown, the stress values immediately decrease at the time of fracture.



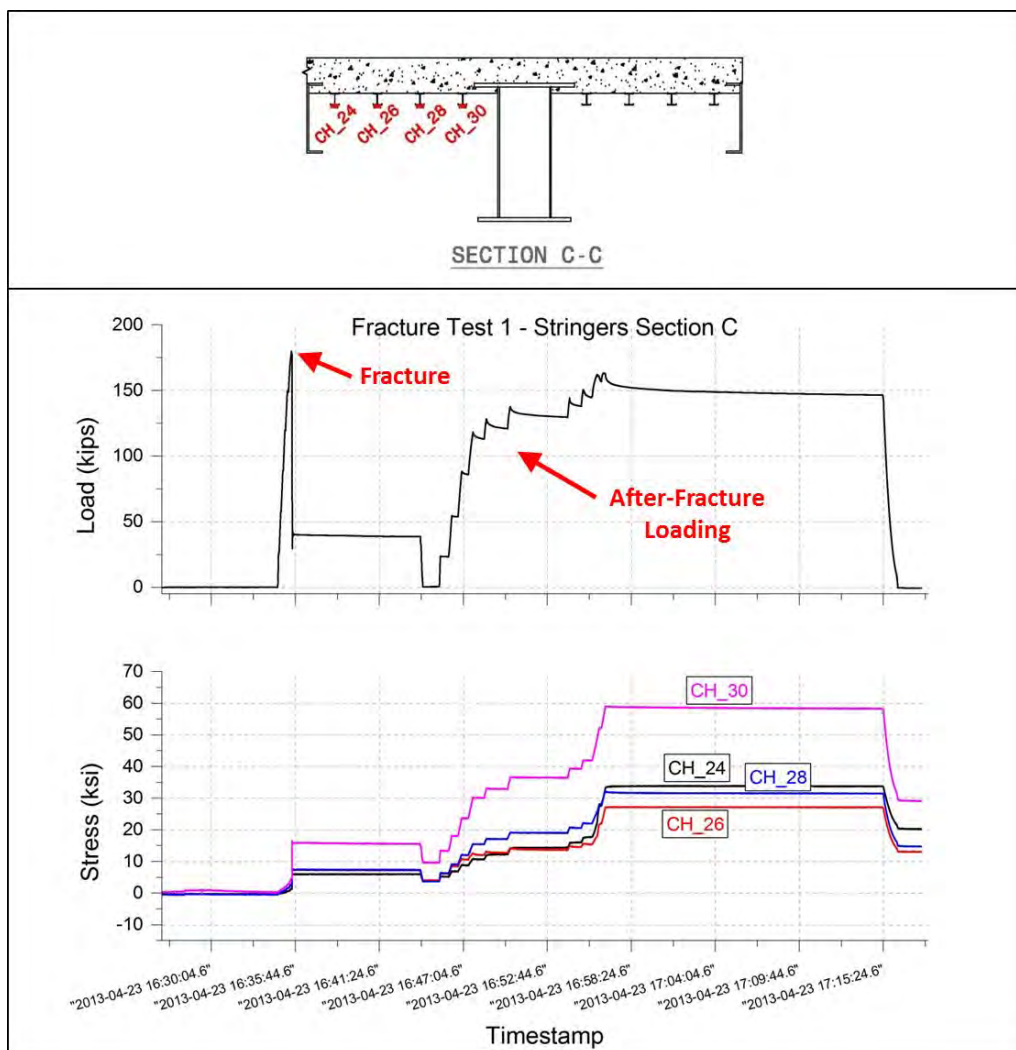
**Figure 6.25: Fracture Test 1 stress results at Section B**

Figure 6.26 shows the stress results of the bottom flanges of the exterior girders at Section B. An increase occurred in the gages when the East RRFC main girder fractured, indicating load redistribution into the exterior girders. The figure also shows the load in the exterior girders continued to increase with increasing load.



**Figure 6.26: Fracture Test 1 stress results at Section B (exterior girders)**

As shown in Figure 6.27, the stress values increased in the stringers of the East RRFC once fracture of the main girder occurred. These secondary members are located near the applied load, causing larger stresses in these members during after-fracture loading. The stringers shown in the figure increased about 6 times the stress measurements at these locations before fracture during Test 5 (Figure 6.12).



**Figure 6.27: Fracture Test 1 stress results at Section C (stringers)**

#### 6.4.1.2. Fracture Test 1 Concrete Deck Response

Damage to the composite concrete deck was observed following Fracture Test 1. As shown in Figure 6.28, separation between the shear connectors on the inner exterior girders and the concrete deck occurred near the supports. The separation can also be seen in Figure 6.29 at the south end of the West RRF. Separation was due to differences in deflection between the RRF and the continuous concrete deck. Concrete spalling was also observed near the inner exterior girders near midspan, where the load was applied. Delamination of the concrete deck occurred during Fracture Test 1, as shown in Figure 6.30. The delamination area was located near midspan of the East RRF under and

around the location of the applied load for this test. The length of the area was about 14 feet and the width was about 3 feet.



**Figure 6.28: Separation of shear stud in concrete deck after Fracture Test 1**



**Figure 6.29: Separation of concrete deck on West RRFC**

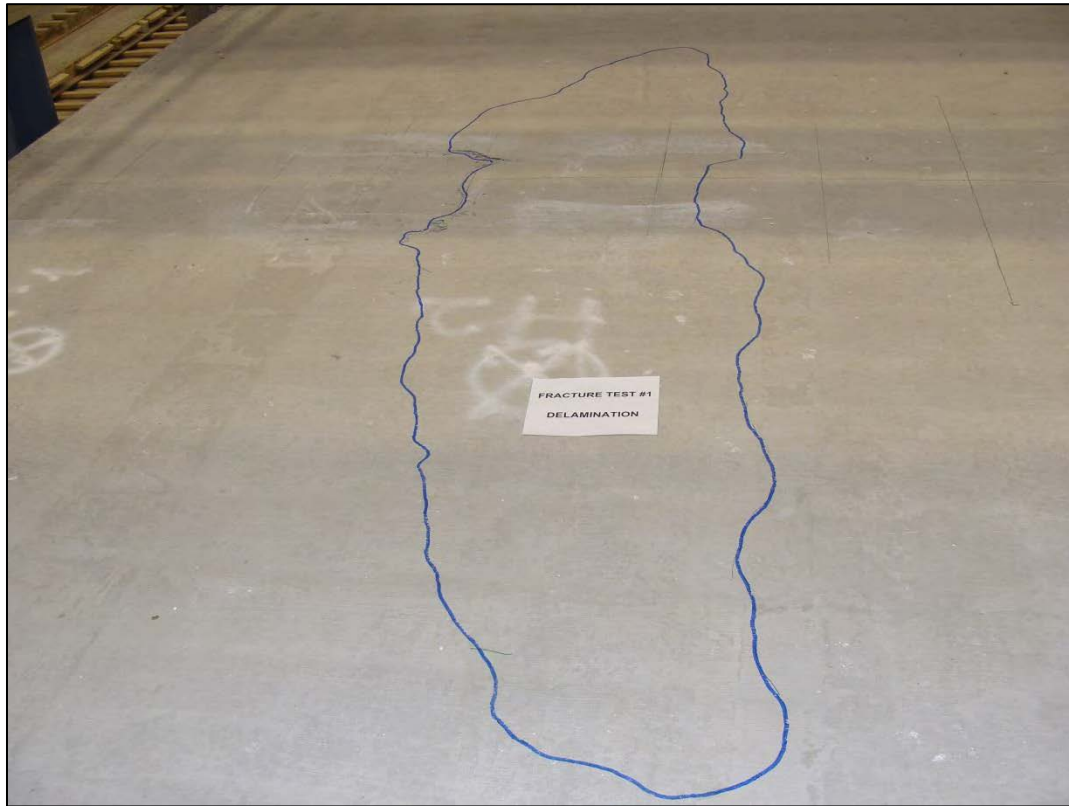


**Figure 6.30: Concrete deck delamination on East RRFC after Fracture Test 1**

#### **6.4.2. Fracture Test 2 Results**

The second fracture test consisted of simulating a fracture in the main girder of the West RRFC, with the East RRFC main girder already fractured. This fracture test demonstrated a worst case scenario of having both RRFC main girders fractured. Set-up of the second fracture test is explained in more detail in Section 5.6.2. As shown in Figure 6.31, fracture of the West RRFC main girder occurred at a relatively low load compared to first fracture. Following fracture of the main girder in the second RRFC, the RRFC bridge was loaded and unloaded several times. The figure shows that the maximum applied load was about 190kips, with both RRFC main girders fractured. Figure 6.32 shows the fractured main girder. As shown, the bottom flange fractured through, and then the crack continued about 2 feet up both webs. The web cracks arrested

approximately 3 inches from the bottom of the concrete deck, where ductile yielding was observed.

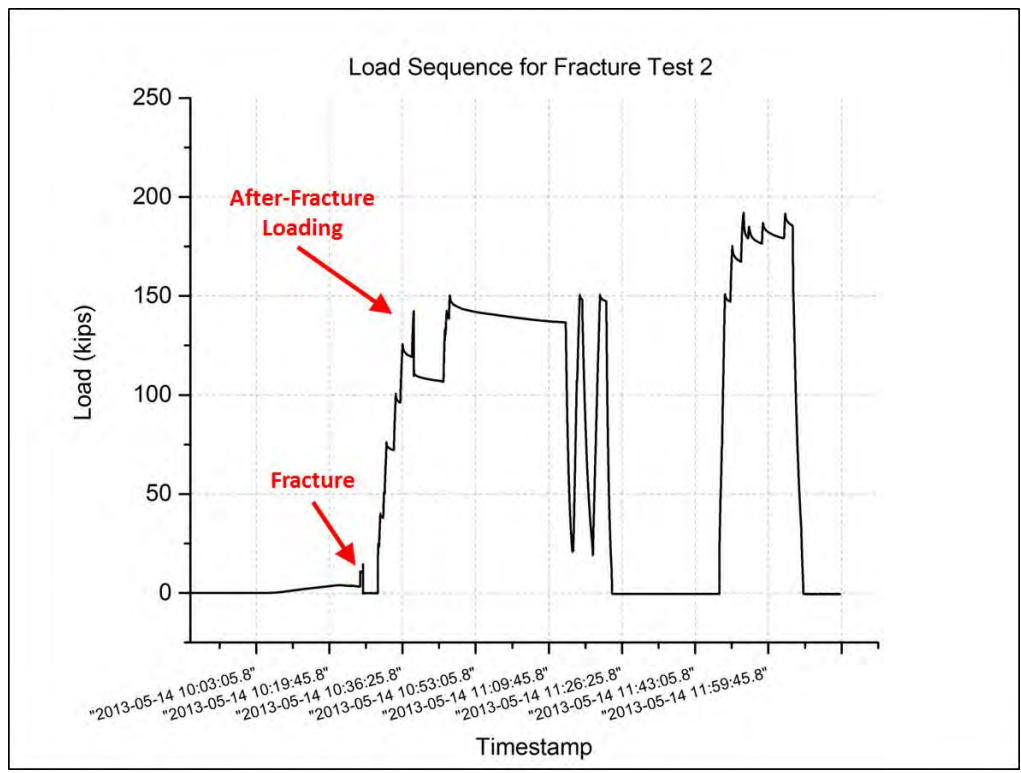


Figure 6.31: Fracture Test 2 load sequence



Figure 6.32: Fracture Test 2 fractured main girder web (A) & bottom flange (B)



#### *6.4.2.1. Fracture Test 2 Load Redistribution*

The main goal of the second fracture test was to observe the behavior of the RRFC bridge under load after both main girders were fractured. Data from strain gages were collected during the test; however, due to a large number of gages not working, the behavior is best shown through the displacement results in the following figures. Complete stress and displacement results for Fracture Test 2 can be found in Appendix D in tabular form. The values presented in the appendix are at an after-fracture load of 0 kips (when the applied load was unloaded after fracture occurred), and at an after-fracture load of 75 kips. It is important to mention that during the higher post-fracture loads, locations of the RRFC material were yielding, and no longer responding with linear-elastic behavior.

The locations of the displacement sensors were modified for Fracture Test 2 to better observe the response of the exterior girders. The revised plans are provided in Appendix D. The modification resulted in moving D\_114 to the West RRFC inner exterior girder near midspan; D\_116 remained on the main girder at the south quarter point and D\_115 remained on the main girder at midspan. D\_113 and D\_117 remained at the supports. Figure 6.33 shows the deflections during the fracture test, including the elastic rebound immediately after fracture. As shown, the main girder at midspan (D\_115) deflected 6.7 inches ( $L/85$ ) due to the maximum after-fracture load of 190 kips. A maximum permanent deflection of 4.5 inches ( $L/125$ ) at midspan remained at this location after removing the load.

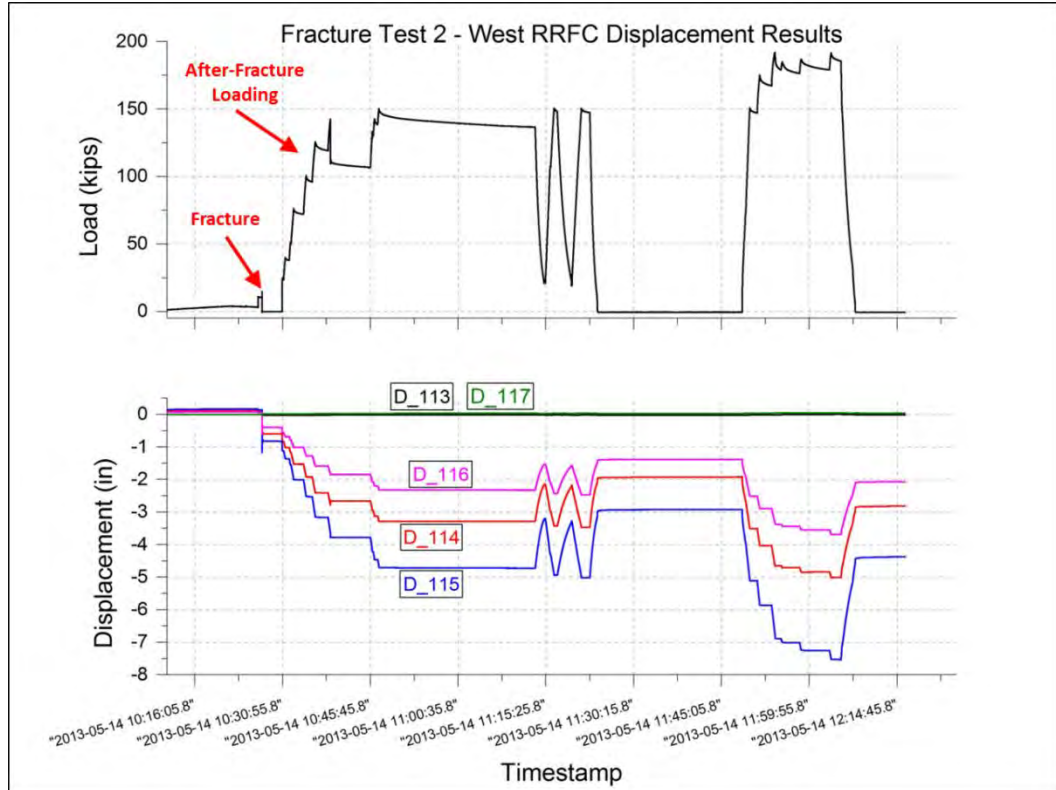


**Figure 6.33: West RRFC displacement results for Fracture Test 2**

The locations of the displacement sensors on the East RRFC were also modified and are presented in Appendix D. During this test, D\_110 and D\_111 were moved to the East RRFC inner exterior girder and outer exterior girder at midspan. D\_109 remained on the main girder at the north quarter point, and D\_108 and D\_112 remained at the supports. As shown in Figure 6.34, the East RRFC inner exterior girder (D\_110) deflected about 2.7 inches ( $L/210$ ) due to the maximum applied load of 190 kips. Both deflection figures above show permanent deflections at most instrumented locations after the applied load was completely removed.

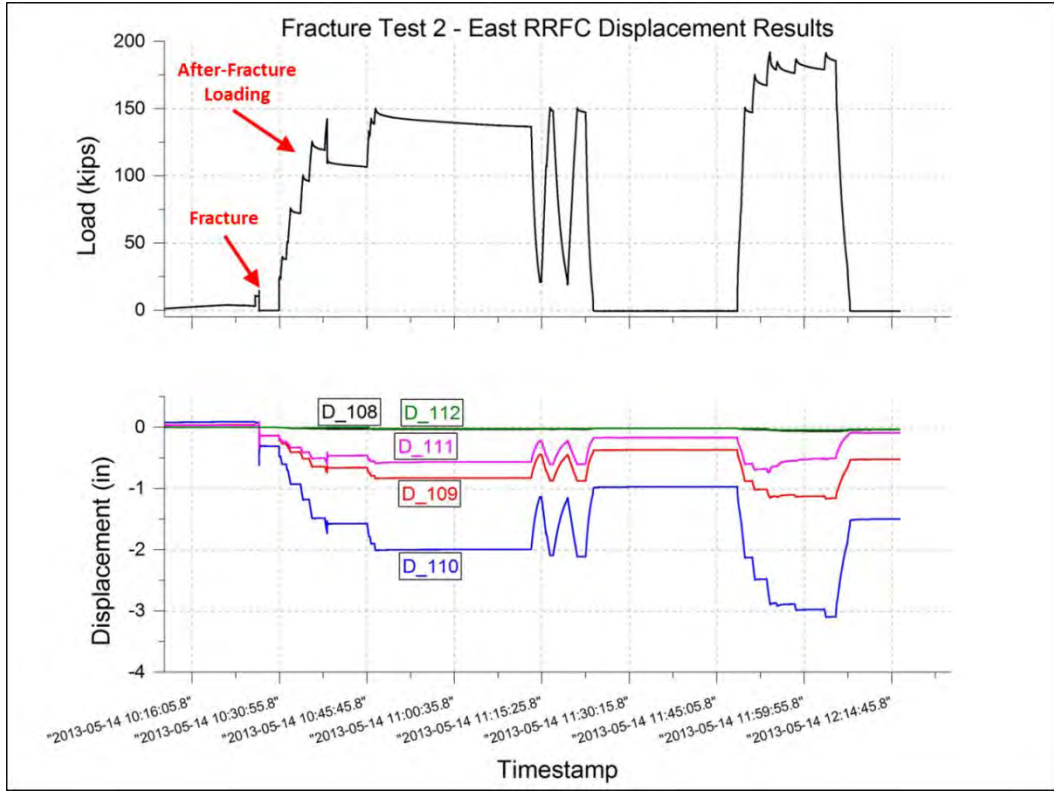


**Figure 6.34: East RRFC displacement results for Fracture Test 2**

Figure 6.35 and Figure 6.36 are images of the RRFC bridge loaded to 190 kips during Fracture Test 2, after both RRFC main girders were fractured. Large deformations can be seen in the RRFC steel structure and the concrete bridge deck. Although large displacements were present, the RRFC bridge remained capable of carrying and redistributing the 190 kip applied point load.



**Figure 6.35: After-fracture loading of RRFC bridge**



**Figure 6.36: After-fracture loading of RRFC bridge (deck view)**

#### 6.4.2.2. *Fracture Test 2 Concrete Deck Response*

Damage to the composite concrete deck was also observed after Fracture Test 2. Additional spalling occurred near the inner exterior girders (between RRFCs) near midspan. As shown in Figure 6.37, additional delamination of the concrete deck also occurred. The location of the delamination was under and around the applied load on the West RRFC. It was a smaller area compared to the delamination on the East RRFC after Fracture Test 1. The area was about 6 feet long and around 2 feet wide.

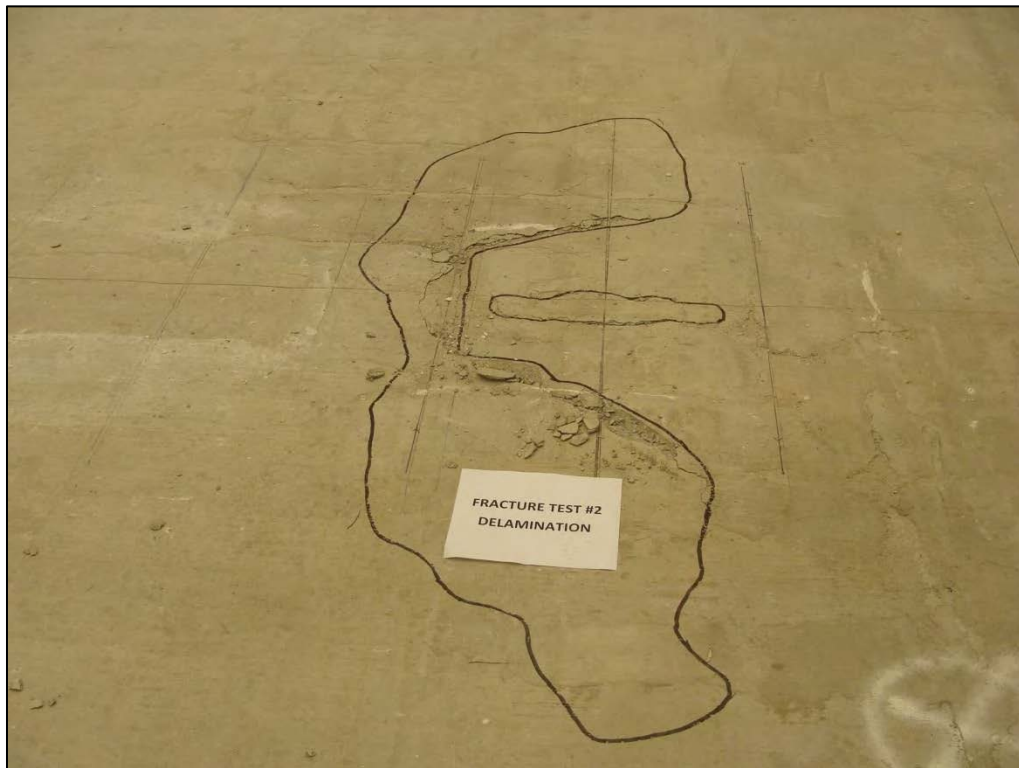


**Figure 6.37: Concrete deck delamination on West RRFC after Fracture Test 2**

## **CHAPTER 7. REVISIONS AND PROPOSED ADDITIONS TO LOAD RATING GUIDELINES**

The main objectives of this research were to evaluate the behavior of railroad flatcar bridges subjected to higher loads, demonstrate load-path redundancy in railroad flatcar bridges, and calibrate and revise the proposed load rating guidelines developed by Provines et al. (2011) in Phase I. The proposed load rating guidelines presented in this chapter were developed as a result of controlled load testing of the full-scale RRFC bridge in the laboratory. These guidelines were created as an addition to the proposed load rating guidelines developed in Phase I (Provines et al., 2011). They are intended to be used with the allowable stress load rating method in *AASHTO The Manual for Bridge Evaluation* (2011).

This chapter begins with discussing any recommended revisions to the proposed load rating guidelines developed in Phase I based on laboratory test results. The chapter continues with a discussion of additions to the proposed load rating guidelines and how they were developed using the instrumentation data. The additions discussed include: (1) load rating based on live load bending stress for RRFC bridges constructed with a composite concrete deck, (2) determining the available capacity in the remaining primary members after fracture occurs in one primary member, and (3) load rating based on live load shear stress.

### **7.1. Revisions to Phase I Load Rating Guidelines**

The proposed load rating guidelines developed in Phase I were focused on accurately estimating the live load bending stress in the longitudinal members of RRFC bridges. The research classified the main girders as primary members and determined that

these members undergo global bending due to the effects of a truck driving across the bridge. A “two stringer” effective section for the main girder was deemed adequate in resisting the global bending effects. This effective section included the structural shape of the main girder and two stringers on either side of the main girder. The research also stated that the exterior girders and stringers are secondary members and should be load rated based on local bending effects (Provines et al., 2011). Detailed information pertaining to the research study and development of these guidelines are discussed in Section 2.2.

Instrumentation data from the load tests performed on the laboratory RRFC bridge with no deck supported the conclusions made in Phase I to estimate the live load response of RRFCs. It was determined that the procedures previously developed accurately predict the response of the flatcars with reasonable conservatism. Therefore, no recommended changes are proposed to the existing load rating guidelines. However, additions regarding the behavior of a RRFC bridge constructed with a composite concrete deck and regarding the shear response are needed. The remaining discussion in this chapter is focused on the development to determine the live load response of RRFC bridges constructed with a composite concrete deck and recommendations for shear load rating.

## **7.2. Railroad Flatcar Bridges Constructed with a Composite Concrete Deck**

The first addition to the proposed load rating guidelines is a refined procedure to load rate bridges constructed from typical RRFCs and a fully composite concrete deck. A typical RRFC is defined as a flatcar with one main box girder and an exterior girder on either side of the main girder. The goal of this addition is to more accurately predict the maximum positive live load bending stress in the primary longitudinal members by using the same live load bending stress equation (Equation 2) developed in Phase I (Provines et al., 2011).

$$\sigma_{LL} = (\alpha) (CDF) \frac{(DF) M_{LL}}{S_{eff}}$$

**Equation 2: Live load bending stress equation developed in Phase I (Provines et al., 2011).**

where:

$\sigma_{LL}$  = Maximum positive live load bending stress

$\alpha$  = Stress modification factor

$CDF$  = Car distribution factor

$DF$  = Distribution factor

$M_{LL}$  = Maximum positive live load moment

$S_{eff}$  = Effective section modulus

The primary members of the RRFC bridge in the laboratory were the main girders and exterior girders. These members carried the majority of the applied load. The main girders and exterior girders were made fully composite with the concrete deck by the use of shear connectors. The exterior girders were unaltered, allowing the ability to weld shear connectors to their top flange. The procedures developed are applicable to flatcars with primary members that are made fully composite with a concrete deck.

The steps to predict the live load bending stress in a primary member begins with calculating the live load moment for a single lane loaded as specified in *AASHTO The Manual for Bridge Evaluation* (2011). This step is typically formed by assuming a beam line model of the bridge and computing the maximum live load moment due to the design truck. Next, the live load moment is distributed to each flatcar by using a distribution factor. The moment within each flatcar is then distributed to each primary member by the car distribution factor. Finally, this moment is resisted by an effective section, which in this case, is the composite section of the member.



The procedures were developed using data from the controlled load tests performed on the RRFC bridge in the laboratory. The refined components of the live load bending stress equation for this application are the effective section, girder distribution factors (distribution factor and car distribution factor), and the stress modification factor. The development of these components is discussed in the following sections.

### **7.2.1. Effective Section**

The effective section to resist live load bending effects for each primary member was developed based on stress measurements from controlled load tests. The primary members include the main girders and exterior girders when utilizing a composite concrete deck. The top flange stress values were near zero, indicating that the neutral axis of the composite section was near this location (as shown in Figure 6.13). Therefore, the bottom flange stress values of the main girders and exterior girders were used in determining the appropriate effective section.

Based on *AASHTO LRFD Bridge Design Specifications* (2012), the structural shape of the member plus its effective width of the concrete deck was assumed to be the effective section for each primary member. The stringers were not included in the effective section calculations. As mentioned, these members were close to the neutral axis of the cross section and did not provide a substantial contribution. The proposed effective section was calibrated using the stress data and was found to adequate when not including the stringers. Figure 7.1 shows the assumed effective sections for each primary member at Section C and Section I (near midspan). The deck widths shown were transformed using a modular ratio of 7 to compute the section properties of the composite section, provided in Table 7.1.

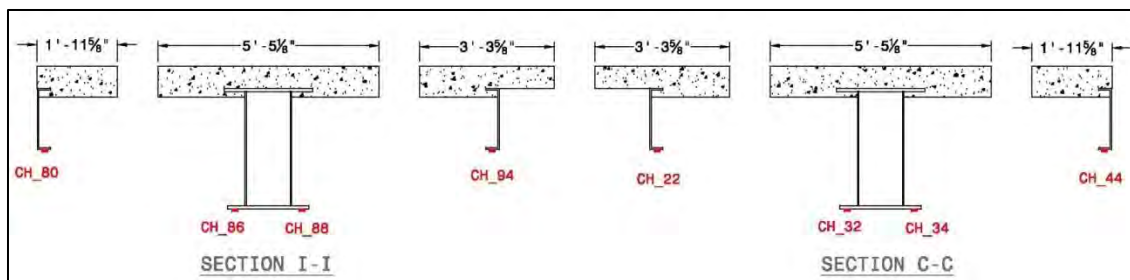


**Figure 7.1: Assumed effective sections for each primary member near midspan**

**Table 7.1: Composite section properties**

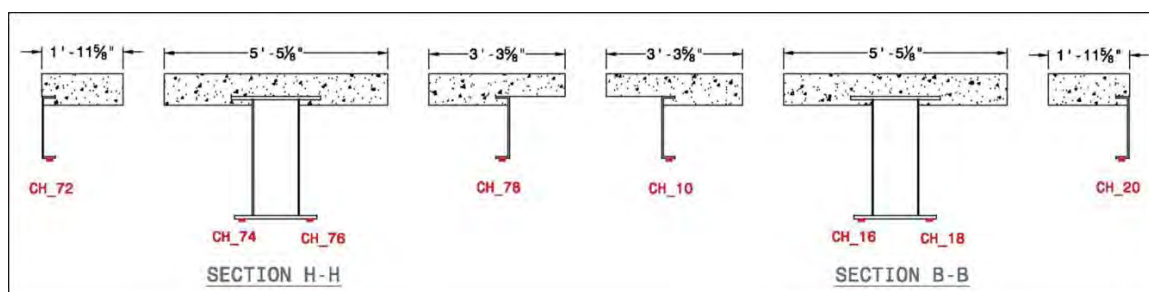
Member	$I$ (in <sup>4</sup> )	$A$ (in <sup>2</sup> )	$y_{bot}$ (in)	$S_{bot}$ (in <sup>3</sup> )
Outer Exterior Girder	1,732	43	17.1	101
Main Girder	31,602	153	28.6	1,105
Inner Exterior Girder	1,985	59	18.2	109

The bridge moment computed using the assumed effective sections was compared to the theoretical bridge moment for Sections C and Section I. The bottom flange stresses, at an applied load of 75 kips, were multiplied by the effective section modulus ( $S_{bot}$ ) for each primary member to obtain the moment in that member. All gages remained below the yield stress at an applied load of 75 kips for the first fracture test, discussed in a later section. Therefore, stress measurements at 75 kips was chosen to be analyzed for before-fracture tests as well. These moments were summed to determine the total bridge moment at that cross section. The theoretical bridge moment was computed based on a beam line model of the bridge, with an applied point load of 75 kips at midspan. These calculations were made for Test 5, Test 6, and Test 10. The results are shown in Table 7.2. The comparison results in an average under-prediction of about 2% between the total bridge moment calculated based on test results and the theoretical bridge moment.

**Table 7.2: Total bridge moment near midspan**

75kip Point Load at Midspan							
RRFC	Member	TEST 5 - SECTIONS C & I		TEST 6 - SECTIONS C & I		TEST 10 - SECTIONS C & I	
		Bottom Flange Stress (ksi)	Member Moment (kft)	Bottom Flange Stress (ksi)	Member Moment (kft)	Bottom Flange Stress (ksi)	Member Moment (kft)
East RRFC (Loaded)	Outer Exterior Girder (CH_44)	4.0	33.7	4.6	39.2	0.7	5.6
	Main Girder (CH_32 & CH_34)	6.5	602.0	6.3	583.6	3.9	360.5
	Inner Exterior Girder (CH_22)	2.9	26.0	3.3	30.4	4.3	39.4
West RRFC (Unloaded)	Inner Exterior Girder (CH_94)	1.7	15.0	1.9	17.0	4.5	41.0
	Main Girder (CH_86 & CH_88)	1.4	125.0	1.4	130.1	4.0	364.2
	Outer Exterior Girder (CH_80)	-0.01	-0.1	-0.03	-0.2	0.7	5.8
Total Bridge Moment (kft)		802		800		817	
Theoretical Bridge Moment (kft)		825		825		825	

A similar comparison was performed for Section B and Section H, near the span quarter points. The assumed effective sections were the same as computed for Section C and Section I. Figure 7.2 shows these effective sections, as well as the strain gage locations. The results of the comparison are shown in Table 7.3 for Test 5, Test 6 and Test 10. An average under-prediction of about 12.5% exists between the total bridge moment calculated based on test results and the theoretical bridge moment. The larger difference between the actual and calculated bridge moment could be attributed to a slight change in the effective section of the members at the quarter point cross section, compared to at midspan.

**Figure 7.2: Assumed effective sections for each primary member near quarter point**

**Table 7.3: Total bridge moment near quarter point**

75kip Point Load at Midspan							
RRFC	Member	TEST 5 - SECTIONS B & H		TEST 6 - SECTIONS B & H		TEST 10 - SECTIONS B & H	
		Bottom Flange Stress (ksi)	Member Moment (kft)	Bottom Flange Stress (ksi)	Member Moment (kft)	Bottom Flange Stress (ksi)	Member Moment (kft)
East RRFC (Loaded)	Outer Exterior Girder (CH_20)	1.9	16.3	1.7	14.3	0.8	6.4
	Main Girder (CH_16 & CH_18)	2.7	244.2	2.7	248.2	1.7	155.8
	Inner Exterior Girder (CH_10)	1.1	10.4	1.0	8.7	1.0	8.8
West RRFC (Unloaded)	Inner Exterior Girder (CH_78)	0.8	6.9	0.7	6.1	1.0	9.4
	Main Girder (CH_74 & CH_76)	0.8	75.3	0.8	75.5	1.8	169.4
	Outer Exterior Girder (CH_72)	0.1	1.0	0.1	1.1	0.8	6.4
Total Bridge Moment (kft)		354		354		356	
Theoretical Bridge Moment (kft)		406		406		406	

### 7.2.2. Girder Distribution Factors Using Spring Analogy

The distribution factor (DF) and car distribution factor (CDF) represent the portion of the total live load bridge moment carried by each flatcar and by each primary member within the flatcar, respectively. These girder distribution factors were determined for the laboratory RRFC bridge based on experimental stress data and the assumed effective sections described in Section 7.2.1.

The spring analogy, developed to predict the live load response of slab-on-girder bridges, was used to determine the distribution factor and car distribution factor for additional cases besides that of the laboratory RRFC bridge. A detailed background of the spring analogy is provided in Section 2.5. In the spring analogy, the girders are represented as parallel rotational springs based on relative stiffness values. The concrete deck is represented by flexible torsion bars between the rotational springs. The live load is applied to the idealized system as applied moments at the center of each wheel location. The simplified model is shown in Figure 7.3. The system is then analyzed to determine the rotational reaction of each spring; these reactions are the girder distribution factors of the actual system (Akinci et al., 2013).

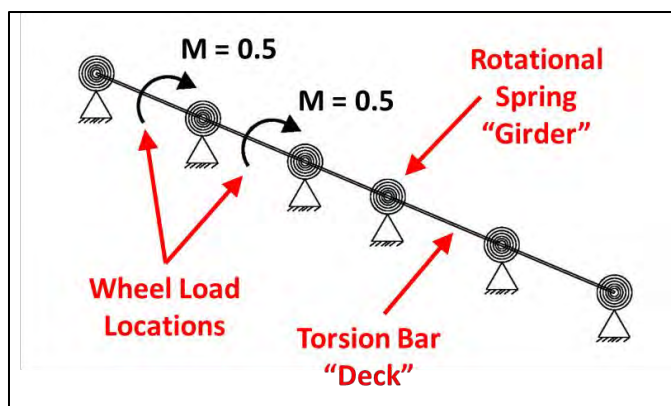


**Figure 7.3: RRFC bridge modeled using the spring analogy**

#### 7.2.2.1. Model Calibration

The idealized model of the RRFC bridge was calibrated in SAP2000 using data from the controlled load tests and the assumed effective section. The rotational stiffness values assigned to each spring were based on relative flexural stiffness values of the composite section of the primary members. The main girder was assigned a rotational stiffness value of unity and the exterior girders were assigned a value equal to the ratio of the moment of inertia of the exterior girder composite section to moment of inertia of the main girder composite section. Uncracked section properties were used and the contribution of rebar and stringers was ignored. The relative stiffness values for the RRFC bridge in the laboratory are shown in Table 7.4.

**Table 7.4: Stiffness values used for spring analogy calibration**

RRFC	Primary Member	Member Label	$I$ (in <sup>4</sup> )	Relative Stiffness
East RRFC (Loaded)	Outer Exterior Girder	EXT <sub>o</sub>	1,732	0.05
	Main Girder	MAIN	31,602	1.00
	Inner Exterior Girder	EXT <sub>i</sub>	1,985	0.06
West RRFC (Unloaded)	Inner Exterior Girder	EXT <sub>i</sub>	1,985	0.06
	Main Girder	MAIN	31,602	1.00
	Outer Exterior Girder	EXT <sub>o</sub>	1,732	0.05

After assigning the rotational stiffness values to the springs, the relative stiffness of the torsion bar in the model was determined by calibrating the model with the actual

girder distribution factors determined from the measured stress values during Test 5, Test 6, and Test 10. The actual girder distribution factors were calculated by dividing the member moment by the total applied moment. The relative stiffness of the torsion bar between one exterior girder and one main girder was calibrated to be 3.3. The relative stiffness of the segment between the two inner exterior girders (i.e., between the flatcars), was determined to be 0.33. These calibrated values accounted for the contribution of the concrete deck, floorbeams, and other elements which assist in the longitudinal load distribution of the live load. Table 7.5 compares the actual girder distribution factors, obtained using measured data, to the girder distribution factors determined by the model.

**Table 7.5: Comparison of actual versus model girder distribution factors (GDF)**

RRFC	Member	Test 5		Test 6		Test 10	
		Actual GDF	Model GDF	Actual GDF	Model GDF	Actual GDF	Model GDF
East RRFC (Loaded)	EXT <sub>o</sub>	0.04	0.04	0.05	0.04	0.01	0.02
	MAIN	0.75	0.75	0.73	0.73	0.44	0.44
	EXT <sub>i</sub>	0.03	0.04	0.04	0.05	0.05	0.03
West RRFC (Unloaded)	EXT <sub>i</sub>	0.02	0.01	0.02	0.01	0.05	0.03
	MAIN	0.16	0.15	0.16	0.16	0.45	0.44
	EXT <sub>o</sub>	0.00	0.00	0.00	0.00	0.01	0.02

The girder distribution factor was separated into a distribution factor and a car distribution factor. The distribution factor represents the portion of the live load moment distributed between each flatcar. The car distribution factor represents the portion of the live load moment in the flatcar distributed to each primary member within that flatcar. The separation of the girder distribution factor into the distribution factor and car distribution factor for Test 5 is shown in Table 7.6. As shown, the model is an adequate representation of the actual data. The results for Test 6 and Test 10 can be found in Appendix E.

**Table 7.6: Test 5 Distribution factors (DF) and car distribution factors (CDF)**

RRFC	Member	Test 5					
		Actual GDF	Model GDF	Actual DF	Model DF	Actual CDF	Model CDF
East RRFC (Loaded)	EXT <sub>0</sub>	0.04	0.04	0.82	0.83	0.05	0.05
	MAIN	0.75	0.75			0.91	0.90
	EXT <sub>1</sub>	0.03	0.04			0.04	0.05
West RRFC (Unloaded)	EXT <sub>1</sub>	0.02	0.01	0.18	0.16	0.11	0.06
	MAIN	0.16	0.15			0.89	0.94
	EXT <sub>0</sub>	0.00	0.00			0.00	0.00

#### 7.2.2.2. Parametric Study

A parametric study was performed on the calibrated spring model to incorporate a variety of geometry cases for RRFC bridges with a fully composite concrete deck. Combinations of the following parameters were studied: (1) the relative flexural stiffness ratio of the exterior girders, (2) the clear distance between flatcars, and (3) the transverse location of the truck wheels. The different values considered for each parameter are presented in Table 7.7, Table 7.8, and Table 7.9. A drawing to define the parameter variables is presented in Figure 7.4.

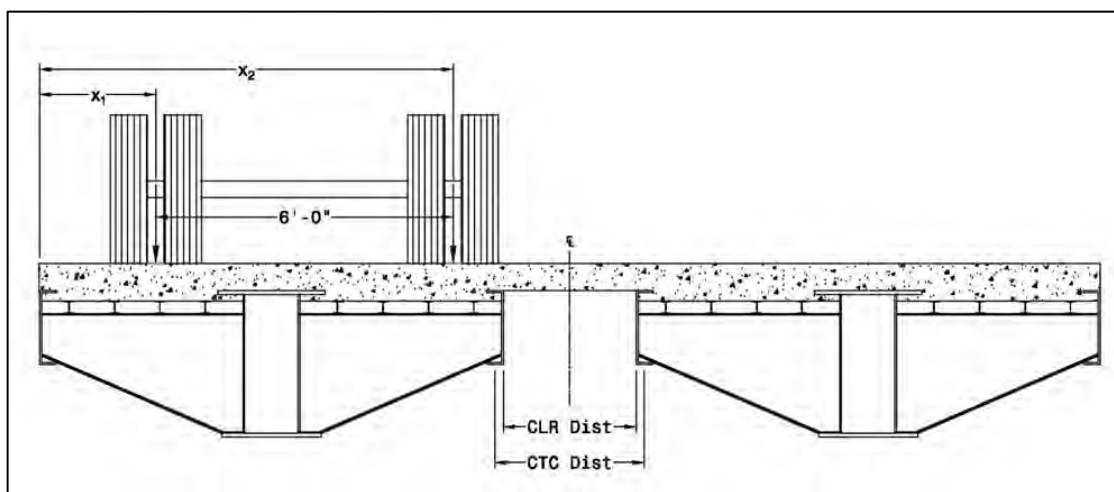


**Figure 7.4: Schematic for “DIST” and “LOC”**

**Table 7.7: Relative flexural stiffness values for parametric study**

Relative Flexural Stiffness						
RRFC	Member	Trial				
		REL1*	REL2	REL3	REL4	REL5
East RRFC (Loaded)	EXT <sub>O</sub>	0.055	0.15	0.25	0.5	0.75
	MAIN	1	1	1	1	1
	EXT <sub>I</sub>	0.063	0.15	0.25	0.5	0.75
West RRFC (Unloaded)	EXT <sub>I</sub>	0.063	0.15	0.25	0.5	1
	MAIN	1	1	1	1	0.75
	EXT <sub>O</sub>	0.055	0.15	0.5	0.5	1

\*Corresponds to laboratory test

**Table 7.8: Distance between flatcars for parametric study**

Distance Between RRFCs		
Trial	Distance (in)	
	Clear Distance	Center-to-Center
DIST1	18	21.9375
DIST2	24	27.9375
DIST3*	32.25	36.1875
DIST4	48	51.9375
DIST5	54	57.9375
DIST6	64.5	68.4375
DIST7	72	75.9375

\*Corresponds to laboratory test

**Table 7.9: Truck wheel locations for parametric study**

Truck Locations		
Trial	Absolute Distance (in)	
	x <sub>1</sub>	x <sub>2</sub>
LOC1	7.875	79.875
LOC2*	18.125	90.125
LOC3	30.125	102.125
LOC4	42.125	114.125
LOC5	66.125	138.125
LOC6	90.375	162.375

\*Corresponds to laboratory test

The relative flexural stiffness values for the exterior girders varied from 5 percent to 75 percent of the main girder flexural stiffness. Trial REL1 in Table 7.7 represents the



actual relative stiffness values for the RRFC bridge in the laboratory. The clear distance between flatcars was varied from 1.5 feet to 6 feet, with DIST3 representing the laboratory bridge. The values shown in Table 7.8 represents the center-to-center distance between the inner exterior girders (between flatcars), or the distance between the representative springs in the model. Finally, the location of the truck varied in the transverse direction of the RRFC bridge, with LOC2 representing the location of the axle load in Test 6 performed on the laboratory bridge. The truck coordinates are relative to the outer face of the East RRFC. Drawings of the different truck locations can be found in Appendix E.

Two studies were performed to determine the distribution factor and car distribution factor for a RRFC bridge with a fully composite concrete deck. The first study involved setting the distance between the adjacent flatcars to a constant value while varying the relative flexural stiffness values and the transverse truck location. The parameter combinations for the first study are shown in Table 7.10. The second study kept a constant transverse truck location and allowed different relative flexural stiffness values with varying distances between the adjacent flatcars, as shown in Table 7.11.

**Table 7.10: Parametric Study 1 combinations**

STUDY 1						
DIST3						
<b>REL1</b>	LOC1	LOC2	LOC3	LOC4	LOC5	LOC6
<b>REL2</b>	LOC1	LOC2	LOC3	LOC4	LOC5	LOC6
<b>REL3</b>	LOC1	LOC2	LOC3	LOC4	LOC5	LOC6
<b>REL4</b>	LOC1	LOC2	LOC3	LOC4	LOC5	LOC6
<b>REL5</b>	LOC1	LOC2	LOC3	LOC4	LOC5	LOC6

**Table 7.11: Parametric Study 2 combinations**

STUDY 2							
LOC2							
<b>REL1</b>	DIST1	DIST2	DIST3	DIST4	DIST5	DIST6	DIST7
<b>REL2</b>	DIST1	DIST2	DIST3	DIST4	DIST5	DIST6	DIST7
<b>REL3</b>	DIST1	DIST2	DIST3	DIST4	DIST5	DIST6	DIST7
<b>REL4</b>	DIST1	DIST2	DIST3	DIST4	DIST5	DIST6	DIST7
<b>REL5</b>	DIST1	DIST2	DIST3	DIST4	DIST5	DIST6	DIST7

### 7.2.2.3. *Distribution Factor Results*

The results of the two parametric studies to determine the distribution factor are presented in this section. It is important to mention that the model determined girder distribution factors, which is the proportion of the total live load bridge moment distributed to each primary member. The girder distribution factors were separated into distribution factors and car distribution factors. Distribution factors are the proportion of the total live load bridge moment distributed to each flatcar.

As expected, both parametric studies showed that the distribution factor depends on the relative flexural stiffness, the transverse location of the truck wheels, and the clear distance between flatcars. The results of Study 1 showed the contribution of the relative flexural stiffness (Figure 7.5) and the transverse location of the truck wheels (Figure 7.6) to the distribution factor. The location of the truck wheels and the distance between the flatcars were kept constant in Figure 7.5. As shown in the figure, as the stiffness of the exterior girders increased relative to the main girder, more of the live load moment remained in the loaded flatcar and less was distributed to the unloaded flatcar. Similar behavior was observed for the other truck location cases when varying the relative flexural stiffness of the exterior girders.

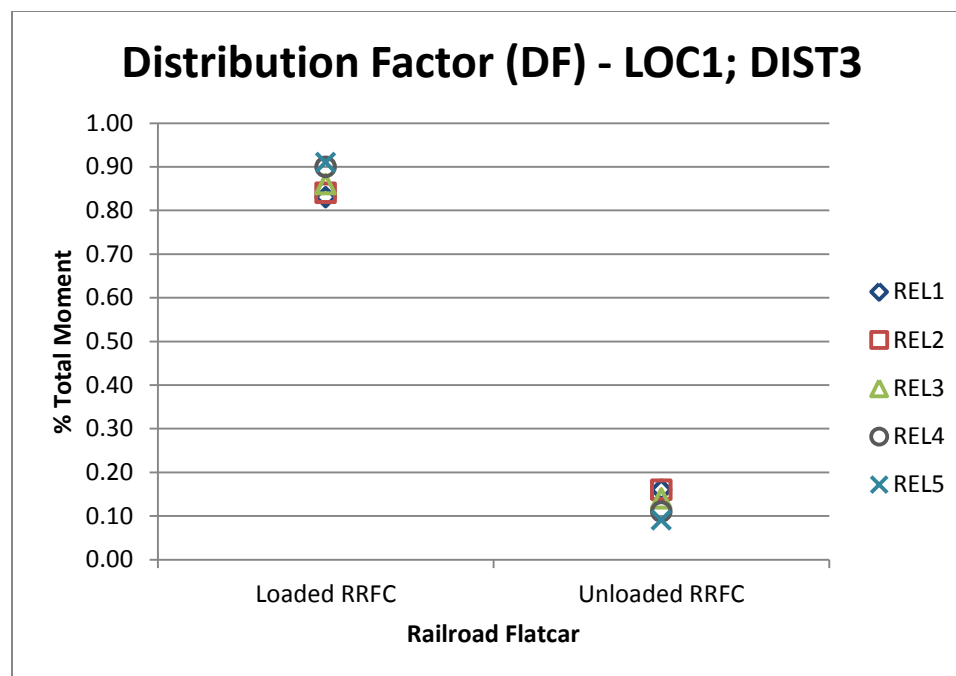


**Figure 7.5: Parametric Study 1 results varying relative stiffness**

The relative flexural stiffness of the members and distance between flatcars were kept constant in Figure 7.6. Drawings of the different truck locations are presented in Appendix E. The figure shows that a larger amount of load was distributed to the unloaded RRFC once the inside wheel ( $X_2$ ) crossed the bridge centerline (LOC5 and LOC6). Similar behavior was seen for the other relative flexural stiffness values considered. In fact, two distinct categories of distribution were observed, as shown in the figure. Specifically the two categories are as follows: (1) when the location of the inside wheel is inside the bridge centerline (LOC1-LOC4) and (2) when the location of the inside wheel crosses the bridge centerline (LOC5 and LOC6). If the first category is satisfied, the distribution factor would also depend on the spacing between the flatcars. The results of the second parametric study showed that as the distance between the two flatcars increases, the load distributed to the unloaded flatcar decreases (Figure 7.7). The distribution factors for the second category were developed as a result of Table 7.12. As shown, the sum of the “loaded” and “unloaded” distribution factors is greater than 1. An envelope of data was considered when determining the distribution factors; therefore, the peak values when considering LOC5 and LOC6 were used. For example, Figure 7.6

shows the peak value of 0.57 when considering LOC5 and LOC6 for the “Loaded RRFC,” controlled by LOC5. The remaining results for Study 1 can be found in tabular form in Appendix E.

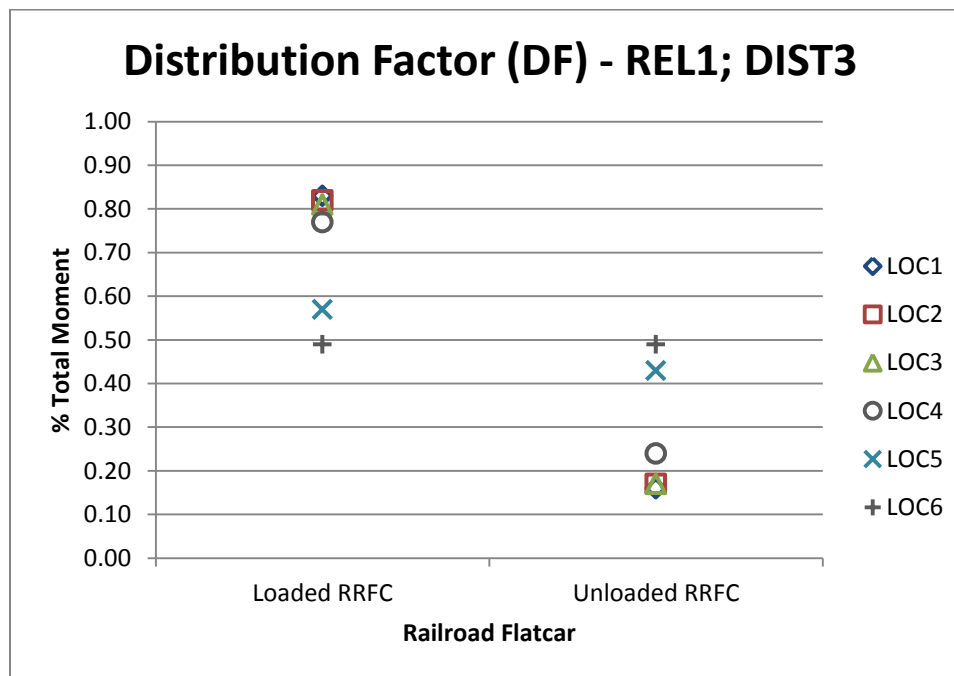


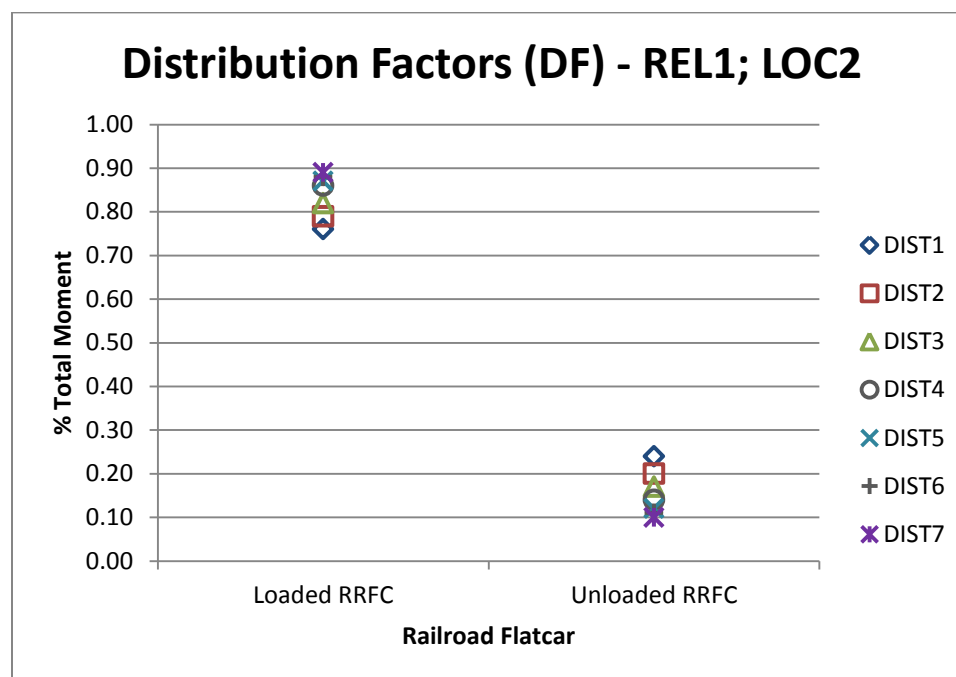
Figure 7.6: Parametric Study 1 results varying truck location

Table 7.12: Maximum distribution factors for LOC5-LOC6

Maximum Distribution Factor (DF)		
LOC5 - LOC6; DIST3		
RRFC	EAST RRFC	WEST RRFC
	(Loaded)	(Unloaded)
REL1	0.57	0.49
REL2	0.57	0.50
REL3	0.57	0.51
REL4	0.58	0.50
REL5	0.59	0.50

Distribution factors were evaluated when varying the distance between two adjacent flatcars in Study 2. Figure 7.7 shows the results of the study for REL1. The figure shows that as the distance between RRFCs increases, the load distributed to the unloaded flatcar decreases. In other words, more of the live load remained in the loaded

RRFC. Similar behavior was observed for the other relative flexural stiffness cases. The remaining results of Study 2 can be found in tabular form in Appendix E.

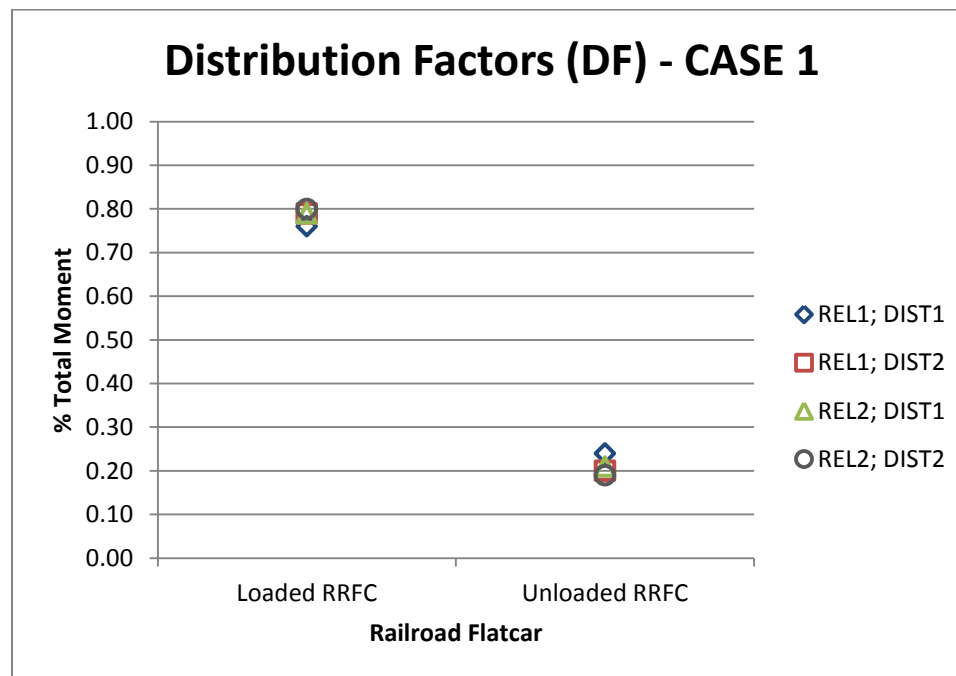


**Figure 7.7: Parametric Study 2 when varying distance between flatcars**

Similar distribution factor values were observed for certain distances between RRFCs. For example, DIST1 and DIST2 showed close-to-similar results, as shown in Figure 7.7. Based on similar distribution factors determined in Study 2, three categories were developed to determine the distribution factors: (1) the distance between RRFCs is less than or equal to 2 feet (DIST 1 and DIST2), (2) the distance between RRFCs is greater than 2 feet and less than or equal to 4 feet (DIST3 and DIST4), and (3) the distance between RRFCs is greater than 4 feet and less than or equal to 6 feet (DIST5-DIST7).

As an example, Figure 7.8 shows the distribution factors for Case 1. Case 1 includes stiffness ratios less than or equal to 15% (REL1 and REL2), and distances between the adjacent flatcars that are less than or equal to 2 feet (DIST1 and DIST2). The figure indicates similar results for these cases; therefore, the distribution factor for the loaded flatcar under these circumstances would be 0.80 (the peak observed value in the

envelope). Similarly, the distribution factor for the unloaded flatcar under these circumstances would be 0.25 (the peak observed value in the envelope). This procedure was performed for eight additional cases and is shown in Appendix E.

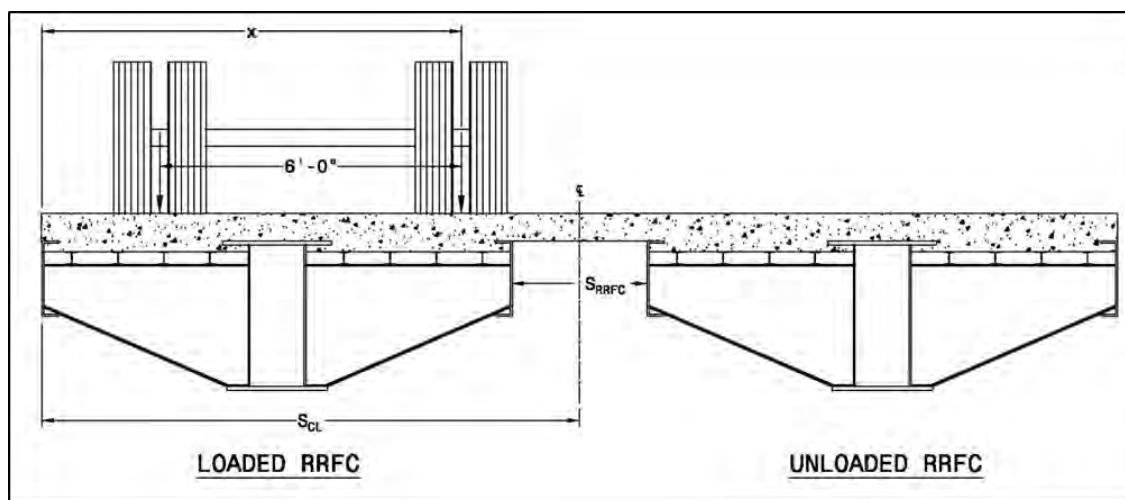


**Figure 7.8: Distribution factors for Case 1**

The results from the parametric studies allowed for the development of simple tables to be used to determine the distribution factors. Table 7.13 provides distribution factors for different cases depending on the relative flexural stiffness, location of the truck, and distance between the flatcars, for a single lane loaded. A useful schematic to determine the appropriate case is shown in Figure 7.9. Table 7.14 was developed to be used to determine the distribution factors for two lanes loaded. These values were determined by assuming worst case scenarios of the single lane loaded data, depending on construction geometry. For example, for a flatcar spacing less than 2 feet and a stiffness ratio less than 15%, the worst loading scenario occurs when the trucks are located inside of the bridge centerline on their respective flatcars. Therefore, each flatcar would have a superimposed distribution factor of 1.05 ( $0.80 + 0.25$ ). Each flatcar is considered “loaded” in the two lanes loaded situation.

**Table 7.13: Distribution factor for calculating live load stress for single lane loaded**

Distribution Factor, $DF$								
Stiffness Ratio, $I_{ext}/I_{main}$	$x \leq S_{CL}$						$S_{CL} < x < (S_{CL} + 6ft)$	
	$S_{RRFC} \leq 2ft$		$2ft < S_{RRFC} \leq 4ft$		$4ft < S_{RRFC} \leq 6ft$		$S_{RRFC} \leq 6ft$	
	Loaded <i>RRFC</i>	Unloaded <i>RRFC</i>	Loaded <i>RRFC</i>	Unloaded <i>RRFC</i>	Loaded <i>RRFC</i>	Unloaded <i>RRFC</i>	Loaded <i>RRFC</i>	Unloaded <i>RRFC</i>
$I_{ext}/I_{main} \leq 15\%$	0.80	0.25	0.90	0.20	0.90	0.15	0.60	0.60
$15\% < I_{ext}/I_{main} \leq 25\%$	0.85	0.20	0.90	0.15	0.95	0.15	0.60	0.60
$25\% < I_{ext}/I_{main} \leq 75\%$	0.90	0.20	0.95	0.15	0.95	0.10	0.60	0.60

**Figure 7.9: Schematic for determining the distribution factor for one lane loaded****Table 7.14: Distribution factor for calculating live load stress for two lanes loaded**

Distribution Factor, $DF$			
Stiffness Ratio, $I_{ext}/I_{main}$	$S_{RRFC} \leq 2ft$	$2ft < S_{RRFC} \leq 4ft$	$4ft < S_{RRFC} \leq 6ft$
	Loaded <i>RRFC</i>	Loaded <i>RRFC</i>	Loaded <i>RRFC</i>
$I_{ext}/I_{main} \leq 15\%$	1.05	1.30	1.50
$15\% < I_{ext}/I_{main} \leq 25\%$	1.05	1.30	1.50
$25\% < I_{ext}/I_{main} \leq 75\%$	1.10	1.35	1.50

#### 7.2.2.4. Car Distribution Factor Results

After the total live load bridge moment is distributed between adjacent flatcars, the moment in each flatcar must be distributed to the primary members. This can be done by applying the car distribution factor. The results of the two parametric studies showed that the car distribution factor mainly depends on the relative flexural stiffness. Figure

7.10 shows the car distribution factor results for Study 1 when varying the truck location. As shown, varying the truck location did not make a substantial impact on the car distribution factor. Figure 7.11 shows the car distribution factor results for Study 2 in which the distance between flatcars was varied. The figure shows that the distance between the flatcars did not greatly influence the car distribution factor. This behavior was observed for the other relative flexural stiffness cases examined. The figures show the primary members relative to their transverse location in the cross section. The outer exterior girder of the East RRFC is represented as member closest to 0 inches, the EAST RRFC main girder follows, and so on. The remaining car distribution factor results from Study 1 and Study 2 can be found in Appendix E.

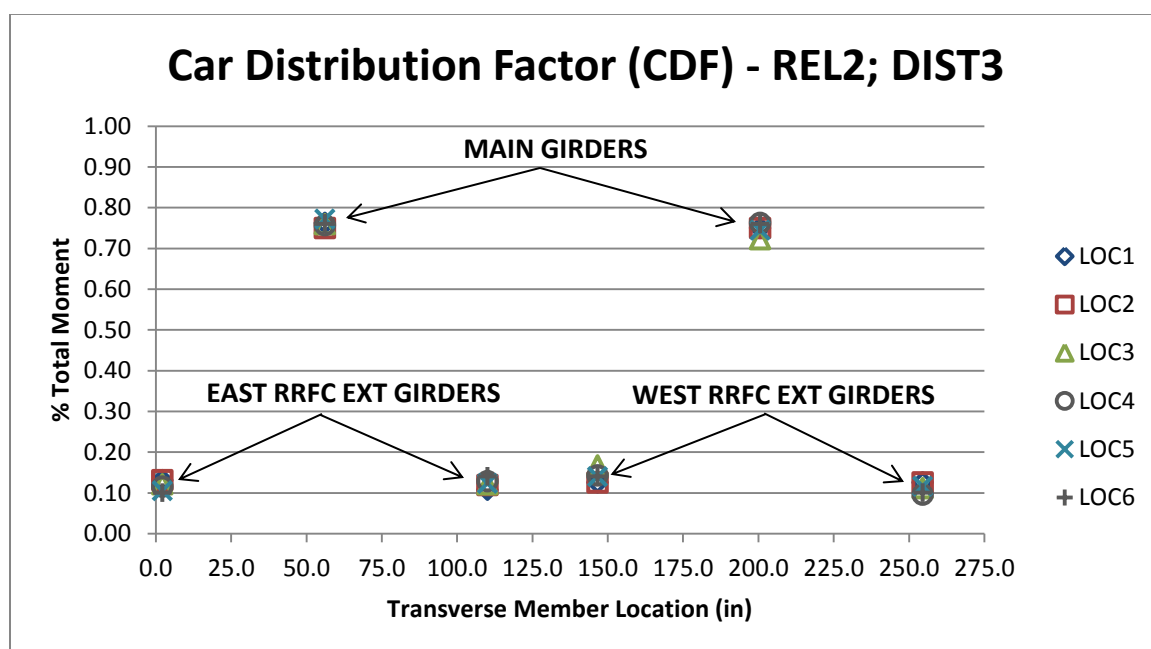
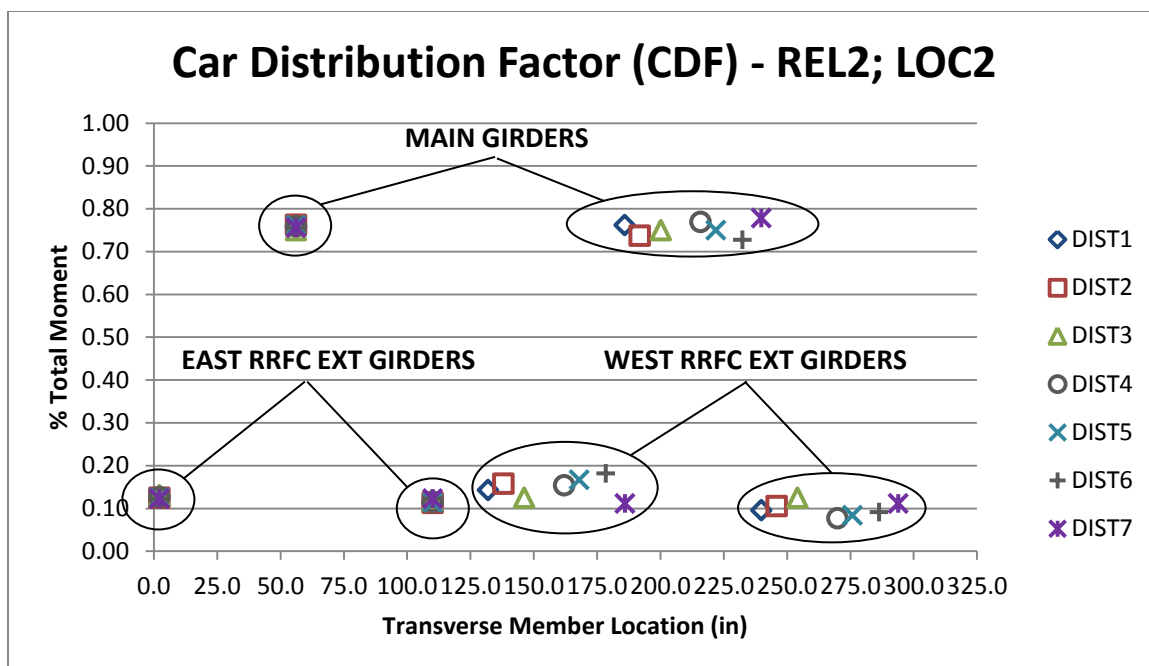


Figure 7.10: Car distribution factor when varying truck location





**Figure 7.11: Car distribution factor when varying distance between flatcars**

The results of the parametric study showed similar car distribution factors for different relative stiffness values. Based on similar car distribution factors, four categories were created to determine the car distribution factor: (1) the stiffness ratio is less than or equal to 5% (REL1), (2) the stiffness ratio is between 5% and 15% (REL2), (3) the stiffness ratio is between 15% and 25% (REL3), and (4) the stiffness ratio is between 25% and 75% (REL4 and REL5). The car distribution factor for each category was developed based on the peak car distribution factors within each category to encompass all of the values considered. Therefore, the sum of the car distribution factors within each flatcar does not equal 1. These peak values are presented in Table 7.15 and Table 7.16. Table 7.17 shows the final development of the car distribution factor to be used when calculating the live load member stress.

**Table 7.15: Maximum car distribution factors for LOC1-LOC6**

Maximum Car Distribution Factor (CDF)		
LOC1 - LOC6; DIST3		
Member	Exterior Girder	Main Girder
REL1	0.08	0.94
REL2	0.17	0.77
REL3	0.24	0.67
REL4	0.36	0.52
REL5	0.44	0.44

**Table 7.16: Maximum car distribution factors for DIST1-DIST7**

Maximum Car Distribution Factor (CDF)		
DIST1-DIST7; LOC2		
Member	Exterior Girder	Main Girder
REL1	0.05	0.94
REL2	0.18	0.78
REL3	0.25	0.67
REL4	0.36	0.50
REL5	0.43	0.40

**Table 7.17: Car distribution factor results for calculating live load stress**

Car Distribution Factor, <i>CDF</i>		
Stiffness Ratio, $I_{ext}/I_{main}$	Longitudinal member	
	<i>Main Girder</i>	<i>Exterior Girder(s)</i>
$I_{ext}/I_{main} \leq 5\%$	0.95	0.05
$5\% < I_{ext}/I_{main} \leq 15\%$	0.80	0.15
$15\% < I_{ext}/I_{main} \leq 25\%$	0.70	0.25
$25\% < I_{ext}/I_{main} \leq 75\%$	0.55	0.45

### 7.2.3. Stress Modification Factor

The stress modification factor was used in Phase I to more accurately match live load stresses calculated with stresses measured in the field (Provines et al., 2011). The stress modification factor when using the procedures to determine live load bending stresses in primary members that are fully composite with a concrete deck is built into the distribution factors and car distribution factors developed herein. Calibration of the spring

analogy model to more accurately predict the behavior of the flatcar bridge allowed for the stress modification factor to equal 1.0. In other words, the live load response was accurately predicted through the distribution factors and car distributions and an additional adjustment was not needed.

### **7.3. Capacity After Fracture**

The controlled fracture tests performed in the laboratory demonstrated that the RRFC bridge was capable of carrying a significant load after fracture occurred. Two fracture tests were performed; the first fracture test involved fracturing the East RRFC main girder near midspan. Data from this fracture test was used to develop procedures to evaluate the remaining capacity of the RRFC bridge after fracture occurs in one main girder. The evaluation considers one fractured main girder near midspan and calculations to determine if adequate capacity remains, assuming the maximum live load moment in the bridge (which occurs near midspan). Data from the uniaxial strain gages near midspan was used to develop the following procedures. Specifically, the data used was from an applied load of 75 kips after fracture occurred. The load was applied as a point load, directly at midspan. The AASHTO HS-20 design truck weighs 72 kips with the load distributed throughout the truck wheels (AASHTO 2012). The design truck load creates less live load moment in the bridge compared to the 75 kip point load. Hence, if the RRFC bridge in the laboratory adequately carried a point load of 75 kips, it was assumed that it can sufficiently carry the HS-20 truck load. It is noted that the laboratory RRFC bridge sustained an applied load of 150 kips after fracturing one main girder.

Two types of loads were considered when developing the procedures to check the bridge capacity after fracture occurred. The first loading was due to redistribution of locked-in stresses immediately after fracture occurred. Locked-in stresses include stress due to dead load and residual stresses “locked-in” a given member. The second loading was due to live load and determining how the bridge system carries the applied load with a fractured primary member. The total stress in a remaining primary member, at a given location, is the sum of the effects due to the two loads. The development to estimate these

effects and evaluate the remaining available capacity is discussed in the following sections.

It is important to mention that the following procedures only apply to bridges with a concrete deck that is fully composite with the primary members. The primary members are described as the exterior girders and main girders; however, composite action between the exterior girders and concrete deck must be met. The procedures do not apply if the exterior girders were altered such that composite action cannot be adequately achieved. Also, the concrete deck must be properly designed following the *AASHTO LRFD Bridge Design Specifications* (2012).

### **7.3.1. Capacity Limit**

The capacity limit to determine if the remaining primary members can adequately carry the live load was determined based on the *AASHTO Manual for Bridge Evaluation* (2011) and comparing to stress measured during the fracture test. In the *AASHTO Manual for Bridge Evaluation* (2011), the capacity limit for allowable stress when considering operating rating is 75% of the yield strength. Operating rating is defined as the “maximum permissible live load to which the structure may be subjected” (AASHTO, 2011). The case of a fracture is seen by the authors as an extreme case in which utilizing the operating level capacity limit is adequate. The capacity limit is not the full yield strength, allowing some reserve capacity to remain.

This capacity limit was compared to the laboratory test data. The maximum total stress compared to the yield stress in the outer exterior girder of the fractured flatcar is shown in Table 7.18. This was the maximum stress measured in the RRFC bridge at this loading point. The yield stress of 48 ksi was determined from material testing performed on the flatcar material. The maximum total stress presented includes the stress due to redistribution of locked-in loads when fracture occurred, plus the effect due to an after-fracture applied point load of 75 kips. As shown, the maximum stress in the member is 80% of the yield strength at this load. Hence, 75% of the yield strength was determined to be a sufficient for the laboratory bridge tested.

**Table 7.18: Maximum total stress in outer exterior girder of fractured flatcar**

Exterior Girder of Fractured RRFC (CH_44)		
Maximum Total Stress (ksi)	Yield (ksi)	Max Stress / Yield
38.4	48.0	0.8

### 7.3.2. Redistribution of Locked-in Loads

The locked-in stresses, or loads, were assumed to be the dead load carried by the fractured member and residual stresses. Residual stresses may be due to manufacturing and welding to create the build-up main member. This section describes how the stresses due to redistributed locked-in loads were calculated based on laboratory testing. These calculations were possible due to the instrumentation data in the laboratory; without instrumentation, engineers can only estimate dead load and not the effects of residual stresses from manufacturing and fabrication.

Table 7.19 shows the stress in the remaining primary members near midspan after fracturing the East RRFC main girder. These stresses are produced by the redistribution of dead load and residual stresses previously carried by the East RRFC main girder (it is noted that since no yielding was observed, the offsets are not attributed to nonlinear behavior). They were determined after fracturing the main girder and unloading any remaining applied load. At this point, there was no contribution to the applied load and any offset of stresses were assumed to be due to the redistribution of dead load and residual stresses once in the now fractured main girder. The moments in each member were calculated using the composite effective section described in Section 7.2.1. The total redistributed moment calculated at this cross section was about 420 kip-ft.

Based on stress measurements, the total dead load moment resisted by the structural shape of the main girder was calculated to be about 350 kip-ft. The calculation conservatively assumed the main girder carried the entire weight of the flatcar, plus a portion of the concrete deck equal to the tributary width used for the effective section calculations. The calculated dead load stress due to the weight of the concrete deck was

compared to the stress measured during the concrete deck pour and matched within 20%; therefore, the previously mentioned assumption was considered acceptable. It was concluded that the redistributed locked-in loads could be determined by assuming that the total dead load moment resisted by the main girder prior to fracture would be redistributed to the other primary members after fracture occurred. It is important to note that the redistribution of residual stresses cannot be estimated without instrumentation measurements and it varies case by case. An example calculation of this evaluation can be found in Appendix G.

The redistributed locked-in stress in a remaining primary member can be calculated similarly to the calculation of the live load stress. The total dead load moment once carried by the fractured member can be distributed to each flatcar by the distribution factor, and then distributed to the intact primary members by the car distribution factor. The effective section of the remaining primary members resisting the moment was assumed the same as when calculating live load stresses. The following sections describe the distribution factor and car distribution factor used to calculate the redistributed locked-in loads.

**Table 7.19: Fracture 1 redistribution of locked-in loads**

Redistribution of Dead Load After Fracture							
FRACTURE TEST 1 - SECTIONS C & I							
RRFC	Member	Redistributed Locked-In Stresses (ksi)	Redistributed Locked-In Moment (kft)	GDF	Car Redistributed Moment (kft)	DF	CDF
East RRFC (Loaded)	Outer Exterior Girder (CH_44)	17.2	145.3	0.34	257.1	0.61	0.57
	Main Girder (CH_32 & CH_34)	0.0	0.0	0.00			0.00
	Inner Exterior Girder (CH_22)	12.3	111.8	0.26			0.43
West RRFC (Unloaded)	Inner Exterior Girder (CH_94)	3.2	28.7	0.07	165.2	0.39	0.17
	Main Girder (CH_86 & CH_88)	1.6	142.7	0.34			0.86
	Outer Exterior Girder (CH_80)	-0.7	-6.3	-0.01			-0.04
Total Redistributed Moment (kft)		422					

### *7.3.2.1. Distribution Factor for Redistribution of Locked-in Loads*

The distribution factor was developed to distribute the moment between flatcars. Table 7.19 presents the portion of the moment distributed to each flatcar based on laboratory testing (DF column). Redistributed locked-in moments were calculated based on stress measurements and the assumed effective sections (as discussed in 7.2.1. ) for the remaining primary members. Distribution factors to redistribute locked-in loads were determined by summing the member moments in each car and dividing by the total moment redistributed, in that cross section. Recall that the East RRFC main girder was fractured. Based on the experimental data, it was suggested to assume 60% of the dead load moment previously carried by the fractured member remains in the fractured flatcar and 40% is distributed to the non-fractured flatcar.

### *7.3.2.2. Car Distribution Factor for Redistribution of Locked-in Loads*

The car distribution factor was developed to distribute the portion of the live load moment in the respective flatcar to the intact primary members. The only primary members remaining in the fractured flatcar were the exterior girders. Experimental data shown in Table 7.19 shows that the outer exterior girder of the fractured flatcar had an actual car distribution factor of 0.57 and the inner exterior girder had an actual car distribution factor of 0.43; however, 0.50 was deemed sufficient; thus, it is sufficient to assume that 50% of the flatcar moment is distributed to each exterior girder.

## **7.3.3. Redistribution of Live Load**

The fractured portion of the main girder can no longer carry live load at the fractured cross section; therefore, a new load path for the bridge system needed to be determined. Figure 7.12 displays the percent of the total moment (i.e., girder distribution factor) for each primary member before and after fracture occurred at an applied load of 75 kips. The members are represented by their location in the transverse direction, assuming 0 inches as the outer face of the East RRFC. The figure shows that the live load moment was mainly redirected into the exterior girders of the fractured flatcar and the main girder of the non-fractured flatcar. These numerical values are also shown in Table

7.20. They were determined based on the measured stresses at these cross sections and the assumed composite effective sections. The live load stress values were calculated by subtracting the measured redistributed locked-in stress from the total stress in the strain gage.

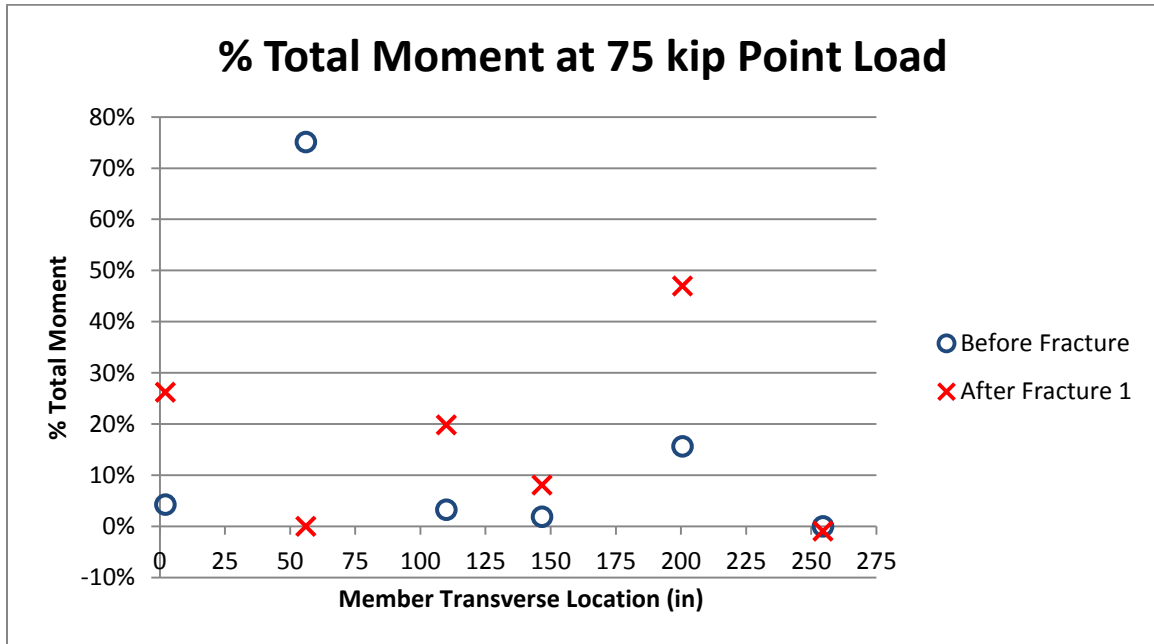


**Figure 7.12: Percent of total moment carried by primary members before and after fracture**



**Table 7.20: Fracture 1 redistribution of live load**

75kip Point Load at Midspan							
FRACTURE TEST 1 - SECTIONS C & I							
RRFC	Member	Live Load Stress (ksi)	Live Load Moment (kft)	GDF	Car Live Load Moment (kft)	DF	CDF
East RRFC (Loaded)	Outer Exterior Girder (CH_44)	21.2	178.8	0.26	314.2	0.46	0.57
	Main Girder (CH_32 & CH_34)	0.0	0.0	0.00			0.00
	Inner Exterior Girder (CH_22)	14.9	135.4	0.20			0.43
West RRFC (Unloaded)	Inner Exterior Girder (CH_94)	6.1	55.1	0.08	369.2	0.54	0.15
	Main Girder (CH_86 & CH_88)	3.5	320.9	0.47			0.87
	Outer Exterior Girder (CH_80)	-0.8	-6.8	-0.01			-0.02
<b>Total Live Load Moment (kft)</b>		<b>683</b>					

The live load stress in a remaining primary member can be calculated using similar procedures described in Section 7.2. , with the exception of using different distribution factors and car distribution factors for the fractured flatcar members. The following sections discuss the development of these factors to be used to determine the live load effects on the intact primary members at midspan. An example of the calculations to determine available capacity after fracture occurs for the laboratory RRFC bridge can be found in Appendix G.

#### 7.3.3.1. Distribution Factor for Redistribution of Live Load

The distribution factor for distributing the live load moment after fracture occurred was developed to distribute the live load moment due to the design truck between adjacent flatcars. As shown in Table 7.20, about 50% of the total live load moment remained in the East RRFC and about 50% was shifted to the West RRFC. Thus, the distribution factor for the fractured flatcar was assumed to be 0.50 if it is the loaded flatcar. If the non-fractured flatcar is the loaded flatcar, the distribution factor of 1.0 should be used. This was determined based on the assumption that the entire live load

applied to the non-fractured flatcar would remain in that flatcar, since the fractured flatcar is now in a flexible state and would not “attract” the load.

When a two lane loaded case is considered, the recommendation is that a distribution factor of 0.50 still be used for the fractured flatcar. This assumes that 50% of the load applied to the fractured flatcar remains in that car, and 50% is distributed to the non-fractured flatcar, as shown from the experimental data for a single lane loaded. Again, it is assumed that the load applied to the non-fractured flatcar would remain in that car, and not get distributed to the fractured flatcar in its flexible state. The non-fractured flatcar would then have a superimposed distribution factor that includes the 50% distributed from the fractured car and its entire load for a combined conservative distribution factor of 1.75.

#### *7.3.3.2. Car Distribution Factor for Redistribution of Live Load*

The car distribution factor was developed to distribute the portion of the live load moment in the flatcar to its primary members. Table 7.20 displays the car distribution factor for the remaining primary members. These portions were determined based on the experimental measurements and the assumed composite effective sections. The car distribution factor for the exterior girders in the fractured flatcar was determined to be 0.50 based on the information provided in the table. It was concluded that the car distribution factors discussed in Section 7.2.2.4. were adequate to use for the non-fractured RRFC.

### **7.4. Shear**

Rectangular rosette strain gages were installed on the webs of the East RRFC exterior girders and main girder. One instrumented cross section (Section J-J) was about 2 feet from the support, in the shallow section of the main girder. The second instrumented cross section (Section K-K) was about 6 feet from the support, where the main girder tapers. Details about the rosettes can be found in Section 4.2. The critical location for shear was at the supports; however, instrumentation was not installed here due to inaccessibility because of the large floorbeam at that location. Higher shear values

were observed in Section J-J because of the shallower section; therefore, the measured results in this section will be discussed further. The location of the rosettes in Section J-J is shown in Figure 7.13, for convenience. As shown, all rosettes were placed at mid-depth of the member webs. Maximum shear in the webs were assumed at these locations.

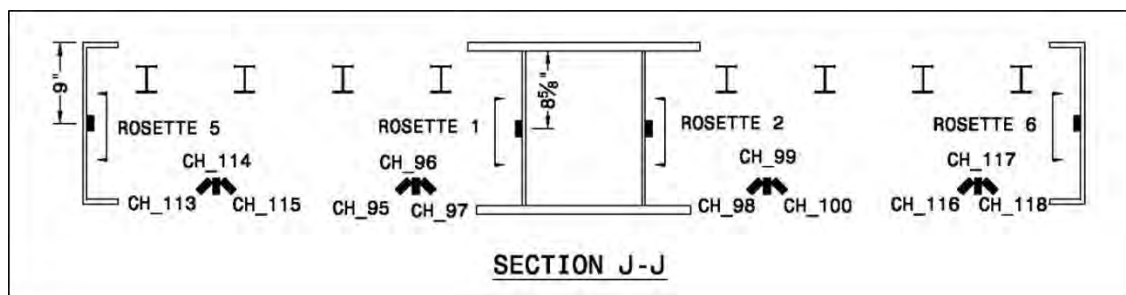


**Figure 7.13: Location of rectangular rosette strain gages on East RRFC**

The principal shear strain at each rosette was calculated using measured data. The principal shear strains were used to determine the maximum shear strain at each location. The maximum shear strain was then converted to maximum shear stress. Finally, maximum shear was calculated by multiplying the maximum shear stress by the respective web area. The maximum shear values, for a load of 150 kips, are shown in Table 7.21 for Test 1. The East RRFC was point loaded at midspan with no deck for Test 1. The total shear at Section J-J calculated in the main girder and exterior girders was about 76 kips, compared to the theoretical shear value of 75 kips. The main girder was the only longitudinal member of the flatcar that was supported at the bearing; therefore, any shear carried by the exterior girders at this location had to get into the support by means of the large floorbeam located at the support (see RRFC drawings in Appendix A). Therefore, it is reasonable and conservative to assume that the main girder carries all of the shear force.

**Table 7.21: Section J-J maximum shear values with no deck**

Section J-J							
Test	Maximum Shear (kips)						
	Main Girder			Exterior Girders			Total Shear
	<i>Rosette 1</i>	<i>Rosette 2</i>	<i>Total</i>	<i>Rosette 5</i>	<i>Rosette 6</i>	<i>Total</i>	
<b>1</b>	33.9	29.9	63.8	6.0	6.1	12.0	75.8

The same calculations previously discussed were used to determine the shear values in the webs of the main girders for Test 5 and Test 7. Measurements from Rosettes 5 and 6 on the exterior girders were not obtained during these tests. The East RRFC and West RRFC were subjected to a point load at midspan for Test 5 and Test 7, respectively. Only the East RRFC main girder was instrumented with rectangular rosette strain gages; therefore, the measurements from both tests were needed to determine the total shear value in the cross section from the loaded RRFC main girder and the unloaded RRFC main girder. These results are shown in Table 7.22 for a load of 150 kips. The total shear in the main girders at this cross section was about 52 kips, compared to the theoretical shear of 75 kips. Therefore, it was assumed that some of the shear force was also being carried by the exterior girders at this cross section. However, because the critical shear location is at the support, it is conservative to assume that the main girder carries all of the shear force in the case of the composite concrete deck.

**Table 7.22: Section J-J maximum shear values with composite concrete deck**

Section J-J			
Test	Maximum Shear (kips)		
	Main Girder		
	<i>Rosette 1</i>	<i>Rosette 2</i>	<i>Total</i>
<b>5</b>	12.7	25.5	38.2
<b>7</b>	11.6	2.6	14.2
<b>Total Shear</b>			52.4

## CHAPTER 8. RESULTS, CONCLUSIONS, & RECOMMENDATIONS

### 8.1. Results

A railroad flatcar bridge consisting of two typical flatcars placed side-by-side was constructed and tested in the laboratory. Typical RRFCs are defined as flatcars with one main box girder and an exterior girder, typically a channel, on either side of the main girder. The flatcars were load tested individually without a concrete deck or connection between them, with a patch of timber decking, and with a fully composite concrete deck. Both main girders of the RRFC bridge were fractured at midspan. After each fracture, the bridge was point loaded to observe the response at the fractured state.

Proposed load rating guidelines were developed for RRFC bridges constructed with a fully composite concrete deck and added to the proposed load rating guidelines developed in Phase I. The guidelines developed herein were based from a series of load tests conducted in the laboratory. Similar to the development of the proposed guidelines in Phase I, those developed in Phase II focused on user-friendly procedures to more accurately load rate RRFC bridges with composite concrete decks (Provines et al., 2011). The proposed load rating guidelines can be found in Appendix F. An example using these guidelines to load rate the RRFC bridge in the laboratory is presented in Appendix G.

Guidelines were also developed to estimate if the remaining longitudinal members have sufficient capacity to carry traffic loads after fracturing one main girder. The guidelines were developed based on controlled load tests performed on the laboratory RRFC bridge after generating a fracture at midspan in one of the two main box girders. The authors believe the procedures are only applicable to bridges constructed with typical RRFCs with the exterior girders and main girders made fully composite with the concrete

deck. The guidelines can be found in conjunction with the previously mentioned load rating guidelines in Appendix F. Example calculations to determine remaining member capacity in the fractured state is available in Appendix G.

## 8.2. Conclusions

Experimental testing of the RRFC bridge in the laboratory resulted in the following key conclusions:

- When loaded individually, both railroad flatcars displayed similar behavior when subjected to the same applied point load. The main box girder carried the majority of the applied load during these individual tests. The applied point load at midspan load in these tests was nearly twice that of typical truck traffic loads.
- Timber decking did not provide any substantial stiffness or load distribution within the RRFC.
- The composite concrete deck provided added stiffness, increased live load capacity, and provided excellent load distribution within a single RRFC and between adjacent RRFCs.
- The main girders and exterior girders were determined to be primary members of RRFC bridges constructed with a composite concrete deck, as long as the members are unaltered and made fully composite with the deck.
- The model developed by Akinci et al. (2013) consisting of rotational springs representing the exterior girders and main girders, and torsional bars representing the concrete deck, was found to be sufficient in predicting the load distribution to each primary member.
- Laboratory testing demonstrated that bridges constructed with typical RRFCs and a composite concrete deck will very likely have load-path redundancy and should not be labeled fracture critical. The exterior girders and main girders must be fully

composite with a properly designed concrete deck for this statement to be applicable. Loads were redistributed into the exterior girders of the fractured RRFC, as well as into the non-fractured RRFC primary members.

- The laboratory RRFC bridge was subjected to loads that far exceed typical truck traffic loads, in the non-fractured and fractured state. The behavior of the bridge during these load tests was satisfactory to the point that even in the fractured state, the bridge resisted loads more than double the HS-20 design load with both main box girders fractured.
- Shear forces are carried by the webs of the main girders when utilizing any type of bridge deck. This is a conservative, yet reasonable assumption based on laboratory test data.

### **8.3. Future Research Recommendations**

A recommendation for future research is the development of a detailed finite element model of the laboratory RRFC bridge that is calibrated using the instrumentation data collected during laboratory testing. Creating a finite element model that adequately portrays the behavior of the laboratory bridge before and after fracture occurred would allow for a parametric study to be executed, enabling a broader characterization of RRFC structural response. A few suggested parameters of the study include: RRFC length, rigidity of the connection between adjacent RRFCs, and stiffness of the bridge deck. The recommended study would assist in determining the level of load redundancy for different flatcar bridge scenarios and geometries.

## LIST OF REFERENCES



## LIST OF REFERENCES

- AAR. (2007). "Design, Fabrication, and Construction of Freight Cars," Manual of Standards and Recommended Practices Section C – Part II. The Association of American Railroads.
- AASHTO. (2011). "The Manual for Bridge Evaluation," Second Edition. American Association of State Highway and Transportation Officials. 2011.
- AASHTO. (2012). "LRFD Bridge Design Specifications," Sixth Edition. American Association of State Highway and Transportation Officials. 2012.
- Akinci, N. O., Liu, J., & Bowman, M. D. (2013). "Spring analogy to predict the 3-D live load response of slab-on-girder bridges," *Engineering Structures*, Vol. 26, pp. 1049-1057. 2013.
- AS 5100. (2004). "AS 5100 Bridge Design Code," Australian Standards. 2004.
- AWS. (2010). "Bridge Welding Code," AASHTO/AWS D1.5M/D1.5:2010. An American National Standard. 2010.
- Bridge Diagnostics, Inc. (1995). "Technique enables flatcar bridges to attain higher load ratings," *Roads & Bridges*, August 1995, pp. 42-43.
- Bridge Diagnostics, Inc. (2002). "Load Testing, Evaluation, and Rating Four Railroad Flatcar Bridge Spans Over Trinity River in Redding, California," Submitted to: Bureau of Reclamation, Water Conveyance Group D-8140. 2002.
- Dhanasekar, M. & Bayissa, W. L. (2011). "Structural adequacy assessment of a disused flat bottom rail wagon as road bridge deck," *Engineering Structures*, Vol. 33, pp. 1838-1849. 2011.

- Diggelmann, L. M., Connor, R. J., & Sherman, R. J. (2012). "Evaluation of Member and Load-Path Redundancy on the US-421 Bridge Over the Ohio River," Confidential Final Report. Purdue University. August 2012.
- Doornink, J. D., Wipf, T. J., & Klaiber, F. W. (2003a). "Railroad Flatcar Bridges for Economical Bridge Replacement Systems," *Proceedings of the 2003 Mid-Continent Transportation Research Symposium*. Ames, Iowa, August 2003.
- Doornink, J. D., Wipf, T. J., & Klaiber, F. W. (2003b). "Use of Railroad Flatcars in Cost-Effective Low-Volume-Road Bridges," *Transportation Research Record Paper No. LVR8-1147*. 2003.
- Idriss, R. L., White, K. R., Woodward, C. B., & Jauregui, D. V. (1995). "Evaluation and testing of a fracture critical bridge," *NDT&E International*, Vol. 28, No. 6, pp. 339-347. 1995.
- Jamtsho, L. & Dhanasekar, M. (2013). "Performance Testing of a Road Bridge Deck Containing Flat Rail Wagons," *Journal of Bridge Engineering*, Vol. 18, April 2013, pp. 308-317.
- McDonald, C. (2011) "An Experimental Research Investigation into Disused Flat Rail Wagons as Bridges with Applications for Low Volume Rural Roads in Australia," Queensland University of Technology. 2011.
- NBIS. (2012). 23 CFR 650, Subpart C National Bridge Inspection Standards, Federal Highway Administration, Washington, D.C., January 2012.
- Neuman, B. J. (2009). "Evaluating the Redundancy of Steel Bridges: Full-Scale Destructive Testing of a Fracture Critical Twin Box-Girder Steel Bridge," M.S. Thesis, The University of Texas at Austin, Austin, TX. 2009.
- Parsons, T. J. (1991). "Bridges Constructed From Railroad Cars," Arkansas State Highway and Transportation Department. Final Report TRC 8901. Arkansas State University. December 1991.
- Peevler, R. (2013). Fountain County Highway Supervisor. Email correspondence.

- Provines, J. T., Connor, R. J., & Sherman, R. J. (2011). "Development of Guidelines for the Rating, Inspection, and Acquisition of Railroad Flatcars for Use as Highway Bridges on Low-Volume Roads," Indiana Local Technical Assistance Program. Final Report. Purdue University. July 2011.
- Roberts, J. (1995a). "A Temporary Bridge," *Science*, Vol. 268, No. 5208, April 14. pp. 261-262.
- Roberts, J. (1995b). "Ready for Anything," *Civil Engineering*, Vol. 65, No. 11, November 1995, pp. 54-55.
- Shurbert, J. (2013). Sales Manager at Irving Materials, Inc. Email correspondence.
- Suprenant, B. (1987a). "Railroad Car Bridges: Asset or Liability?" Montana Rural Technical Assistance Program. Montana State University. Bozeman, MT. May 1987.
- Suprenant, B. (1987b). "Railroad cars offer option for economical bridges," *Roads & Bridges*, Vol. 25, No. 11, November 1987, pp. 58-61.
- Washer, G., Connor, R. J., Ciolko, A., Kogler, R., Fish, P., & Forsyth, D. (2011), "Guidelines for Reliability-Based Bridge Inspection Practices," NCHRP 12-82. *Transportation Research Board*.
- Wattenburg, W. H., McCallen, D. B., & Murray R. C. (1995). "A Modular Steel Freeway Bridge: Design Concept and Earthquake Resistance," *Science*, Vol. 268, No. 5208, April 14, 1995, pp. 279-281.
- Wipf, T. J., Klaiber, F. W., Witt, J., & Threadgold, T. L. (1999). "Use of Railroad Flat Cars for Low-Volume Road Bridges," Iowa Department of Transportation Project TR-421. Iowa State University. August 1999.
- Wipf, T. J., Klaiber, F. W., & Doornink, J. D. (2003). "Demonstration Project using Railroad Flatcars for Low-Volume Road Bridges," Iowa Department of Transportation Project TR-444. Iowa State University. February 2003.
- Wipf, T. J., Klaiber F. W., Boomsma, H. A., & Palmer, K. S. (2007a). "Field Testing of Railroad Flatcar Bridges Volume I: Single Spans," Iowa Department of Transportation Project TR-498. Iowa State University. August 2007.

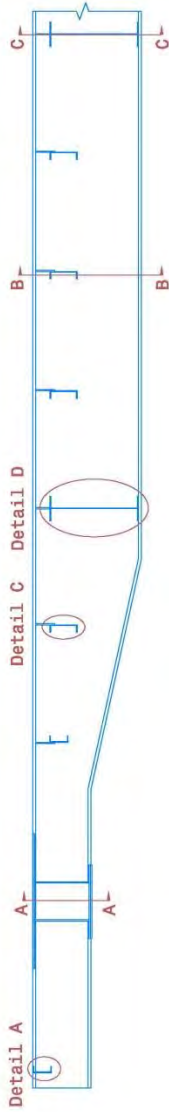
Wipf, T. J., Klaiber, F. W., Mass, J. J., Keierleber, B., & Witt, J. (2007b). "Field Testing of Railroad Flatcar Bridges Volume II: Multiple Spans," Iowa Department of Transportation Project TR-498. Iowa State University. August 2007.

## APPENDICES

**APPENDIX A. RAILROAD FLATCAR DIMENSIONS**

# RRFC DIMENSIONS

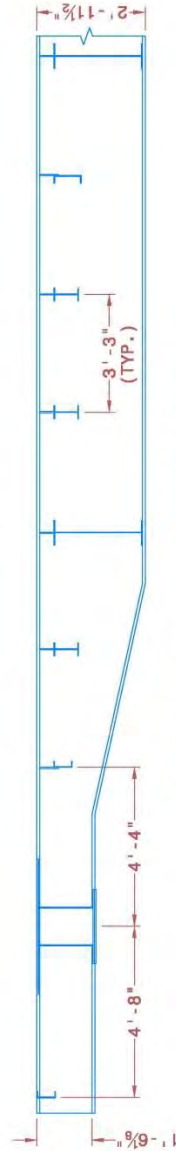
SHEET NO.:  
**1 of 3**



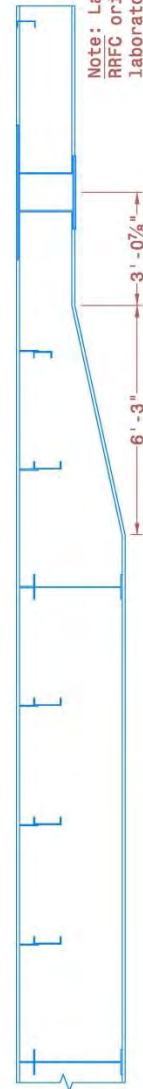
ELEVATION VIEW - NORTHWEST SECTION



ELEVATION VIEW - SOUTHWEST SECTION



ELEVATION VIEW - NORTHEAST SECTION

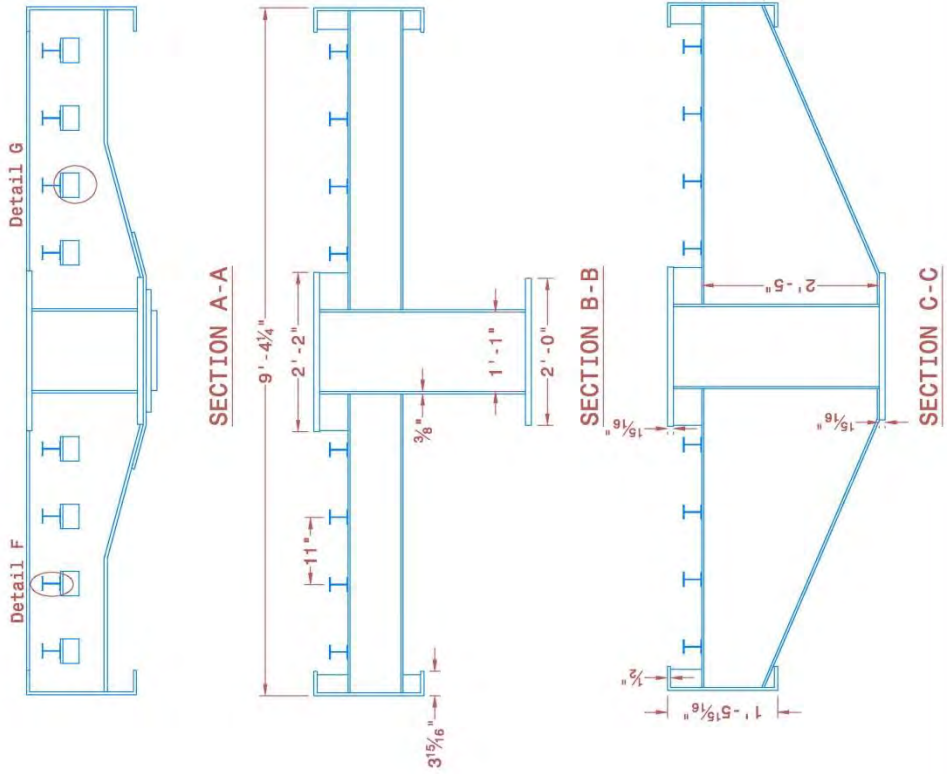


ELEVATION VIEW - SOUTHEAST SECTION

Note: Labels based on RRFC orientation in laboratory. Elevation view drawings do not show exterior girders or stringers.

# RRFC DIMENSIONS

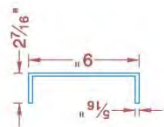
SHEET NO.:  
**2 of 3**



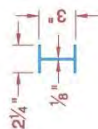


# RRFC DIMENSIONS

SHEET NO. :  
**3 of 3**



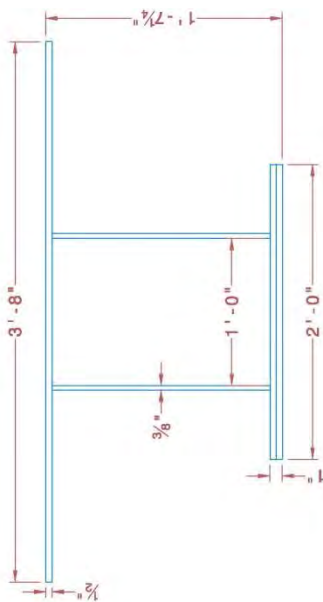
DETAIL C



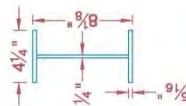
DETAIL F



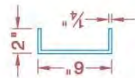
DETAIL G



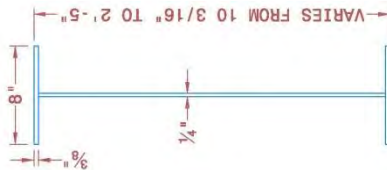
DETAIL B



DETAIL E



DETAIL A

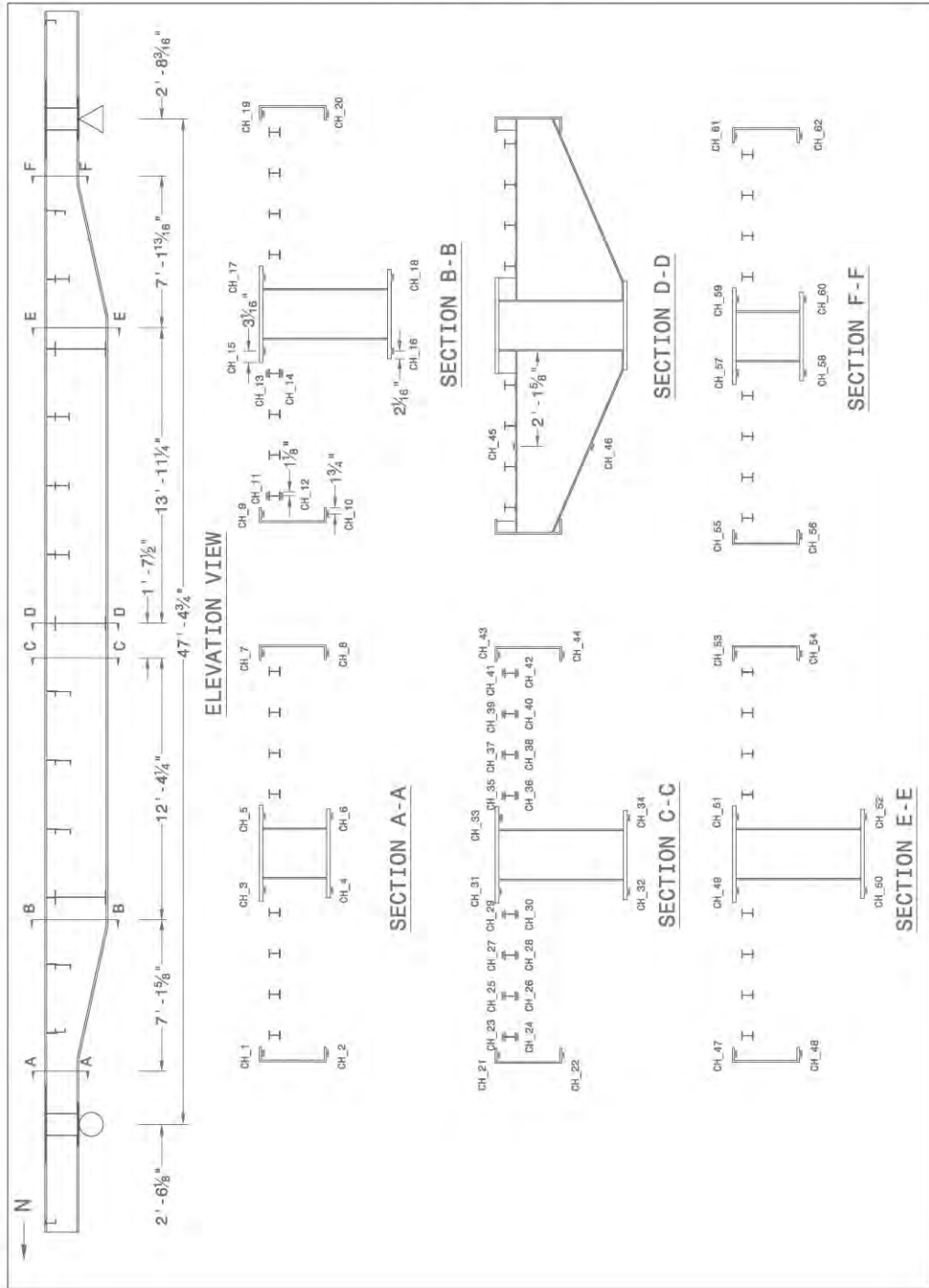


DETAIL D

**APPENDIX B. INSTRUMENTATION PLANS**

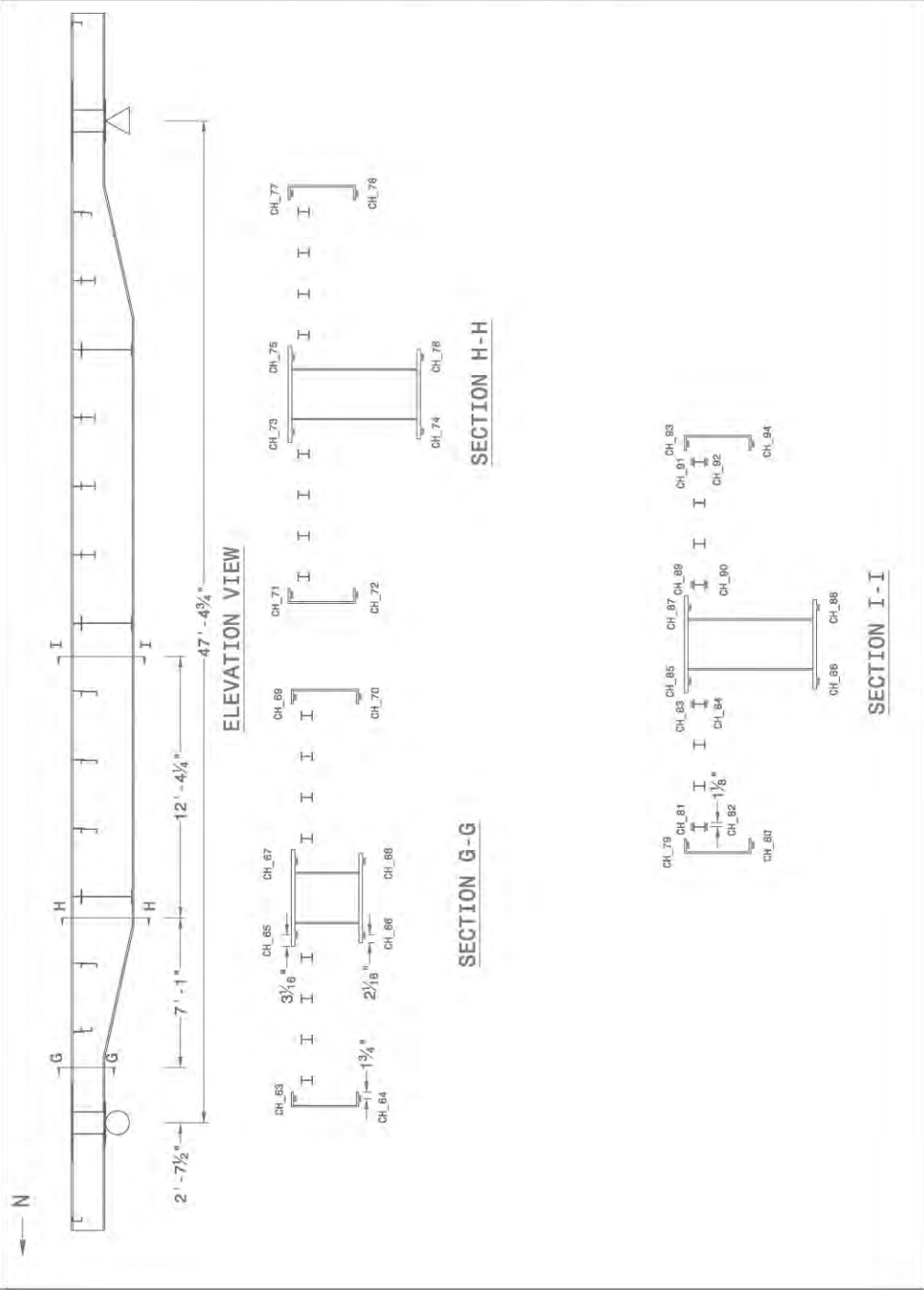
# STRAIN GAGE PLANS EAST RRFC

SHEET NO. :  
**1 of 3**



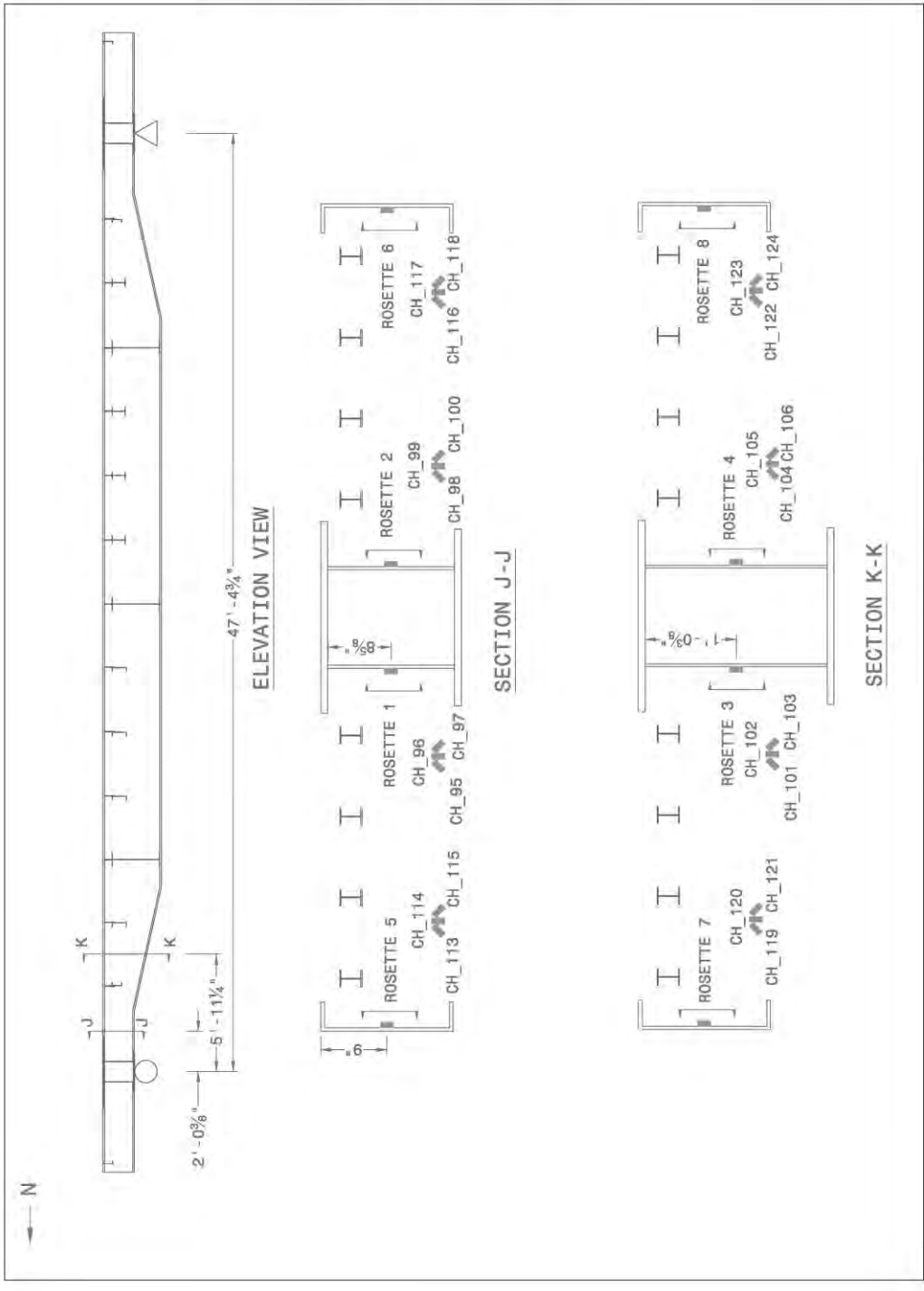
# STRAIN GAGE PLANS WEST RRFC

SHEET NO. :  
**2 of 3**



# ROSETTE PLANS EAST RRFC

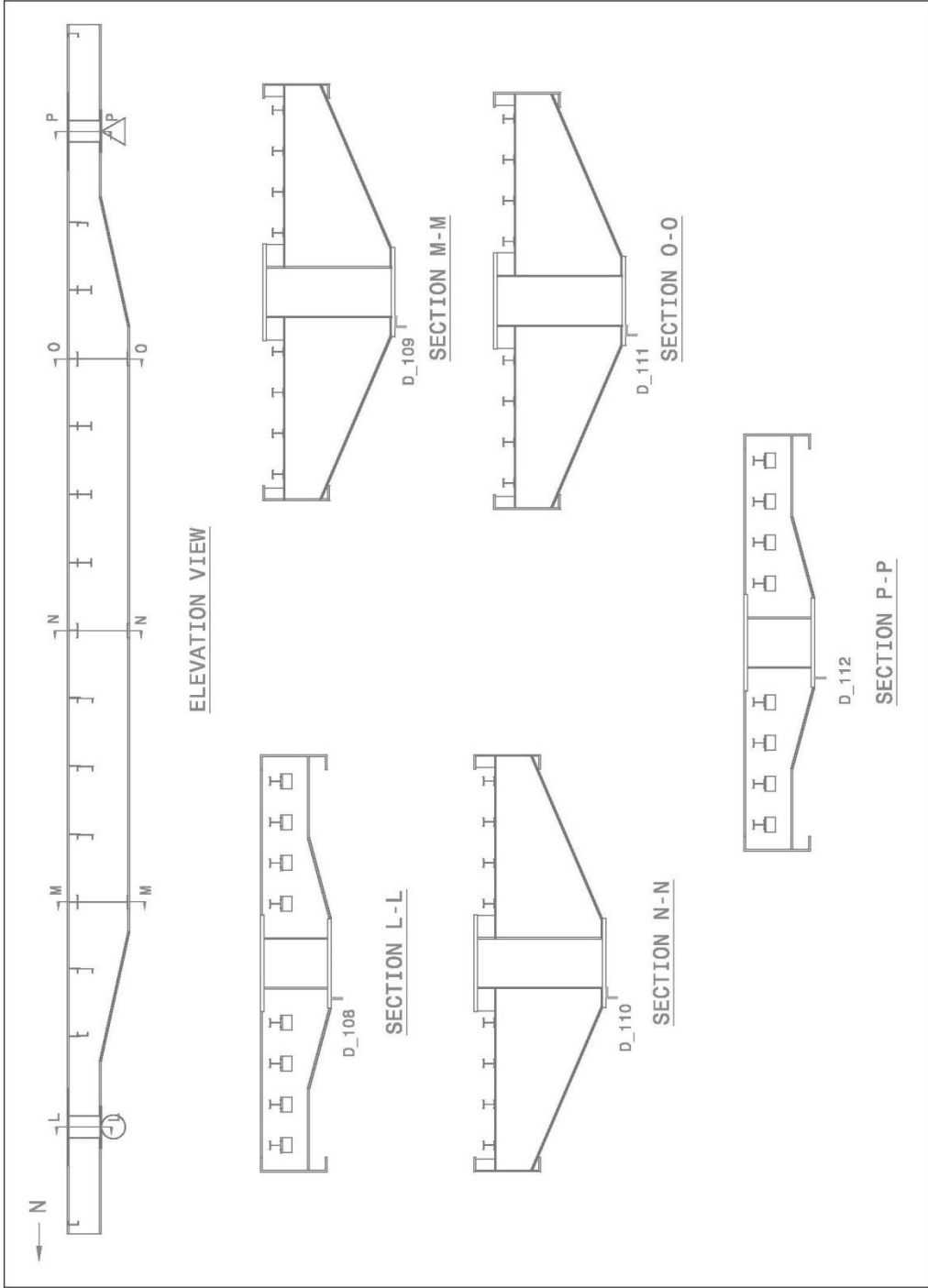
SHEET NO. :  
**3 of 3**



# DISPLACEMENT SENSORS EAST RRFC - TESTS 1-8, 11

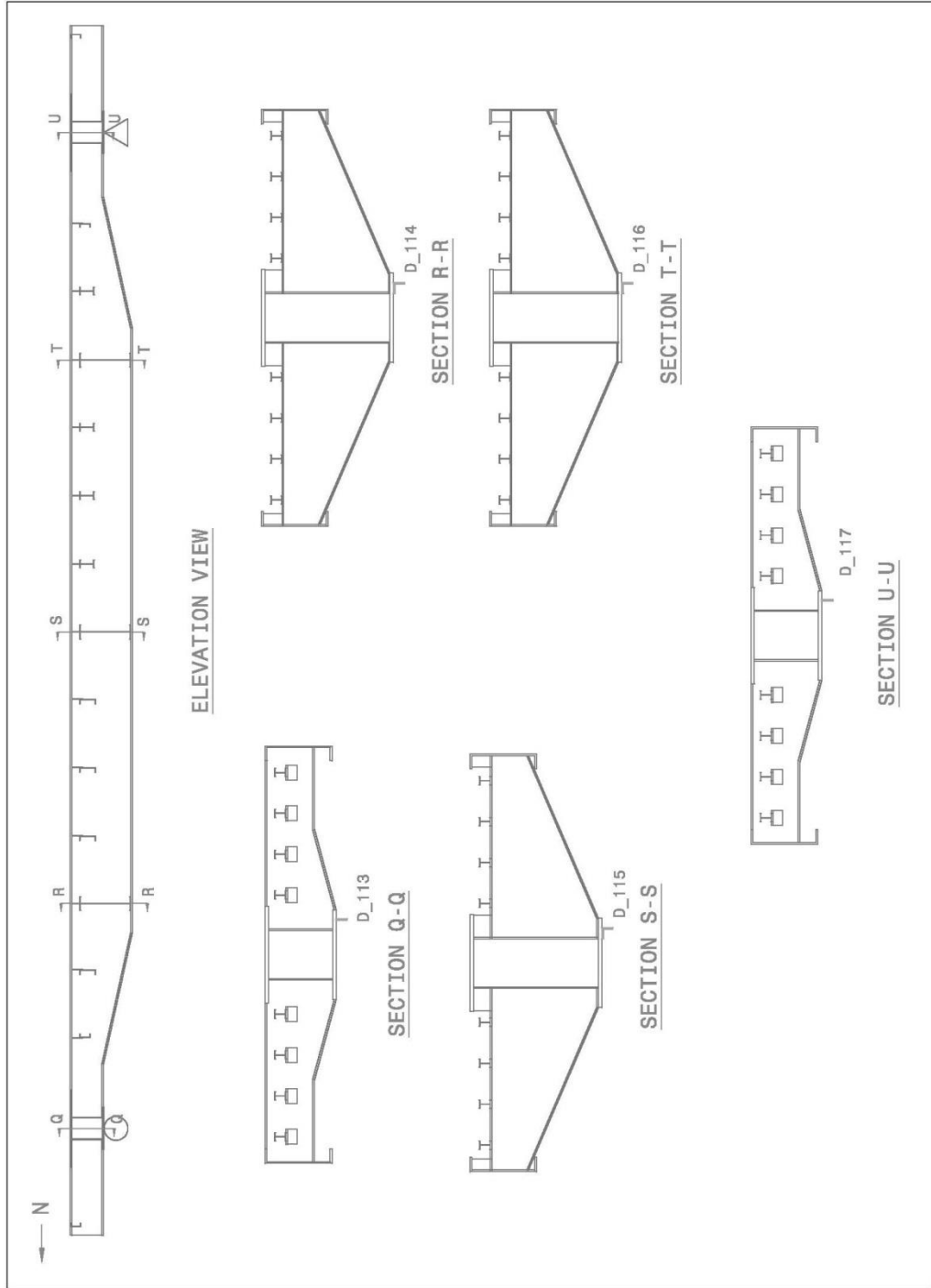
SHEET NO.:

1 of 2



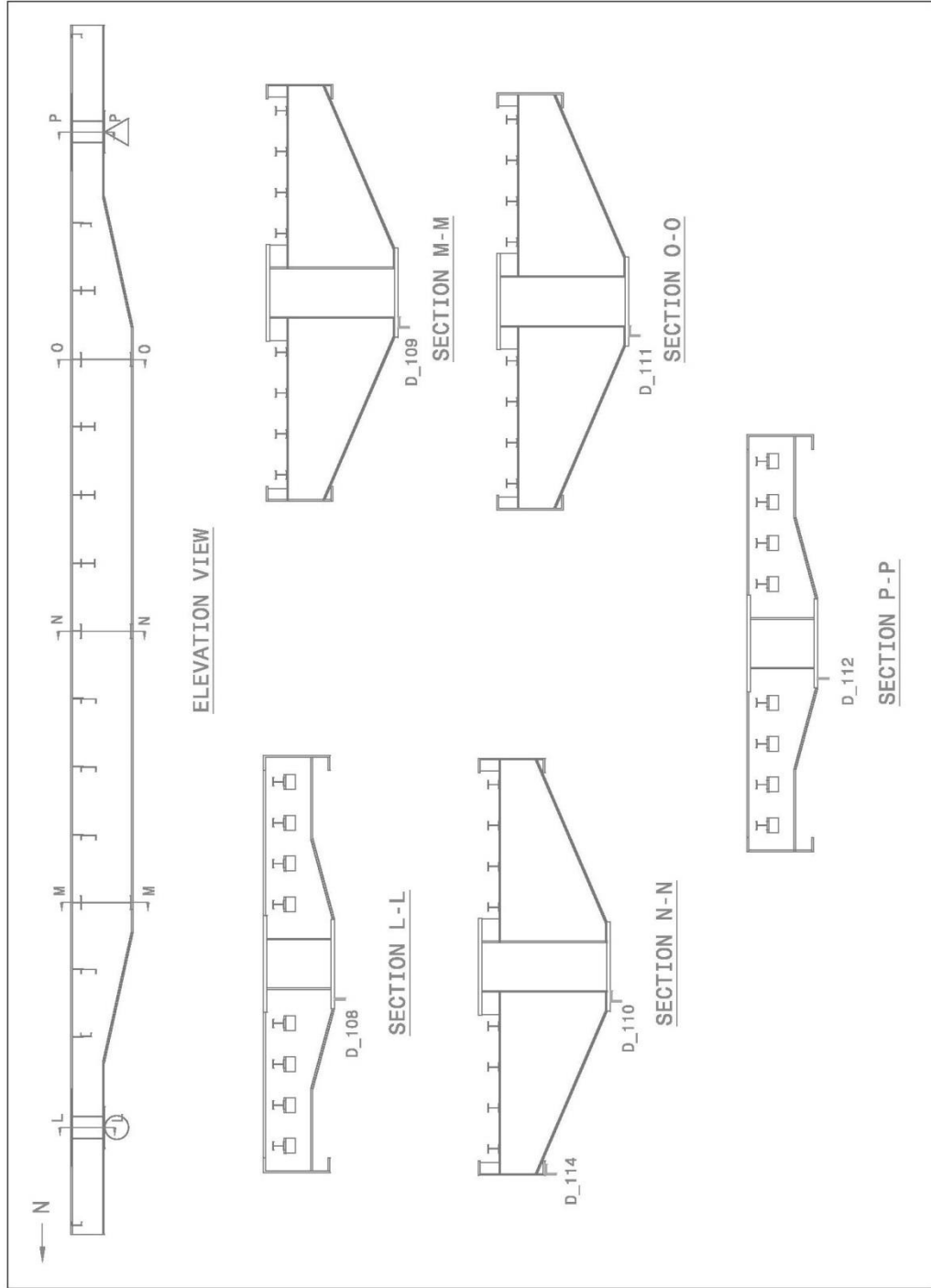
# DISPLACEMENT SENSORS WEST RRFC - TESTS 1-8, 11

SHEET NO. :  
**2 of 2**



# DISPLACEMENT SENSORS EAST RRFC - FRACTURE 1

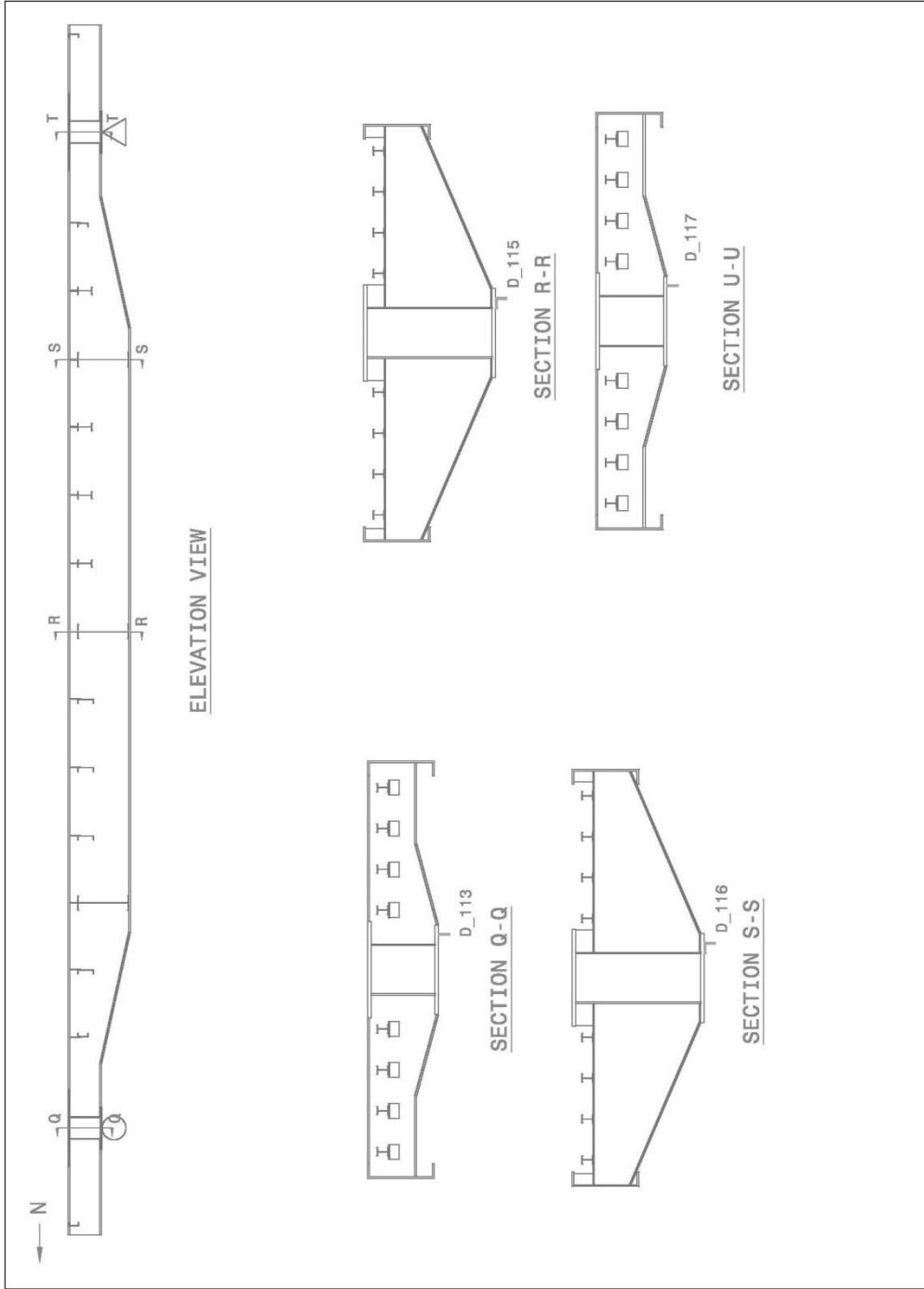
SHEET NO. :  
**1 of 2**





# DISPLACEMENT SENSORS WEST RRFC - FRACTURE 1

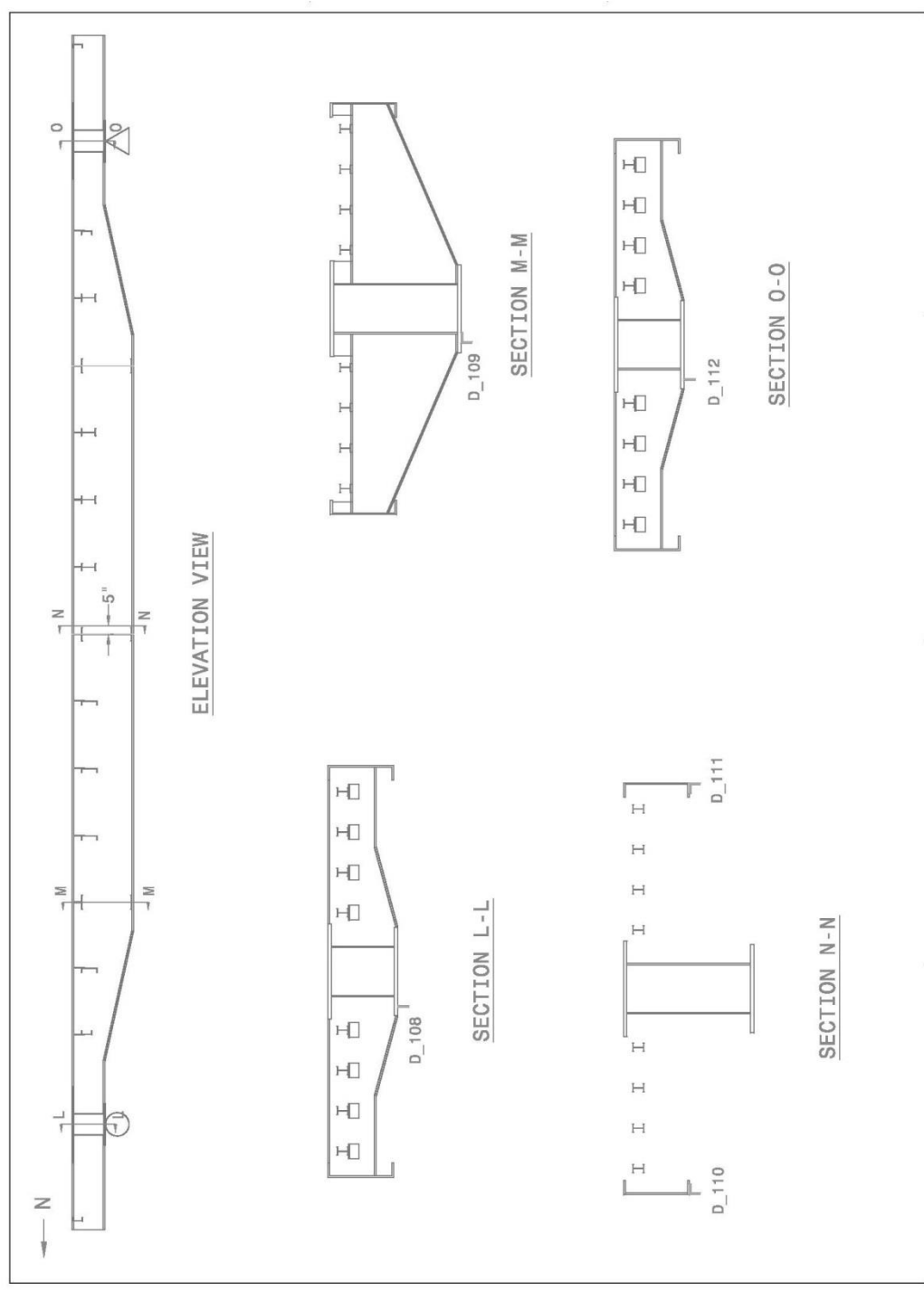
SHEET NO.:  
**2 of 2**



# DISPLACEMENT SENSORS EAST RRFC - FRACTURE 2

SHEET NO.:

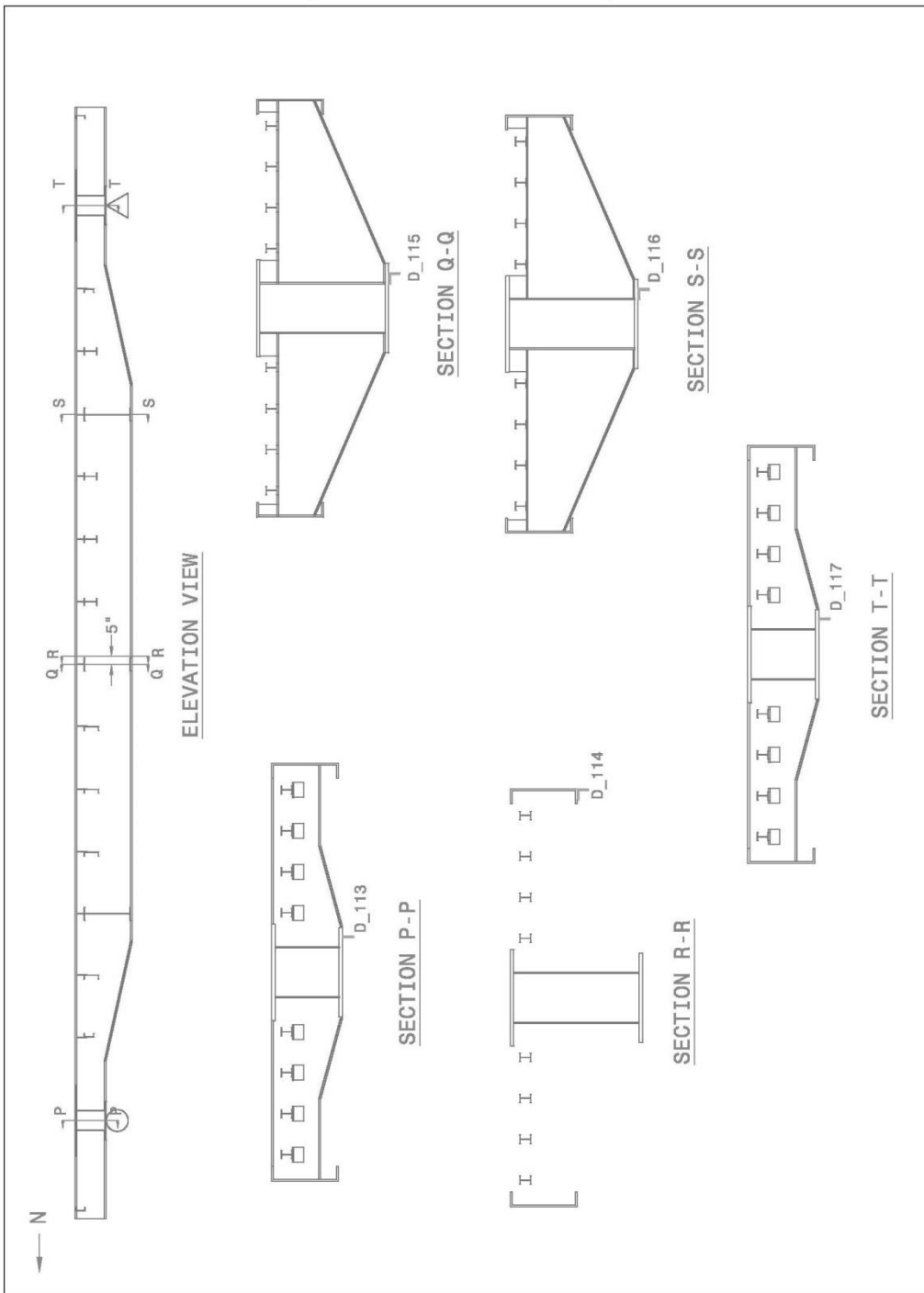
# 1 of 2



# DISPLACEMENT SENSORS WEST RRFC - FRACTURE 2

SHEET NO.:

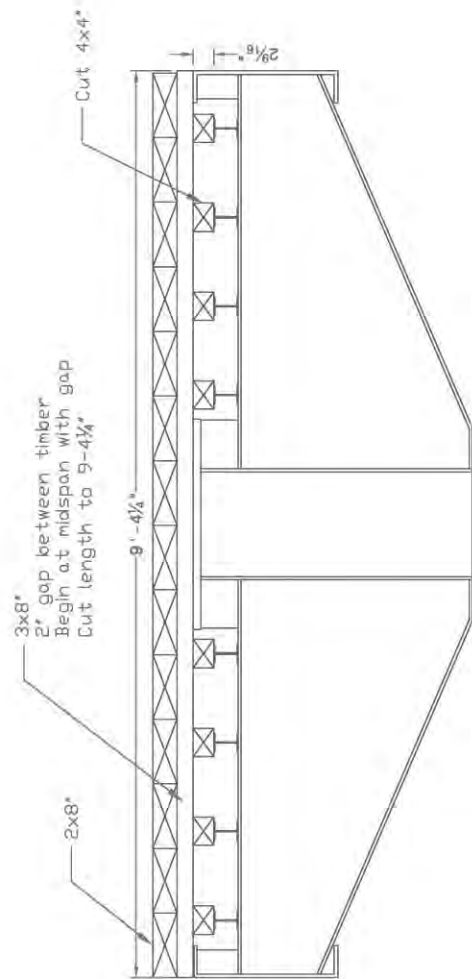
2 of 2



**APPENDIX C. RAILROAD FLATCAR BRIDGE DECK DESIGNS**

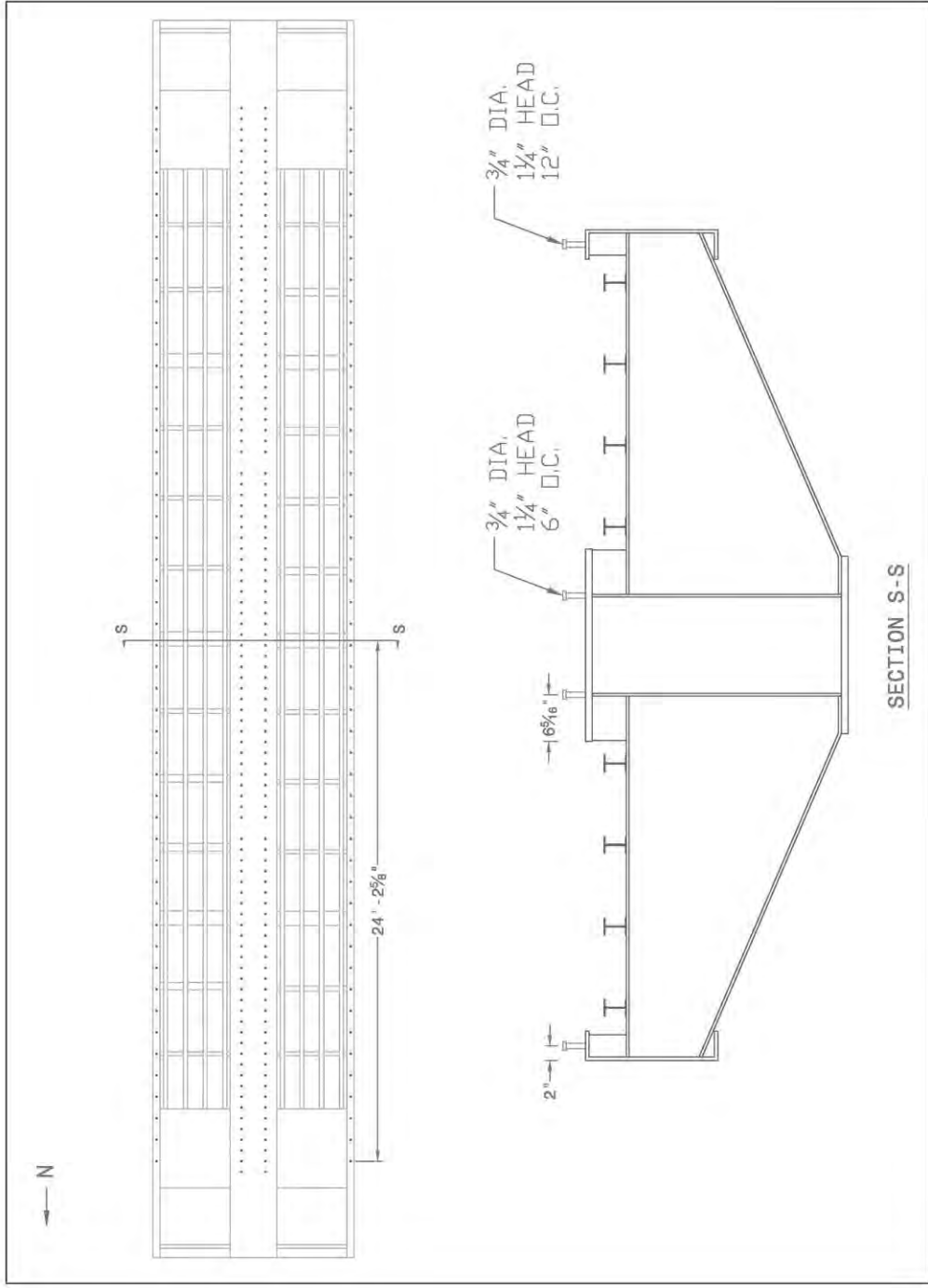
# TIMBER DECK

SHEET NO. :  
**1 of 1**



# SHEAR CONNECTORS

SHEET NO.:  
**1 of 1**



## DECK DESIGN FOR STEEL SUPERSTRUCTURE

### Procedure

Design the bridge deck as per AASHTO LRFD chapter 9.

### Assumptions

1. Strip Method
2. Approximate dead load for deck design as  $\frac{\omega \cdot L^2}{10}$
3. Limiting strain in concrete is 0.003.

### References

1. AASHTO LRFD
2. Indiana Design Manual

### Given

#### Concrete

$$f_c := 6 \text{ ksi}$$

$$\gamma_c := 145 \text{ pcf}$$

#### Section properties (Steel)

$$b_f := 3.9375 \text{ in}$$

$$t_f := 0.5 \text{ in}$$

$$t_w := \frac{7}{16} \text{ in}$$

$$f_{y,\text{rebar}} := 60 \text{ ksi}$$

$$E_s := 29000 \text{ ksi}$$

#### Section properties (Slab)

$$X_{ws} := 0 \text{ in}$$

$$d_s := 6.5 \text{ in}$$

$$l_s := d_s - X_{ws} = 6.5 \text{ in}$$

$$c_b := 1 \text{ in}$$

#### *AASHTO 9.7.2.4*

Compressive strength of concrete

Assumed density of reinforced concrete

Exterior girder top flange width

Exterior girder top flange thickness

Exterior girder web thickness

Yield strength of steel reinforcement

Elastic modulus of steel components

Depth of sacrificial wearing surface

Total depth of slab

Design depth of the slab

#### *AASHTO 5.12.3*

Bottom cover

$$c_t := 1 \text{ in}$$

AASHTO 5.12.3  
Top cover - using 1" for lab testing

$$b_{\text{strip}} := 1 \text{ ft}$$

$$d := d_s - X_{\text{wss}} - c_b = 5.5 \text{ in}$$

#### Section Properties (Future Wearing Surface)

$$DL_{\text{fws}} := 35 \text{ psf}$$

#### Bridge cross section details

$$S := 32.1875 \text{ in} = 2.68 \text{ ft}$$

Spacing between inner exterior girders

$$S_{\text{eff}} := S - t_w = 2.65 \text{ ft}$$

AASHTO 9.7.2.4  
Effective girder spacing

$$W_{\text{bridge}} := 256 \text{ in} = 21.33 \text{ ft}$$

Bridge width

#### Load Factors

$$\eta_D := 1.00$$

AASHTO 1.3.3  
Ductility factor

$$\eta_R := 1.00$$

AASHTO 1.3.4  
Redundancy factor  
>= 1.05 for nonredundant members  
= 1.00 for conventional levels of red

$$\eta_I := 1.00$$

AASHTO 1.3.5  
Importance factor

$$\eta := \eta_D \cdot \eta_R \cdot \eta_I = 1$$

AASHTO 1.3.2.1  
Load modifier

$$\gamma_{p,DC} := 1.25$$

AASHTO Table 3.4.1-2  
Components and attachments

$$\gamma_{p,DW} := 1.5$$

AASHTO Table 3.4.1-2  
Wearing surfaces

$$\gamma_{LL} := 1.75$$

AASHTO Table 3.4.1-1  
Live load  
Strength | Case

$$\phi_b := 0.9$$

#### Loads



$$\frac{b_f}{4} = 0.98\text{-in}$$

AASHTO 4.6.2.1.6

Design section for negative moments and shear forces, assuming steel I-beams

$$M_{s,LL,n} := 2.48\text{kip}\cdot\text{ft}$$

AASHTO Table A4-1

Live load moment

#### Service (Positive)

Dead load approximated using Assumption 1.  
Live load from AASHTO Table A4-1.

$$w_{s,slab,p} := \gamma_c \cdot b_{strip} \cdot d_s = 0.08 \cdot \frac{\text{kip}}{\text{ft}}$$

$$M_{s,slab,p} := \frac{1}{10} \cdot w_{s,slab,p} \cdot S_{eff}^2 = 0.05 \cdot \text{kip}\cdot\text{ft}$$

Slab dead load moment (per foot)

$$M_{s,fws,p} := \frac{1}{10} \cdot DL_{fws} \cdot b_{strip} \cdot S_{eff}^2 = 0.02 \cdot \text{kip}\cdot\text{ft}$$

Future wearing surface moment (per foot)

$$M_{s,LL,p} := 4.68\text{kip}\cdot\text{ft}$$

AASHTO Table A4-1

Live load moment (per foot)

#### Service (Negative)

$$M_{s,slab,n} := M_{s,slab,p} = 0.05 \cdot \text{kip}\cdot\text{ft}$$

Slab dead load moment (per foot)

$$M_{s,fws,n} := M_{s,fws,p} = 0.02 \cdot \text{kip}\cdot\text{ft}$$

Future wearing surface moment (per foot)

#### Factored (Positive)

$$M_{u,slab,p} := \eta \cdot \gamma_p \cdot DC \cdot M_{s,slab,p} = 0.07 \cdot \text{kip}\cdot\text{ft}$$

$$M_{u,fws,p} := \eta \cdot \gamma_p \cdot DW \cdot M_{s,fws,p} = 0.04 \cdot \text{kip}\cdot\text{ft}$$

$$M_{u,LL,p} := \eta \cdot \gamma_{LL} \cdot M_{s,LL,p} = 8.19 \cdot \text{kip}\cdot\text{ft}$$

#### Factored (Negative)

$$M_{u,slab,n} := \eta \cdot \gamma_p \cdot DC \cdot M_{s,slab,n} = 0.07 \cdot \text{kip}\cdot\text{ft}$$

$$M_{u,fws,n} := \eta \cdot \gamma_p \cdot DW \cdot M_{s,fws,n} = 0.04 \cdot \text{kip}\cdot\text{ft}$$

$$M_{u,LL,n} := \eta \cdot \gamma_{LL} \cdot M_{s,LL,n} = 4.34 \cdot \text{kip}\cdot\text{ft}$$

#### Total moments for service

$$M_{s,p} := \frac{M_{s,slab,p} + M_{s,fws,p} + M_{s,LL,p}}{ft} = 4.76 \cdot \text{kip} \cdot \frac{ft}{ft}$$

$$M_{s,n} := \frac{M_{s,slab,n} + M_{s,fws,n} + M_{s,LL,n}}{ft} = 2.56 \cdot \text{kip} \cdot \frac{ft}{ft}$$

**Total factored moments**

$$M_{u,p} := \frac{M_{u,slab,p} + M_{u,fws,p} + M_{u,LL,p}}{ft} = 8.3 \cdot \text{kip} \cdot \frac{ft}{ft}$$

$$M_{u,n} := \frac{M_{u,slab,n} + M_{u,fws,n} + M_{u,LL,n}}{ft} = 4.45 \cdot \text{kip} \cdot \frac{ft}{ft}$$

**Transverse Reinforcement - Positive Moment Design (Bottom Bars)**

Choose #5 @10      $A_s := 0.31 \text{ in}^2$       $d_b := 0.625 \text{ in}$       $A_{f,p} := \left( \frac{1 \text{ ft}}{10 \text{ in}} \right) \cdot A_s = 0.37 \text{ in}^2$

$$d_p := d_s - X_{ws} - c_b - \frac{d_b}{2} \quad d_p = 5.19 \text{ in}$$

$$a := \frac{A_{f,p} \cdot f_y \cdot \text{rebar}}{0.85 \cdot f_c \cdot b_{\text{strip}}} \quad a = 0.36 \text{ in}$$

$$\phi M_{n,p} := \frac{\phi_b \cdot A_{f,p} \cdot f_y \cdot \text{rebar} \cdot \left( d_p - \frac{a}{2} \right)}{ft} \quad \phi M_{n,p} = 8.38 \frac{1}{ft} \cdot \text{kip} \cdot ft$$

$$\frac{\phi M_{n,p}}{M_{u,p}} = 1.01 \quad \text{OK} \quad M_{u,p} = 8.3 \frac{1}{ft} \cdot \text{kip} \cdot ft$$

Determine if the section is tension controlled:

$$\epsilon_{cu} := 0.003 \quad \beta_1 := 0.85 \quad c := \frac{a}{\beta_1} = 0.43 \text{ in}$$

$$\epsilon_s := \frac{\epsilon_{cu}}{c} \cdot (d_p - c) \quad \epsilon_s = 0.03 > 0.005 \quad \text{OK} \quad \text{Therefore } \phi = 0.9$$

Check for crack control (positive):

$$s_p \leq \frac{700 \cdot \gamma_e}{\beta_s \cdot f_{ss}} - 2 \cdot d_e$$

$$\gamma_e := 1$$

AASHTO 5.7.3.4-1  
Spacing of mild steel

Assume class 1

$$d_{c,p} := c_b - \frac{d_b}{2} = 0.69 \text{ in}$$

$$\beta_{s,p} := 1 + \frac{d_{c,p}}{0.7 \cdot (t_s - d_{c,p})} = 1.17$$

$$f_{ss} = \frac{M_{ss}(d - c)}{I_t} \cdot n$$

$$M_{ss,p} := M_{s,p}$$

Service level positive moment

$$\rho_p := \frac{A_{f,p}}{b_{\text{strip}} \cdot d_p} \quad \rho_p = 5.98 \times 10^{-3}$$

$$k_1 := 1$$

AASHTO 5.4.2.4-1

$$E_c := 33000 \cdot k_1 \cdot \left( \frac{\gamma_c}{k_{cf}} \right)^{1.5} \cdot \sqrt{f_c \cdot \text{ksi}} = 4.46 \times 10^3 \cdot \text{ksi}$$

Modulus of elasticity for concrete

$$n := \frac{E_s}{E_c} = 6.5$$

$$k_p := \sqrt{\rho_p^2 \cdot n^2 + 2\rho_p \cdot n} - \rho_p \cdot n \quad k_p = 0.24$$

$$c_{s,p} := k_p \cdot d_p = 1.26 \text{ in}$$

Depth to the neutral axis at service (positive)

$$I_{t,p} := \frac{1}{3} \cdot b_{\text{strip}} \cdot c_{s,p}^3 + n \cdot A_{f,p} \cdot (d_p - c_{s,p})^2 = 45.29 \cdot \text{in}^4$$

Transformed moment of inertia

$$f_{ss,p} := M_{ss,p} \cdot f_t \cdot \frac{(d_p - c_{s,p})}{I_{t,p}} \cdot n \quad f_{ss,p} = 32.2 \cdot \text{ksi}$$

$$s_p := \frac{700 \cdot \gamma_c \cdot \frac{\text{kip}}{\text{in}}}{\beta_{s,p} \cdot f_{ss,p}} - 2 \cdot d_{c,p} = 17.22 \text{ in} > 8 \text{ in} \quad \text{OK}$$

Minimum Reinforcement:

$$\phi M_n \geq \min(1.2 \cdot M_{cr}, 1.33 M_u)$$

AASHTO 5.7.3.3.2

$$M_{cr} = S_c \cdot (f_r + f_{cpe}) - M_{dne} \left( \frac{S_e}{S_{nc}} - 1 \right) \geq S_c \cdot f_r$$

$$S_c := \frac{b_{strip} \cdot t_s^2}{6} = 84.5 \cdot \text{in}^3 \quad f_r := 0.37 \sqrt{f_c \cdot \text{ksi}} = 906.31 \text{ psi} \quad \text{Section modulus and modulus of rupture}$$

$$M_{cr} := S_c \cdot f_r \quad M_{cr} = 6.38 \cdot \text{kip} \cdot \text{ft} \quad \text{Cracking moment}$$

$$\min \left( 1.2 \cdot \frac{M_{cr}}{\text{ft}}, 1.33 M_{u,p} \right) = 7.66 \frac{1}{\text{ft}} \cdot \text{kip} \cdot \text{ft} < \phi M_{n,p} = 8.38 \frac{1}{\text{ft}} \cdot \text{kip} \cdot \text{ft} \quad \text{OK}$$

### Transverse Reinforcement - Negative Moment Design (Top Bars)

$$\text{Choose \#5 @ 10} \quad A_s := 0.31 \text{ in}^2 \quad d_b := 0.625 \text{ in} \quad \Delta_{f,n} := \left( \frac{1 \text{ ft}}{10 \text{ in}} \right) \cdot A_s = 0.372 \cdot \text{in}^2$$

$$d_n := d_s - X_{ws} - c_1 - \frac{d_b}{2} \quad d_n = 5.19 \cdot \text{in}$$

$$a := \frac{\Delta_{f,n} \cdot f_{y,\text{rebar}}}{0.85 \cdot f_c \cdot b_{strip}} \quad a = 0.36 \cdot \text{in}$$

$$\phi M_{n,n} := \frac{\phi_b \cdot \Delta_{f,n} \cdot f_{y,\text{rebar}} \cdot \left( d_n - \frac{a}{2} \right)}{\Omega} \quad \phi M_{n,n} = 8.38 \frac{1}{\text{ft}} \cdot \text{kip} \cdot \text{ft}$$

$$\frac{\phi M_{n,n}}{M_{u,n}} = 1.88 \quad \text{OK}$$

Determine if the section is tension controlled:

$$\epsilon_{cu} := 0.003 \quad \beta_1 := 0.85 \quad c := \frac{a}{\beta_1} = 0.43 \cdot \text{in}$$

$$\epsilon_s := \frac{\epsilon_{cu}}{c} \cdot (d - c) \quad \epsilon_s = 0.04 > 0.005 \quad \text{OK} \quad \text{Therefore } \phi = 0.9$$

Check for crack control (positive):

$$s_p \leq \frac{700 \cdot \gamma_e}{\beta_s \cdot f_{ss}} - 2 \cdot d_c \quad \text{AASHTO 5.7.3.4-1} \\ \text{Spacing of mild steel}$$

$$\gamma_e := 1 \quad \text{Assume class 1}$$

$$d_{c,n} := c_t - \frac{d_b}{2} = 0.69 \text{ in}$$

$$\beta_{s,n} := 1 + \frac{d_{c,n}}{0.7 \cdot (t_s - d_{c,n})} = 1.17$$

$$f_{ss} = \frac{M_{ss}(d - c)}{I_t} \cdot n$$

$$M_{ss,n} := M_{s,n}$$

Service level positive moment

$$\rho_n := \frac{A_{f,n}}{b_{strip} \cdot d_n} \quad \rho_n = 5.9759 \times 10^{-3}$$

$$k_n := \sqrt{\rho_n^2 \cdot n^2 + 2\rho_n \cdot n} - \rho_n \cdot n \quad k_n = 0.24$$

$$c_{s,n} := k_n \cdot d_n = 1.26 \text{ in}$$

Depth to the neutral axis at service (positive)

$$I_{t,n} := \frac{1}{3} \cdot b_{strip} \cdot c_{s,n}^3 + n \cdot A_{f,n} \cdot (d_n - c_{s,n})^2 = 45.29 \cdot \text{in}^4$$

Transformed moment of inertia

$$f_{ss,n} := M_{ss,n} \cdot \text{ft} \cdot \frac{(d_n - c_{s,n})}{I_{t,n}} \cdot n \quad f_{ss,n} = 17.32 \cdot \text{ksi}$$

$$s_n := \frac{700 \cdot \gamma_e \cdot \frac{\text{kip}}{\text{in}}}{\beta_{s,n} \cdot f_{ss,n}} - 2 \cdot d_{c,n} = 33.21 \cdot \text{in} \geq 6 \text{ in} \quad \text{OK}$$

Minimum Reinforcement:

$$\phi M_n \geq \min(1.2 \cdot M_{cr}, 1.33 M_u)$$

AASHTO 5.7.3.3.2

$$M_{cr} = S_c \left( f_r + f_{cpe} \right) - M_{dnc} \left( \frac{S_c}{S_{nc}} - 1 \right) \geq S_c \cdot f_r$$

$$\min \left( 1.2 \cdot \frac{M_{cr}}{\text{ft}}, 1.33 M_{u,n} \right) = 5.91 \frac{1}{\text{ft}} \cdot \text{kip} \cdot \text{ft} < \phi M_{n,n} = 8.38 \frac{1}{\text{ft}} \cdot \text{kip} \cdot \text{ft} \quad \text{OK}$$

**Longitudinal Reinforcement (AASHTO 9.7.2.5)**

$$A_{s,\text{min},\text{bot}} := 0.27 \frac{\text{in}^2}{\text{ft}}$$

Choose #5 @ 12

$$A_{s,\text{bot}} := 0.31 \frac{\text{in}^2}{\text{ft}}$$

$$A_{s,\text{min},\text{top}} := 0.18 \frac{\text{in}^2}{\text{ft}}$$

Choose #5 @ 12

$$A_{s,\text{top}} := 0.31 \frac{\text{in}^2}{\text{ft}}$$

**Shrinkage and Temperature Reinforcement (AASHTO 5.10.8)**

$$A_s \geq \frac{1.3 \cdot b \cdot h}{2 \cdot (b + h) \cdot f_y}$$

$$\frac{1.3 \cdot b_{\text{strip}} \cdot d_s \cdot \frac{\text{kip}}{\text{in}\cdot\text{ft}}}{2 \cdot (b_{\text{strip}} + d_s) \cdot f_{y,\text{rebar}}} = 0.046 \frac{1}{\text{ft}} \cdot \text{in}^2$$

&lt;

$$A_{s,\text{top}} = 0.31 \frac{1}{\text{ft}} \cdot \text{in}^2$$

$$A_{s,\text{bot}} = 0.31 \frac{1}{\text{ft}} \cdot \text{in}^2$$

$$A_{f,p} = 0.37 \cdot \text{in}^2$$

$$A_{f,n} = 0.37 \cdot \text{in}^2$$

OK

$$0.11 \cdot \frac{\text{in}^2}{\text{ft}} < A_s < 0.60 \frac{\text{in}^2}{\text{ft}}$$

OK

**Distribution Reinforcement (AASHTO 9.7.3.2)**

$$A_{\text{secondary},\text{req}} := \min \left( .67, \frac{2.2}{\sqrt{\frac{S_{\text{eff}}}{\text{ft}}}} \right) = 67.9\%$$

$$A_{\text{secondary},\text{req}} \cdot \frac{A_{f,p}}{\text{ft}} = 0.25 \frac{1}{\text{ft}} \cdot \text{in}^2$$

$$A_{s,\text{bot}} = 0.31 \frac{1}{\text{ft}} \cdot \text{in}^2$$

OK

**Minimum Spacing Between Mats (AASHTO 5.10.3.1.1)**

$$1.5 \cdot d_b = 0.94 \cdot \text{in}$$

Primary Reinforcement (Transverse direction):

Use #5 at 10" for top reinforcement and #5 at 10" for bottom reinforcement.

Secondary Reinforcement (Longitudinal direction):

Use #5 at 12" for top reinforcement and #5 at 12" for bottom reinforcement.

**APPENDIX D. LABORATORY TEST RESULTS**

<b>Test 1 - No Deck (150 kips)</b>					
Channel	Avg Stress (ksi)	Channel	Avg Stress (ksi)	Channel	Avg Stress (ksi)
CH_1	-5.31	CH_32	20.29	CH_95	-7.53
CH_2	0.04	CH_33	-16.78	CH_96	-1.16
CH_3	-3.37	CH_34	21.49	CH_97	6.05
CH_4	4.97	CH_35	-8.66	CH_98	7.89
CH_5	-1.78	CH_36	-4.45	CH_99	1.16
CH_6	4.56	CH_37	-5.71	CH_100	-4.05
CH_7	-5.97	CH_38	-1.79	CH_101	-2.05
CH_8	0.52	CH_39	-5.15	CH_102	-0.35
CH_9	-6.82	CH_40	-1.37	CH_103	2.61
CH_10	2.57	CH_41	-6.67	CH_104	1.84
CH_11	-3.80	CH_42		CH_105	-0.13
CH_12	-1.51	CH_43	-11.38	CH_106	-1.13
CH_13	-4.10	CH_44	8.45	LOADCELL	150.03
CH_14	-0.95	CH_45	0.37	D_108 (in)	-0.01
CH_15	-6.48	CH_46	2.35	D_109 (in)	-0.82
CH_16	9.16	CH_47	-6.79	D_110 (in)	-1.20
CH_17	-6.80	CH_48	3.12	D_111 (in)	-0.84
CH_18	9.12	CH_49	-6.78	D_112 (in)	-0.05
CH_19	-6.87	CH_50	9.26	CH_113	-0.48
CH_20	3.35	CH_51	-6.48	CH_114	0.24
CH_21	-11.19	CH_52	10.23	CH_115	-1.06
CH_22	9.32	CH_53	-6.86	CH_116	-0.96
CH_23	-6.99	CH_54	3.04	CH_117	0.33
CH_24	-3.19	CH_55	-6.10	CH_118	-0.44
CH_25	-5.31	CH_56	0.90	CH_119	-0.53
CH_26	-1.08	CH_57	-2.37	CH_120	0.51
CH_27	-5.70	CH_58	4.38	CH_121	-1.20
CH_28	-1.39	CH_59	-2.27	CH_122	-0.84
CH_29	-9.18	CH_60	4.96	CH_123	0.82
CH_30	-4.52	CH_61	-5.32	CH_124	-0.14
CH_31	-16.44	CH_62	-0.02		



<b>Test 2 - No Deck (150 kips)</b>			
<b>Channel</b>	<b>Avg Stress (ksi)</b>	<b>Channel</b>	<b>Avg Stress (ksi)</b>
<b>CH_63</b>	-6.21	<b>CH_88</b>	21.74
<b>CH_64</b>	0.86	<b>CH_89</b>	-9.02
<b>CH_65</b>	-2.32	<b>CH_90</b>	-4.91
<b>CH_66</b>	4.57	<b>CH_91</b>	-7.28
<b>CH_67</b>	-2.80	<b>CH_92</b>	-3.35
<b>CH_68</b>	5.09	<b>CH_93</b>	-11.59
<b>CH_69</b>	-5.82	<b>CH_94</b>	8.96
<b>CH_70</b>	0.13	<b>LOADCELL</b>	150.03
<b>CH_71</b>	-6.93	<b>D_113 (in)</b>	-0.01
<b>CH_72</b>	2.80	<b>D_114 (in)</b>	-0.84
<b>CH_73</b>	-6.67	<b>D_115 (in)</b>	-1.20
<b>CH_74</b>	9.76	<b>D_116 (in)</b>	-0.83
<b>CH_75</b>	-6.65	<b>D_117 (in)</b>	-0.04
<b>CH_76</b>	10.28	<b>CH_113</b>	-0.01
<b>CH_77</b>	-7.03	<b>CH_114</b>	-0.02
<b>CH_78</b>	3.16	<b>CH_115</b>	-0.01
<b>CH_79</b>	-11.13	<b>CH_116</b>	-0.01
<b>CH_80</b>	8.46	<b>CH_117</b>	-0.02
<b>CH_81</b>	-7.24	<b>CH_118</b>	-0.01
<b>CH_82</b>	-3.71	<b>CH_119</b>	0.01
<b>CH_83</b>	-9.36	<b>CH_120</b>	0.02
<b>CH_84</b>	-4.99	<b>CH_121</b>	-0.01
<b>CH_85</b>	-16.75	<b>CH_122</b>	0.01
<b>CH_86</b>	21.50	<b>CH_123</b>	-0.01
<b>CH_87</b>	-16.91	<b>CH_124</b>	-0.02

<b>Test 3 -Timber Deck (150 kips)</b>					
Channel	Avg Stress (ksi)	Channel	Avg Stress (ksi)	Channel	Avg Stress (ksi)
CH_1	-5.37	CH_32	19.98	CH_95	-7.48
CH_2	-0.01	CH_33	-15.97	CH_96	-1.20
CH_3	-3.29	CH_34	21.53	CH_97	6.11
CH_4	5.12	CH_35	-10.71	CH_98	7.75
CH_5	-1.90	CH_36	-2.74	CH_99	1.15
CH_6	4.49	CH_37	-5.47	CH_100	-4.02
CH_7	-5.84	CH_38	-1.70	CH_101	-1.99
CH_8	0.58	CH_39	-4.54	CH_102	-0.32
CH_9	-6.87	CH_40	-1.38	CH_103	2.67
CH_10	2.53	CH_41	-6.56	CH_104	1.80
CH_11	-3.82	CH_42	-2.97	CH_105	-0.13
CH_12	-1.48	CH_43	-11.48	CH_106	-1.10
CH_13	-4.07	CH_44	8.47	LOADCELL	150.00
CH_14	-0.95	CH_45	0.47	D_108 (in)	-0.01
CH_15	-6.47	CH_46	2.24	D_109 (in)	-0.81
CH_16	9.10	CH_47	-6.85	D_110 (in)	-1.18
CH_17	-6.76	CH_48	3.12	D_111 (in)	-0.82
CH_18	9.11	CH_49	-6.71	D_112 (in)	-0.04
CH_19	-6.75	CH_50	9.27	CH_113	-0.49
CH_20	3.24	CH_51	-6.47	CH_114	0.23
CH_21	-11.22	CH_52	10.15	CH_115	-1.09
CH_22	9.31	CH_53	-6.78	CH_116	-0.93
CH_23	-6.99	CH_54	2.96	CH_117	0.32
CH_24	-3.17	CH_55	-6.14	CH_118	-0.42
CH_25	-5.45	CH_56	0.80	CH_119	-0.55
CH_26	-0.96	CH_57	-2.17	CH_120	0.51
CH_27	-5.71	CH_58	4.57	CH_121	-1.20
CH_28	-1.30	CH_59	-2.42	CH_122	-0.84
CH_29	-10.09	CH_60	4.69	CH_123	0.79
CH_30	-3.62	CH_61	-5.32	CH_124	-0.13
CH_31	-16.07	CH_62	0.09		

<b>Test 4 -Timber Deck (75 kips)</b>					
Channel	Avg Stress (ksi)	Channel	Avg Stress (ksi)	Channel	Avg Stress (ksi)
CH_1	-2.75	CH_32	9.70	CH_95	-3.82
CH_2	-0.15	CH_33	-7.89	CH_96	-0.71
CH_3	-1.50	CH_34	10.80	CH_97	3.11
CH_4	2.77	CH_35	-4.49	CH_98	3.87
CH_5	-1.19	CH_36	-2.35	CH_99	0.61
CH_6	2.18	CH_37	-4.63	CH_100	-2.13
CH_7	-2.71	CH_38	1.05	CH_101	-0.98
CH_8	0.24	CH_39	-6.77	CH_102	-0.19
CH_9	-3.02	CH_40	3.58	CH_103	1.38
CH_10	0.60	CH_41	-2.48	CH_104	0.91
CH_11	-1.80	CH_42	-1.79	CH_105	-0.05
CH_12	-0.80	CH_43	-6.45	CH_106	-0.63
CH_13	-2.05	CH_44	5.11	LOADCELL	75.00
CH_14	-0.52	CH_45	1.28	D_108 (in)	-0.01
CH_15	-3.30	CH_46	-3.74	D_109 (in)	-0.42
CH_16	4.62	CH_47	-2.86	D_110 (in)	-0.60
CH_17	-3.46	CH_48	0.89	D_111 (in)	-0.43
CH_18	4.66	CH_49	-3.50	D_112 (in)	-0.03
CH_19	-2.81	CH_50	4.62	CH_113	-0.38
CH_20	1.03	CH_51	-3.35	CH_114	0.11
CH_21	-6.21	CH_52	5.19	CH_115	-0.49
CH_22	5.27	CH_53	-2.78	CH_116	-0.40
CH_23	-5.88	CH_54	0.90	CH_117	0.18
CH_24	0.00	CH_55	-3.28	CH_118	-0.30
CH_25	-3.96	CH_56	0.39	CH_119	-0.35
CH_26	1.42	CH_57	-0.93	CH_120	0.26
CH_27	-5.50	CH_58	2.43	CH_121	-0.51
CH_28	1.26	CH_59	-1.50	CH_122	-0.31
CH_29	-5.02	CH_60	2.37	CH_123	0.46
CH_30	-1.97	CH_61	-2.25	CH_124	-0.05
CH_31	-8.39	CH_62	-0.20		

<b>Concrete Pour</b>							
Channel	Final Stress (ksi)	Channel	Final Stress (ksi)	Channel	Final Stress (ksi)	Channel	Final Stress (ksi)
CH_1	-0.28	CH_32	2.56	CH_63	-0.66	CH_94	1.80
CH_2	0.07	CH_33	-2.63	CH_64	0.28	CH_95	-2.70
CH_3	-0.60	CH_34	3.35	CH_65	-0.89	CH_96	-1.03
CH_4	1.35	CH_35	-1.03	CH_66	0.55	CH_97	2.55
CH_5	-0.62	CH_36	-0.15	CH_67	-0.55	CH_98	1.33
CH_6	0.21	CH_37	-1.25	CH_68	1.61	CH_99	-0.38
CH_7	-0.82	CH_38	-0.13	CH_69	-0.77	CH_100	-0.42
CH_8	0.36	CH_39	-0.99	CH_70	0.05	CH_101	-0.55
CH_9	-1.78	CH_40	-0.13	CH_71	0.14	CH_102	1.45
CH_10	1.05	CH_41	-1.32	CH_72	0.60	CH_103	1.23
CH_11	-0.89	CH_42	0.00	CH_73	-2.37	CH_104	0.27
CH_12	0.02	CH_43	-1.52	CH_74	2.06	CH_105	-0.33
CH_13	-0.97	CH_44	0.69	CH_75	-1.82	CH_106	0.17
CH_14	0.09	CH_45	0.07	CH_76	2.00	LOADCELL	NA
CH_15	-1.54	CH_46	-1.21	CH_77	-2.21	D_108 (in)	-0.02
CH_16	1.81	CH_47	-1.28	CH_78	1.22	D_109 (in)	-0.11
CH_17	-1.67	CH_48	0.84	CH_79	-1.83	D_110 (in)	-0.16
CH_18	1.65	CH_49	-0.63	CH_80	1.39	D_111 (in)	-0.13
CH_19	-1.10	CH_50	1.81	CH_81	-1.70	D_112 (in)	-0.04
CH_20	0.85	CH_51	-0.96	CH_82	-0.13	CH_113	0.80
CH_21	-1.54	CH_52	2.43	CH_83	-2.64	CH_114	0.72
CH_22	1.88	CH_53	-0.89	CH_84	-0.46	CH_115	0.00
CH_23	-1.23	CH_54	0.88	CH_85	-2.15	CH_116	-1.27
CH_24	-0.66	CH_55	-0.96	CH_86	3.44	CH_117	-0.09
CH_25	-1.03	CH_56	0.69	CH_87	-2.57	CH_118	0.33
CH_26	0.12	CH_57	-0.35	CH_88	3.13	CH_119	1.18
CH_27	-1.35	CH_58	1.30	CH_89	-2.06	CH_120	0.53
CH_28	-0.16	CH_59	-1.07	CH_90	0.00	CH_121	1.10
CH_29	-1.76	CH_60	0.62	CH_91	-1.83	CH_122	0.21
CH_30	-0.78	CH_61	0.00	CH_92	-0.46	CH_123	0.13
CH_31	-2.65	CH_62	0.33	CH_93	-1.92	CH_124	0.09

<b>Test 5 - Concrete Deck (150 kips)</b>							
Channel	Avg Stress (ksi)	Channel	Avg Stress (ksi)	Channel	Avg Stress (ksi)	Channel	Avg Stress (ksi)
CH_1	-0.33	CH_32	13.78	CH_63	-0.03	CH_94	3.30
CH_2	1.54	CH_33	-2.01	CH_64	1.36	CH_95	-2.93
CH_3	-0.21	CH_34	12.37	CH_65	-0.12	CH_96	-0.91
CH_4	1.03	CH_35	-0.46	CH_66	-0.49	CH_97	2.08
CH_5	0.07	CH_36	1.29	CH_67	0.09	CH_98	7.17
CH_6	3.50	CH_37	-0.08	CH_68	2.02	CH_99	1.35
CH_7	0.10	CH_38	1.58	CH_69	-0.03	CH_100	-2.97
CH_8	-0.17	CH_39	-0.06	CH_70	-0.56	CH_101	0.10
CH_9	-0.46	CH_40	1.52	CH_71	0.03	CH_102	-0.53
CH_10	2.28	CH_41	-0.36	CH_72	0.23	CH_103	1.21
CH_11	-0.03	CH_42		CH_73	-0.13	CH_104	3.98
CH_12	0.29	CH_43	-1.99	CH_74	1.99	CH_105	-0.01
CH_13	-0.19	CH_44	7.98	CH_75	-0.29	CH_106	-2.48
CH_14	0.42	CH_45	0.43	CH_76	1.28	LOADCELL	149.98
CH_15	-0.43	CH_46	4.53	CH_77	-0.39	D_108 (in)	-0.01
CH_16	5.45	CH_47	-0.46	CH_78	1.52	D_109 (in)	-0.32
CH_17	-0.58	CH_48	2.21	CH_79	0.26	D_110 (in)	-0.48
CH_18	5.16	CH_49	-0.50	CH_80	-0.02	D_111 (in)	-0.32
CH_19	-0.86	CH_50	5.90	CH_81	0.14	D_112 (in)	-0.01
CH_20	3.86	CH_51	-0.68	CH_82	0.22	D_113 (in)	0.00
CH_21		CH_52	5.17	CH_83	-0.03	D_114 (in)	-0.09
CH_22	5.73	CH_53	-1.09	CH_84	0.14	D_115 (in)	-0.13
CH_23	-0.03	CH_54	3.64	CH_85	-0.17	D_116 (in)	-0.09
CH_24	0.73	CH_55	-0.26	CH_86	3.83	D_117 (in)	-0.01
CH_25	-0.14	CH_56	1.38	CH_87		CH_125	0.10
CH_26	1.21	CH_57	-0.29	CH_88	1.60	CH_126	0.06
CH_27	-0.02	CH_58	0.62	CH_89	-0.05	CH_127	
CH_28	1.25	CH_59	-0.03	CH_90	0.17	CH_128	
CH_29	-0.48	CH_60	3.37	CH_91	-0.24	CH_129	0.00
CH_30	1.72	CH_61		CH_92	0.48	CH_130	0.01
CH_31	-2.00	CH_62	-0.32	CH_93	-0.73		

<b>Test 6 - Concrete Deck (150 kips)</b>							
Channel	Avg Stress (ksi)	Channel	Avg Stress (ksi)	Channel	Avg Stress (ksi)	Channel	Avg Stress (ksi)
CH_1	-0.27	CH_32	13.40	CH_63	-0.06	CH_94	3.75
CH_2	1.54	CH_33	-1.83	CH_64	1.41	CH_95	-2.97
CH_3	-0.25	CH_34	11.95	CH_65	-0.13	CH_96	-0.94
CH_4	1.00	CH_35	-0.81	CH_66	-0.51	CH_97	2.11
CH_5	0.03	CH_36	1.46	CH_67	0.10	CH_98	7.35
CH_6	3.58	CH_37	0.30	CH_68	2.03	CH_99	1.36
CH_7	0.14	CH_38	2.36	CH_69	0.08	CH_100	-3.02
CH_8	-0.32	CH_39	-0.16	CH_70	-0.67	CH_101	0.09
CH_9	-0.48	CH_40	2.42	CH_71	-0.03	CH_102	-0.54
CH_10	1.92	CH_41	-0.21	CH_72	0.26	CH_103	1.22
CH_11	-0.07	CH_42	2.33	CH_73	-0.12	CH_104	4.05
CH_12	0.25	CH_43		CH_74	1.92	CH_105	0.00
CH_13	-0.14	CH_44	9.28	CH_75	-0.30	CH_106	-2.47
CH_14	0.44	CH_45	1.40	CH_76	1.36	LOADCELL	150.06
CH_15	-0.47	CH_46	0.94	CH_77	-0.34	D_108 (in)	-0.01
CH_16	5.47	CH_47	-0.51	CH_78	1.34	D_109 (in)	-0.32
CH_17	-0.66	CH_48	1.88	CH_79	0.27	D_110 (in)	-0.48
CH_18	5.31	CH_49	-0.46	CH_80	-0.05	D_111 (in)	-0.32
CH_19	-0.88	CH_50	6.03	CH_81	0.18	D_112 (in)	-0.01
CH_20	3.39	CH_51	-0.59	CH_82	0.26	D_113 (in)	0.00
CH_21		CH_52	5.33	CH_83	0.03	D_114 (in)	-0.10
CH_22	6.69	CH_53	-1.08	CH_84	0.22	D_115 (in)	-0.13
CH_23	-0.84	CH_54	3.17	CH_85	-0.17	D_116 (in)	-0.10
CH_24	1.54	CH_55	-0.25	CH_86	4.07	D_117 (in)	-0.01
CH_25		CH_56	1.40	CH_87		CH_125	0.12
CH_26	1.98	CH_57	-0.34	CH_88	1.58	CH_126	0.12
CH_27	-0.44	CH_58	0.65	CH_89	-0.07	CH_127	
CH_28	1.71	CH_59	0.09	CH_90	0.22	CH_128	
CH_29	-0.61	CH_60	3.42	CH_91	-0.20	CH_129	0.03
CH_30	1.55	CH_61		CH_92	0.62	CH_130	0.03
CH_31	-1.67	CH_62	-0.44	CH_93	-0.72		

<b>Test 7 - Concrete Deck (150 kips)</b>							
Channel	Avg Stress (ksi)	Channel	Avg Stress (ksi)	Channel	Avg Stress (ksi)	Channel	Avg Stress (ksi)
CH_1	0.21	CH_32	1.34	CH_63	-0.07	CH_94	5.86
CH_2	-0.50	CH_33	-0.24	CH_64	-0.23	CH_95	-2.33
CH_3	0.12	CH_34	3.80	CH_65	0.09	CH_96	-0.46
CH_4	1.85	CH_35	-0.10	CH_66	3.43	CH_97	2.26
CH_5	-0.11	CH_36	0.09	CH_67	-0.28	CH_98	-0.83
CH_6	-0.53	CH_37	0.03	CH_68	1.00	CH_99	-0.39
CH_7	-0.09	CH_38	0.18	CH_69	-0.36	CH_100	0.19
CH_8	1.25	CH_39	0.09	CH_70	1.70	CH_101	-1.75
CH_9	-0.52	CH_40	0.16	CH_71	-0.76	CH_102	0.10
CH_10	1.36	CH_41	0.10	CH_72	3.73	CH_103	2.13
CH_11	-0.25	CH_42	0.18	CH_73	-0.94	CH_104	-0.90
CH_12	0.02	CH_43	0.19	CH_74	5.22	CH_105	-0.34
CH_13	-0.02	CH_44	0.06	CH_75	-0.39	CH_106	1.10
CH_14	0.24	CH_45	-0.27	CH_76	6.35	LOADCELL	149.97
CH_15	-0.59	CH_46	-2.69	CH_77	-0.32	D_108 (in)	-0.01
CH_16	1.00	CH_47	-0.63	CH_78	2.54	D_109 (in)	-0.09
CH_17	-0.09	CH_48	1.34	CH_79	-2.08	D_110 (in)	-0.12
CH_18	1.83	CH_49	-0.42	CH_80	8.23	D_111 (in)	-0.09
CH_19	0.03	CH_50	1.20	CH_81	-0.40	D_112 (in)	0.00
CH_20	0.14	CH_51	-0.08	CH_82	1.59	D_113 (in)	-0.01
CH_21		CH_52	1.90	CH_83	-0.43	D_114 (in)	-0.32
CH_22	3.11	CH_53	0.21	CH_84	1.40	D_115 (in)	-0.47
CH_23	-0.34	CH_54	0.19	CH_85	-2.08	D_116 (in)	-0.32
CH_24	0.05	CH_55	-0.21	CH_86	12.11	D_117 (in)	-0.01
CH_25	-0.52	CH_56	-0.70	CH_87		CH_125	0.26
CH_26	0.01	CH_57	-0.18	CH_88	14.71	CH_126	0.35
CH_27	-0.36	CH_58	2.24	CH_89	-0.78	CH_127	
CH_28	0.08	CH_59	-0.10	CH_90	1.51	CH_128	
CH_29	-0.20	CH_60	-0.46	CH_91	0.11	CH_129	0.17
CH_30	0.06	CH_61		CH_92	1.54	CH_130	0.15
CH_31	-0.53	CH_62	1.33	CH_93			

<b>Test 8 - Concrete Deck (150 kips)</b>							
Channel	Avg Stress (ksi)	Channel	Avg Stress (ksi)	Channel	Avg Stress (ksi)	Channel	Avg Stress (ksi)
CH_1	0.26	CH_32	1.42	CH_63	-0.11	CH_94	6.94
CH_2	-0.62	CH_33	-0.23	CH_64	-0.32	CH_95	-2.41
CH_3	0.16	CH_34	4.02	CH_65	0.11	CH_96	-0.49
CH_4	1.91	CH_35	-0.03	CH_66	3.47	CH_97	2.32
CH_5	-0.12	CH_36	0.14	CH_67	-0.30	CH_98	-0.82
CH_6	-0.55	CH_37	0.04	CH_68	1.07	CH_99	-0.37
CH_7	-0.13	CH_38	0.18	CH_69	-0.37	CH_100	0.17
CH_8	1.30	CH_39	0.13	CH_70	1.70	CH_101	-1.74
CH_9	-0.54	CH_40	0.18	CH_71	-0.78	CH_102	0.14
CH_10	1.15	CH_41	0.14	CH_72	3.22	CH_103	2.16
CH_11	-0.25	CH_42	0.16	CH_73	-0.87	CH_104	-0.92
CH_12	-0.01	CH_43	0.18	CH_74	5.32	CH_105	-0.32
CH_13	-0.04	CH_44	-0.05	CH_75	-0.44	CH_106	1.07
CH_14	0.29	CH_45	-0.29	CH_76	6.40	LOADCELL	150.07
CH_15	-0.52	CH_46	-2.98	CH_77	-0.42	D_108 (in)	-0.01
CH_16	1.09	CH_47	-0.66	CH_78	2.21	D_109 (in)	-0.09
CH_17	-0.09	CH_48	1.28	CH_79	-2.34	D_110 (in)	-0.13
CH_18	1.79	CH_49	-0.39	CH_80	9.51	D_111 (in)	-0.10
CH_19	0.03	CH_50	1.31	CH_81	-0.70	D_112 (in)	0.00
CH_20	0.19	CH_51	-0.11	CH_82	2.37	D_113 (in)	-0.01
CH_21		CH_52	1.95	CH_83	-0.56	D_114 (in)	-0.32
CH_22	3.58	CH_53	0.24	CH_84	1.63	D_115 (in)	-0.46
CH_23	-0.33	CH_54	0.17	CH_85	-1.75	D_116 (in)	-0.31
CH_24	0.18	CH_55	-0.20	CH_86	11.61	D_117 (in)	-0.01
CH_25	-0.41	CH_56	-0.84	CH_87		CH_125	0.20
CH_26	0.04	CH_57	-0.09	CH_88	14.39	CH_126	0.24
CH_27	-0.40	CH_58	2.23	CH_89	-0.67	CH_127	
CH_28	0.08	CH_59	-0.14	CH_90	1.40	CH_128	
CH_29	-0.21	CH_60	-0.49	CH_91	0.15	CH_129	0.10
CH_30	0.11	CH_61		CH_92	2.32	CH_130	0.05
CH_31	-0.47	CH_62	1.38	CH_93			



<b>Test 9 - Concrete Deck (150 kips)</b>							
Channel	Avg Stress (ksi)	Channel	Avg Stress (ksi)	Channel	Avg Stress (ksi)	Channel	Avg Stress (ksi)
CH_1	0.39	CH_32	4.96	CH_63	-0.43	CH_94	12.37
CH_2	-1.32	CH_33	-0.80	CH_64	2.14	CH_95	-5.14
CH_3	0.35	CH_34	10.38	CH_65	-0.26	CH_96	-1.11
CH_4	3.01	CH_35	-0.45	CH_66	-0.20	CH_97	4.54
CH_5	-0.26	CH_36	0.14	CH_67	0.25	CH_98	0.30
CH_6	-0.18	CH_37	-0.42	CH_68	3.13	CH_99	-0.28
CH_7	-0.47	CH_38	0.13	CH_69	-0.19	CH_100	-0.40
CH_8	2.18	CH_39	-0.37	CH_70	-1.48	CH_101	-2.80
CH_9	-0.23	CH_40	0.06	CH_71	-0.64	CH_102	-0.10
CH_10	1.75	CH_41	-0.47	CH_72	1.28	CH_103	3.84
CH_11	-0.21	CH_42	-0.12	CH_73	-0.35	CH_104	-0.60
CH_12	0.17	CH_43	-0.38	CH_74	3.57	CH_105	-0.51
CH_13	-0.10	CH_44	0.18	CH_75	-0.28	CH_106	1.16
CH_14	0.65	CH_45	-0.39	CH_76	3.93	LOADCELL	150.01
CH_15	-0.56	CH_46	-5.97	CH_77	0.15	D_108 (in)	-0.02
CH_16	3.39	CH_47	-0.52	CH_78	1.88	D_109 (in)	-0.59
CH_17	-0.30	CH_48	2.25	CH_79	-0.43	D_110 (in)	-0.33
CH_18	3.49	CH_49	-0.36	CH_80	0.20	D_111 (in)	-0.05
CH_19	-0.60	CH_50	3.79	CH_81	-0.48	D_112 (in)	-0.01
CH_20	1.20	CH_51	-0.35	CH_82	-0.20	D_113 (in)	-0.01
CH_21		CH_52	3.67	CH_83	-0.44	D_114 (in)	-0.59
CH_22	11.73	CH_53	-0.19	CH_84	0.25	D_115 (in)	-0.33
CH_23		CH_54	0.95	CH_85	-0.85	D_116 (in)	-0.05
CH_24	2.46	CH_55	0.09	CH_86	10.09	D_117 (in)	-0.01
CH_25		CH_56	-1.56	CH_87		CH_125	-1.83
CH_26	2.57	CH_57	0.29	CH_88	5.28	CH_126	0.17
CH_27	-0.13	CH_58	3.66	CH_89	-0.35	CH_127	
CH_28	1.86	CH_59	-0.24	CH_90	1.31	CH_128	
CH_29	-0.36	CH_60	-0.58	CH_91	0.07	CH_129	-1.64
CH_30	1.07	CH_61		CH_92	3.90	CH_130	-0.94
CH_31	-1.20	CH_62	2.31	CH_93			

<b>Test 10 - Concrete Deck (150 kips)</b>							
Channel	Avg Stress (ksi)	Channel	Avg Stress (ksi)	Channel	Avg Stress (ksi)	Channel	Avg Stress (ksi)
CH_1	0.32	CH_32	6.06	CH_63	-0.34	CH_94	9.02
CH_2	-0.62	CH_33	-0.93	CH_64	1.60	CH_95	-4.37
CH_3	0.23	CH_34	9.60	CH_65	-0.21	CH_96	-0.99
CH_4	2.44	CH_35	-0.44	CH_66	0.32	CH_97	3.76
CH_5	-0.20	CH_36	0.30	CH_67	0.11	CH_98	1.33
CH_6	0.42	CH_37	-0.34	CH_68	2.51	CH_99	0.01
CH_7	-0.30	CH_38	0.31	CH_69	-0.07	CH_100	-0.76
CH_8	1.60	CH_39	-0.34	CH_70	-0.74	CH_101	-2.05
CH_9	-0.36	CH_40	0.22	CH_71	-0.53	CH_102	-0.04
CH_10	1.93	CH_41	-0.43	CH_72	1.51	CH_103	3.02
CH_11	-0.23	CH_42	0.08	CH_73	-0.36	CH_104	0.18
CH_12	0.23	CH_43	-0.72	CH_74	3.51	CH_105	-0.38
CH_13	-0.12	CH_44	1.33	CH_75	-0.29	CH_106	0.47
CH_14	0.54	CH_45	1.52	CH_76	3.85	LOADCELL	150.06
CH_15	-0.47	CH_46	-0.65	CH_77	0.01	D_108 (in)	-0.02
CH_16	3.32	CH_47	-0.59	CH_78	2.06	D_109 (in)	-0.23
CH_17	-0.38	CH_48	2.36	CH_79	-0.67	D_110 (in)	-0.33
CH_18	3.45	CH_49	-0.44	CH_80	1.38	D_111 (in)	-0.22
CH_19	-0.52	CH_50	3.76	CH_81	-0.46	D_112 (in)	-0.01
CH_20	1.52	CH_51	-0.37	CH_82	0.02	D_113 (in)	-0.01
CH_21		CH_52	3.63	CH_83	-0.46	D_114 (in)	-0.23
CH_22	8.67	CH_53	-0.22	CH_84	0.35	D_115 (in)	-0.32
CH_23	-1.06	CH_54	1.23	CH_85	-0.93	D_116 (in)	-0.22
CH_24	2.07	CH_55	0.04	CH_86	9.37	D_117 (in)	0.00
CH_25		CH_56	-0.87	CH_87		CH_125	-0.96
CH_26	2.50	CH_57	0.25	CH_88	6.45	CH_126	0.15
CH_27	-0.40	CH_58	2.94	CH_89	-0.52	CH_127	
CH_28	1.90	CH_59	-0.21	CH_90	1.60	CH_128	
CH_29	-0.60	CH_60	-0.04	CH_91	0.13	CH_129	-0.75
CH_30	1.36	CH_61	0.08	CH_92	2.94	CH_130	-0.39
CH_31	-1.51	CH_62	1.77	CH_93			

<b>Test 11 - Concrete Deck (150 kips)</b>							
Channel	Avg Stress (ksi)	Channel	Avg Stress (ksi)	Channel	Avg Stress (ksi)	Channel	Avg Stress (ksi)
CH_1	-0.32	CH_32	5.58	CH_63	-0.03	CH_94	1.15
CH_2	0.76	CH_33	-0.91	CH_64	0.66	CH_95	-1.12
CH_3	-0.11	CH_34	4.68	CH_65	-0.08	CH_96	-0.36
CH_4	0.14	CH_35	-0.31	CH_66	-0.32	CH_97	0.70
CH_5	0.02	CH_36	0.32	CH_67	0.08	CH_98	3.19
CH_6	1.55	CH_37	-0.41	CH_68	0.90	CH_99	0.65
CH_7	0.06	CH_38	0.39	CH_69	-0.11	CH_100	-1.31
CH_8	-0.31	CH_39	-0.43	CH_70	-0.38	CH_101	0.20
CH_9	-0.17	CH_40	0.23	CH_71	-0.06	CH_102	-0.21
CH_10	0.94	CH_41	-0.42	CH_72	0.16	CH_103	0.26
CH_11	0.03	CH_42	0.25	CH_73	-0.08	CH_104	1.84
CH_12	0.17	CH_43	-1.00	CH_74	0.73	CH_105	0.03
CH_13	-0.02	CH_44	2.88	CH_75	-0.13	CH_106	-1.22
CH_14	0.17	CH_45	0.06	CH_76	0.59	LOADCELL	150.03
CH_15	-0.17	CH_46	1.00	CH_77	-0.13	D_108 (in)	-0.01
CH_16	2.08	CH_47	-1.39	CH_78	0.46	D_109 (in)	-0.17
CH_17	-0.31	CH_48	5.32	CH_79	0.11	D_110 (in)	-0.28
CH_18	2.18	CH_49	-0.69	CH_80	0.03	D_111 (in)	-0.27
CH_19	-0.40	CH_50	10.39	CH_81	0.07	D_112 (in)	-0.01
CH_20	1.36	CH_51	-0.80	CH_82	0.11	D_113 (in)	0.00
CH_21		CH_52	9.58	CH_83	-0.07	D_114 (in)	-0.05
CH_22	1.92	CH_53	-1.55	CH_84	0.03	D_115 (in)	-0.06
CH_23	-0.21	CH_54	6.96	CH_85	-0.10	D_116 (in)	-0.05
CH_24	0.11	CH_55	-0.28	CH_86	1.86	D_117 (in)	-0.01
CH_25	-0.54	CH_56	2.34	CH_87		CH_125	0.15
CH_26	0.23	CH_57	-0.37	CH_88	0.68	CH_126	0.10
CH_27	-0.33	CH_58	3.09	CH_89	-0.12	CH_127	
CH_28	0.23	CH_59	-0.03	CH_90		CH_128	
CH_29	-0.21	CH_60	4.80	CH_91	-0.28	CH_129	0.25
CH_30	0.31	CH_61		CH_92	0.06	CH_130	0.19
CH_31	-0.66	CH_62	1.39	CH_93			

<b>Test 12 - Concrete Deck (150 kips)</b>							
Channel	Avg Stress (ksi)	Channel	Avg Stress (ksi)	Channel	Avg Stress (ksi)	Channel	Avg Stress (ksi)
CH_1	0.39	CH_32	0.66	CH_63	-0.07	CH_94	2.02
CH_2	-0.36	CH_33	-0.11	CH_64	-0.30	CH_95	-1.24
CH_3	0.14	CH_34	1.86	CH_65	0.04	CH_96	-0.21
CH_4	0.79	CH_35	-0.10	CH_66	1.37	CH_97	1.14
CH_5	-0.10	CH_36	0.01	CH_67	-0.13	CH_98	-0.51
CH_6	-0.41	CH_37	-0.03	CH_68	0.12	CH_99	-0.21
CH_7	-0.02	CH_38	0.08	CH_69	0.01	CH_100	0.07
CH_8	0.60	CH_39	0.04	CH_70	0.76	CH_101	-0.90
CH_9	-0.22	CH_40	0.12	CH_71	-0.37	CH_102	
CH_10	0.40	CH_41	0.04	CH_72	1.25	CH_103	1.06
CH_11	-0.16	CH_42	0.06	CH_73	-0.39	CH_104	-0.53
CH_12	-0.01	CH_43	0.07	CH_74	2.08	CH_105	-0.16
CH_13	-0.03	CH_44	0.03	CH_75	-0.20	CH_106	0.55
CH_14	0.07	CH_45	-0.15	CH_76	2.39	LOADCELL	150.03
CH_15	-0.17	CH_46	-1.23	CH_77	-0.16	D_108 (in)	0.00
CH_16	0.51	CH_47	-0.77	CH_78	1.05	D_109 (in)	-0.05
CH_17	-0.07	CH_48	1.28	CH_79	-1.05	D_110 (in)	
CH_18	0.64	CH_49	-0.24	CH_80	2.77	D_111 (in)	-0.05
CH_19	-0.02	CH_50	0.62	CH_81	-0.51	D_112 (in)	0.00
CH_20	0.11	CH_51	-0.08	CH_82	0.19	D_113 (in)	0.00
CH_21		CH_52	1.55	CH_83	-0.32	D_114 (in)	-0.18
CH_22	1.12	CH_53	0.30	CH_84	0.40	D_115 (in)	-0.36
CH_23	-0.51	CH_54	-0.01	CH_85	-0.85	D_116 (in)	-0.27
CH_24	-0.03	CH_55	-0.26	CH_86	4.61	D_117 (in)	-0.01
CH_25		CH_56	-0.19	CH_87		CH_125	0.15
CH_26	-0.09	CH_57	-0.06	CH_88	5.93	CH_126	0.13
CH_27	-0.25	CH_58	1.57	CH_89	-0.20	CH_127	
CH_28	0.01	CH_59	-0.11	CH_90	0.00	CH_128	
CH_29	-0.14	CH_60	-0.23	CH_91	-0.12	CH_129	0.49
CH_30	-0.03	CH_61		CH_92	0.33	CH_130	0.31
CH_31	-0.39	CH_62	0.81	CH_93			

<b>Fracture Test 1 (After-Fracture Load: 0 kips)</b>							
Channel	Avg Stress (ksi)	Channel	Avg Stress (ksi)	Channel	Avg Stress (ksi)	Channel	Avg Stress (ksi)
CH_1	1.31	CH_29	-3.86	CH_57	0.94	CH_85	-0.28
CH_2	1.23	CH_30	9.67	CH_58	-2.38	CH_86	2.60
CH_3	1.03	CH_31	6.19	CH_59	1.35	CH_87	
CH_4	-2.16	CH_32		CH_60	-0.07	CH_88	0.51
CH_5	1.07	CH_33		CH_61		CH_89	0.09
CH_6	0.11	CH_34		CH_62	-1.05	CH_90	
CH_7	3.25	CH_35	-2.08	CH_63	0.21	CH_91	-0.51
CH_8	-0.90	CH_36	8.03	CH_64	0.69	CH_92	0.47
CH_9	1.64	CH_37	-1.70	CH_65	0.00	CH_93	
CH_10	1.26	CH_38	4.33	CH_66	-0.47	CH_94	3.16
CH_11	1.22	CH_39	1.44	CH_67	0.11	LOADCELL	0.32
CH_12	1.84	CH_40	5.69	CH_68	1.26	D_108	0.00
CH_13	1.45	CH_41	2.33	CH_69		D_109	-0.30
CH_14	1.03	CH_42	3.44	CH_70	-1.19	D_110	
CH_15	0.01	CH_43		CH_71	-0.40	D_111	
CH_16	-1.13	CH_44	17.21	CH_72	-0.41	D_112	0.01
CH_17	0.37	CH_45	0.72	CH_73	-0.16	D_113	-0.01
CH_18	-1.94	CH_46	9.69	CH_74	0.90	D_114	-0.38
CH_19	1.91	CH_47	1.12	CH_75	0.13	D_115	-0.08
CH_20	-0.12	CH_48	-1.24	CH_76	0.77	D_116	-0.06
CH_21		CH_49	0.23	CH_77	0.21	D_117	0.00
CH_22	12.26	CH_50	-1.28	CH_78		CH_125	0.80
CH_23	0.62	CH_51	0.51	CH_79	0.36	CH_126	0.82
CH_24	3.76	CH_52	-0.89	CH_80	-0.74	CH_127	
CH_25		CH_53	4.77	CH_81	-0.02	CH_128	
CH_26	4.03	CH_54	0.49	CH_82	-0.17	CH_129	0.91
CH_27		CH_55	0.51	CH_83	-0.03	CH_130	1.03
CH_28	3.64	CH_56	0.86	CH_84	0.09		

<b>Fracture Test 1 (After-Fracture Load: 75 kips)</b>							
Channel	Avg Stress (ksi)	Channel	Avg Stress (ksi)	Channel	Avg Stress (ksi)	Channel	Avg Stress (ksi)
CH_1	1.44	CH_29	-1.10	CH_57	0.75	CH_85	-0.61
CH_2	2.61	CH_30	21.35	CH_58	-3.70	CH_86	7.90
CH_3	0.85	CH_31	12.26	CH_59	1.56	CH_87	
CH_4	-3.42	CH_32		CH_60	2.09	CH_88	2.18
CH_5	1.02	CH_33		CH_61		CH_89	0.14
CH_6	2.26	CH_34		CH_62	-2.37	CH_90	
CH_7	3.55	CH_35	-1.31	CH_63	-0.14	CH_91	-0.38
CH_8	-1.97	CH_36	17.65	CH_64	2.33	CH_92	1.56
CH_9	2.12	CH_37	-1.30	CH_65	-0.17	CH_93	
CH_10	3.63	CH_38	11.39	CH_66	-1.41	CH_94	9.22
CH_11	1.45	CH_39	4.60	CH_67	0.39	LOADCELL	75.02
CH_12	2.44	CH_40	13.60	CH_68	3.88	D_108	0.00
CH_13	1.46	CH_41	4.69	CH_69		D_109	-0.75
CH_14	0.97	CH_42	10.33	CH_70	-2.55	D_110	
CH_15	-0.19	CH_43		CH_71	-0.67	D_111	
CH_16	1.08	CH_44	38.37	CH_72	-0.64	D_112	0.01
CH_17	-0.27	CH_45	1.83	CH_73	-0.36	D_113	-0.02
CH_18	-1.70	CH_46	21.49	CH_74	3.23	D_114	-0.94
CH_19	2.35	CH_47	1.26	CH_75	-0.25	D_115	-0.23
CH_20	2.52	CH_48	-0.64	CH_76	2.46	D_116	-0.16
CH_21		CH_49	-0.21	CH_77	0.29	D_117	-0.01
CH_22	27.16	CH_50	0.94	CH_78		CH_125	0.87
CH_23	3.18	CH_51	-0.23	CH_79	0.37	CH_126	1.07
CH_24	8.15	CH_52	0.58	CH_80	-1.54	CH_127	
CH_25		CH_53	4.62	CH_81	-0.09	CH_128	
CH_26	10.11	CH_54	2.09	CH_82	-0.29	CH_129	1.56
CH_27		CH_55	0.29	CH_83	-0.17	CH_130	1.54
CH_28	10.93	CH_56	2.29	CH_84	0.13		

<b>Fracture Test 2 (After-Fracture Load: 0 kips)</b>							
Channel	Avg Stress (ksi)	Channel	Avg Stress (ksi)	Channel	Avg Stress (ksi)	Channel	Avg Stress (ksi)
CH_1	0.20	CH_29	0.05	CH_57	-0.02	CH_85	
CH_2	-1.08	CH_30	2.58	CH_58	1.12	CH_86	
CH_3	0.13	CH_31	0.55	CH_59	-0.15	CH_87	
CH_4	0.71	CH_32		CH_60	-0.82	CH_88	
CH_5	-0.02	CH_33		CH_61		CH_89	-1.61
CH_6	-0.48	CH_34		CH_62	0.50	CH_90	
CH_7	-0.20	CH_35	0.41	CH_63	1.28	CH_91	4.06
CH_8	0.60	CH_36	2.02	CH_64	-0.63	CH_92	9.13
CH_9	0.84	CH_37	0.07	CH_65	0.43	CH_93	
CH_10	-0.06	CH_38	1.43	CH_66	0.06	CH_94	23.30
CH_11		CH_39	0.62	CH_67	0.08	LOADCELL	-0.09
CH_12	0.43	CH_40	1.67	CH_68	-0.93	D_108	0.00
CH_13	-0.07	CH_41	0.40	CH_69		D_109	-0.14
CH_14	-0.02	CH_42	0.91	CH_70	0.99	D_110	-0.31
CH_15	0.06	CH_43		CH_71	1.83	D_111	-0.13
CH_16		CH_44	3.00	CH_72	1.47	D_112	0.00
CH_17	-0.15	CH_45	0.04	CH_73	-0.33	D_113	-0.02
CH_18	1.01	CH_46	-0.04	CH_74	-0.23	D_114	-0.60
CH_19	0.25	CH_47	-0.08	CH_75	-0.28	D_115	-0.82
CH_20	0.56	CH_48	0.22	CH_76	-1.68	D_116	-0.40
CH_21		CH_49	-0.08	CH_77	0.93	D_117	0.02
CH_22	5.46	CH_50	0.20	CH_78		CH_125	-0.32
CH_23	0.49	CH_51	-0.19	CH_79		CH_126	-2.06
CH_24	1.33	CH_52	0.75	CH_80	24.02	CH_127	
CH_25		CH_53		CH_81	2.66	CH_128	
CH_26	2.30	CH_54	-0.16	CH_82	8.62	CH_129	0.08
CH_27		CH_55	0.45	CH_83	-0.48	CH_130	0.01
CH_28	1.72	CH_56	-1.33	CH_84	15.85		

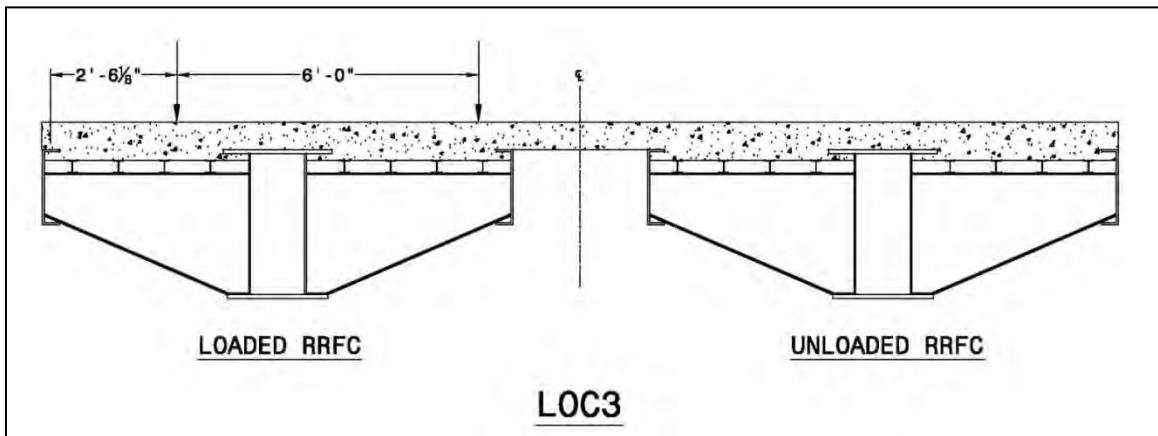
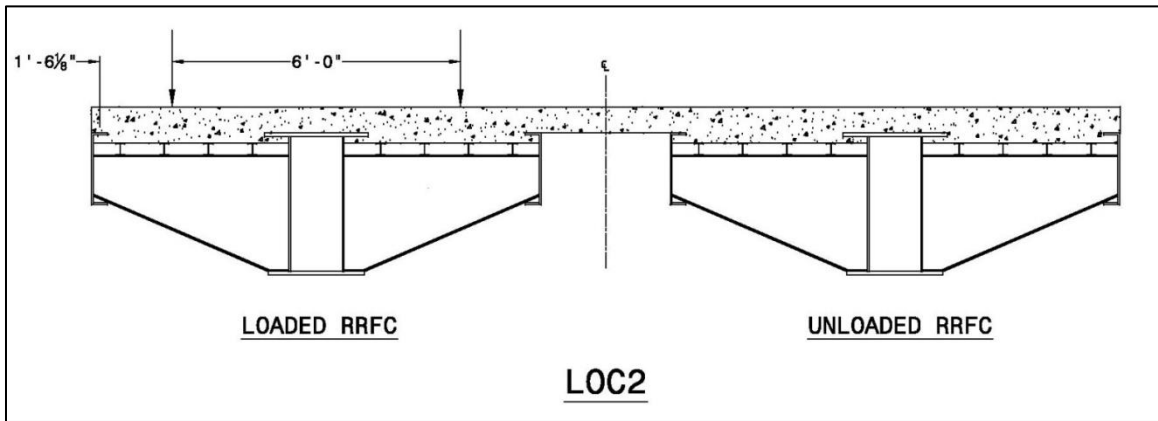
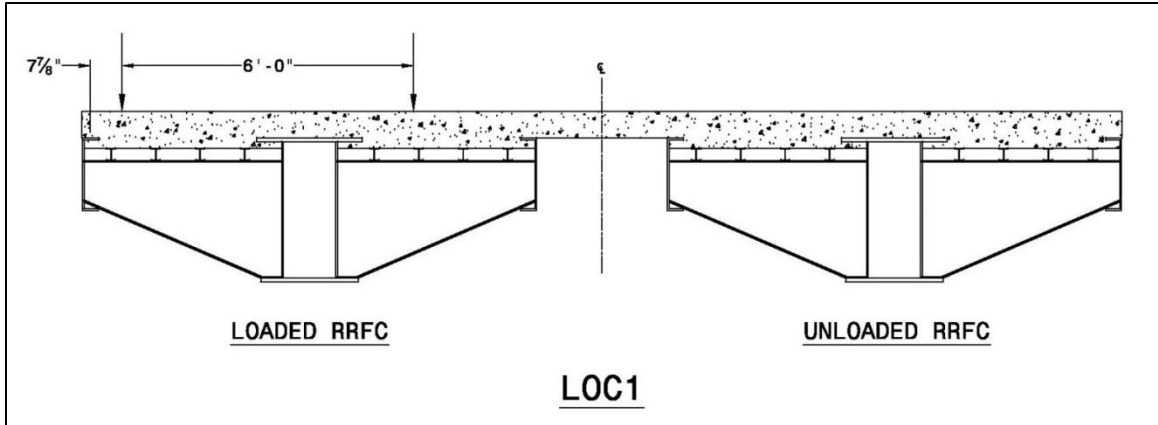
<b>Fracture Test 2 (After-Fracture Load: 75 kips)</b>							
Channel	Avg Stress (ksi)	Channel	Avg Stress (ksi)	Channel	Avg Stress (ksi)	Channel	Avg Stress (ksi)
CH_1	0.40	CH_29	2.73	CH_57	-0.04	CH_85	
CH_2	-2.30	CH_30	7.67	CH_58	3.30	CH_86	
CH_3	0.14	CH_31	2.48	CH_59	-0.65	CH_87	
CH_4	2.45	CH_32		CH_60	-1.46	CH_88	
CH_5	-0.38	CH_33		CH_61		CH_89	-3.17
CH_6	-1.32	CH_34		CH_62	1.87	CH_90	
CH_7	-0.50	CH_35	0.73	CH_63	1.69	CH_91	7.70
CH_8	1.88	CH_36	6.63	CH_64	-0.98	CH_92	19.05
CH_9	1.39	CH_37	0.12	CH_65	0.25	CH_93	
CH_10	1.05	CH_38	4.46	CH_66	1.80	CH_94	49.34
CH_11		CH_39	1.87	CH_67	-0.49	LOADCELL	74.98
CH_12	0.88	CH_40	4.66	CH_68	-0.92	D_108	-0.01
CH_13	-0.15	CH_41	1.56	CH_69		D_109	-0.40
CH_14	0.25	CH_42	3.61	CH_70	4.02	D_110	-0.92
CH_15	-0.40	CH_43		CH_71	3.40	D_111	-0.33
CH_16		CH_44	9.92	CH_72	4.20	D_112	-0.01
CH_17	-0.51	CH_45	0.24	CH_73	-1.06	D_113	-0.02
CH_18	2.95	CH_46	0.87	CH_74	1.17	D_114	-1.51
CH_19	0.57	CH_47	-0.62	CH_75	-0.98	D_115	-1.98
CH_20	1.63	CH_48	1.11	CH_76	1.27	D_116	-1.00
CH_21		CH_49	-0.34	CH_77	1.65	D_117	0.02
CH_22	16.16	CH_50	1.15	CH_78		CH_125	-0.53
CH_23	0.85	CH_51	-0.54	CH_79		CH_126	-2.88
CH_24	4.58	CH_52	2.37	CH_80	52.63	CH_127	
CH_25		CH_53		CH_81	6.45	CH_128	
CH_26	5.75	CH_54	-0.21	CH_82	18.56	CH_129	-1.15
CH_27		CH_55	1.01	CH_83	-2.39	CH_130	-0.78
CH_28	4.79	CH_56	-2.64	CH_84	33.40		

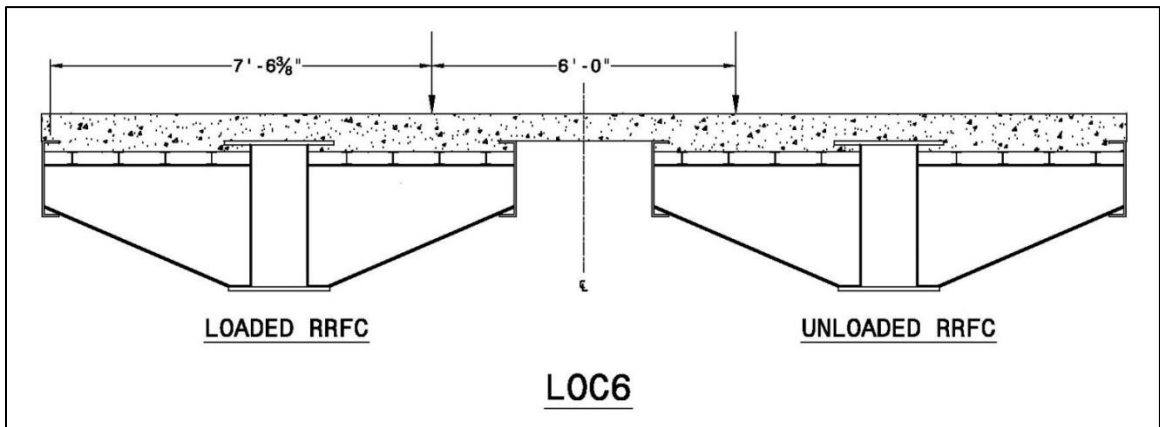
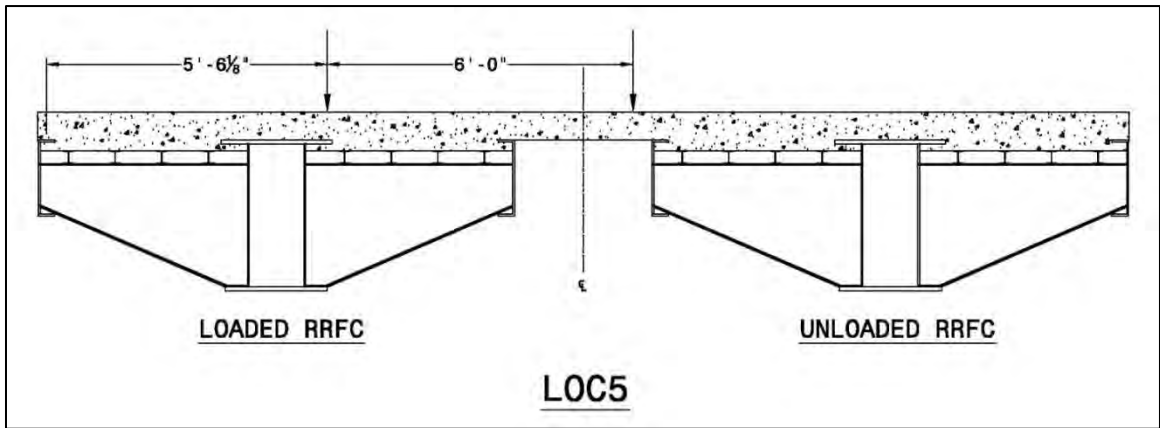
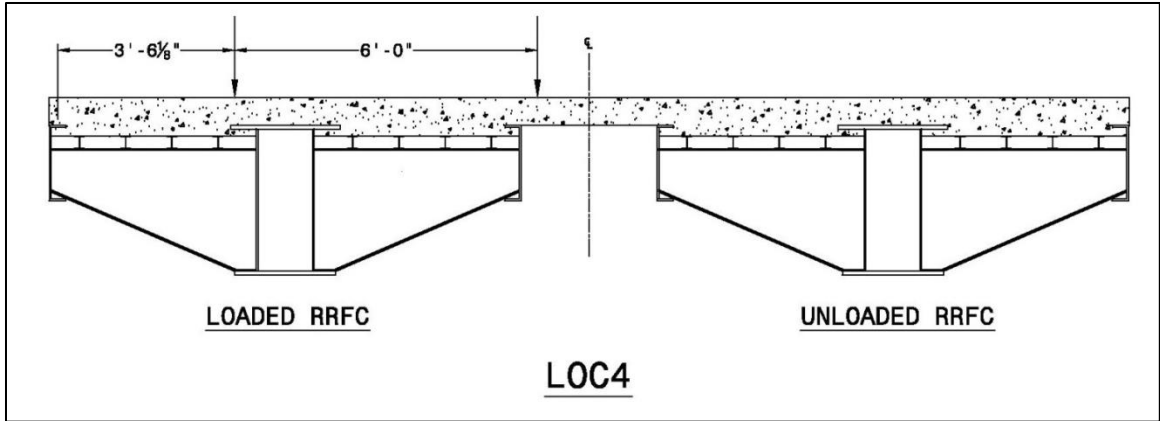


**APPENDIX E. DEVELOPMENT OF PROPOSED GUIDELINES**

RRFC	Member	Test 6					
		Actual GDF	Model GDF	Actual DF	Model DF	Actual CDF	Model CDF
East RRFC (Loaded)	EXT <sub>0</sub>	0.05	0.04	0.82	0.82	0.06	0.05
	MAIN	0.73	0.73			0.89	0.89
	EXT <sub>1</sub>	0.04	0.05			0.05	0.06
West RRFC (Unloaded)	EXT <sub>1</sub>	0.02	0.01	0.18	0.17	0.11	0.06
	MAIN	0.16	0.16			0.89	0.94
	EXT <sub>0</sub>	0.00	0.00			0.00	0.00

RRFC	Member	Test 10					
		Actual GDF	Model GDF	Actual DF	Model DF	Actual CDF	Model CDF
East RRFC	EXT <sub>0</sub>	0.01	0.02	0.50	0.49	0.02	0.04
	MAIN	0.44	0.44			0.88	0.90
	EXT <sub>1</sub>	0.05	0.03			0.10	0.06
West RRFC	EXT <sub>1</sub>	0.05	0.03	0.51	0.49	0.10	0.06
	MAIN	0.45	0.44			0.88	0.90
	EXT <sub>0</sub>	0.01	0.02			0.02	0.04





**Parametric Study 1 Results:**

REL1 DIST3	Distribution Factor (DF)	
	EAST RRFC	WEST RRFC
	(Loaded)	(Unloaded)
LOC1	0.83	0.16
LOC2	0.82	0.17
LOC3	0.81	0.17
LOC4	0.77	0.24
LOC5	0.57	0.43
LOC6*	0.49	0.49

REL2 DIST3	Distribution Factor (DF)	
	EAST RRFC	WEST RRFC
	(Loaded)	(Unloaded)
LOC1	0.84	0.16
LOC2	0.84	0.16
LOC3	0.83	0.18
LOC4	0.78	0.21
LOC5	0.57	0.43
LOC6*	0.50	0.50

REL3 DIST3	Distribution Factor (DF)	
	EAST RRFC	WEST RRFC
	(Loaded)	(Unloaded)
LOC1	0.86	0.14
LOC2	0.85	0.14
LOC3	0.84	0.15
LOC4	0.79	0.21
LOC5	0.57	0.42
LOC6*	0.51	0.51

REL4 DIST3	Distribution Factor (DF)	
	EAST RRFC	WEST RRFC
	(Loaded)	(Unloaded)
LOC1	0.90	0.11
LOC2	0.88	0.11
LOC3	0.88	0.13
LOC4	0.82	0.19
LOC5	0.58	0.43
LOC6*	0.50	0.50

RELS DIST3	Distribution Factor (DF)	
	EAST RRFC	WEST RRFC
	(Loaded)	(Unloaded)
LOC1	0.91	0.09
LOC2	0.90	0.10
LOC3	0.90	0.10
LOC4	0.84	0.17
LOC5	0.59	0.41
LOC6*	0.50	0.50

\*Both RRFCs can be assumed “loaded”

REL1; DIST3						
Member #	1	2	3	4	5	6
Rel. Stiffness	0.055	1	0.063	0.063	1	0.055
Car Distribution Factor (CDF)						
LOC1	0.06	0.88	0.06	0.06	0.94	0.00
LOC2	0.05	0.89	0.06	0.06	0.94	0.00
LOC3	0.05	0.89	0.06	0.06	0.94	0.00
LOC4	0.05	0.88	0.06	0.08	0.88	0.04
LOC5	0.05	0.89	0.05	0.07	0.88	0.05
LOC6	0.04	0.90	0.06	0.06	0.90	0.04

REL2; DIST3						
Member #	1	2	3	4	5	6
Rel. Stiffness	0.15	1	0.15	0.15	1	0.15
Car Distribution Factor (CDF)						
LOC1	0.13	0.76	0.11	0.13	0.75	0.13
LOC2	0.13	0.75	0.12	0.13	0.75	0.13
LOC3	0.12	0.76	0.12	0.17	0.72	0.11
LOC4	0.12	0.76	0.13	0.14	0.76	0.10
LOC5	0.11	0.77	0.12	0.14	0.74	0.12
LOC6	0.10	0.76	0.14	0.14	0.76	0.10

REL3; DIST3						
Member #	1	2	3	4	5	6
Rel. Stiffness	0.25	1	0.25	0.25	1	0.25
Car Distribution Factor (CDF)						
LOC1	0.19	0.65	0.16	0.21	0.64	0.14
LOC2	0.18	0.66	0.16	0.21	0.64	0.14
LOC3	0.17	0.65	0.18	0.20	0.67	0.13
LOC4	0.16	0.66	0.18	0.24	0.62	0.14
LOC5	0.16	0.67	0.18	0.21	0.64	0.14
LOC6	0.16	0.65	0.20	0.20	0.65	0.16

REL4; DIST3						
Member #	1	2	3	4	5	6
Rel. Stiffness	0.5	1	0.5	0.5	1	0.5
Car Distribution Factor (CDF)						
LOC1	0.28	0.49	0.23	0.36	0.45	0.18
LOC2	0.26	0.49	0.25	0.36	0.45	0.18
LOC3	0.25	0.49	0.26	0.31	0.46	0.23
LOC4	0.23	0.50	0.27	0.32	0.47	0.21
LOC5	0.22	0.52	0.26	0.33	0.47	0.21
LOC6	0.22	0.48	0.30	0.30	0.48	0.22

REL5; DIST3						
Member #	1	2	3	4	5	6
Rel. Stiffness	0.75	1	0.75	0.75	1	0.75
Car Distribution Factor (CDF)						
LOC1	0.33	0.40	0.27	0.44	0.33	0.22
LOC2	0.31	0.40	0.29	0.40	0.40	0.20
LOC3	0.29	0.40	0.31	0.40	0.40	0.20
LOC4	0.27	0.40	0.32	0.41	0.35	0.24
LOC5	0.25	0.42	0.32	0.41	0.37	0.22
LOC6	0.24	0.40	0.36	0.36	0.40	0.24

**Parametric Study 2 Results:**

REL1 LOC 2	Distribution Factor (DF)	
	EAST RRFC	WEST RRFC
	(Loaded)	(Unloaded)
DIST1	0.76	0.24
DIST2	0.79	0.20
DIST3	0.82	0.17
DIST4	0.86	0.14
DIST5	0.87	0.12
DIST6	0.88	0.11
DIST7	0.89	0.10

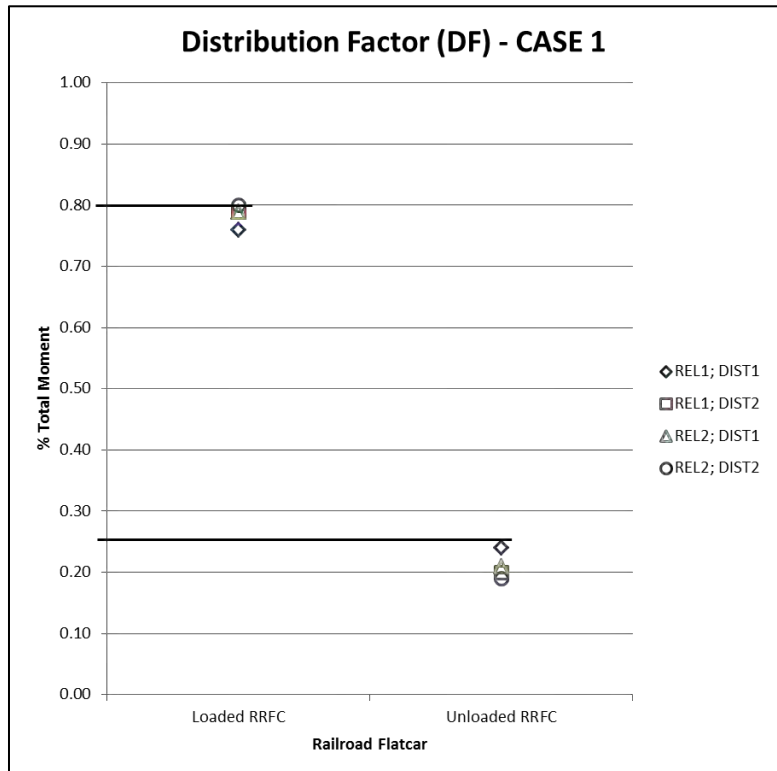
REL2 LOC 2	Distribution Factor (DF)	
	EAST RRFC	WEST RRFC
	(Loaded)	(Unloaded)
DIST1	0.79	0.21
DIST2	0.80	0.19
DIST3	0.84	0.16
DIST4	0.87	0.13
DIST5	0.88	0.12
DIST6	0.90	0.11
DIST7	0.90	0.09

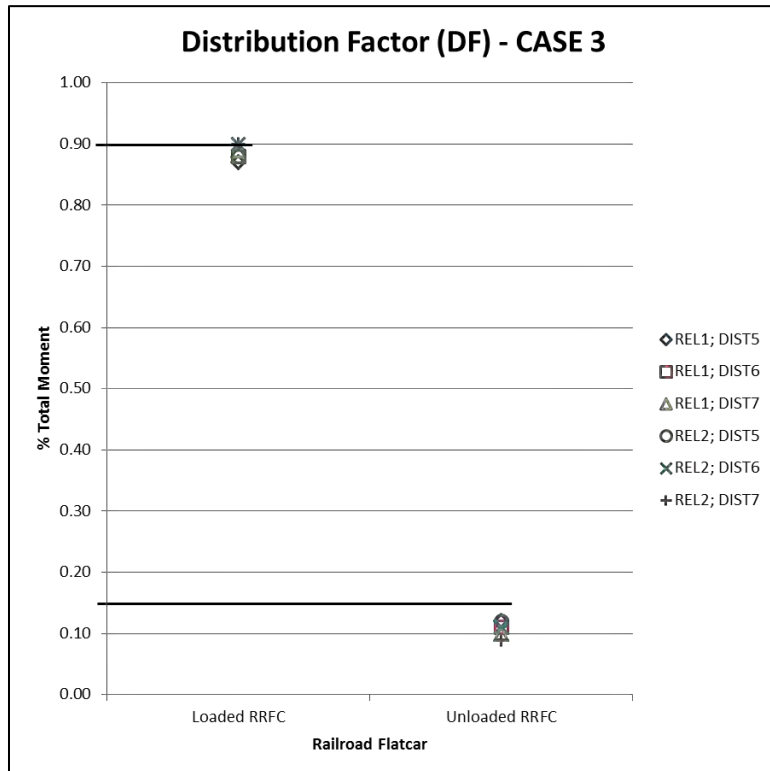
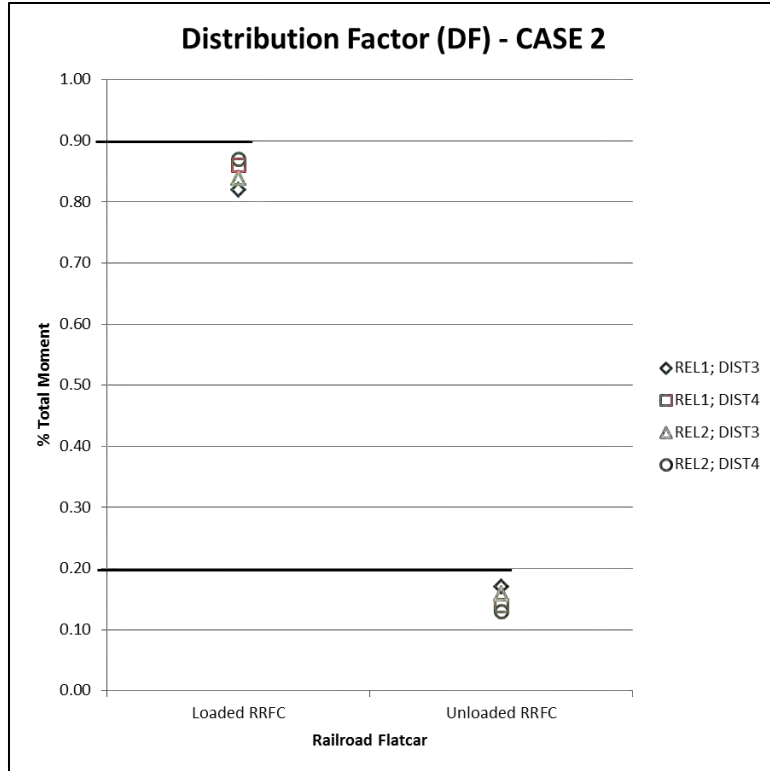
REL3 LOC 2	Distribution Factor (DF)	
	EAST RRFC	WEST RRFC
	(Loaded)	(Unloaded)
DIST1	0.81	0.19
DIST2	0.83	0.18
DIST3	0.85	0.14
DIST4	0.89	0.12
DIST5	0.89	0.11
DIST6	0.90	0.09
DIST7	0.92	0.08

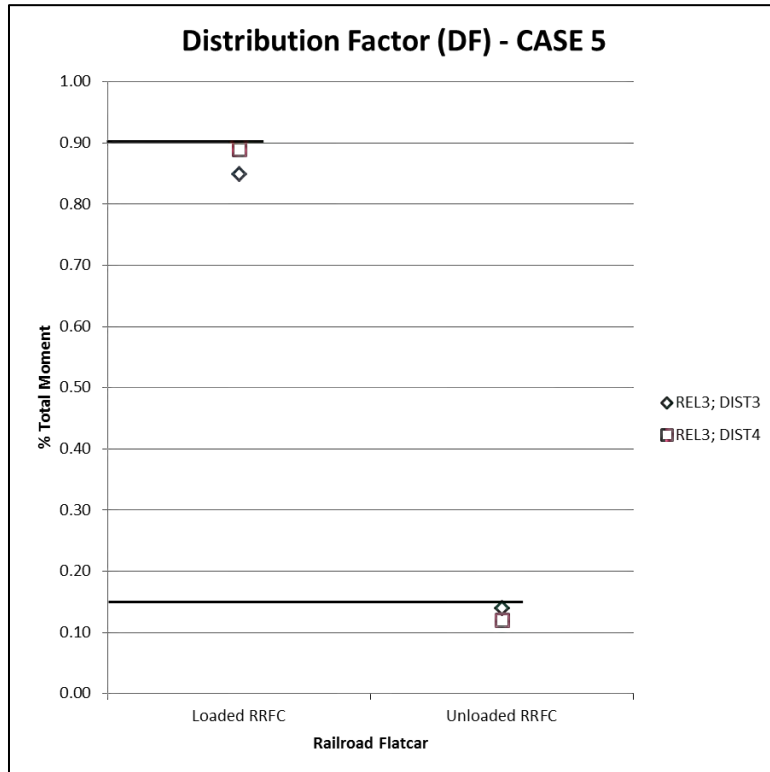
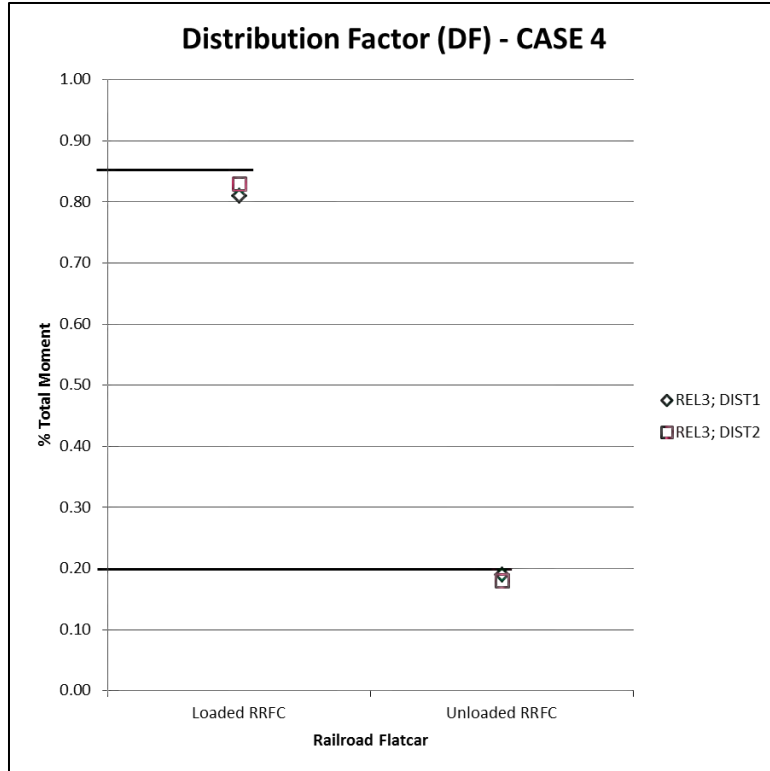


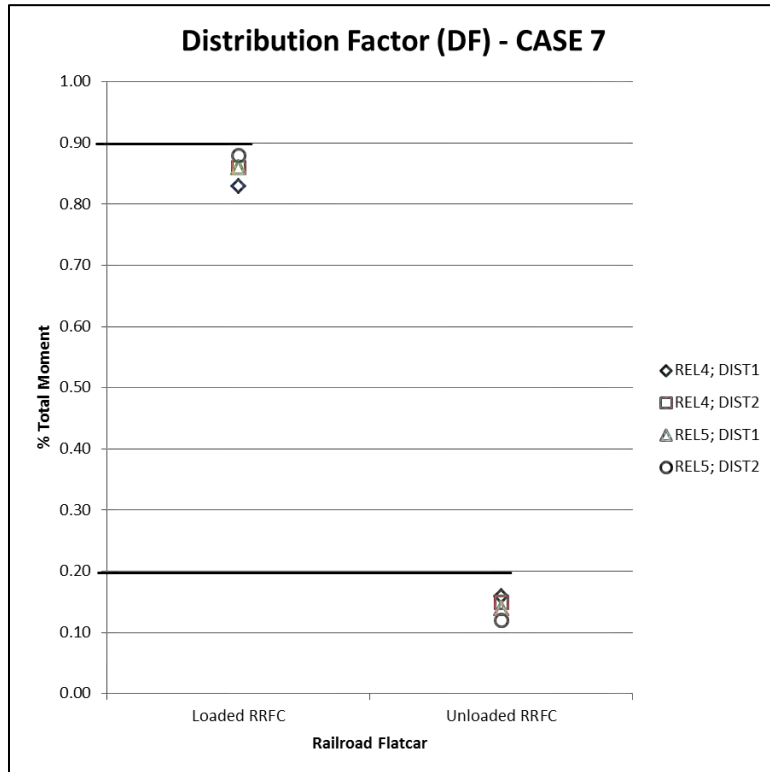
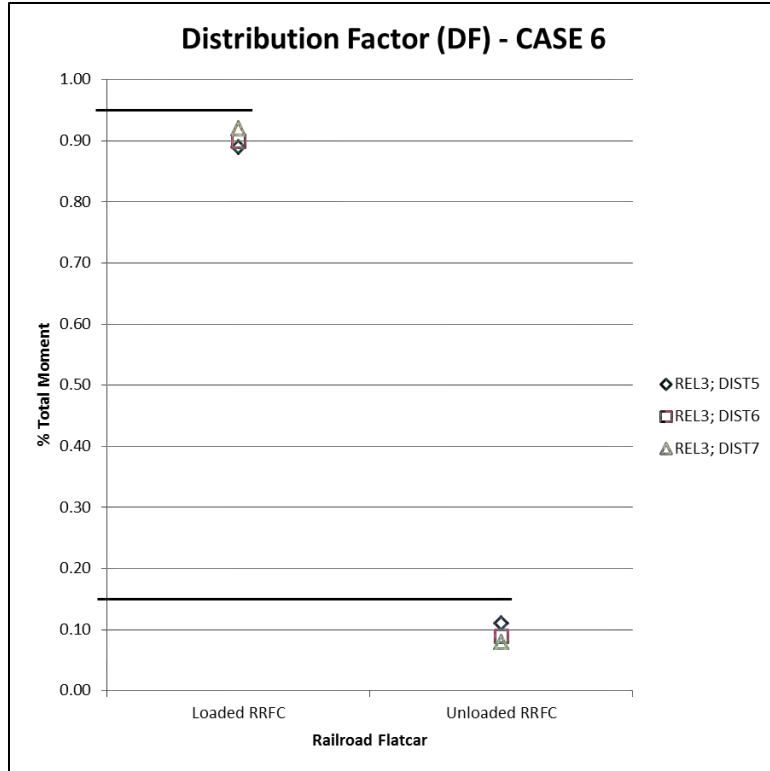
REL4 LOC 2	Distribution Factor (DF)	
	EAST RRFC	WEST RRFC
	(Loaded)	(Unloaded)
DIST1	0.83	0.16
DIST2	0.86	0.15
DIST3	0.88	0.11
DIST4	0.92	0.09
DIST5	0.92	0.09
DIST6	0.92	0.06
DIST7	0.93	0.06

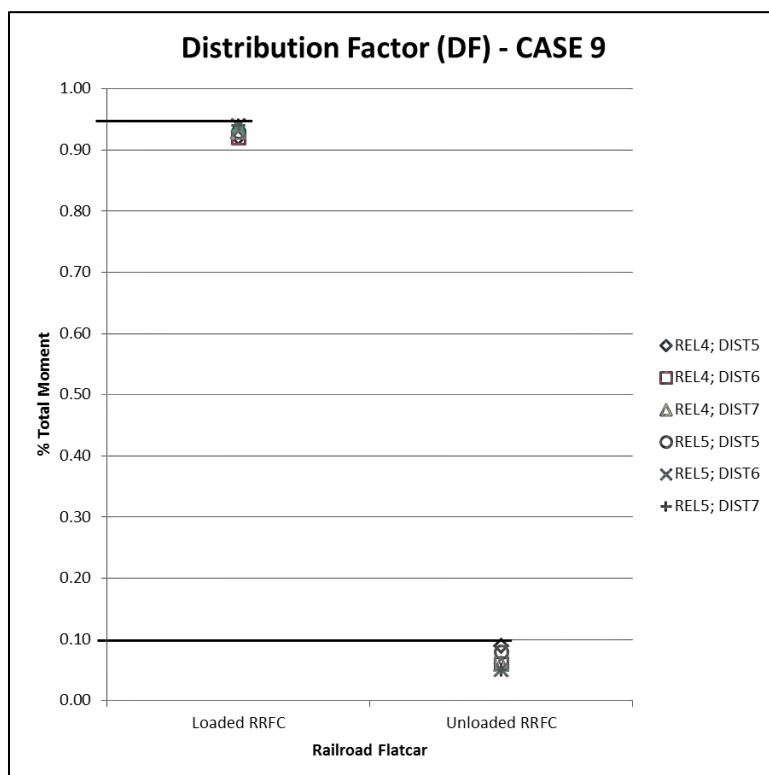
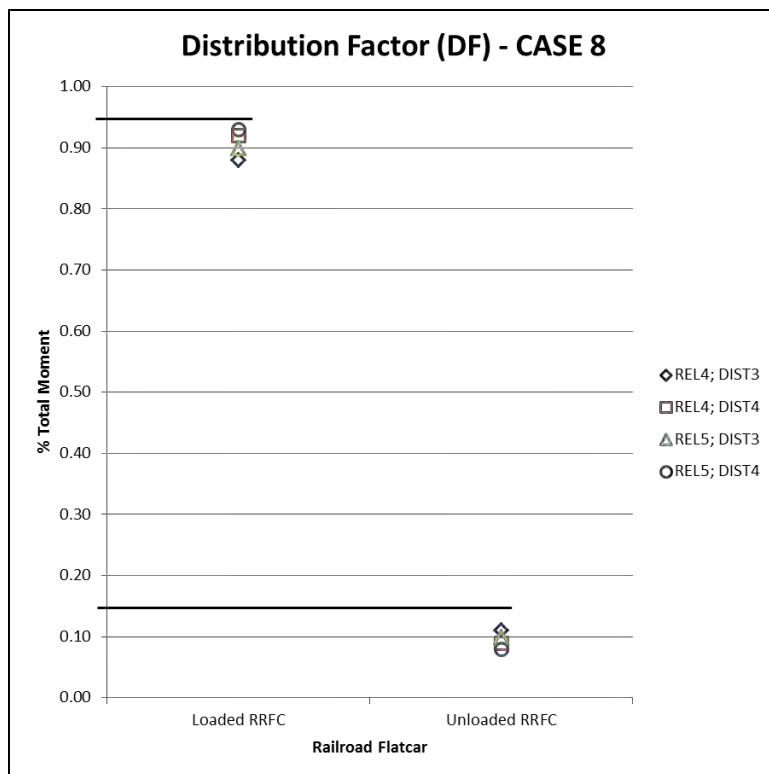
REL5 LOC 2	Distribution Factor (DF)	
	EAST RRFC	WEST RRFC
	(Loaded)	(Unloaded)
DIST1	0.86	0.14
DIST2	0.88	0.12
DIST3	0.90	0.10
DIST4	0.93	0.08
DIST5	0.93	0.08
DIST6	0.94	0.05
DIST7	0.94	0.05











REL1; LOC2						
Member #	1	2	3	4	5	6
Rel. Stiffness	0.055	1	0.063	0.063	1	0.055
Car Distribution Factor (CDF)						
DIST1	0.05	0.89	0.05	0.08	0.88	0.04
DIST2	0.05	0.89	0.06	0.10	0.90	0.00
DIST3	0.05	0.89	0.06	0.06	0.94	0.00
DIST4	0.06	0.88	0.06	0.07	0.93	0.00
DIST5	0.06	0.89	0.06	0.00	1.00*	0.00
DIST6	0.06	0.89	0.06	0.00	1.00*	0.00
DIST7	0.06	0.89	0.06	0.00	1.00*	0.00

\*Assumed outliers –A small amount of the total live load moment is actually being distributed into the unloaded flatcar for DIST5-DIST7 (see DF tables). This small amount was shown to be mainly carried by the main girder, resulting in a CDF of 1.0. This value is believed to be too conservative; therefore, it was taken out for the development of the CDF.

REL2; LOC2						
Member #	1	2	3	4	5	6
Rel. Stiffness	0.15	1	0.15	0.15	1	0.15
Car Distribution Factor (CDF)						
DIST1	0.13	0.76	0.11	0.14	0.76	0.10
DIST2	0.13	0.76	0.11	0.16	0.74	0.11
DIST3	0.13	0.75	0.12	0.13	0.75	0.13
DIST4	0.13	0.76	0.11	0.15	0.77	0.08
DIST5	0.13	0.76	0.11	0.17	0.75	0.08
DIST6	0.12	0.76	0.12	0.18	0.73	0.09
DIST7	0.12	0.76	0.12	0.11	0.78	0.11

REL3; LOC2						
Member #	1	2	3	4	5	6
Rel. Stiffness	0.25	1	0.25	0.25	1	0.25
Car Distribution Factor (CDF)						
DIST1	0.19	0.65	0.16	0.21	0.63	0.16
DIST2	0.18	0.65	0.17	0.22	0.61	0.17
DIST3	0.18	0.66	0.16	0.21	0.64	0.14
DIST4	0.18	0.65	0.17	0.25	0.58	0.17
DIST5	0.18	0.65	0.17	0.18	0.64	0.18
DIST6	0.18	0.66	0.17	0.22	0.67	0.11
DIST7	0.17	0.65	0.17	0.25	0.63	0.13

<b>REL4; LOC2</b>						
<b>Member #</b>	<b>1</b>	<b>2</b>	<b>3</b>	<b>4</b>	<b>5</b>	<b>6</b>
<b>Rel. Stiffness</b>	0.5	1	0.5	0.5	1	0.5
<b>Car Distribution Factor (CDF)</b>						
<b>DIST1</b>	0.27	0.49	0.24	0.31	0.50	0.19
<b>DIST2</b>	0.27	0.49	0.24	0.33	0.47	0.20
<b>DIST3</b>	0.26	0.49	0.25	0.36	0.45	0.18
<b>DIST4</b>	0.26	0.49	0.25	0.33	0.44	0.22
<b>DIST5</b>	0.26	0.49	0.25	0.33	0.44	0.22
<b>DIST6</b>	0.26	0.49	0.25	0.33	0.50	0.17
<b>DIST7</b>	0.26	0.49	0.25	0.33	0.50	0.17

<b>REL5; LOC2</b>						
<b>Member #</b>	<b>1</b>	<b>2</b>	<b>3</b>	<b>4</b>	<b>5</b>	<b>6</b>
<b>Rel. Stiffness</b>	0.75	1	0.75	0.75	1	0.75
<b>Car Distribution Factor (CDF)</b>						
<b>DIST1</b>	0.31	0.40	0.29	0.43	0.36	0.21
<b>DIST2</b>	0.32	0.40	0.28	0.42	0.33	0.25
<b>DIST3</b>	0.31	0.40	0.29	0.40	0.40	0.20
<b>DIST4</b>	0.31	0.40	0.29	0.38	0.38	0.25
<b>DIST5</b>	0.31	0.40	0.29	0.38	0.38	0.25
<b>DIST6</b>	0.31	0.39	0.30	0.40	0.40	0.20
<b>DIST7</b>	0.31	0.39	0.30	0.40	0.40	0.20

**APPENDIX F. PROPOSED GUIDELINES FOR LOAD RATING BRIDGES  
CONSTRUCTED FROM RAILROAD FLATCARS**



## Proposed Guidelines for Load Rating Bridges Constructed from Railroad Flatcars

<p><b>1-INTRODUCTION</b></p> <p><b>1.1-General</b></p> <p>These guidelines describe a procedure for determining the stresses due to live load moment when performing a load rating of the longitudinal flexural members of railroad flatcar (RRFC) bridges. The dead load bending stress may be calculated using traditional structural analysis techniques. Shear stresses to be used for rating may also be determined through the use of traditional structural analysis techniques.</p>	<p><b>C1</b></p> <p><b>C1.1</b></p> <p>Retired railroad flatcars are commonly used as bridges on low-volume roads in rural areas. The objective of these guidelines is to provide conservative but reasonable methods to rate these types of structures. The procedures are heavily based on data obtain from field instrumentation of several RRFC bridges and laboratory testing.</p> <p>Laboratory testing showed that it is reasonable and conservative to assume that the webs of the main girders carry all of the shear force (Washeski, 2013).</p> <p>All references to the AASHTO LRFD Bridge Design Specifications and the AASHTO Manual for Bridge Evaluation are assumed to be the most current version.</p>
<p><b>1.2-Scope</b></p> <p>These guidelines are intended to be used for simply supported, single span RRFC bridges. Deck types which may be included consist of steel plate, timber, or concrete.</p> <p>The procedure described herein shall be used to determine the maximum live load bending stresses in primary and secondary longitudinal members.</p> <p>Primary members are defined as the main load carrying elements of a RRFC bridge. These consist of the main box girder(s) for a typical RRFC. For RRFC bridges constructed from boxcars and RRFC bridges constructed with a fully composite concrete deck, the main box girder and exterior longitudinal girders may be considered primary members.</p> <p>Secondary members are defined as the structural elements which transfer load to the primary members of RRFC bridges. These consist of the exterior girders, stringers, and</p>	<p><b>C1.2</b></p> <p>Bridges in which the RRFC was cast in place with the abutment (i.e., integral abutments) can be considered simply supported for these guidelines.</p> <p>Research suggests that composite action under service loads may be assumed when the main longitudinal members are built-up riveted members. For welded built up members or rolled shapes, shear studs must be present.</p>

## Proposed Guidelines for Load Rating Bridges Constructed from Railroad Flatcars

transverse members for RRFCs except as described above.

The maximum positive live load bending stress for primary members shall be determined based on global bending of the structure. For secondary members, the maximum positive live load bending stress shall be determined based on local bending of the element. The local bending stress shall then be added to the global stress to determine the total stress at a particular location.

Typical RRFCs are defined as those constructed with either one or two main box girders, and generally contain one exterior girder on either side of the flatcar. There is typically a system of three or four longitudinal stringers located between the main girder and exterior girders, found on each side of the main girder.

These guidelines are intended to be applicable for RRFCs utilizing all types of longitudinal connections. A longitudinal connection is defined as the connection between side by side RRFCs.

Figure 1 provides an example of railroad cars which are meant to be included within the

The exterior girders of typical RRFCs are generally constructed with channels, while the stringers are generally constructed with inverted T-shapes, I-shapes, or Z-shapes. Although these are typical features, the exterior girders and stringers are often constructed using different structural shapes.

The cross section and behavior of bridges built using a boxcar differs from other RRFCs. Instead of a box girder, the main longitudinal member typically consists of two Z-shapes facing opposite directions with their top flanges welded together. Therefore these rating procedures differentiate between RRFCs constructed from boxcars and other cross sections.

Boxcars have been used as bridges after their sides and tops have been removed. These types of cars have also been referred to as “car haulers.” The two Z-shapes used to form the main girder generally contain a steel plate welded to the top flanges of each shape.

It is not recommended boxcars be used as bridges.

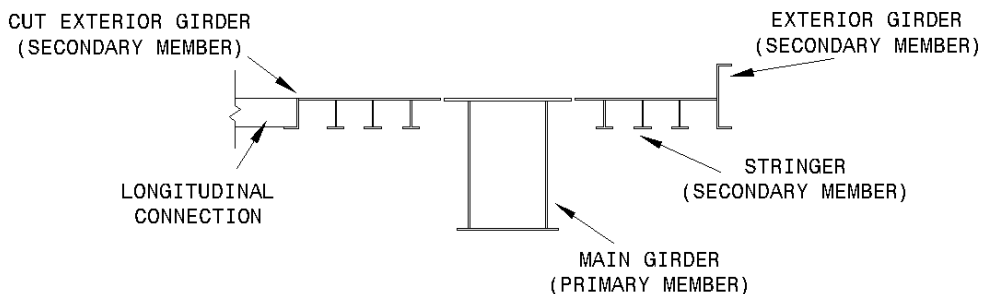
Typically RRFC bridges are constructed by placing two (or more) RRFCs side by side. The exterior girders of adjacent RRFCs are commonly cut to form the longitudinal connection. This connection typically extends longitudinally along the length of the bridge.

Based on field studies of RRFC bridges (Provines, 2011; Wipf et. al. 2007a; Wipf et.

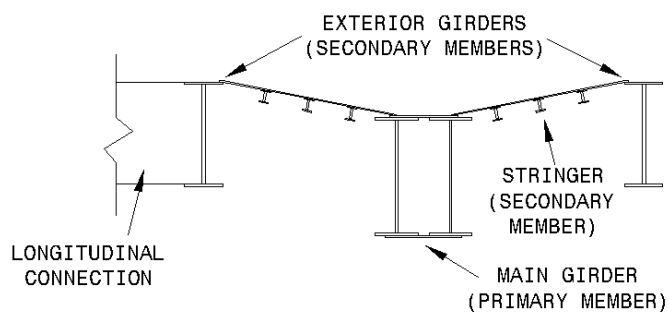
## Proposed Guidelines for Load Rating Bridges Constructed from Railroad Flatcars

scope of these guidelines. The figure also provides examples of which elements are defined as primary members or secondary members. Examples presented in the figure are not meant to be an all-inclusive list of railroad car types for which these guidelines are eligible, but are simply presented to provide engineers with additional guidance for load rating RRFC bridges.

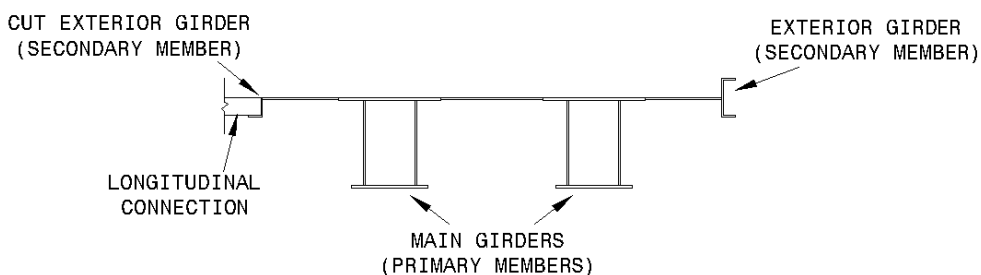
al. 2007b), there is a wide range of longitudinal connections used to connect adjacent flatcars. Particular longitudinal connection types were generally seen to be consistent within a particular area or county.



**TYPICAL RRFC: SINGLE BOX GIRDER FLATCAR WITH SMALL EXTERIOR GIRDERS**



**TYPICAL RRFC: SINGLE BOX GIRDER FLATCAR WITH LARGE EXTERIOR GIRDERS**



**TYPICAL RRFC: TWO-BOX GIRDER FLATCAR**

## Proposed Guidelines for Load Rating Bridges Constructed from Railroad Flatcars

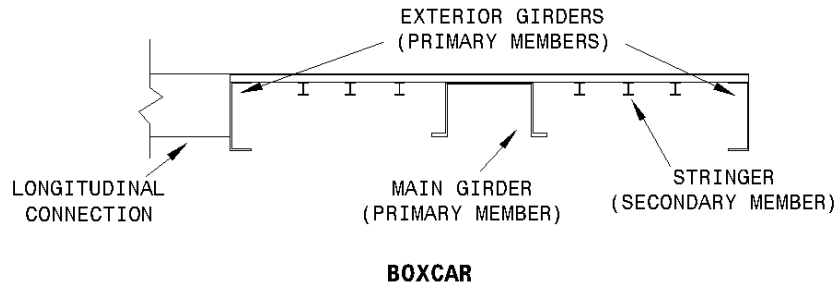


**Figure 1.1: Examples of railroad cars included in scope & member definitions**

### 1.2.1–Material Properties

The elastic modulus of a steel RRFC may be assumed to be 29,000 ksi.

The yield strength ( $F_y$ ) and ultimate strength ( $F_u$ ) of a steel RRFC shall be determined using one of the following methods:

- Recorded from the structural plans of the RRFC
- Material testing of sample taken from RRFC
- An assumed value of  $F_y = 36$  ksi;  $F_u = 58$  ksi

The elastic modulus of concrete, if used as bridge deck, shall be determined based on *AASHTO The Manual for Bridge Evaluation*.

### 1.2.2–Dynamic Load Allowance

The static effects of the truck loads shall be increased by 33 percent to account for the dynamic effects due to moving vehicles.

### C1.2.1

Based on coupon tests from multiple types of RRFCs (Wipf et. al. 2007a; Wipf et. al. 2007b), 29,000 ksi is an acceptable assumed elastic modulus value to be used when performing a load rating on a RRFC bridge.

Based on discussions with several railroad companies and railroad car manufacturers (Provines, 2011), the main structural elements of RRFCs have been constructed with high-strength low-alloy steels with yield strengths ranging from 50-70 ksi since the 1970's. However before the 1970's, RRFC were most likely constructed with steels with a yield strength of either 36 or 50 ksi. Therefore an assumption of a yield strength of 36 ksi is conservative. Coupon tests from multiple types of RRFCs (Wipf et. al. 2007a; Wipf et. al. 2007b), confirmed that 36 ksi is an acceptable assumed yield strength value.

### C1.2.2

Based on field instrumentation studies investigating the dynamic behavior of RRFC bridges (Wipf et. al. 2007a; Wipf et. al. 2007b), a 33 percent increase in the static bending stress provided conservative estimates

## Proposed Guidelines for Load Rating Bridges Constructed from Railroad Flatcars

	<p>for the dynamic bending stress. Although the measured dynamic impact factor varied between different RRFC bridges, a value of 33 percent was chosen to be consistent with current load rating procedures in <i>AASHTO The Manual for Bridge Evaluation</i>.</p>
<p><b>1.2.3–Fatigue &amp; Fracture Provisions</b></p> <p>The fatigue limit state of a RRFC bridge need not be explicitly evaluated if the ADTT (or heavy vehicle traffic) is such that road can be classified as low-volume road over the life of the bridge. Sound engineering judgment shall be used when determining whether or not the RRFC bridge can be considered low-volume.</p> <p>If fatigue cracks are found in the RRFC during routine inspections, the fatigue life shall not be considered sufficient and a fatigue evaluation shall be performed to determine the cause of the cracking and mitigation strategy.</p>	<p><b>C1.2.3</b></p> <p>The stress ranges and number of cycles a RRFC experiences during its railroad service life are most likely much greater than those experienced during its life as a low volume road bridge. Flatcars are typically designed for heavy loads, sometimes up to 70-110 tons as discussed in Article C2.1.2, which are much greater than the majority of vehicles crossing a typical RRFC bridge. In a study investigating the use of RRFCs as low-volume road bridges (Wipf et. al. 1999), many agencies which use RRFC bridges were contacted and all of which verified that fatigue had not been an issue.</p> <p>If there are concerns regarding the susceptibility of fracture, Charpy V-Notch (CVN) tests may be performed on a material sample from the appropriate component of the RRFC. The CVN results can be correlated to fracture toughness, which provides a measure of a material’s resistance to fracture. However, in lieu of a full fitness-for-service (FFS) assessment, the CVN data may be compared to existing requirements for bridge steels.</p>
<p><b>1.3–Approach</b></p> <p>The maximum positive live load bending stress determined by these guidelines are intended to be used in conjunction with <i>AASHTO The Manual for Bridge Evaluation</i>. These guidelines are intended to be applicable for the allowable stress load rating procedure. Other checks, (e.g., local buckling) shall be performed per the <i>AASHTO The Manual for</i></p>	<p><b>C1.3</b></p> <p>These guidelines are not applicable to the load and resistance factor rating (LRFR) or the load factor rating (LFR) because load and resistance factors were not developed. Further research is required if either of these two procedures is to be used.</p>

## Proposed Guidelines for Load Rating Bridges Constructed from Railroad Flatcars

<i>Bridge Evaluation.</i>	
<p><b>2–BRIDGES CONSTRUCTED FROM TYPICAL RRFCS</b></p> <p>The following sections describe the procedures to be used for determining the maximum positive live load bending stress in bridges constructed from typical RRFCS.</p> <p>The provisions in this section apply to RRFCS with all deck types except those with a composite concrete deck. RRFCS with composite concrete decks are addressed in Article 4.</p>	<p><b>C2</b></p> <p>Research has shown (Washeski, 2013) that RRFCS which utilize a composite concrete deck possess superior load distribution characteristics than timber or thin steel plate decks. Hence, these structures are evaluated with separate provisions.</p>
<p><b>2.1–Determination of Maximum Positive Live Load Bending Stress in Primary Members</b></p> <p>This section describes the procedures which shall be used for determining the maximum positive live load bending stress in primary members.</p>	<p><b>C2.1</b></p> <p>As stated in Article 1.2, the primary members of typical RRFCS consist of the main box girder(s) located near the center of a flatcar.</p>
<p><b>2.1.1–General Equation</b></p> <p>The following general expression shall be used in determining the maximum positive live load bending stress:</p> $\sigma_{LL} = (\alpha) (CDF) \frac{(DF) M_{LL}}{S_{eff}} \quad (2.1.1-1)$ <p>where:</p> <p><math>\sigma_{LL}</math> = Maximum positive live load bending stress</p> <p><math>\alpha</math> = Stress modification factor as specified in Article 2.1.1.5</p> <p><math>CDF</math> = Car distribution factor as specified in</p>	<p><b>C2.1.1</b></p> <p>The general equation for the determination of the maximum positive live load bending stress was developed through field instrumentation and controlled load testing of several RRFCS bridges (Provines, 2011).</p>

## Proposed Guidelines for Load Rating Bridges Constructed from Railroad Flatcars

<p>Article 2.1.1.3</p> <p><math>DF</math> = Distribution factor as specified in Article 2.1.1.2</p> <p><math>M_{LL}</math> = Maximum positive live load moment as specified in Article 2.1.1.1</p> <p><math>S_{eff}</math> = Effective section modulus as specified in Article 2.1.1.4</p>	
<p><b>2.1.1.1–Maximum Positive Live Load Moment</b></p> <p>The maximum positive live load moment (<math>M_{LL}</math>) shall be determined using procedures described in <i>AASHTO The Manual for Bridge Evaluation</i>.</p>	<p><b>C2.1.1.1</b></p>
<p><b>2.1.1.2–Distribution Factor</b></p> <p>The following expression shall be used in determining the distribution factor (DF):</p> $DF = MP \leq 1.0 \quad (2.1.1.2-1)$ <p>where:</p> <p><math>DF</math> = Distribution factor</p> <p><math>MP</math> = Moment proportion as specified in Article 2.1.1.2.1</p>	<p><b>C2.1.1.2</b></p> <p>The distribution factor is intended to represent load distribution <u>between</u> flatcars. It is differentiated from the car distribution factor, which is intended to represent load distribution <u>within</u> a flatcar.</p> <p>The distribution factor, as determined by Eq. 2.1.1.2-1, was developed based on field instrumentation results in which RRFC bridges were loaded with one tandem axle test truck (Provines, 2011). Even if a bridge was loaded with two trucks, the data suggested that the moment proportion described in Article 2.1.1.2.1 would provide a conservative distribution factor.</p>
<p><b>2.1.1.2.1–Moment Proportion</b></p> <p>The moment proportion (MP) shall be determined based on the lever rule, as described in the <i>AASHTO LRFD Bridge Design Specifications</i>. The lever rule shall be</p>	<p><b>C2.1.1.2.1</b></p> <p>The load tests which resulted in the development of Eq. 2.1.1.2-1 were performed on bridges which were constructed of two RRFCs connected side-by-side (Provines,</p>

## Proposed Guidelines for Load Rating Bridges Constructed from Railroad Flatcars

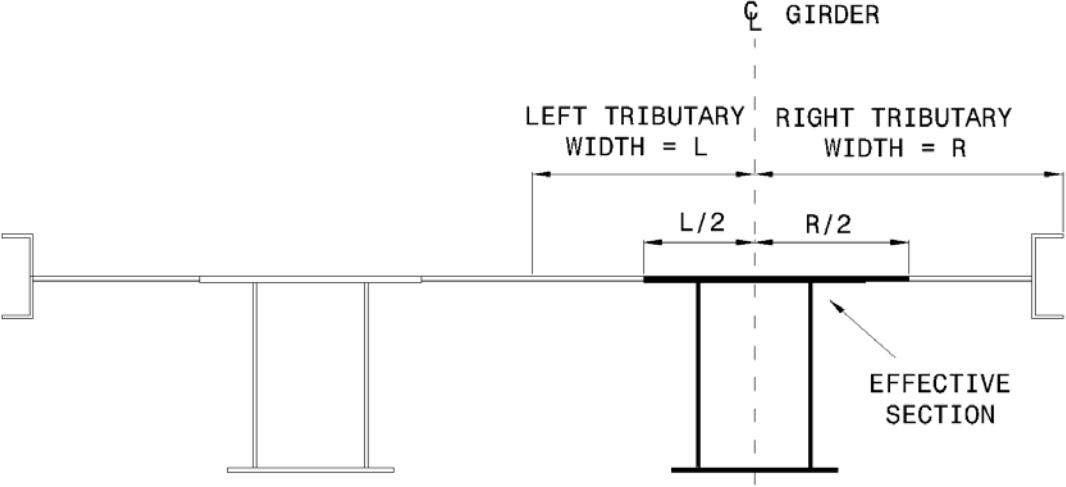
<p>used to distribute the live load moment to each of the RRFCs. The reactions used when computing the lever rule shall be located at the centerline of each RRFC. The moment proportion shall be determined as follows:</p> <ul style="list-style-type: none"> <li>• If the longitudinal connection between RRFCs can be considered a rigid connection: <math>MP = \text{Result from lever rule}</math></li> <li>• If the longitudinal connection between RRFCs cannot be considered a rigid connection or if there is no longitudinal connection: <math>MP = 1.0</math></li> </ul>	<p>2011). It is reasonable to believe the lever rule provides conservative results for bridges with either less than two or more than two RRFCs in the cross section. For instance, if a bridge was constructed of a single RRFC, the lever rule result would be equal to 1.0. The lever rule should also be conservative if used on a bridge constructed with three RRFCs side-by-side. If a truck was located on one of the outside flatcars, according to the lever rule the flatcar on the opposite side would carry zero load provided the truck did not cross the centerline of the middle flatcar. The lever rule, and Eq. 2.1.1.2-1, were used to predict stresses in multiple RRFC bridges in which field instrumentation was used (Wipf et. al. 2003; Wipf et. al. 2007a). Good correlation was found to exist between the calculated and field measured stresses.</p> <p>The lever rule is based on the assumption of a rigid deck. This assumption is violated if the longitudinal connection is not stiff enough in the transverse direction to be considered rigid, therefore no load can be transferred from one RRFC to the other.</p> <p>The evaluation of whether or not a longitudinal connection is sufficiently stiff to transfer moment from one RRFC to another should be determined through analysis and engineering judgment.</p>
<p><b>2.1.1.3–Car Distribution Factor</b></p> <p>The car distribution factor (<i>CDF</i>) shall be determined as follows:</p> <ul style="list-style-type: none"> <li>• For RRFCs with one main box girder: <math>CDF = 1.0</math></li> </ul>	<p><b>C2.1.1.3</b></p> <p>Based on field instrumentation results for RRFCs with only one main box girder, that main girder carries the entire global live load moment (Provines, 2011). In other words, it is not distributed to any other members (i.e., the exterior girders) within the flatcar.</p>



## Proposed Guidelines for Load Rating Bridges Constructed from Railroad Flatcars

<ul style="list-style-type: none"> <li>For RRFCs with two main box girders:</li> </ul> $CDF = \frac{3}{4}$	<p>No RRFCs with two main box girders were field tested in the study (Provines, 2011). However, based on stress results from the single box girder RRFCs and boxcars, it seems reasonably conservative to assign a car distribution factor of 3/4 for RRFCs with two main box girders.</p>
<p><b>2.1.1.4–Effective Section</b></p> <p>The effective section modulus (<math>S_{eff}</math>) for bridges with RRFCs containing one main box girder shall be determined based on the following effective sections:</p> <ul style="list-style-type: none"> <li>For bridges which are constructed with RRFCs containing large exterior girders, the effective section shall consist of the entire RRFC, including the main girder, exterior girders, and any other structural longitudinal elements. Large exterior girders are defined as those which have a moment of inertia of at least 15% of the moment of inertia of the main girder.</li> <li>For bridges which are constructed with RRFCs containing small exterior girders, the effective section shall consist of the main box girder and two stringers on each side of the main girder. Small exterior girders are defined as those which have a moment of inertia of less than 15% of the moment of inertia of the main girder.</li> </ul> <p>The <math>S_{eff}</math> for bridges with RRFCs containing two main box girders shall be determined based on the shaded effective section shown in Figure 2. The effective section shall include any longitudinal structural elements within the section and shall have a</p>	<p><b>C2.1.1.4</b></p> <p>Results from field instrumentation of RRFC bridges with large exterior girders (Provines, 2011) showed it is conservative to assume the entire flatcar participates in global bending. Results from other field instrumentation studies confirmed this assumption to be reasonably conservative (Wipf et. al. 2003; Wipf et. al. 2007a).</p> <p>Results from a field instrumentation study showed (Provines, 2011) it is conservative to assume only two stringers on either side of the main girder participate in global bending of RRFCs with smaller exterior girders.</p> <p>Although no RRFCs with two main box girders were tested, it is reasonable to believe the effective section for these types of cars is similar to RRFCs with one box girder. For RRFCs with one box girder, two stringers on each side represents roughly half the distance between the edge of the main girder and the</p>

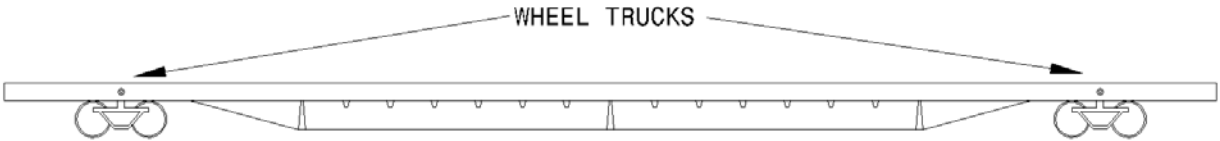
## Proposed Guidelines for Load Rating Bridges Constructed from Railroad Flatcars

<p>minimum section of at least the box girder.</p>	<p>edge of the flatcar. The effective section shown in the figure is based on the idea that half the distance between the main girder and the edge of the flatcar is participating in global bending.</p>
 <p><b>Figure 2.1: Effective section for typical 2-box girder RRFC</b></p>	
<p>The dimensions used for determining the effective section shall be obtained through field measurements or as-built drawings. Any deterioration, such as corrosion or cracks, in structural members shall be considered in these dimensions.</p>	
<p><b>2.1.1.5–Stress Modification Factor</b></p> <p>The stress modification factor (<math>\alpha</math>) shall be taken equal to 0.75</p>	<p><b>C2.1.1.5</b></p> <p>The stress modification factor was developed based on the field instrumentation test results to more accurately, but still conservatively, match stresses calculated using Eq.2.1.1-1 with those measured during field testing (Provines, 2011). The stress modification factor of 0.75 was also verified through the results of previous field instrumentation studies of RRFC bridges (Wipf et. al. 2003; Wipf et. al. 2007a). Although no bridges with RRFCs containing two box girders were tested in the field</p>

## Proposed Guidelines for Load Rating Bridges Constructed from Railroad Flatcars

	instrumentation study, it is reasonable to assume stress modification factor of 0.75 would be conservative for these types of structures.								
<p><b>2.1.2–Alternative Load Rating Procedure</b></p> <p>An acceptable alternative approach to load rating the <u>primary</u> members of RRFC bridges is to ensure the maximum live load on the bridge is always less than the live load limit of the flatcar. For this to be an acceptable load rating approach, the RRFC shall be supported on its wheel trucks, which are defined as the locations where the original wheels attached to the flatcar (shown in Figure 3). The RRFC shall be in good condition and the original design live load limit shall be properly documented. The RRFC shall also have been designed after 1964.</p>	<p><b>C2.1.2</b></p> <p>The design live load of a RRFC is called the live load limit. The live load limit is stenciled onto some RRFCs.</p> <p>RRFCs are designed to be supported at the wheel trucks, thus their performance is better when they are supported at these locations. The specifications stated in Article 2.1.2 imply that flatcars which have been cut to fit a particular span length are ineligible for the alternative load rating procedure.</p> <p>There was no standard loading for RRFCs prior to 1964, when the Association of American Railroads (AAR) Design Specifications were issued. Currently (AAR 2007) there are three major classifications of design live loads for RRFCs, which can be seen in Table C1.</p> <p><b>Table C1: Design live loads for RRFCs</b></p> <table border="1" data-bbox="976 1230 1503 1491"> <thead> <tr> <th>Live Load Limit kips (tons)</th> <th>Gross Rail Load kips (tons)</th> </tr> </thead> <tbody> <tr> <td>140 (70)</td> <td>220 (110)</td> </tr> <tr> <td>200 (100)</td> <td>263 (131.5)</td> </tr> <tr> <td>220 (110)</td> <td>286 (143)</td> </tr> </tbody> </table> <p>In Table C1, the live load limit refers to the maximum live load that can be applied to the flatcar while the gross rail load refers to the maximum vertical load on the flatcar, including the live load plus the self weight of the flatcar.</p> <p>The live load values presented in Table C1 can be applied to a RRFC in a number of different load cases, as per <i>AAR Manual of</i></p>	Live Load Limit kips (tons)	Gross Rail Load kips (tons)	140 (70)	220 (110)	200 (100)	263 (131.5)	220 (110)	286 (143)
Live Load Limit kips (tons)	Gross Rail Load kips (tons)								
140 (70)	220 (110)								
200 (100)	263 (131.5)								
220 (110)	286 (143)								

## Proposed Guidelines for Load Rating Bridges Constructed from Railroad Flatcars

	<p><i>Standards and Recommended Practices Section C – Part II</i> (AAR 2007).</p> <p>In a literature review performed regarding the use of RRFCs as low-volume road bridges (Provines, 2011), it was not confirmed if the values in Table C1 date back to 1964 or if they were issued in a newer Specification; therefore the design loads for each particular RRFC must be known and documented when using the alternative load rating approach as specified in Article 2.1.2.</p>
	
<p><b>Figure 2.2: Location of wheel trucks on typical RRFC</b></p>	
<p><b>2.2–Determination of Maximum Positive Live Load Bending Stress in Secondary Members</b></p> <p>This section describes the procedures which shall be used for determining the maximum positive live load bending stress in secondary members. The local bending stress shall then be added to the global stress to determine the total stress at a particular location.</p>	<p><b>C2.2</b></p> <p>As stated in Article 1.2, the secondary members of typical RRFCs consist of the exterior girders and stringers.</p>
<p><b>2.2.1–RRFCs With Two Box Girders</b></p> <p>The following methods shall be acceptable for determining the maximum positive live load bending stress in secondary members of RRFCs with two box girders:</p>	<p><b>C2.2.1</b></p> <p>No bridges constructed with RRFCs consisting of two box girders were tested through the use of field instrumentation (Provines, 2011). Due to their large difference in geometry, it was not reasonable to presume the methods developed for RRFCs with one box girder would produce conservative stress results for RRFCs constructed with two box</p>

## Proposed Guidelines for Load Rating Bridges Constructed from Railroad Flatcars

<ul style="list-style-type: none"> <li>• Orthotropic plate theory equations found in the <i>AASHTO LRFD Bridge Design Specifications</i></li> <li>• Finite element analysis</li> <li>• Field instrumentation and testing</li> <li>• Any reasonable and accepted engineering method</li> </ul>	<p>girders.</p> <p>Engineering judgment should be practiced when performing one of the four methods listed in Article 2.2.2.</p>
<p><b>2.2.2–General Equation For RRFCs With One Box Girder</b></p> <p>The following general expression shall be used in determining the maximum positive live load bending stress in secondary members of RRFCs with one box girder:</p> $\sigma_{LL} = \frac{(DF) M_{LL}}{S_{eff}} \quad (2.2.2-1)$ <p>where:</p> <p><math>\sigma_{LL}</math> = Maximum positive live load bending stress</p> <p><math>DF</math> = Distribution factor as specified in Article 2.2.2.2</p> <p><math>M_{LL}</math> = Maximum positive live load moment as specified in Article 2.2.2.1</p> <p><math>S_{eff}</math> = Effective section modulus as specified in Article 2.2.2.3.</p>	<p><b>C2.2.2</b></p> <p>The general equation for the determination of the maximum positive live load bending stress in secondary members was developed through field instrumentation and controlled load testing of several RRFC bridges (Provines, 2011).</p>
<p><b>2.2.2.1–Maximum Positive Live Load Moment</b></p> <p>If the center-to-center span of the secondary member between adjacent transverse members is five feet or less, the following expression shall be used when determining the maximum positive live load moment:</p>	<p><b>C2.2.2.1</b></p>

## Proposed Guidelines for Load Rating Bridges Constructed from Railroad Flatcars

$M_{LL} = \frac{PL}{4} \quad (2.2.2-1)$ <p>where:</p> <p><math>P</math> = Weight of single rear axle wheel load</p> <p><math>L</math> = Center to center span of secondary member between adjacent transverse members</p> <p>If the center-to-center span of the secondary member between adjacent transverse members is greater than five feet, the tandem and single axle wheel loads shall be positioned to establish the maximum positive live load moment. Moment equations for simply supported spans shall be used.</p>	<p>Based on field measurements of RRFCs (Provines, 2011), the simply supported moment equation yielded conservative, but reasonable stresses in secondary members.</p> <p>The weight of a single rear axle wheel load can be determined by taking the weight of a rear axle of a design truck and dividing it by 4. The axle weight is divided by 2 because the rear axles (32 kip in HS-20 truck) in the AASHTO design trucks represent a pair of tandem axles. It has been shown through field testing that the presence of each individual axle causes local bending of secondary members. The single axle weight can then be divided by 2 again to represent the weight of each wheel load.</p> <p>Although all of the RRFC bridges tested through the use of field instrumentation had secondary members with spans of less than five feet, it is reasonable to use the simply supported moment equations for determining moments on secondary members with greater span lengths.</p> <p>Eq. 2.2.2-1 cannot be used for spans greater than five feet because the entire tandem can be located on the span.</p>
<p><b>2.2.2.2–Distribution Factor</b></p> <p>The distribution factor (<math>DF</math>) for secondary members shall be calculated as follows:</p> <ul style="list-style-type: none"> <li>• If <math>\frac{l_1}{l_2} \geq 3</math>:</li> </ul> $DF = 1$ <ul style="list-style-type: none"> <li>• If <math>3 &gt; \frac{l_1}{l_2} \geq 2</math>:</li> </ul> $DF = \frac{4}{5}$	<p><b>C2.2.2.2</b></p> <p>Field instrumentation test results (Provines, 2011) showed if one secondary member was at least three times as stiff any other secondary member in the group, it could attract all of the live load moment. The results also showed that if the secondary members of a group were of relatively similar stiffness (e.g., less than two times as stiff), the maximum portion of the live load moment any stringer experienced was 3/5. A linear interpolation between these two</p>

## Proposed Guidelines for Load Rating Bridges Constructed from Railroad Flatcars

<ul style="list-style-type: none"> <li>• If <math>\frac{I_1}{I_2} &lt; 2</math>:</li> </ul> $DF = \frac{3}{5}$ <p>where:</p> <p><math>I_1</math> = moment of inertia of secondary member being rated</p> <p><math>I_2</math> = largest moment of inertia of secondary member within group not being rated</p> <p>A group of secondary members shall be defined as those on one side of the main girder.</p> <p>The moment of inertia shall be determined based on the effective sections prescribed in Article 2.2.2.3.</p>	<p>results was reasonably done for secondary members with a relative stiffness between 2 and 3.</p> <p>A group of secondary members typically consists of one exterior girder, which may be cut if it is used to form the longitudinal connection, and three stringers.</p>
<p><b>2.2.2.3–Effective Section</b></p> <p>The effective section modulus (<math>S_{eff}</math>) shall be determined based on whether the secondary member has been cut and whether it is rigidly attached to a steel deck. A cut secondary member is defined as one which has had a portion of its structural shape removed. The effective section modulus shall be determined based on the following effective sections:</p> <ul style="list-style-type: none"> <li>• For exterior girders which are not cut and are rigidly attached to a steel deck, the effective section shall consist of the structural shape of the exterior girder.</li> <li>• For exterior girders which have been cut and are rigidly attached to a steel deck, the effective section shall consist of the remaining portion of the structural shape and a portion of the</li> </ul>	<p><b>C2.2.2.3</b></p> <p>Many exterior girders which are located on the inside of the bridge, adjacent to another RRFC, are cut in the field in order to form a longitudinal connection between RRFCs.</p> <p>Field testing results (Provines, 2011) showed portions of the steel deck participated in local bending if the secondary member was rigidly connected to the deck.</p>

## Proposed Guidelines for Load Rating Bridges Constructed from Railroad Flatcars

<p>steel deck with a width equal to the width of the bottom flange of the structural shape of the exterior girder.</p> <ul style="list-style-type: none"> <li>• For exterior girders which are not rigidly attached to a steel deck, the effective section shall consist of the structural shape of the exterior girder.</li> <li>• For stringers which are rigidly attached to a steel deck, the effective section shall consist of the structural shape and a portion of the steel deck with a width equal to the width of the bottom flange of the structural shape of the stringer.</li> <li>• For stringers, which are not rigidly attached to a steel deck, the effective section shall consist of the structural shape of the stringer.</li> </ul>	
<p><b>3-BRIDGES CONSTRUCTED FROM BOXCARS</b></p> <p>The following sections describe the procedures which shall be used for determining the maximum positive live load bending stress in bridges constructed from boxcars.</p>	<p><b>C3</b></p>
<p><b>3.1-Determination of Maximum Positive Live Load Bending Stress in Primary Members</b></p> <p>This section describes the procedures which shall be used for determining the maximum positive live load bending stress in primary members. The local bending stress shall then be added to the global stress to determine the total stress at a particular location.</p>	<p><b>C3.1</b></p> <p>As stated in Article 1.2, the primary members of boxcars consist of the main girder and the two exterior girders.</p>
<p><b>3.1.1-General Equation</b></p>	<p><b>C3.1.1</b></p>



## Proposed Guidelines for Load Rating Bridges Constructed from Railroad Flatcars

<p>The following general expression shall be used in determining the maximum positive live load bending stress:</p> $\sigma_{LL} = (\alpha)(CDF) \frac{(DF) M_{LL}}{S_{eff}} \quad (3.1.1-1)$ <p>where:</p> <p><math>\sigma_{LL}</math> = Maximum positive live load bending stress</p> <p><math>\alpha</math> = Stress modification factor as specified in Article 3.1.1.5</p> <p><math>CDF</math> = Car distribution factor as specified in Article 3.1.1.3</p> <p><math>DF</math> = Distribution factor as specified in Article 3.1.1.2</p> <p><math>M_{LL}</math> = Maximum positive live load moment as specified in Article 3.1.1.1</p> <p><math>S_{eff}</math> = Effective section modulus as specified in Article 3.1.1.4</p>	<p>The general equation for the determination of the maximum positive live load bending stress was developed through field instrumentation and controlled load testing of a bridge constructed of boxcars (Provines, 2011).</p>
<p><b>3.1.1.1–Maximum Positive Live Load Moment</b></p> <p>The maximum positive live load moment (<math>M_{LL}</math>) shall be determined using procedures described in <i>AASHTO The Manual for Bridge Evaluation</i>.</p>	<p><b>C3.1.1.1</b></p>
<p><b>3.1.1.2–Distribution Factor</b></p> <p>The following expression shall be used in determining the distribution factor (DF):</p> $DF = MP \leq 1.0 \quad (3.1.1.2-1)$	<p><b>C3.1.1.2</b></p> <p>The distribution factor is intended to represent load distribution <u>between</u> boxcars. It is differentiated from the car distribution factor, which is intended to represent load distribution <u>within</u> a boxcar.</p>

## Proposed Guidelines for Load Rating Bridges Constructed from Railroad Flatcars

<p>where:</p> <p><math>DF</math> = Distribution factor</p> <p><math>MP</math> = Moment proportion as specified in Article 3.1.1.2.1</p>	
<p><b>3.1.1.2.1–Moment Proportion</b></p> <p>The moment proportion (MP) shall be determined based on the lever rule, as described in the <i>AASHTO LRFD Bridge Design Specifications</i>. The lever rule shall be used to distribute the live load moment to each of the boxcars. The reactions used for when computing the lever rule shall be located at the centerline of each boxcar. The moment proportion shall be determined as follows:</p> <ul style="list-style-type: none"> <li>• If the longitudinal connection between boxcars can be considered a rigid connection:  <math>MP</math> = Result from lever rule</li> <li>• If the longitudinal connection between boxcars cannot be considered a rigid connection, or if there is no longitudinal connection:  <math>MP</math> = 1.0</li> </ul>	<p><b>C3.1.1.2.1</b></p> <p>The load tests which resulted in the development of Eq. 3.1.1.2-1 were performed on a bridge which was constructed of two boxcars connected side-by-side. It is reasonable to believe the lever rule provides conservative results for bridges using either less than two or more than two boxcars in the cross section. For instance, if a bridge was constructed of a single boxcar, the lever rule result would be equal to 1.0. The lever rule would be conservative if used on a bridge constructed with three boxcars side-by-side. If a truck was located on one of the outside boxcars, according to the lever rule the boxcar on the opposite side would carry zero load provided the truck did not cross the centerline of the middle boxcar.</p> <p>The lever rule is based on the assumption of a rigid deck. This assumption is violated if the longitudinal connection is not stiff enough in the transverse direction to be considered rigid, therefore no load can be transferred from one boxcar to the other.</p> <p>The evaluation of whether or not a longitudinal connection is stiff enough to transfer moment from one boxcar to another should be determined through the use of the bridge inspection report and engineering judgment.</p>
<p><b>3.1.1.3–Car Distribution Factor</b></p> <p>The car distribution factor (CDF) shall be</p>	<p><b>C3.1.1.3</b></p>

## Proposed Guidelines for Load Rating Bridges Constructed from Railroad Flatcars

<p>determined as follows:</p> <ul style="list-style-type: none"> <li>For main girders:</li> </ul> $CDF = \frac{3}{4}$ <ul style="list-style-type: none"> <li>For exterior girders:</li> </ul> $CDF = \frac{3}{5}$	<p>The car distribution factors for each primary member of a boxcar were developed through field instrumentation results. The CDF values represent maximum distribution factors within a boxcar seen in the results.</p>
<p><b>3.1.1.4–Effective Section</b></p> <p>The effective section modulus (<math>S_{eff}</math>) shall be determined based on the following effective sections:</p> <ul style="list-style-type: none"> <li>For main girders, the effective section shall consist of the structural shapes which make up the main girder.</li> <li>For the exterior girders, the effective section shall consist of the structural shape of the exterior girder.</li> </ul>	<p><b>C3.1.1.4</b></p> <p>Based on the load testing and stress results (Provines, 2011), the effective sections of the primary members of boxcar consist only of the structural shapes used to construct those members. Dissimilar to effective sections for typical RRFCs, the secondary members did not participate in global bending resistance.</p>
<p><b>3.1.1.5–Stress Modification Factor</b></p> <p>The stress modification factor (<math>\alpha</math>) shall be taken equal to 0.75.</p>	<p><b>C3.1.1.5</b></p> <p>The stress modification factor was developed through field instrumentation test results to more accurately, but still conservatively, match stresses calculated using Eq.3.1.1-1 with those measured during field testing (Provines, 2011).</p>
<p><b>3.2–Determination of Maximum Positive Live Load Bending Stress in Secondary Members</b></p> <p>The following methods shall be acceptable for determining the maximum positive live load bending stress in secondary members of</p>	<p><b>C3.2</b></p> <p>Based on the limited field testing data from a single boxcar bridge, no conclusive specific methods for determining bending stress in</p>

## Proposed Guidelines for Load Rating Bridges Constructed from Railroad Flatcars

<p>boxcars:</p> <ul style="list-style-type: none"> <li>• Orthotropic plate theory equations found in the <i>AASHTO LRFD Bridge Design Specifications</i></li> <li>• Finite element analysis</li> <li>• Field instrumentation and testing</li> <li>• Any reasonable and accepted engineering method</li> </ul>	<p>secondary members were developed.</p>
<p><b>4-BRIDGES CONSTRUCTED FROM TYPICAL RRFCs WITH A COMPOSITE CONCRETE DECK</b></p> <p>The following sections describe the procedures to be used for determining the maximum positive live load bending stress in bridges constructed from typical RRFCs with a fully composite concrete deck.</p>	<p><b>C4</b></p>
<p><b>4.1-Determination of Maximum Positive Live Load Bending Stress in Primary Members</b></p> <p>The following conditions must be satisfied to use the procedures in Article 4.1:</p> <ul style="list-style-type: none"> <li>• The primary members of a bridge constructed with typical RRFCs and a fully composite concrete deck include the main box girder and the two exterior girders;</li> <li>• The primary members shall be fully composite with the concrete deck;</li> <li>• The concrete deck shall have the ability to transfer load within a single flatcar; and</li> <li>• The concrete deck shall have the ability to transfer load between flatcars;</li> </ul>	<p><b>C4.1</b></p> <p>Research has demonstrated that the main box girder and the two exterior girders function as primary load carrying members when a composite concrete deck is present (Washeleski, 2013). If the exterior members are altered during installation, this assumption may not be valid and further evaluation should be performed.</p> <p>Laboratory testing showed that composite action between the flatcar member and the concrete deck was achieved when shear connectors were designed using procedures described in <i>AASHTO LRFD Bridge Design Specifications</i> (Washeleski, 2013).</p> <p>Exterior girders that were altered, or cut,</p>

## Proposed Guidelines for Load Rating Bridges Constructed from Railroad Flatcars

	<p>are not assumed to be capable of achieving composite action.</p> <p>Composite action can be achieved through the use of shear studs, rivet heads extending from built-up members into the concrete deck, or other acceptable means of transferring load from the concrete deck to the RRFC.</p> <p>Field instrumentation results from a bridge constructed of a flatcar with riveted built-up members showed composite action with its concrete deck (Provines, 2011).</p>
<p><b>4.1.1–General Equation</b></p> <p>The following general expression shall be used in determining the maximum positive live load bending stress:</p> $\sigma_{LL} = (\alpha) (CDF) \frac{(DF) M_{LL}}{S_{eff}} \quad (4.1.1-1)$ <p>where:</p> <p><math>\sigma_{LL}</math> = Maximum positive live load bending stress</p> <p><math>\alpha</math> = Stress modification factor as specified in Article 4.1.1.5</p> <p><math>CDF</math> = Car distribution factor as specified in Article 4.1.1.3</p> <p><math>DF</math> = Distribution factor as specified in Article 4.1.1.2</p> <p><math>M_{LL}</math> = Maximum positive live load moment for one lane loaded as specified in Article 4.1.1.1</p> <p><math>S_{eff}</math> = Effective section modulus as specified in Article 4.1.1.4</p>	<p><b>C4.1.1</b></p> <p>The general equation for the determination of the maximum positive live load bending stress was developed through field instrumentation and controlled load testing of several RRFC bridges (Provines, 2011).</p> <p>The application of this equation for RRFC bridges with a fully composite concrete deck was refined through instrumentation and controlled load testing of a full-scale RRFC bridge in the laboratory (Washeleski, 2013).</p>
<p><b>4.1.1.1–Maximum Positive Live Load Moment</b></p>	<p><b>C4.1.1.1</b></p>

## Proposed Guidelines for Load Rating Bridges Constructed from Railroad Flatcars

<p>The maximum positive live load moment for a single lane loaded (<math>M_{LL}</math>) shall be determined using procedures described in <i>AASHTO The Manual for Bridge Evaluation</i>.</p>	
<p><b>4.1.1.2–Distribution Factor</b></p> <p>The following expression shall be used in determining the distribution factor (DF):</p> $DF = MP \leq 1.0 \quad (4.1.1.2-1)$ <p>where:</p> <p><math>DF</math> = Distribution factor</p> <p><math>MP</math> = Moment proportion as specified in Article 4.1.1.2.1</p>	<p><b>C4.1.1.2</b></p> <p>The distribution factor is intended to represent load distribution <u>between</u> flatcars. It is differentiated from the car distribution factor, which is intended to represent load distribution <u>within</u> a flatcar.</p>
<p><b>4.1.1.2.1–Moment Proportion</b></p> <p>The moment proportion (MP) shall be determined using Table 4.1 for one lane loaded, schematically shown in Figure 4.1, and Table 4.2 for two lanes loaded.</p>	<p><b>C4.1.1.2.1</b></p> <p>The lever rule to determine the moment proportion may still be used in this application; however, laboratory testing showed it provides overly conservative results (Washelseki 2013).</p> <p>The moment proportion values in the tables provided were developed using a torsional spring analogy to predict more accurate live load responses between the flatcars (Washeski, 2013; Akinci 2013). The spring analogy was calibrated using the experimental data collected during laboratory testing on a RRFC bridge constructed with two typical RRFCs and a fully composite concrete deck (Washeski, 2013).</p> <p>The moment proportions provided encompass a moment envelope obtained through a parametric study using the spring analogy (Washeski, 2013). Hence, the proportions do not always sum to 1.0.</p> <p>The parametric study was performed for bridges constructed of two RRFCs connected</p>

Proposed Guidelines for Load Rating Bridges Constructed from Railroad Flatcars

side-by-side. The lever rule may be used for bridges with either less than two or more than two RRFCs in the cross section, as described in Article C2.1.1.2.1.

The application of the moment proportion tables is based on the assumption of a properly designed and constructed concrete deck to transfer load between the flatcars. The application is also based on the assumption that the main girders and exterior girders are fully composite with the concrete deck, as described in Article 4.1.

**Table 4.1: Moment proportion for one lane loaded**

Moment Proportion, <i>MP</i>								
Stiffness Ratio, $I_{ext}/I_{main}$	$x \leq S_{CL}$						$S_{CL} < x < (S_{CL} + 6ft)$	
	$S_{RRFC} \leq 2ft$		$2ft < S_{RRFC} \leq 4ft$		$4ft < S_{RRFC} \leq 6ft$		$S_{RRFC} \leq 6ft$	
	<i>Loaded RRFC</i>	<i>Unloaded RRFC</i>	<i>Loaded RRFC</i>	<i>Unloaded RRFC</i>	<i>Loaded RRFC</i>	<i>Unloaded RRFC</i>	<i>Loaded RRFC</i>	<i>Unloaded RRFC</i>
$I_{ext}/I_{main} \leq 15\%$	0.80	0.25	0.90	0.20	0.90	0.15	0.60	0.60
$15\% < I_{ext}/I_{main} \leq 25\%$	0.85	0.20	0.90	0.15	0.95	0.15	0.60	0.60
$25\% < I_{ext}/I_{main} \leq 75\%$	0.90	0.20	0.95	0.15	0.95	0.10	0.60	0.60

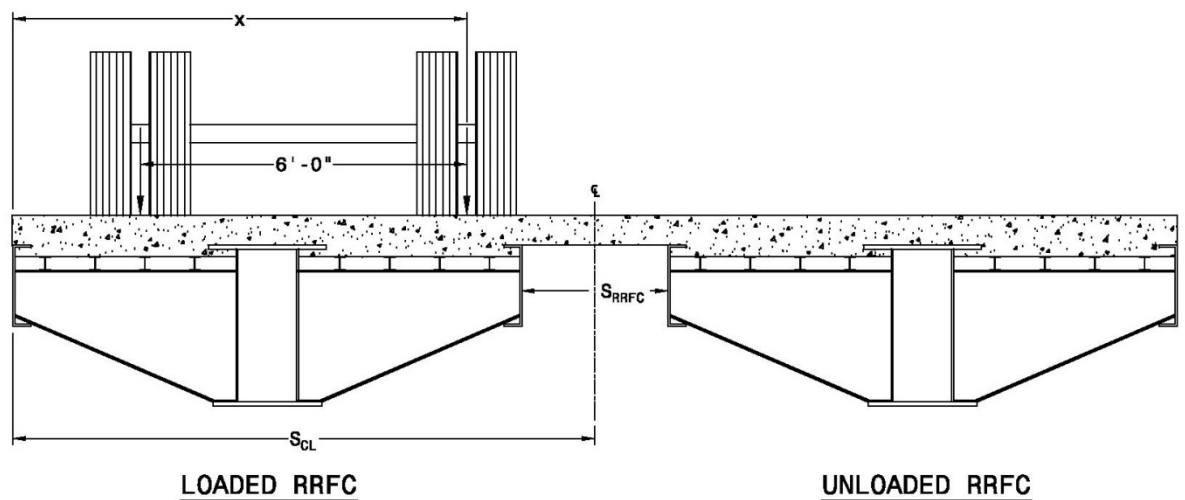


**Figure 4.1: Schematic for determining the moment proportion for one lane loaded**

## Proposed Guidelines for Load Rating Bridges Constructed from Railroad Flatcars

**Table 4.2: Moment proportion for two lanes loaded**

Moment Proportion, $MP$			
Stiffness Ratio, $I_{ext}/I_{main}$	$S_{RRFC} \leq 2\text{ft}$	$2\text{ft} < S_{RRFC} \leq 4\text{ft}$	$4\text{ft} < S_{RRFC} \leq 6\text{ft}$
	<i>Loaded RRFC</i>	<i>Loaded RRFC</i>	<i>Loaded RRFC</i>
$I_{ext}/I_{main} \leq 15\%$	1.05	1.30	1.50
$15\% < I_{ext}/I_{main} \leq 25\%$	1.05	1.30	1.50
$25\% < I_{ext}/I_{main} \leq 75\%$	1.10	1.35	1.50

where:

$I_{ext}$  = Moment of inertia about the strong axis of the exterior girder composite section

$I_{main}$  = Moment of inertia about the strong axis of the main girder composite section

$S_{CL}$  = Distance from outside face of loaded flatcar to bridge centerline

$S_{RRFC}$  = Clear distance between flatcars

$\chi$  = Distance from outside face of loaded flatcar to location of inside wheel of truck axle

**4.1.1.3–Car Distribution Factor**

The car distribution factor (CDF) shall be determined as specified in Table 4.3.

**Table 4.3: Car distribution factor**

Car Distribution Factor, $CDF$		
Stiffness Ratio, $I_{ext}/I_{main}$	Longitudinal member	
	<i>Main Girder</i>	<i>Exterior Girder(s)</i>
$I_{ext}/I_{main} \leq 5\%$	0.95	0.05
$5\% < I_{ext}/I_{main} \leq 15\%$	0.80	0.15
$15\% < I_{ext}/I_{main} \leq 25\%$	0.70	0.25
$25\% < I_{ext}/I_{main} \leq 75\%$	0.50	0.40

**C.4.1.1.3**

Based on laboratory test results for a bridge constructed with two RRFCs and a fully composite concrete deck, the main girder and exterior girders within a flatcar were found to carry the entire “global” live load moment (Washeski, 2013). The CDF represents the distribution of the moment within a flatcar between the primary members.

The CDFs were developed using laboratory test data and through an analytical parametric study (Washeski, 2013; Akinci 2013).

The application of the CDF provided in the table is based on the assumption of a properly designed and constructed concrete deck to transfer load within the flatcars. The application is also based on the assumption



## Proposed Guidelines for Load Rating Bridges Constructed from Railroad Flatcars

<p>where:</p> <p><math>I_{ext}</math> = Moment of inertia about the strong axis of the exterior girder composite section</p> <p><math>I_{main}</math> = Moment of inertia about the strong axis of the main girder composite section</p>	<p>that the main girders and exterior girders are fully composite with the concrete deck, as described in Article 4.1.</p>
<p><b>4.1.1.4–Effective Section</b></p> <p>The effective section modulus (<math>S_{eff}</math>) shall consist of the structural shape of the member and its effective flange width of the concrete deck slab, as described in the <i>AASHTO LRFD Bridge Design Specifications</i>.</p>	<p><b>C.4.1.1.4</b></p> <p>Results from laboratory testing of a bridge constructed with typical RRFCs and a fully composite concrete deck showed it is reasonable to assume the structural shape of the flatcar member and its effective width of the concrete deck slab as the effective section of the longitudinal member, presuming the member is composite with the concrete deck (Washeleski, 2013).</p>
<p><b>4.1.1.5–Stress Modification Factor</b></p> <p>The stress modification factor (<math>\alpha</math>) shall be taken equal to 1.0.</p>	<p><b>C4.1.1.5</b></p> <p>The stress modification factor described in Article 2.1.1.5 was developed based on the field instrumentation test results to more accurately, but still conservatively, match stresses calculated using Eq.2.1.1-1 with those measured during field testing (Provines, 2011).</p> <p>The stress modification factor is to be taken as 1.0 for the application of a bridge constructed with typical RRFCs and a fully composite concrete deck. Since considerably more instrumentation was installed in the laboratory and more rigorous analytical modeling of load distribution was developed, the provisions provided herein for RRFC bridges constructed with a composite concrete deck yield more accurate estimates of the actual stress in the members. Hence, no adjustment factor is needed when using the distribution factors provided in Tables 4.1, 4.2, and 4.3.</p> <p>If the lever rule is used to determine the</p>

## Proposed Guidelines for Load Rating Bridges Constructed from Railroad Flatcars

	distribution factor, the stress modification factor may be taken as 0.75.
<p><b>4.2–Determination of Maximum Positive Live Load Bending Stress in Secondary Members</b></p> <p>The local bending stresses in secondary members (e.g., stringers) of RRFC bridges with concrete decks may be neglected.</p>	<p><b>C4.2</b></p> <p>It has been shown through field and laboratory testing that when a concrete deck is present, the local bending effects of secondary members, such as stringers, are negligible (Provines, 2011, Washeleski, 2013)).</p>
<p><b>4.3–Determination of Available Capacity After Fracture of a Main Girder</b></p> <p>This section describes the procedures which may be used for determining if a typical RRFC with a composite concrete deck has adequate remaining capacity if fracture of a main girder were to occur. These provisions are intended to be utilized to rationally establish if members of a RRFC should be classified as a fracture critical member and hence subjected to more rigorous field inspection.</p> <p>The conditions listed in Article 4.1 must be satisfied to use the following procedure.</p> <p>The provisions may be applied for RRFCs with bearing to bearing span lengths of up to 60 feet.</p> <p>No provisions are required for evaluation of fracture of an exterior girder as these members do not carry the major proportion of the dead or live load moments as do the main girders. Hence, fracture of the main girder is the only critical scenario.</p> <p>The stress in the remaining primary</p>	<p><b>C4.3</b></p> <p>The procedures in this section were developed from laboratory testing of a bridge constructed with typical RRFCs and a fully composite concrete deck. The laboratory research conducted a controlled fracture of the tension flange of one main girder (Washeleski, 2013).</p> <p>Laboratory testing showed that the composite concrete deck played a significant role in transferring load to the remaining primary members after fracture occurred (Washeleski, 2013). It is not recommended to use the following procedures if the conditions in Article 4.1 are not satisfied.</p> <p>The simplified procedures recommended herein were developed based on a RRFC with a bearing to bearing span of nearly 48 feet. The results are believed to be applicable up to bearing to bearing span lengths of up to 60 feet. For clear span lengths greater than 60 feet, additional analysis should be performed. The approach simply determines if the stress in the remaining members remains below an acceptable level under various load conditions in the faulted state.</p> <p>Failure of an exterior member, such as a typical channel beam that is often utilized was</p>

## Proposed Guidelines for Load Rating Bridges Constructed from Railroad Flatcars

<p>members shall not exceed <math>0.75F_y</math> under any of the load conditions investigated</p>	<p>not found to be a critical failure mechanism. If the structure possess sufficient capacity when a main girder fails, it is clear failure of an exterior beam would not be a critical case.</p> <p>Since this is considered an extreme event, the limit of <math>0.75F_y</math> was selected to be a reasonable upper bound stress in the steel components.</p> <p>The procedures and distribution factors recommended herein are intended to provide simple, yet reasonably conservative estimates of the proportion of the moments distributed to the remaining intact members.</p>
<p><b>4.3.1–Redistribution of Dead Load</b></p> <p>This section describes the procedures for determining the redistribution of dead loads to the remaining primary members after fracture occurs in the tension flange of a primary member.</p>	<p><b>C4.3.1</b></p> <p>Locked in stresses include both dead load stresses, fabrication stresses, and other residual stresses. The redistribution of these stresses is in addition to the original gravity load stresses in the member under consideration. Obviously, it is not possible to quantify fabrication and residual stresses for in-service bridges. The laboratory testing showed those effects were relatively small compared to those associated with applied dead load stress due to the self-weight of the car and concrete (Washeski, 2013).</p>
<p><b>4.3.1.1–General Equation</b></p> <p>The following general expression shall be used in determining the redistributed dead load stress:</p> $\sigma_{RD} = (\alpha) (CDF) \frac{(DF) M_{RD}}{S_{eff}} \quad (4.3.1.1-1)$ <p>where:</p> <p><math>\sigma_{RD}</math> = Redistributed dead load stress</p> <p><math>\alpha</math> = Stress modification factor as specified in</p>	<p><b>C4.3.1.1</b></p>

## Proposed Guidelines for Load Rating Bridges Constructed from Railroad Flatcars

<p>Article 4.3.1.6</p> <p><math>CDF</math> = Car distribution factor as specified in Article 4.3.1.4</p> <p><math>DF</math> = Distribution factor as specified in Article 4.3.1.3</p> <p><math>M_{RD}</math> = Redistributed moment as specified in Article 4.3.1.2</p> <p><math>S_{eff}</math> = Effective section modulus as specified in Article 4.3.1.5</p>	
<p><b>4.3.1.2–Maximum Redistributed Moment (<math>M_{RD}</math>)</b></p> <p>The assumed moment due to redistribution of dead load after fracture occurs (<math>M_{RD}</math>) may be taken as the dead load moment carried by the main girder before the fracture occurred.</p>	<p><b>C4.3.1.2</b></p> <p>Dead load stresses should be calculated using traditional structural analysis techniques. Laboratory research results found this assumption to be reasonable in estimating the redistributed moment due to dead load after fracture occurs (Washeski, 2013).</p>
<p><b>4.3.1.3–Distribution Factor</b></p> <p>The distribution factor (DF) for redistributed dead load may be used as follows:</p> <ul style="list-style-type: none"> <li>• For the fractured flatcar, <math>DF = 0.60</math></li> <li>• For the non-fractured flatcar, <math>DF = 0.40</math></li> </ul>	<p><b>C4.3.1.3</b></p> <p>The distribution factor is intended to represent load distribution between flatcars. The distribution factors were developed based on laboratory testing and analysis when a controlled fracture was simulated in the tension flange of one main girder of a bridge constructed with typical RRFCs and a fully composite concrete deck (Washeski, 2013).</p>
<p><b>4.3.1.4–Car Distribution Factor</b></p> <p>The car distribution factor (CDF) for redistributed dead load shall be determined as follows:</p> <ul style="list-style-type: none"> <li>• For the fractured flatcar, <math>CDF = 0.50</math></li> </ul>	<p><b>C4.3.1.4</b></p> <p>The car distribution factor is intended to represent load distribution within a flatcar.</p> <p>The car distribution factor of 0.50 for the</p>

## Proposed Guidelines for Load Rating Bridges Constructed from Railroad Flatcars

<ul style="list-style-type: none"> <li>• For the non-fractured flatcar, CDF values in Article 4.1.1.3</li> </ul>	<p>remaining primary members in the fractured flatcar is based on the assumption that the remaining members are the exterior girders.</p>
<p><b>4.3.1.5 –Effective Section</b></p> <p>The effective section modulus (<math>S_{eff}</math>) for determining the redistributed dead load in a specified member shall consist of the structural shape of the member and its effective flange width of the concrete deck slab, as described in the <i>AASHTO LRFD Bridge Design Specifications</i>.</p>	<p><b>C4.3.1.5</b></p>
<p><b>4.3.1.6–Stress Modification Factor</b></p> <p>The stress modification factor (<math>\alpha</math>) for determining the redistributed dead load shall be taken equal to 1.0.</p>	<p><b>C4.3.1.6</b></p>
<p><b>4.3.2–Determination of Maximum Positive Live Load Bending Stress in Remaining Primary Members</b></p> <p>Eq. 4.1.1-1 shall be used to determine the maximum positive live load bending stress in the remaining primary members after fracture occurs in the tension flange of a primary member.</p>	<p><b>C4.3.2</b></p>
<p><b>4.3.2.1–Maximum Positive Live Load Moment</b></p> <p>The maximum positive live load moment for a single lane loaded (<math>M_{LL}</math>) shall be determined using procedures described in <i>AASHTO The Manual for Bridge Evaluation</i>.</p>	<p><b>C4.3.2.1</b></p>
<p><b>4.3.2.2–Distribution Factor</b></p> <p>The distribution factor (DF) for determining the live load stress shall be used as</p>	<p><b>C4.3.2.2</b></p> <p>The distribution factor is intended to represent load distribution between flatcars.</p>

## Proposed Guidelines for Load Rating Bridges Constructed from Railroad Flatcars

<p>follows for one lane loaded:</p> <ul style="list-style-type: none"> <li>• For the fractured flatcar, <math>DF = 0.50</math></li> <li>• For the non-fractured flatcar, <math>DF = 1.0</math></li> </ul> <p>The distribution factor (DF) shall be used as follows for two lanes loaded:</p> <ul style="list-style-type: none"> <li>• For the fractured flatcar, <math>DF = 0.50</math></li> <li>• For the non-fractured flatcar, <math>DF = 1.75</math></li> </ul>	<p>Based on laboratory testing, when the fractured flatcar was loaded, 50% of the applied load was transferred to the non-fractured flatcar (Washeski, 2013). If the non-fractured flatcar is loaded, it is conservatively specified that 100% of the live load moment is to be carried by that car since it is much stiffer than the failed car. The DF of 1.75 for two lanes loaded was specified for the same reason.</p>
<p><b>4.3.2.3–Car Distribution Factor</b></p> <p>The car distribution factor (CDF) for determining the live load stress shall be determined as follows:</p> <ul style="list-style-type: none"> <li>• For the fractured flatcar, <math>CDF = 0.50</math></li> <li>• For the non-fractured flatcar, CDF values in Article 4.1.1.3</li> </ul>	<p><b>C4.3.2.3</b></p> <p>The car distribution factor is intended to represent load distribution within a flatcar.</p> <p>The car distribution factor of 0.50 for the remaining primary members in the fractured flatcar is based from the assumption that the remaining members are the exterior girders.</p>
<p><b>4.3.2.4 –Effective Section</b></p> <p>The effective section modulus (<math>S_{eff}</math>) shall consist of the structural shape of the member and the effective flange width of the concrete deck slab, as described in the <i>AASHTO LRFD Bridge Design Specifications</i>.</p>	<p><b>C4.3.2.4</b></p> <p>Results from laboratory testing of a bridge constructed with typical RRFs and a fully composite concrete deck showed it is reasonable to assume the structural shape of the flatcar member and the effective width of the concrete deck slab as the effective section of the longitudinal member, presuming the member is fully composite with the concrete deck (Washeski, 2013).</p>
<p><b>4.3.2.5–Stress Modification Factor</b></p> <p>The stress modification factor (<math>\alpha</math>) shall be taken equal to 1.0.</p>	<p><b>C4.3.2.5</b></p>

**APPENDIX G. LOAD RATING AND FRACTURE CAPACITY EXAMPLE**

## Load Rating Using Proposed Guidelines

### Laboratory RRFC Bridge - Composite Concrete Deck

**The following conditions must be satisfied to use the load rating procedure:**

1. The primary members shall be composite with the concrete deck
2. The concrete deck shall have the ability to transfer load within a single flatcar
3. The concrete deck shall have the ability to transfer load between flatcars

**Guidelines and Specifications:**

1. AASHTO The Manual for Bridge Evaluation 2011 (*AASHTO*)
2. Proposed Guidelines for Load Rating Bridges Constructed from Railroad Flatcars (*Guidelines*)

**Define Steel Properties:**

$$F_y := 48\text{ksi}$$

Yield strength of steel from material tests

$$E_s := 29000\text{ksi}$$

Assumed elastic modulus of steel

$$\gamma_{\text{steel}} := 490 \frac{\text{lb} \cdot \text{f}}{\text{ft}^3}$$

Assumed unit weight of steel

*Guidelines 1.2.1*

**Define Concrete Properties:**

$$f_c := 5730\text{psi}$$

28 day compressive strength of concrete (typically can assume 4000-6000psi)

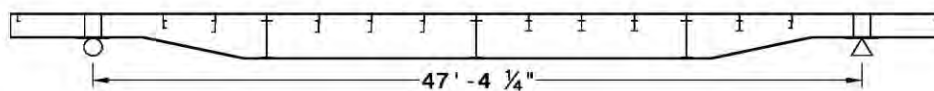
$$w_{\text{conc}} := 150 \frac{\text{lb} \cdot \text{f}}{\text{ft}^3}$$

Assumed unit weight of reinforced concrete

$$E_c := 57\text{ksi} \sqrt{\frac{f_c}{\text{psi}}} = 4314.7\text{ksi}$$

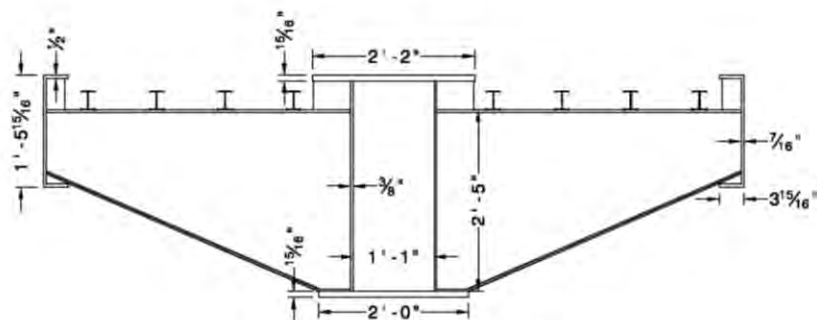
Elastic modulus of concrete

**Define Bridge Dimensions and Parameters:**

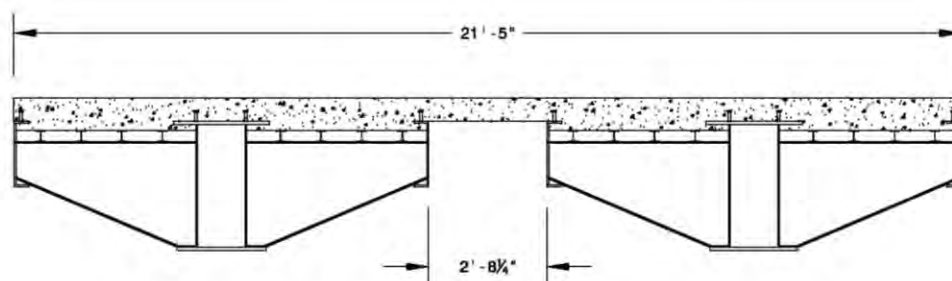


**ELEVATION VIEW**

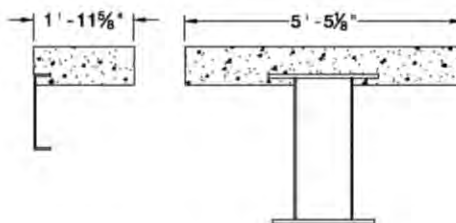




**SECTION DIMENSIONS AT MIDSPAN**



**BRIDGE WIDTH AT MIDSPAN**



**CONCRETE DECK TRIBUTARY WIDTHS**

$$L_{RRFC} = 58\text{ft}$$

Length of RRFC

$$L_{\text{span}} = 47\text{ft} + 4.75\text{in} = 47.4\text{ft}$$

Span length from center of wheel truck to center of wheel truck

$$W_{\text{bridge}} = 21\text{ft} + 5\text{in}$$

Bridge width

$$S_{RRFC} = 2\text{ft} + 8.25\text{in}$$

Clear spacing between RRFCs

$$W_{RRFC} := \frac{36000}{L_{RRFC}} \text{ lbf} = 620.7 \frac{\text{lbf}}{\text{ft}}$$

Weight of one RRFC

$$A_{mg} := 72.1 \text{ in}^2$$

Cross sectional area of main girder (computed using AutoCAD)

$$A_{eg} := 11.6 \text{ in}^2$$

Cross sectional area of exterior girder (computed using AutoCAD)

$$I_{mg} := 16364 \text{ in}^4$$

Main girder moment of inertia (computed using AutoCAD)

$$I_{eg} := 483 \text{ in}^4$$

Exterior girder moment of inertia (computed using AutoCAD)

$$y_{b,mg} := 18.2 \text{ in}$$

Distance from neutral axis to extreme tension fiber of main girder (computed using AutoCAD)

$$y_{b,eg} := 9.0 \text{ in}$$

Distance from neutral axis to extreme tension fiber of exterior girder (computed using AutoCAD)

#### Determine Composite Section Properties:

##### Note:

-Concrete deck width must be transformed to an effective flange width before computing section properties

$$n := \frac{E_s}{E_c} = 7$$

Modular ratio used to transform concrete deck width to be used in composite section property calculations (e.g.  $(1'-11 \frac{5}{8}'' ) / 7 = 3 \frac{3}{8}''$ )

$$I_{mg,comp} := 31602 \text{ in}^4$$

Composite moment of inertia of main girder (computed using AutoCAD)

$$I_{eg,comp} := 1732 \text{ in}^4$$

Composite moment of inertia of exterior girder (computed using AutoCAD)

$$y_{b,comp,mg} := 28.6 \text{ in}$$

Distance from neutral axis to extreme tension fiber of main girder composite section (computed using AutoCAD)

Distance from neutral axis to

$$y_{b,comp,eg} = 17.1 \text{ in}$$

extreme tension fiber of exterior girder composite section (computed using AutoCAD)

$$W_{\text{guardrail}} := 0 \frac{\text{lb}\cdot\text{ft}}{\text{ft}}$$

Weight of guardrail system for entire bridge

$$I = 0.33$$

*Guidelines 1.2.2*

Impact factor

$$A_1 := 1.0$$

*AASHTO 6B.5.2*

Allowable Stress

$$A_2 := 1.0$$

### **Rating of Primary Members for SINGLE LANE Loaded:**

#### **Note:**

- Based on global bending in primary members
- Rating performed on bottom flange of girder (location of maximum positive bending stress)
- Rating performed on loaded RRFC (controls)

#### **Determine Capacity of Members, C:**

$$C = 0.55 \cdot F_y = 26.4 \text{ ksi}$$

*AASHTO Table 6B.6.2.1-1*

### **Rating of Loaded Main Girder:**

#### **Determine Effective Section Modulus, Seff:**

$$S_{mg} := \frac{I_{mg}}{y_{b,mg}} = 899.1 \cdot \text{in}^3$$

Section modulus of main girder

$$S_{effmg} := \frac{I_{mg,comp}}{y_{b,comp,mg}} = 1105 \cdot \text{in}^3$$

Effective section modulus of main girder composite section

### **DETERMINE DEAD LOAD BENDING STRESS, D:**

*Guidelines 1.1*

#### **Note:**

- Only the structural shape of the flatcar member resists dead load

#### **Determine Stress in Main Girder due to RRFC Weight:**

$$M_{RRFC} := \frac{W_{RRFC} \cdot L_{span}^2}{8} = 174 \cdot \text{kip}\cdot\text{ft}$$

Assume main girder carries weight single RRFC

$$\sigma_{RRFC} = \frac{M_{RRFC}}{S_{mg}} = 2.3 \text{ ksi}$$

Stress in main girder due to RRFC weight

**Determine Stress in Main Girder due to Concrete Deck:**

$$w_{deckmg} := (65.1875 \text{ in})(9 \text{ in}) \cdot w_{conc} = 611.1 \frac{\text{lb}}{\text{ft}}$$

Portion of concrete deck carried by the main girder

$$M_{deckmg} = \frac{w_{deckmg} \cdot L_{span}^2}{8} = 171.6 \text{ kip} \cdot \text{ft}$$

Dead load moment at midspan due to concrete deck

$$\sigma_{deckmg} = \frac{M_{deckmg}}{S_{mg}} = 2.3 \text{ ksi}$$

Stress in main girder due to concrete deck

**Determine Total Dead Load Stress in Main Girder:**

$$D := \sigma_{RRFC} + \sigma_{deckmg} = 4.6 \text{ ksi}$$

Total dead load bending stress in main girder

**DETERMINE LIVE LOAD BENDING STRESS, L:**

**Note:**

-The composite section (structural shape of the member and its effective flange width of the concrete deck slab) resists live load

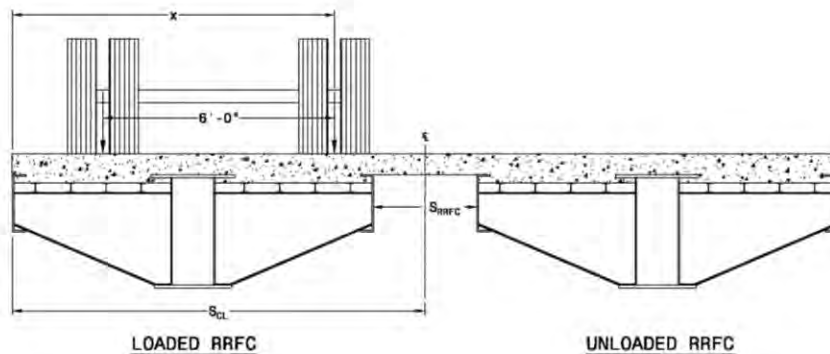
$$M_{LL} := 580 \text{ kip} \cdot \text{ft}$$

*AASHTO Table C6B-1*

Maximum live load moment due to HS-20 truck at midspan

$$\frac{I_{eg,comp}}{I_{mg,comp}} = 5\%$$

Stiffness ratio to be used to determine DF and CDF

**Determine Moment Proportion, MP:**

$$x := 7\text{ft} + 8\text{in}$$

$$S_{CL} := \frac{W_{\text{bridge}}}{2} = 10.7\text{-ft}$$

$$S_{RRFC} = 2.7\text{-ft}$$

$$MP := \begin{cases} 0.90 & \text{if } x \leq S_{CL} \\ 0.60 & \text{if } S_{CL} < x < S_{CL} + 6\text{ft} \end{cases}$$

$$MP = 0.9$$

Location of inside truck wheel take from outside face of loaded RRFC

Distance from outside face of loaded flatcar to centerline of bridge

Clear spacing between RRFCs

*Guidelines 4.1.1.2.1*

Moment proportion from Table, depending on truck location

Represents proportion of live load moment distributed to loaded flatcar

**Determine Distribution Factor, DF:**

$$DF := MP = 0.9$$

$$DF \leq 1 = 1 \quad \text{OKAY}$$

*Guidelines 4.1.1.2*

Represents load distribution between RRFCs

**Determine Maximum Positive Live Load Bending Stress:**

$$\alpha := 1.0$$

*Guidelines 4.1.1.5*

Stress modification factor

*Guidelines 4.1.1.3*

$$CDF = 0.95$$

$$L = \alpha \cdot CDF \cdot \frac{DF \cdot M_{LL}}{S_{effmg}} = 5.39 \text{ ksi}$$

Car distribution factor for main girder (proportion of flatcar moment distributed to main girder)

*Guidelines 4.1.1.-1*

Live load bending stress for main girder

#### **DETERMINE RATING FACTOR, RF:**

$$RF = \frac{C - A_1 \cdot D}{A_2 \cdot L \cdot (1 + I)} = 3.04$$

Rating factor

#### **DETERMINE RATING IN TONS, RT:**

$$RT = \begin{cases} RF \cdot 36\text{ton} & \text{if } RF \leq 1 \\ (36\text{ton}) & \text{otherwise} \end{cases}$$

$$RT = 36 \text{ ton}$$

Inventory load rating when considering global bending effects on the main girder

#### **Rating of Loaded Exterior Girders:**

##### **Determine Effective Section Modulus, Seff:**

$$S_{eg} = \frac{I_{eg}}{y_{b,eg}} = 53.7 \text{ in}^3$$

Section modulus of exterior girder

$$S_{effeg} = \frac{I_{eg,comp}}{y_{b,comp,eg}} = 101.3 \text{ in}^3$$

Effective section modulus of exterior girder composite section

#### **DETERMINE DEAD LOAD BENDING STRESS, D:**

*Guidelines 1.1*

##### **Note:**

-Only the structural shape of the flatcar member resists dead load

##### **Determine Stress in Exterior Girder due to Self Weight:**

$$w_{eg} = A_{eg} \cdot \gamma_{steel} = 39.5 \frac{\text{lb}}{\text{ft}}$$

Exterior girder self weight

$$M_{eg} := \frac{w_{eg} \cdot L_{span}^2}{8} = 11 \text{ kip}\cdot\text{ft}$$

Exterior girder self weight moment  
(Note: Conservative to use the entire bridge span length, may find reasonable to use span length between floor beams)

$$\sigma_{eg} := \frac{M_{eg}}{S_{eg}} = 2.5 \text{ ksi}$$

Stress in exterior girder due to self weight

#### Determine Stress in Exterior Girder due to Concrete Deck:

$$w_{deckeg} := (5\text{m})(9\text{m}) \cdot w_{conc} = 46.9 \frac{\text{lb}}{\text{ft}}$$

Portion of concrete deck carried by the exterior girder (tributary width taken as the distance between the exterior girder and neighboring stringer, 5 inches)

$$M_{deckeg} := \frac{w_{deckeg} \cdot L_{span}^2}{8} = 13.2 \text{ kip}\cdot\text{ft}$$

Dead load moment at midspan due to concrete deck

$$\sigma_{deckeg} := \frac{M_{deckeg}}{S_{eg}} = 2.9 \text{ ksi}$$

Stress in main girder due to concrete deck

#### Determine Total Dead Load Stress in Exterior Girder:

$$D := \sigma_{eg} + \sigma_{deckeg} = 5.4 \text{ ksi}$$

Total dead load bending stress in exterior girder

#### DETERMINE LIVE LOAD BENDING STRESS, L:

##### **Note:**

-The composite section (structural shape of the member and its effective flange width of the concrete deck slab) resists live load

$$M_{LL} := 580 \text{ kip}\cdot\text{ft}$$

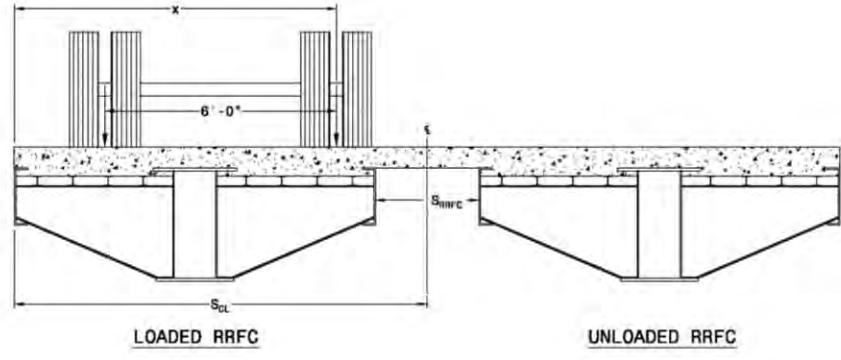
*AASHTO Table C6B-1*

Maximum live load moment due to HS-20 truck at midspan

$$\frac{I_{eg,comp}}{I_{mg,comp}} = 5.96$$

Stiffness ratio to be used to determine DF and CDF

**Determine Moment Proportion, MP:**



$$x := 7\text{ft} + 8\text{in}$$

Location of inside truck wheel take from outside face of loaded RRFC

$$S_{CL} := \frac{W_{\text{bridge}}}{2} = 10.7\text{-ft}$$

Distance from outside face of loaded RRFC to centerline of bridge

$$S_{RRFC} = 2.7\text{-ft}$$

Clear spacing between RRFCs

$$MP := \begin{cases} 0.90 & \text{if } x \leq S_{CL} \\ 0.60 & \text{if } S_{CL} < x < S_{CL} + 6\text{ft} \end{cases}$$

*Guidelines 4.1.1.2.1*

Moment proportion from Table, depending on truck location

$$MP = 0.9$$

Represents proportion of live load moment distributed to loaded RRFC

**Determine Distribution Factor, DF:**

$$DF := MP = 0.9$$

*Guidelines 4.1.1.2*

Represents load distribution between RRFCs

$$DF \leq 1 = 1 \quad \text{OKAY}$$

**Determine Maximum Positive Live Load Bending Stress:**

$$\alpha := 1.0$$

*Guidelines 4.1.1.5*

Stress modification factor

*Guidelines 4.1.1.3*



$$CDF = 0.05$$

$$L = \alpha \cdot CDF \cdot \frac{DF \cdot M_{LL}}{S_{effeg}} = 3.09 \text{ ksi}$$

**DETERMINE RATING FACTOR, RF:**

$$RF := \frac{C - A_1 \cdot D}{A_2 \cdot L \cdot (1 + D)} = 5.1$$

**DETERMINE RATING IN TONS, RT:**

$$RT := \begin{cases} RF \cdot 36 \text{ ton} & \text{if } RF \leq 1 \\ (36 \text{ ton}) & \text{otherwise} \end{cases}$$

$$RT = 36 \text{ ton}$$

Car distribution factor for main girder (proportion of car moment distributed to exterior girder)

*Guidelines 4.1.1.-1*

Live load bending stress for exterior girder

Rating factor

Inventory load rating when considering global bending effects on the exterior girder

**Available Capacity After Fracture**

**Must meet the following provisions:**

1. Composite action between main girders and concrete deck
2. Composite action between exterior girders and concrete deck
3. Adequate design of reinforced concrete deck

**Determine Capacity of Members, C:**

$$C = 0.75 \cdot F_y = 36 \text{ ksi}$$

*Guidelines 4.3*

**Available Capacity of FRACTURED Railroad Flatcar:**

**Exterior Girders:**

**Determine Dead Load Bending Stress Before Fracture:**

$$\sigma_D = \sigma_{eg} + \sigma_{deckeg} = 5.4 \text{ ksi}$$

Dead load bending stress in exterior girder before fracture

**Determine Redistributed Dead Load and Locked-In Bending Stress After Fracture:**

$$DF := 0.60$$

*Guidelines 4.3.1.3*

Portion of redistributed dead load in fractured RRFC

$$CDF := 0.50$$

*Guidelines 4.3.1.4*

Portion of redistributed dead load in single exterior girder

$$M_{DL,mg} := (M_{RRFC} + M_{deckmg}) = 345.9 \text{ kip}\cdot\text{ft}$$

*Guidelines 4.3.1.2*

Redistributed dead load moment (assumed to be dead load original carried by main girder before fracture)

$$\sigma_{RD} := \frac{DF \cdot CDF \cdot M_{DL,mg}}{S_{effeg}} = 12.3 \text{ ksi}$$

Redistributed dead load stress in exterior girder

**Determine Live Load Bending Stress After Fracture:**

$$DF := 0.50$$

*Guidelines 4.3.2.2*

Portion of live load in fractured RRFC

$$CDF := 0.50$$

*Guidelines 4.3.2.3*

Portion of live load in single exterior girder

$$M_{LL} := 580 \text{ kip}\cdot\text{ft}$$

*AASHTO Table C6B-1*

Maximum live load moment due to HS-20 truck at midspan

$$\sigma_{LL} := \frac{DF \cdot CDF \cdot M_{LL}}{S_{effeg}} = 17.2 \text{ ksi}$$

Live load bending stress in exterior girder

**Determine Total Bending Stress After Fracture:**

$$\sigma_{tot} := \sigma_D + \sigma_{RD} + \sigma_{LL} = 34.9 \text{ ksi}$$

Total bending stress in exterior girder

$$\sigma_{tot} < C = 1$$

If less than capacity, okay.

### Available Capacity of UNFRACTURED Railroad Flatcar:

**Note:**

-Based on single lane loaded

### Exterior Girders:

#### Determine Dead Load Bending Stress Before Fracture:

$$\sigma_D := \sigma_{eg} + \sigma_{deckeg} = 5.4 \text{ ksi}$$

Dead load bending stress in exterior girder before fracture

#### Determine Redistributed Dead Load and Locked-In Bending Stress After Fracture:

$$DF := 0.40$$

*Guidelines 4.3.1.3*

Portion of redistributed dead load in unfractured RRFC

$$CDF := 0.05$$

*Guidelines 4.3.1.4*

Portion of redistributed dead load in single exterior girder

$$M_{DL,mg} := M_{RRFC} + M_{deckmg} = 345.9 \text{ kip-ft}$$

Redistributed dead load moment (assumed to be dead load original carried by main girder before fracture)

$$\sigma_{RD} := \frac{DF \cdot CDF \cdot M_{DL,mg}}{S_{effeg}} = 0.8 \text{ ksi}$$

Redistributed dead load stress in exterior girder

#### Determine Live Load Bending Stress After Fracture:

$$DF := 1.0$$

*Guidelines 4.3.2.3*

Portion of live load in unfractured RRFC

$$CDF := 0.05$$

*Guidelines 4.3.2.4*

Portion of live load in single exterior girder

$$M_{LL} := 580 \text{ kip-ft}$$

*AASHTO Table C6B-1*

Maximum live load moment due to HS-20 truck at midspan

$$\sigma_{LL} := \frac{DF \cdot CDF \cdot M_{LL}}{S_{effeg}} = 3.4 \text{ ksi}$$

Live load bending stress in exterior girder

**Determine Total Bending Stress After Fracture:**

$$\sigma_{tot} := \sigma_D + \sigma_{RD} + \sigma_{LL} = 9.7 \text{ ksi}$$

Total bending stress in exterior girder

$$\sigma_{tot} < C = 1$$

If less than capacity, okay.

**Main Girder:**

**Determine Dead Load Bending Stress Before Fracture:**

$$\sigma_D := \sigma_{RRFC} + \sigma_{deckmg} = 4.6 \text{ ksi}$$

Dead load bending stress in exterior girder before fracture

**Determine Redistributed Dead Load and Locked-In Bending Stress After Fracture:**

$$DF := 0.40$$

*Guidelines 4.3.1.3*

Portion of redistributed dead load in unfractured RRFC

$$CDF := 0.90$$

*Guidelines 4.3.1.4*

Portion of redistributed dead load in unfractured main girder

$$M_{DL,mg} := M_{RRFC} + M_{deckmg} = 345.9 \text{ kip-ft}$$

Redistributed dead load moment (assumed to be dead load original carried by main girder before fracture)

$$\sigma_{RD} := \frac{DF \cdot CDF \cdot M_{DL,mg}}{S_{effmg}} = 1.4 \text{ ksi}$$

Redistributed dead load stress in unfractured main girder

**Determine Live Load Bending Stress After Fracture:**

$$DF := 1.0$$

$$CDF := 0.90$$

$$M_{LL} := 580 \text{ kip}\cdot\text{ft}$$

$$\sigma_{LL} = \frac{DF \cdot CDF \cdot M_{LL}}{S_{effmg}} = 5.7 \text{ ksi}$$

*Guidelines 4.3.2.3*

Portion of live load in unfractured RRFC

*Guidelines 4.3.2.4*

Portion of live load in unfractured main girder

*AASHTO Table C6B-1*

Maximum live load moment due to HS-20 truck at midspan

Live load bending stress in unfractured main girder

**Determine Total Bending Stress After Fracture:**

$$\sigma_{tot} := \sigma_D + \sigma_{RD} + \sigma_{LL} = 11.6 \text{ ksi}$$

$$\sigma_{tot} < C = 1$$

Total bending stress in unfractured main

If less than capacity, okay.

**APPENDIX H. GUIDANCE FOR ESTABLISHING RELIABILITY-BASED  
INSPECTION INTERVAL FOR RRFC BRIDGES WITH FULLY COMPOSITE  
CONCRETE DECKS**

Currently, bridges in the United States are inspected at a fixed interval of 24 months under the National Bridge Inspection Standards (NBIS). This interval is set without regard for the current condition and known characteristics of the bridges. The Code of Federal Regulations (CFR) permits the extension of the interval to 48 months if a State-tendered written proposal with supporting data is approved by the Federal Highway Administration (FHWA). However, more recently the FHWA has begun shifting toward an approach that utilizes rational, reliability-based bridge inspection practices. To that end, a recent National Cooperative Highway Research Program (NCHRP) project conducted at the University of Missouri and Purdue University developed a reliability-based bridge inspection (RBI) method (Washer et al., 2011). The goal of the methodology is to improve the safety and reliability of bridges while optimizing the allocation of bridge inspection resources. The RBI practices differ from traditional approaches that are calendar-based because the establishment of the interval, or inspection frequency, is not fixed. Instead, reliability-based engineering analysis is used to assess the specific needs of a bridge or family of bridges. This is achieved by analyzing the likelihood of anticipated or potential damage modes and the associated consequences. The more comprehensive theory and development of the RBI method is beyond the scope of this report and will not be discussed herein. If further information is desired, the reader is referred to the NCHRP 12-82 final report (Washer et al., 2011). Rather, the purpose of the following guidelines is to demonstrate, by way of an example, the application of the RBI procedure with results that could be expected for a similar RRFC structure. It should also be noted that the anticipated damage modes and associated consequences used for the following example were established by the Reliability Assessment Panel (RAP) made up of Indiana Department of Transportation (INDOT) bridge engineers and their consultants during the INDOT implementation phase of NCHRP 12-82.

In order to apply the RBI method to the laboratory RRFC, several assumptions were made. The first of those assumptions was that the average daily truck traffic (ADTT) is low, meaning less than 100 trucks per day. This was a reasonable assumption considering that RRFC bridges are used primarily on low-volume, rural roads. The

current condition ratings for the deck and superstructure were considered to be 7 and 6, respectively.

**Reliability-Based Inspection Interval:**

<b>Corrosion Profile -- Concrete Bridge Deck</b>		
<b>Attribute</b>	<b>Points</b>	<b>Score</b>
D.4 Poor Deck Drainage and Ponding		
Ponding/Ineffective Drainage	10	10
No problems noted	0	
<b>Attribute</b>	<b>Points</b>	<b>Score</b>
D.6 Year of Construction		
Concrete Decks		
Pre 1950	10	
1950-1970	6	
1970-1990	3	3
1990+	0	
D.10 Deck Overlays		
Has overlay	15	
Does not have overlay	0	0
D.8 Concrete Mix Design		
Not high performance concrete	15	15
High performance concrete	0	
D.11 Minimum Concrete Cover		
Unknown	15	
<1.5 in	15	
1.5in - 2.5in	7	7
2.5in +	0	
D.12 Reinforcement Type		
Uncoated carbon steel	15	15
Has Protective Coating or is made from corrosion resistant metal	0	
L.3 Exposure Environment		
Severe/Marine	20	
Moderate/Industrial	10	10
Benign	0	



L.5 Rate of De-Icing Chemical Application		
High (Northern Districts)	20	
Moderate (Middle Districts)	15	15
Low (Southern Districts)	10	
None	0	
C.5 Maintenance Cycle		
No routine maintenance	20	
Some limited maintenance	10	10
Regular maintenance	0	
Corrosion Profile Point Total	140	85

Table H.1 above contains the Points (points possible for the given attribute) and the Score (points assigned by the evaluator for the RRFC). Notice that the attribute *L.3 Exposure Environment* was assumed for this case to be *Moderate/Industrial*, a typical condition for rural bridges, as well as *Moderate* for *L.5 Rate of De-icing Chemical Application*.

**Table H.2 Corrosion damage mode for the concrete deck**

<b>Corrosion Damage -- Concrete Bridge Deck</b>		
<b>Attribute</b>	<b>Points</b>	<b>Score</b>
L.1 Average Daily Truck Traffic Concrete Bridge Deck		
ADTT $\geq$ 2500	15	
$500 \leq$ ADTT < 2500	10	
$100 \leq$ ADTT < 500	5	
ADTT < 100	0	0
C.1 Current Condition Rating		
Current rating is 5 or below	20	
Current rating is 6	5	
Current rating is 7+	0	0
C.8 Corrosion Induced Cracking		
Significant corrosion induced cracking	20	
Moderate corrosion induced cracking	10	
Minor corrosion induced cracking	5	
No corrosion induced cracking	0	0
C.9 General Cracking		
Widespread or severe cracking	15	
Moderate cracking present	10	
Minor or no cracking	0	0

C.10 Delaminations		
Unknown	20	
Significant (>20% by area) delamination	20	
Moderate (5-20% by area) delamination	10	
Minor, localized (<5% by area) delamination	5	
No delamination present	0	0
C.11 Presence of Repaired Areas		
Significant amount of repaired areas	10	
Moderate amount of repaired areas	6	
Minor amount of repaired areas	3	
No repaired areas	0	0
	<b>Points</b>	<b>Score</b>
<b>Attribute</b>		
C.12 Presence of Spalling		
Significant spalling (>10% by area with exposed rebar or strands)	20	
Moderate spalling (greater than 1 inch deep or 6 inches diameter exposed reinforcement)	15	
Minor spalling (less than 1 inch deep or 6 inches in diameter)	5	
No spalling	0	0
C.13 Efflorescence/Staining		
Severe to Moderate efflorescence with rust staining; severe efflorescence without rust staining	15	
Moderate efflorescence without rust staining	10	
Minor efflorescence	5	
No efflorescence	0	0
<b>Corrosion Damage, Deck Total</b>	<b>275</b>	<b>85</b>
<b>Corrosion Damage, Deck Ranking</b>		<b>1.24</b>
		<b>Low</b>
<b>Consequence Factor</b>		<b>Low</b>

The occurrence factor in Table H.2 was obtained by dividing the total assigned points by the total points possible ( $85/275 = 1.24$ , Low). (Note that the total assigned points included the total from Table H.1, which captured a general corrosion attribute overview of this bridge and would be included in any concrete reinforcement corrosion-related damage mode. Since the RRFC was a steel superstructure, it only applied to the concrete deck.) A *Low* occurrence factor is assigned for the ratio that is greater than 1

and less than 2. The consequence factor was determined subjectively by the evaluator. In this case it was assumed that if the damage mode considered were to occur on the bridge, the corrosion would cause spalling and/or delamination. A worst case scenario would be spalls falling from the deck underside. However, it was considered a *Low* consequence assuming that the bridge crossed over a small, non-navigable water way with no pedestrian, water craft, or vehicular traffic. Additionally, since it's an assumed low-volume road, the consequence of spalling on the topside of the deck would also be relatively insignificant. If the assumed scenario would have been different, e.g. high-volume road beneath the bridge (which is doubtful for a RRFC bridge), the consequence for the spalling would probably have been higher since the potential would then exist for debris impacting traffic below.

**Table H.3 Fatigue damage mode for the steel superstructure**

<i>Fatigue Damage -- Steel Girder</i>		
<b>Attribute</b>	<b>Points</b>	<b>Score</b>
D.6 Year of Construction		
Steel Girders, Fatigue		
Unknown	15	
Pre 1975	15	
1976-1984	10	10
1985-1993	5	
1994+	0	
D.16 Element Connection Type		
Elements connected with welds	15	15
Elements connected with rivets	7	
Elements connected with high strength bolts	0	
D.17 Worst Fatigue Detail Category		
Fatigue detail category E or E*	20	20
Fatigue detail category D	15	
Fatigue detail category A, B, B* or C	0	
L.1 Average Daily Truck Traffic		
Steel Girders		
ADTT $\geq$ 2500	15	
500 $\leq$ ADTT < 2500	10	
100 $\leq$ ADTT < 500	5	
ADTT < 100	0	0
L.7 Remaining Fatigue Life		

	Unknown	10	
	Insufficient remaining life	7	
	Sufficient remaining life	3	3
	Infinite remaining life	0	
C.19	Presence of fatigue cracks due to secondary, or out-of-plane stresses		
	Unknown	15	
	Out-of-plane fatigue cracks exist	15	
	Out-of-plane fatigue cracks exist and have been arrested or retrofitted	5	
	No out-of-plane fatigue cracks exist	0	0
Fatigue Damage Total		90	48
Fatigue Damage Ranking			2.13
			Moderate
Consequence Factor			Moderate

Fatigue damage was another anticipated, or possible, mode of damage for the RRFC superstructure, see Table H.3 **Table H.** It was assumed that the remaining fatigue life was sufficient. This means that the fatigue life of the superstructure would be expected to be at least the length of the longest possible inspection interval, or 6 years. Although a fatigue evaluation was not performed for the RRFC, it was known by the evaluator that the stress ranges produced by the equivalent of legal live loads did not exceed the constant amplitude fatigue threshold of the most fatigue-susceptible detail on the structure. Thus, it may be possible that the fatigue life was infinite. However, since a formal fatigue evaluation was not actually performed, the evaluator conservatively assumed a sufficient remaining life rather than an infinite remaining life. The occurrence factor scored as *Moderate*. The consequence factor was conservatively determined to also be *Moderate* by the evaluator assuming that the worst case scenario for the fatigue damage mode would be pop-in fracture and loss of load carrying capacity of one of the primary members. It was established during the laboratory testing that the RRFC with fully composite concrete deck was not fracture critical. Thus, the loss of load carrying capacity of one of the primary members would not cause collapse of the structure, minimizing the potential consequence of fatigue damage.

**Table H.4 Corrosion damage mode of the steel superstructure**

<b>Corrosion Damage -- Steel Girder</b>		
<b>Attribute</b>	<b>Points</b>	<b>Score</b>
D.5 Use of Open Decking		
Has Open Deck	20	
Does not have open deck	0	0
D.13 Built Up Member		
Element is built up member	15	
Element is not a built up member	0	0
D.15 Constructed of Weathering Steel		
Element is NOT weather steel	10	10
Element is properly detailed weathering steel	0	
L.3 Exposure Environment		
Severe/Marine	20	
Moderate/Industrial	10	10
Benign	0	
L.5 Rate of De-Icing Chemical Application		
High (Northern Districts)	20	
Moderate (Middle Districts)	15	15
Low (Southern Districts)	10	
None	0	
<b>Attribute</b>	<b>Points</b>	<b>Score</b>
L.6 Subjected to Overspray Steel Girder		
Severe overspray exposure	20	
Moderate overspray exposure	10	
Low overspray exposure	0	0
Not over a roadway	0	
C.4 Joint Condition		
Significant amount of leakage at joints	20	
Joints have moderate leakage or are debris filled	15	15
Joints are present but not leaking	5	
Bridge is jointless	0	
C.7 Quality of Deck Drainage System		

Deck drains directly onto superstructure or substructure components, or ponding on deck results from poor drainage	15	
Drainage issues resulting in drainage onto superstructure or substructure or moderate ponding on deck; effects may be localized	7	
Adequate drainage	0	0
<b>C.17 Coating Condition</b>		
Coating system in very poor condition, limited or no effectiveness for corrosion protection, great than 3% rusting	15	
Coating system is in poor condition, 1%-3% rusting, substantially effective for corrosion protection	7	7
Coating is in fair to good condition, effective for corrosion protection	0	
<b>C.21 Presence of Active Corrosion</b>		
Significant amount of active corrosion present	20	
Moderate amount of active corrosion present	15	
Minor amount of active corrosion present	7	7
No active corrosion present	0	
<b>C.5 Maintenance Cycle</b>		
No routine maintenance	15	
Some limited maintenance	7	7
Regular maintenance	0	
<b>Corrosion Damage, Superstructure Total</b>	<b>190</b>	<b>71</b>
<b>Corrosion Damage, Superstructure Ranking</b>		<b>1.49</b>
		<b>Low</b>
<b>Consequence Factor</b>		<b>Moderate</b>

Table H.4 above contains the evaluation of the corrosion damage mode for the steel superstructure. Similar assumptions were made for the environmental factors as those made for the corrosion of the deck. Additionally, it was assumed that if this bridge was in the field, end joints would exist on the structure and would have some leaking occurring, but the deck would be otherwise draining properly. The consequence factor was evaluated at *Moderate*, with a similar worst case scenario as that for the fatigue damage mode; loss of load carrying capacity of one of the primary members.

**Table H.5 Fracture damage mode for the steel superstructure**

<b>Fracture Damage -- Steel Girder</b>		
<b>Attribute</b>	<b>Points</b>	<b>Score</b>
D.3 Minimum Vertical Clearance Steel Girder		
≤14'	15	
14' < X ≤15'	12	
15' < X ≤17'	7	
>17'	0	
No under traffic	0	0
D.6 Year of Construction Steel Girders, Fracture		
Unknown	20	
Pre 1975	20	
1976-1984	10	10
1985-1993	5	
1994-2008	3	
2009+	0	
D.14 Constructed of High Performance Steel		
Element is NOT high performance steel	10	10
Element is high performance steel	0	
L.1 Average Daily Truck Traffic Steel Girders		
ADTT ≥ 2500	15	
500 ≤ ADTT < 2500	10	
100 ≤ ADTT < 500	5	
ADTT < 100	0	0
L.7 Remaining Fatigue Life		
Unknown	10	
Insufficient remaining life	7	
Sufficient remaining life	3	3
Infinite remaining life	0	
	<b>Points</b>	<b>Score</b>
C.6 Previously Impacted		
Has been previously impacted	20	
Has NOT been previously impacted	0	0
C.19 Presence of Fatigue Cracks due to Secondary or Out-of-Plane Stress		

Unknown	15	15
Out of plane fatigue cracks	15	
Out of plane fatigue cracks exist and have been arrested or retrofitted	5	
No out of plane fatigue cracks	0	0
C.20 Non-Fatigue Related Cracks or Defects		
Non-fatigue related cracks or defects present	10	
Non fatigue related cracks or defects are NOT present	0	0
<b>Fracture Total</b>	<b>115</b>	<b>38</b>
<b>Fracture Ranking</b>		<b>1.32</b>
		<b>Low</b>
<b>Consequence Factor</b>		<b>Moderate</b>

Table H.5 contains the assessment for the fracture damage mode of the steel superstructure. This damage mode is very similar to the fatigue damage mode since the end result of the fatigue damage mode is fracture. However, the added element of traffic impact must be evaluated as well. It was assumed that the bridge would be over a small, non-navigable water way with no under traffic potentially impacting the bridge. Additionally, it was known that the steel was type A36 steel and not high performance steel. High performance steel is known to have superior fracture resistance.

**Table H.6 Summary of results for reliability-based inspection interval of RRFC with fully composite deck**

Element	Damage Mode	Occurrence Factor (O)		Consequence Factor (C)		Maximum Interval
Deck	Corrosion	Low	2	Low	1	72 months
Steel Girders	Fatigue	Moderate	3	Moderate	2	48 months
	Corrosion	Low	2	Moderate	2	72 months
	Fracture	Low	2	Moderate	2	72 months
Substructure	Corrosion	Remote	1	Low	1	96 months
<b>Inspection Interval:</b>						<b>48 months</b>

Table H.6 provides the summary of results for the reliability-based engineering analysis for the laboratory RRFC. Several assumptions were made in order to evaluate the bridge as if it was in the field. Each of those assumptions has been explained above. It



can be seen in table that the controlling damage mode for the RRFC bridge is fatigue in the steel superstructure with a maximum inspection interval of 48 months.

This example illustrates the reliability-based engineering analysis that would go into determining the inspection interval of a RRFC bridge similar to the one tested in the laboratory using the approach developed by Washer et al. Each RRFC may differ slightly in existing conditions, design attributes, loading attributes, and consequence of occurrences, thus possibly changing the inspection interval. Each RRFC bridge should be evaluated by a qualified person taking all of these factors into consideration.